

明治
丙申
三陸發嘯之實況



A Tale of Earthquakes and Landscapes

What landscapes can tell us about Subduction zone earthquake cycles



Bar Oryan

Green Postdoctoral Scholar

Scripps Institution of Oceanography, UCSD



boryan@ucsd.edu

GREAT MEGATHURST EARTHQUAKES IN THE PAST 20 YEARS

1. 2004 Sumatra-Andaman Earthquake (Mw 9.3)

- **Date:** December 26, 2004
- **Location:** Off the west coast of northern Sumatra, Indonesia
- **Impact:** Triggered a catastrophic tsunami, causing over 230,000 deaths across 14 countries.



2. 2010 Maule Earthquake (Mw 8.8)

- **Date:** February 27, 2010
- **Location:** Offshore Maule region, Chile
- **Impact:** Over 500 fatalities and extensive infrastructure damage.

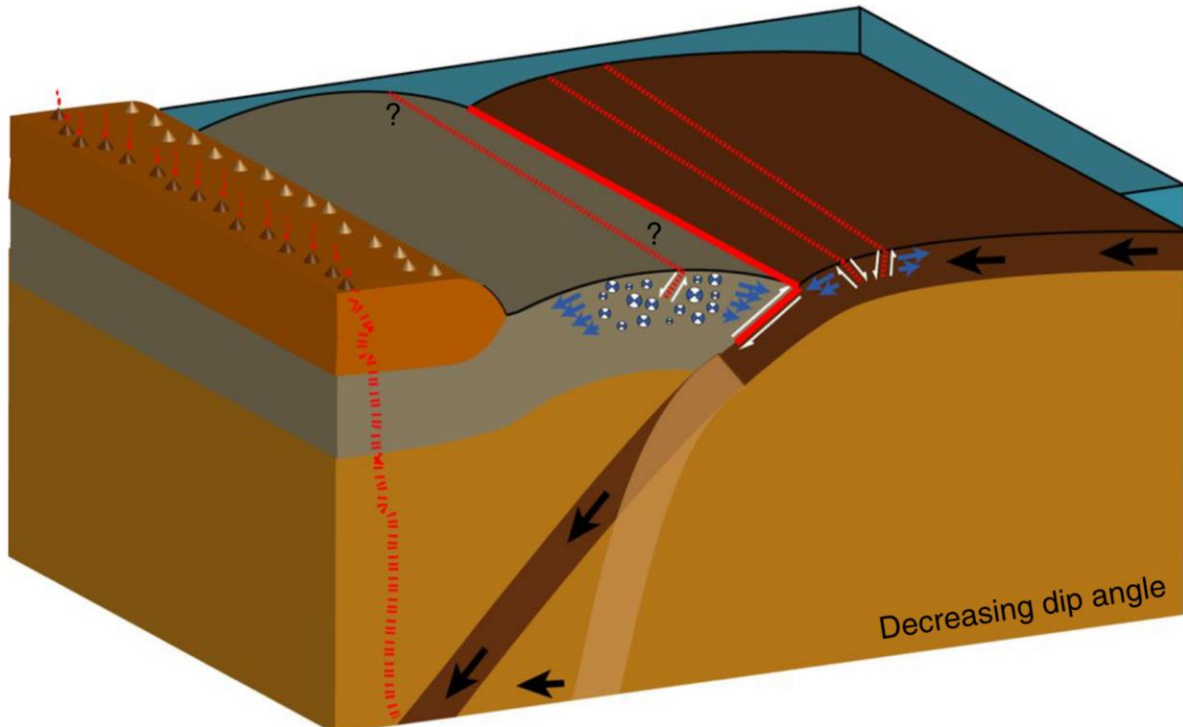
3. 2011 Tōhoku Earthquake (Mw 9.1)

- **Date:** March 11, 2011
- **Location:** Off the east coast of Honshu, Japan
- **Impact:** Generated a massive tsunami, leading to nearly 16,000 deaths and the Fukushima nuclear disaster.



MY RESEARCH INTERESTS

Thermomechanical numerical modeling and study how slow changes of subducting slabs geometry over millions of years affect megathrust hazard

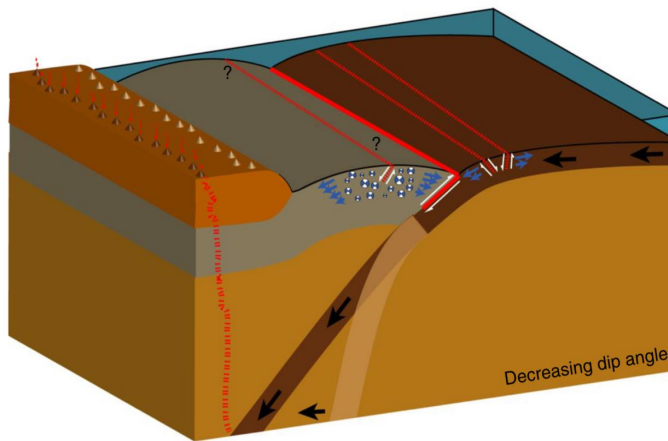


Oryan & Buck, 2020, *Nature geoscience*



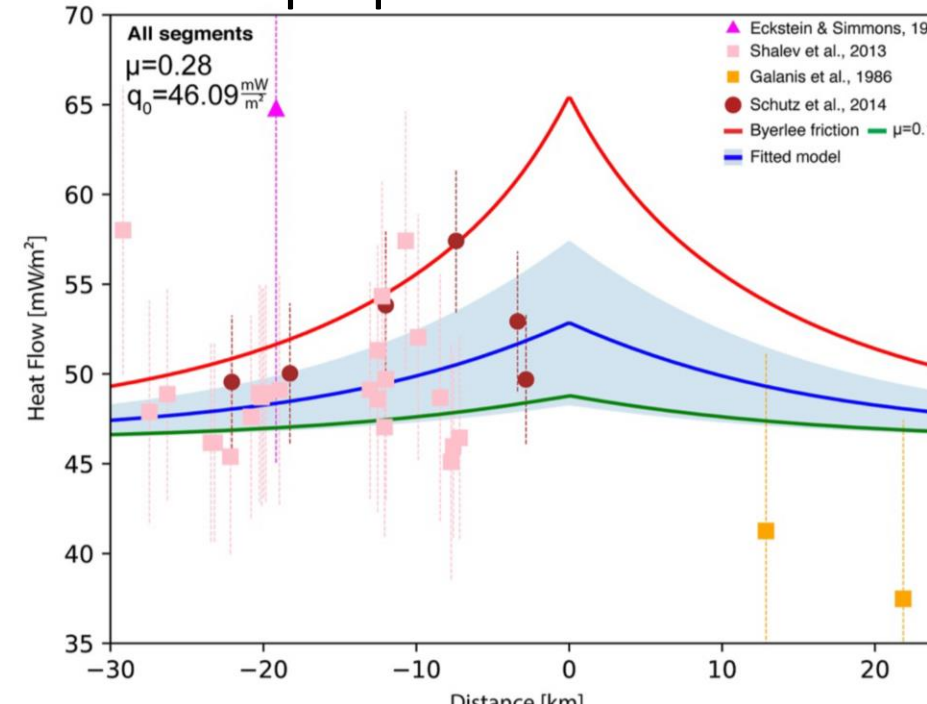
MY RESEARCH INTERESTS

Thermomechanical numerical modeling and study how slow changes of subducting slabs geometry over millions of years affect megathrust hazard



Oryan & Buck, 2020, *Nature geoscience*

Analysis of **heat flow** data to constrain frictional properties of faults

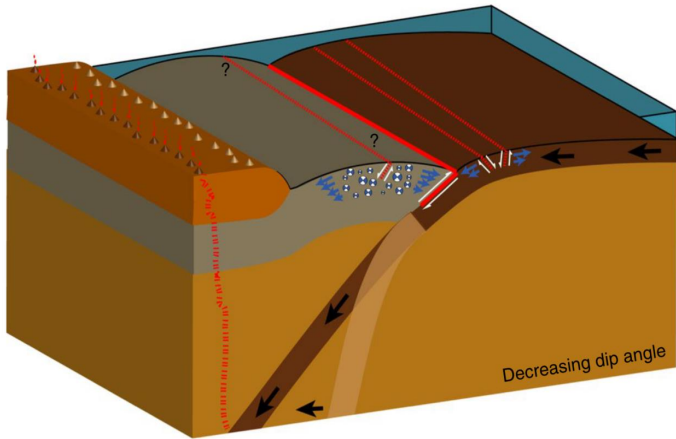


Oryan & Savage ,2021, *G³*



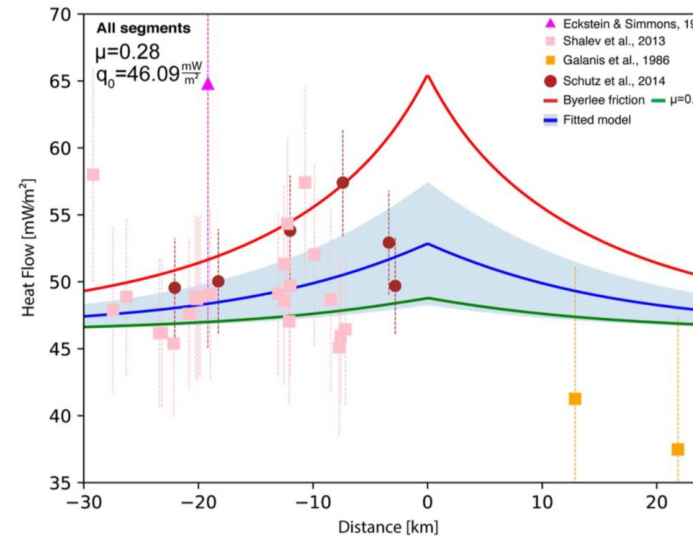
MY RESEARCH INTERESTS

Thermomechanical numerical modeling and study how slow changes of subducting slabs geometry over millions of years affect megathrust hazard



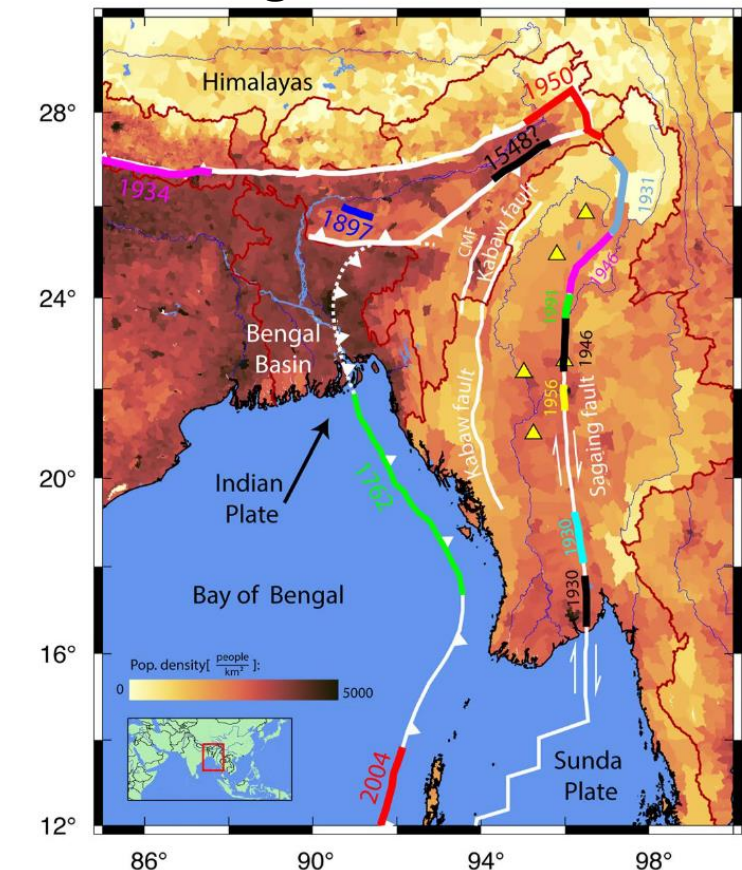
Oryan & Buck, 2020, *Nature geoscience*

Analysis of **heat flow** data to constrain frictional properties of faults



Oryan & Savage ,2021, G^3

Inversion of Indo-Burma **geodetic** data to constrain megathrust hazard



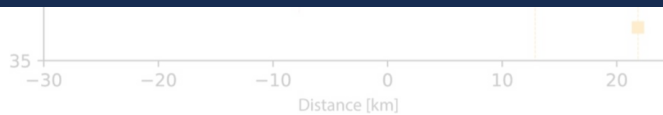
Oryan et al., 2023, JGR



MY RESEARCH INTERESTS

Inversion of Indo-Burma
geodetic data to constrain

I am a **geophysicist** interested in studying
subduction earthquake cycles and associated
hazard using an **interdisciplinary** approach
ranging a broad range of timescales

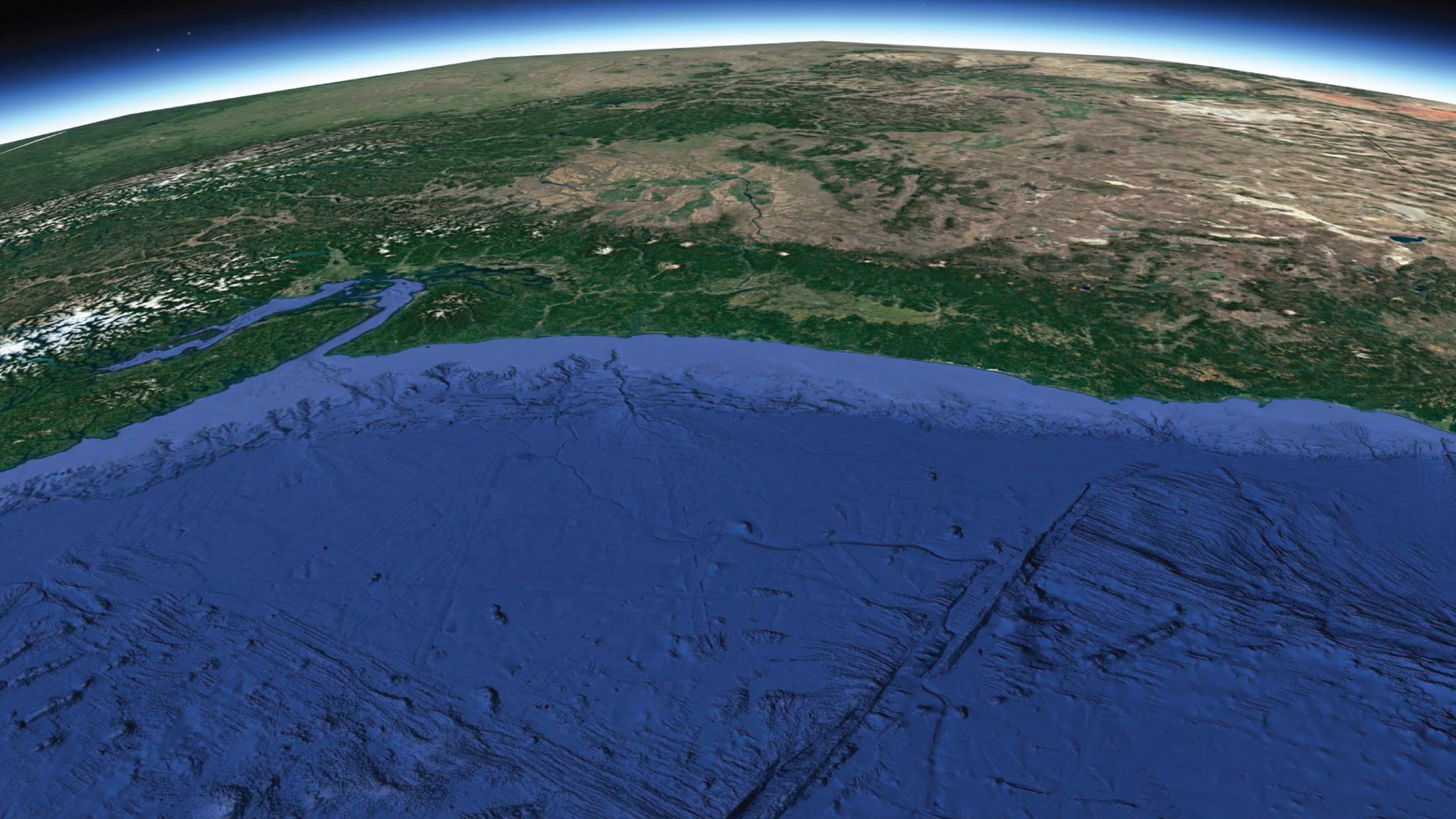


Oryan & Savage ,2021, *G³*

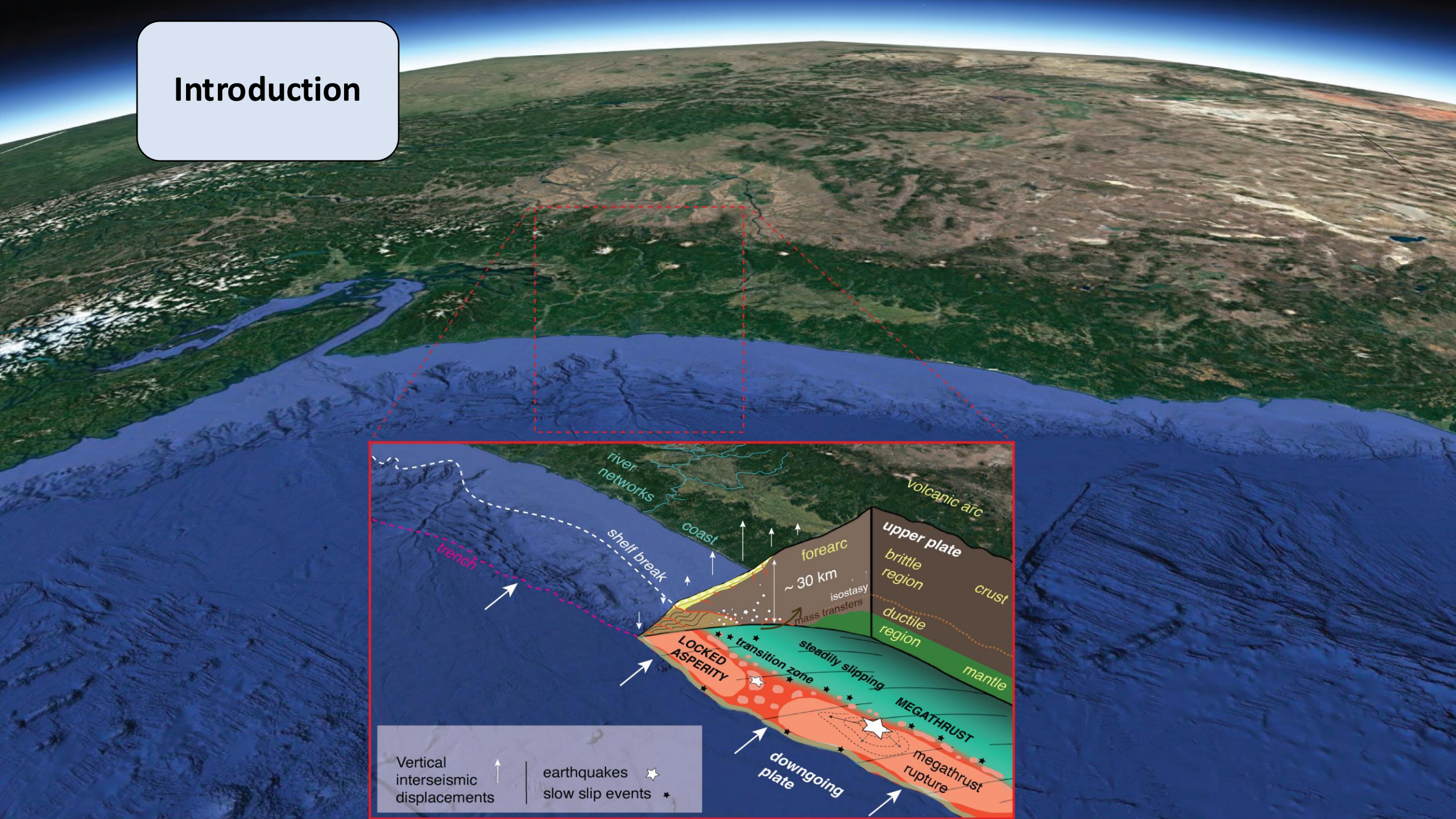


Oryan et al., 2023, JGR

Oryan & Buck, 2020, *Nature geoscience*

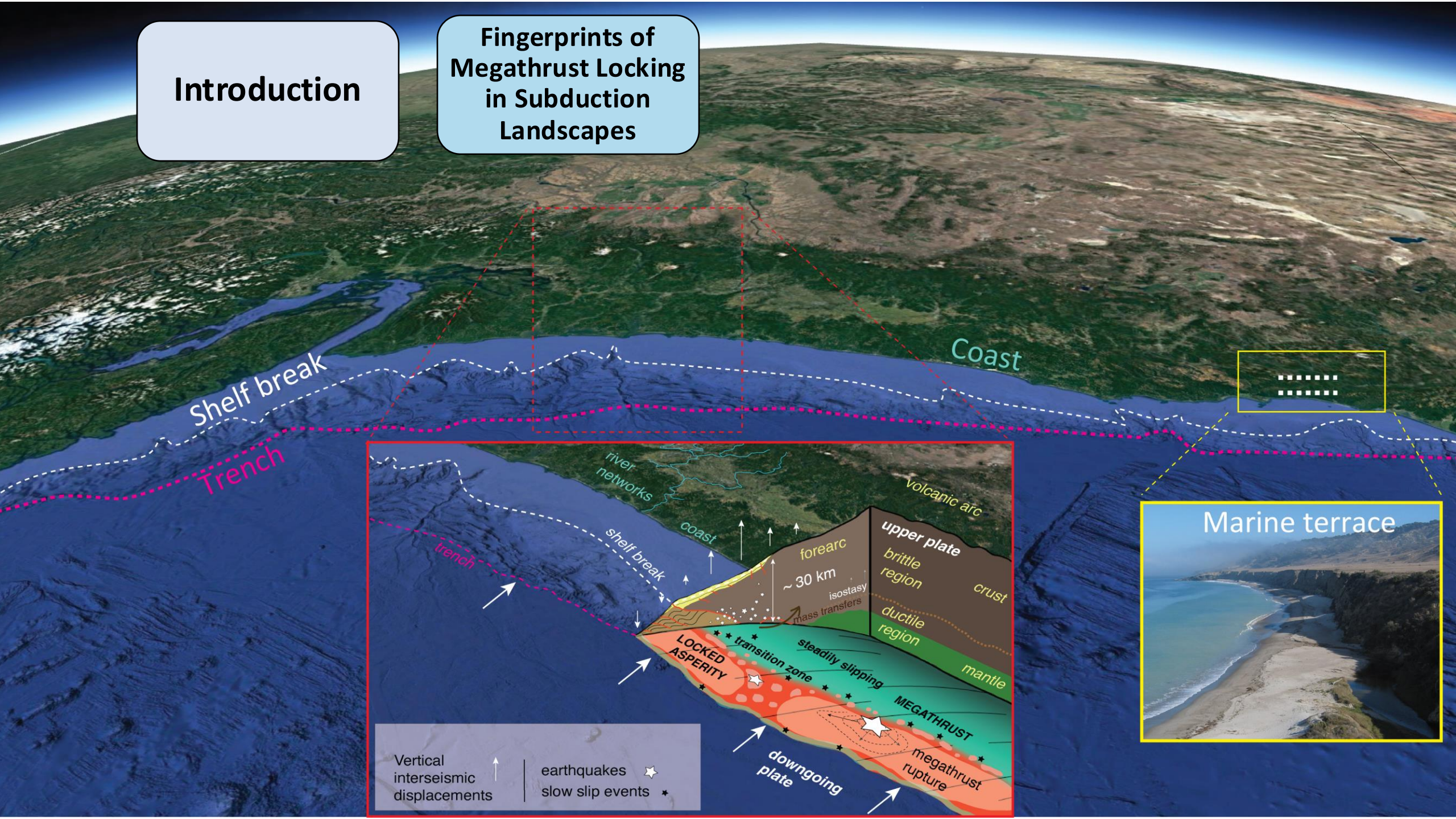


Introduction



Introduction

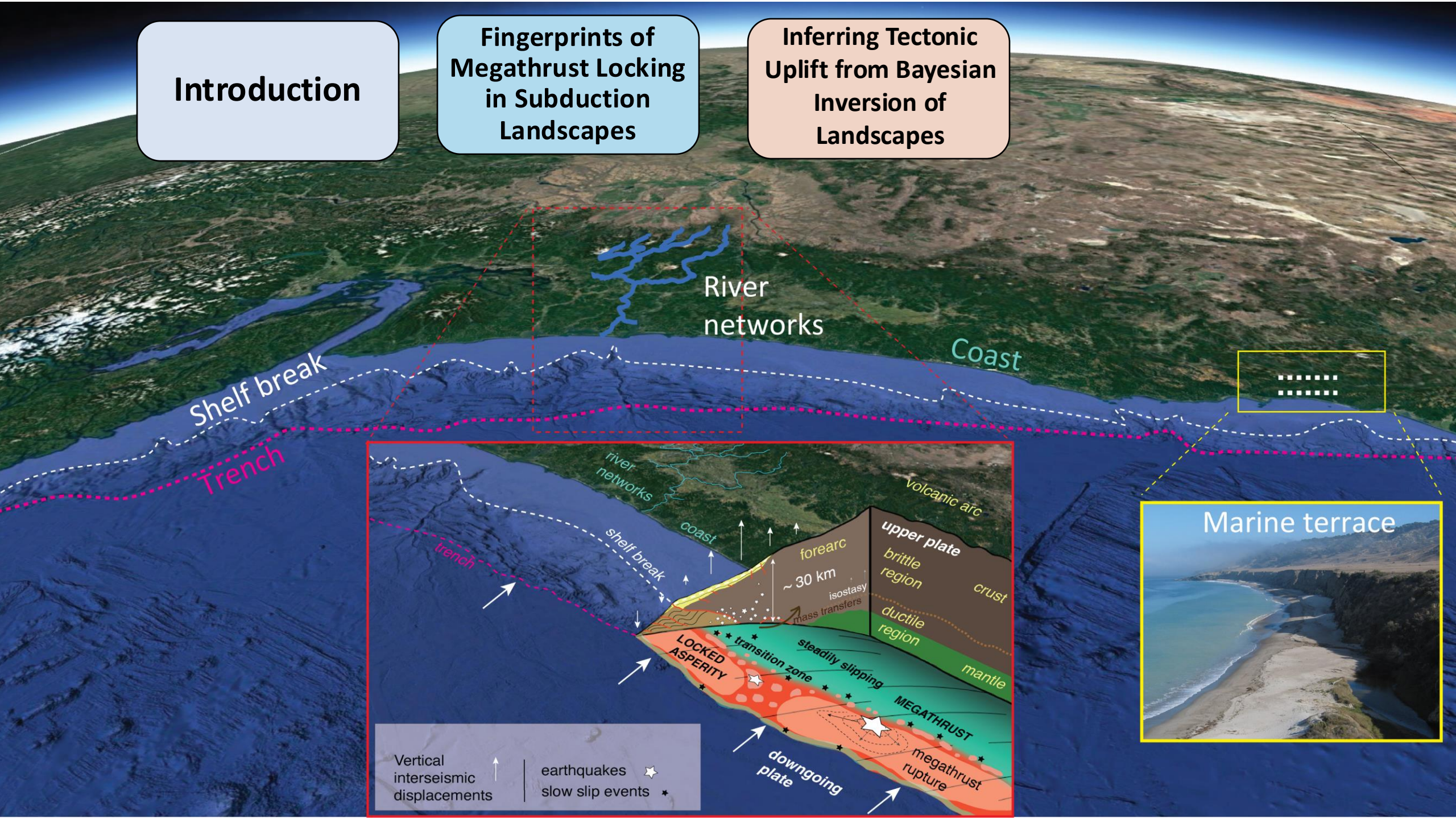
Fingerprints of Megathrust Locking in Subduction Landscapes



Introduction

Fingerprints of Megathrust Locking in Subduction Landscapes

Inferring Tectonic Uplift from Bayesian Inversion of Landscapes

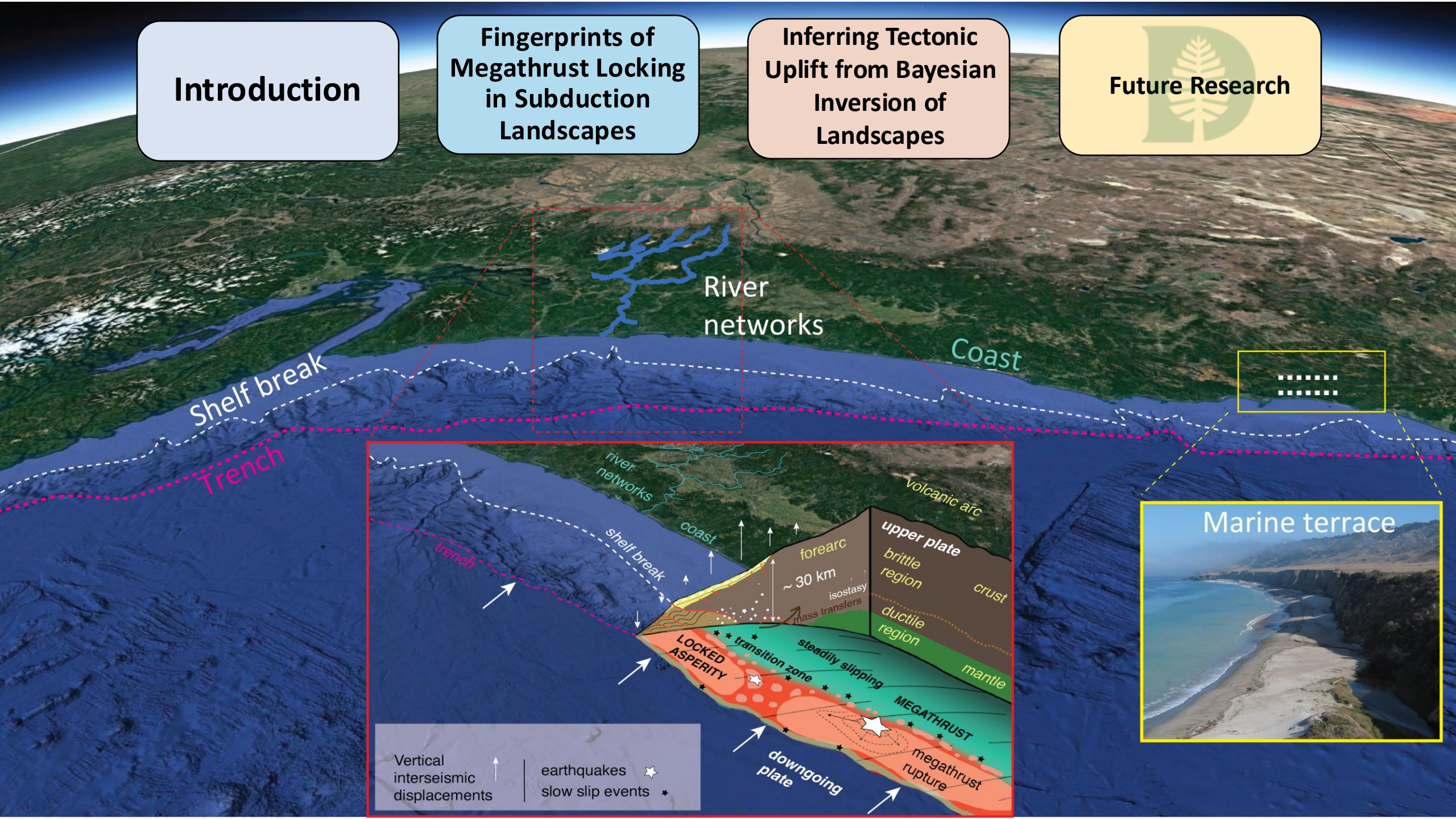


Introduction

Fingerprints of Megathrust Locking in Subduction Landscapes

Inferring Tectonic Uplift from Bayesian Inversion of Landscapes

Future Research

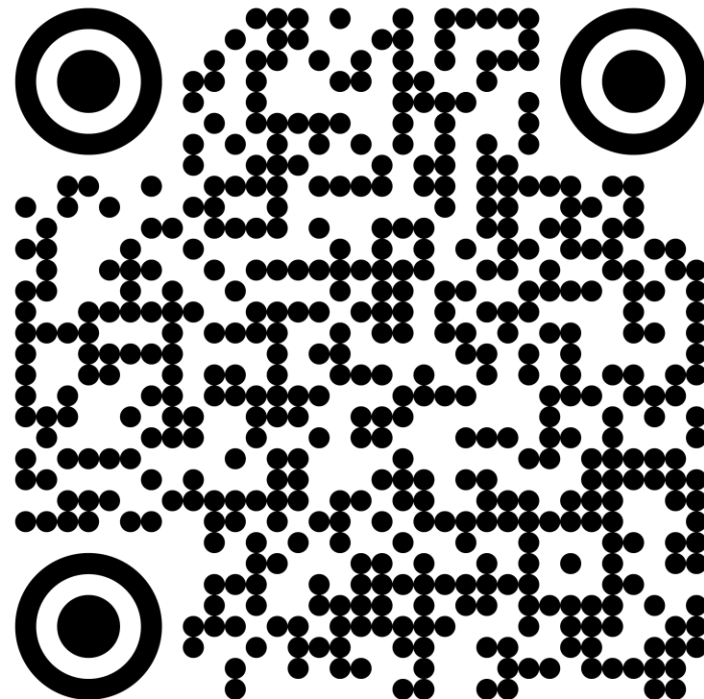


Introduction

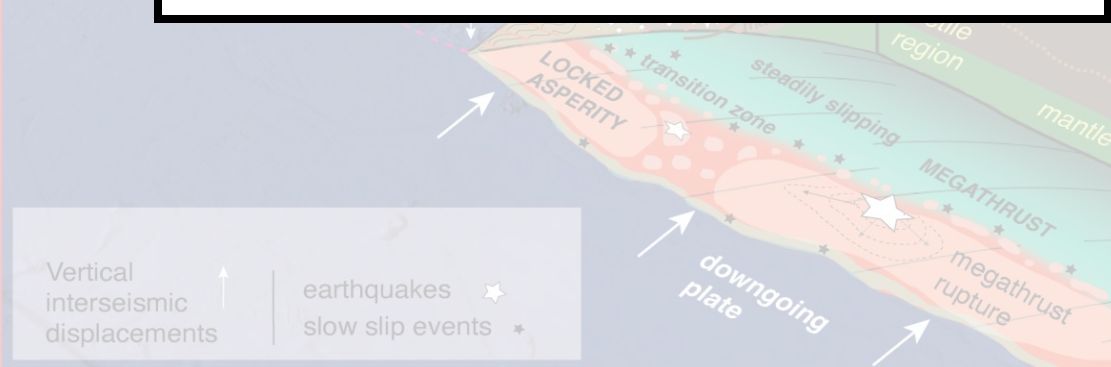
Fingerprints of Megathrust Locking in Subduction Landscapes

Inferring Tectonic Uplift from Bayesian Inversion of Landscapes

Future Research

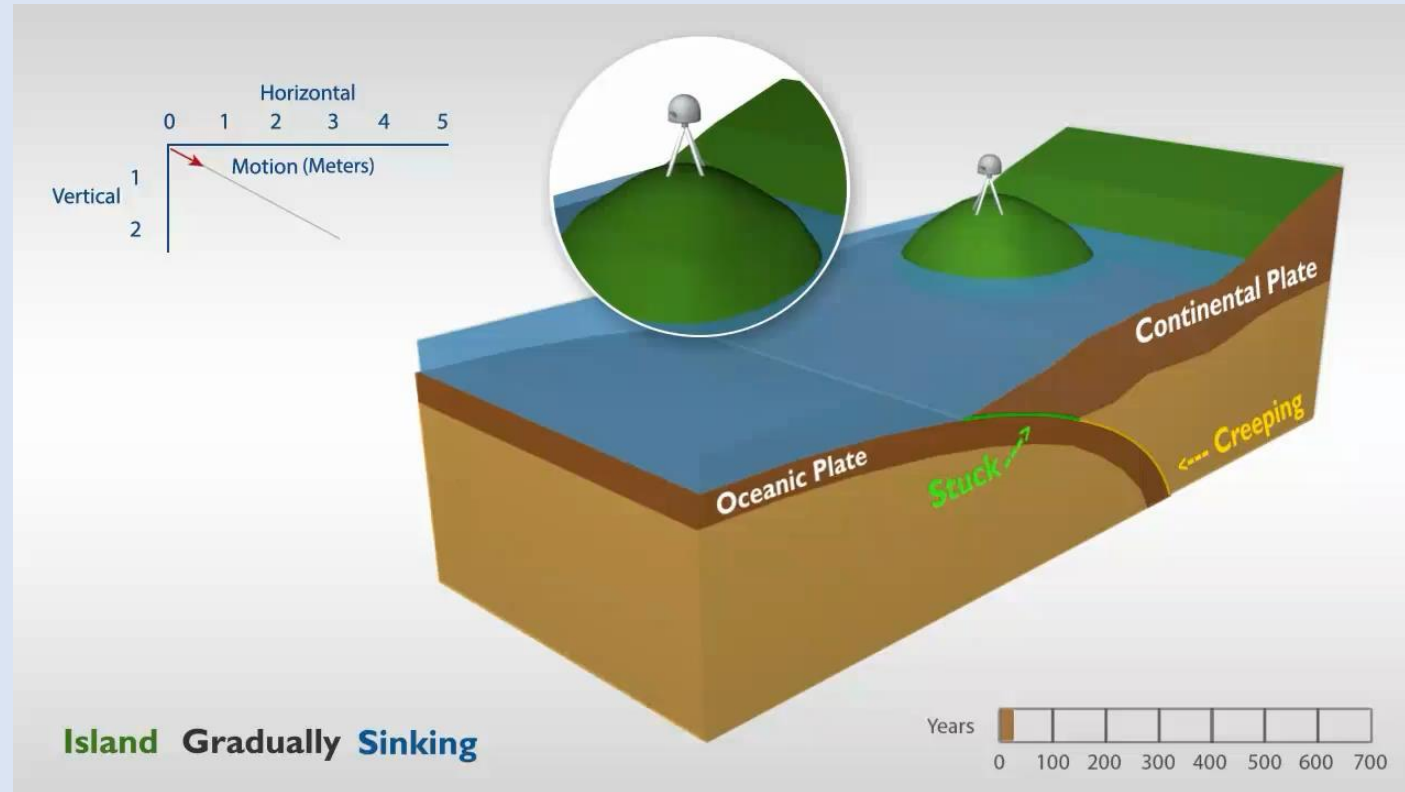


Scan me for slides and references.



Marine terrace

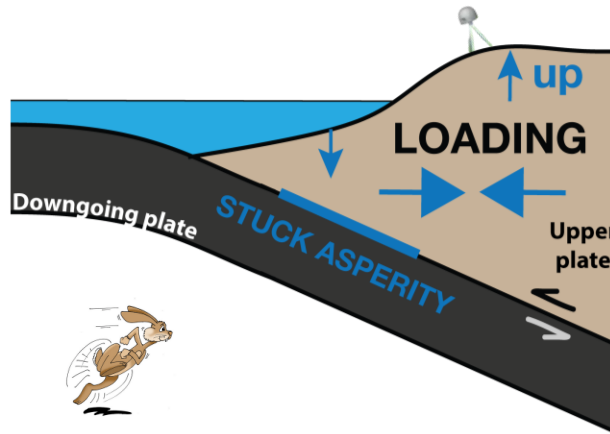
Section 1 - Introduction



EARTHQUAKE CYCLES IN SUBDUCTION ZONES

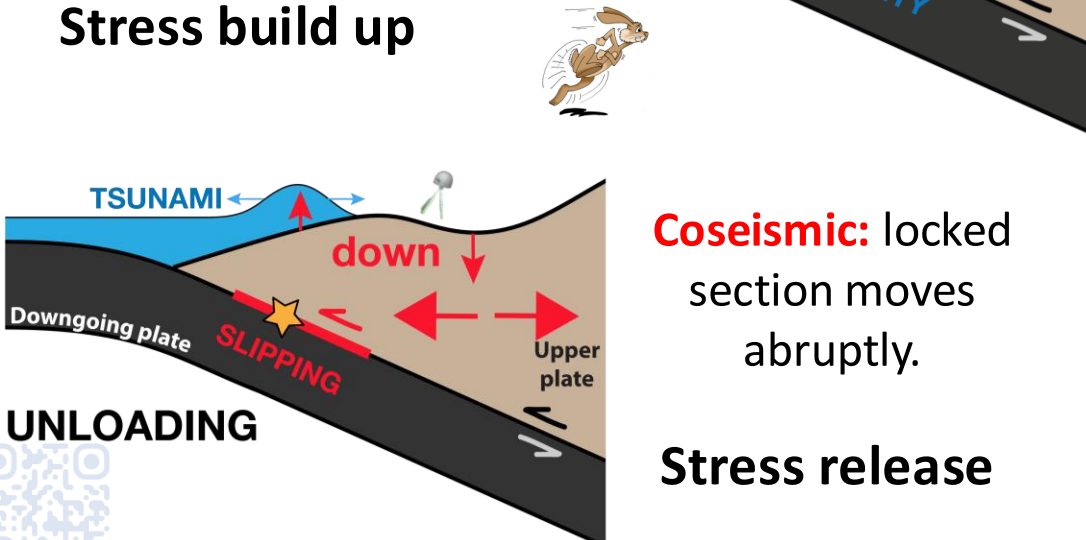


Long-term: downgoing plate descends beneath the upper plate in stick-slip fashion.



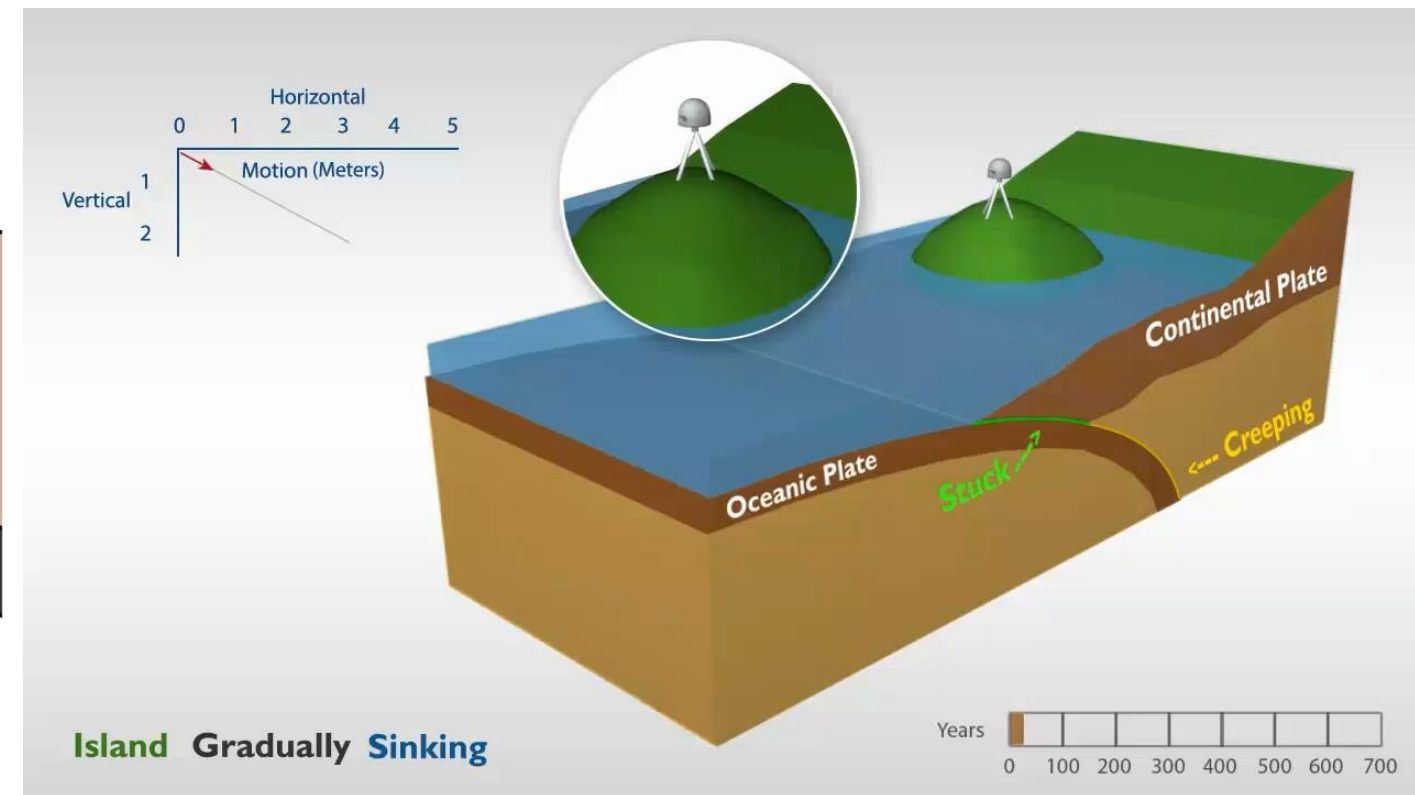
Interseismic: locked section is “stuck”. Creeping section moves slowly.

Stress build up



Coseismic: locked section moves abruptly.

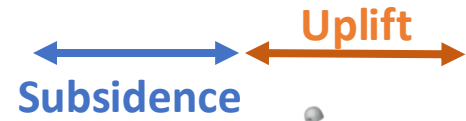
Stress release



EARTHQUAKE CYCLES IN SUBDUCTION ZONES



Long-term: downgoing plate descends beneath the upper plate in stick-slip fashion.



Subsidence

Uplift

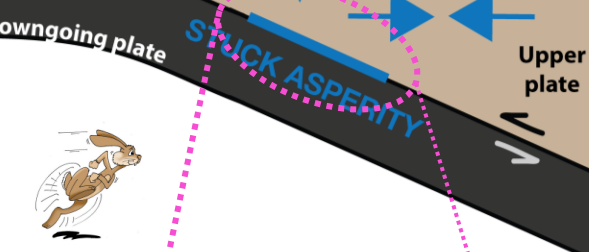
LOADING

up

Dowgoing plate

Stuck Asperity

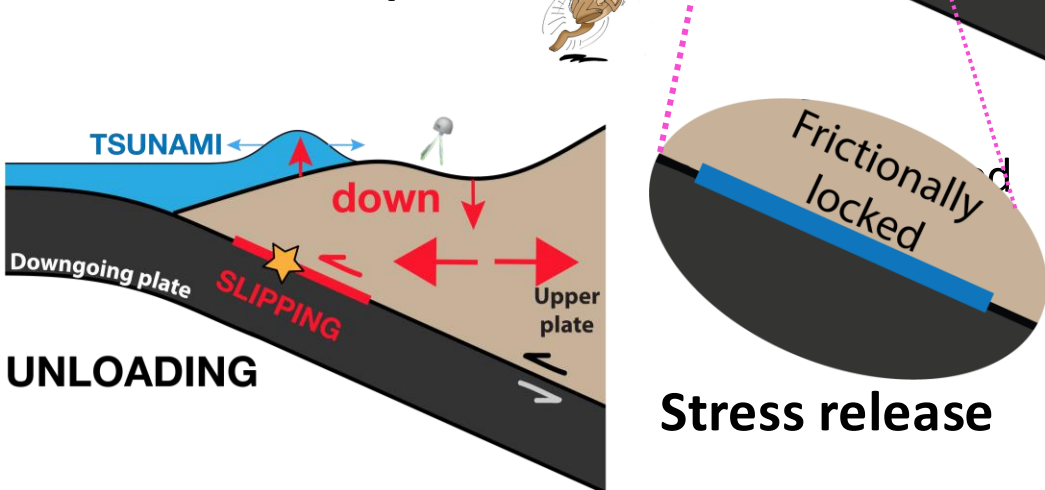
Upper plate



Interseismic: locked section is “stuck”.

Creeping section moves slowly.

Stress build up



TSUNAMI

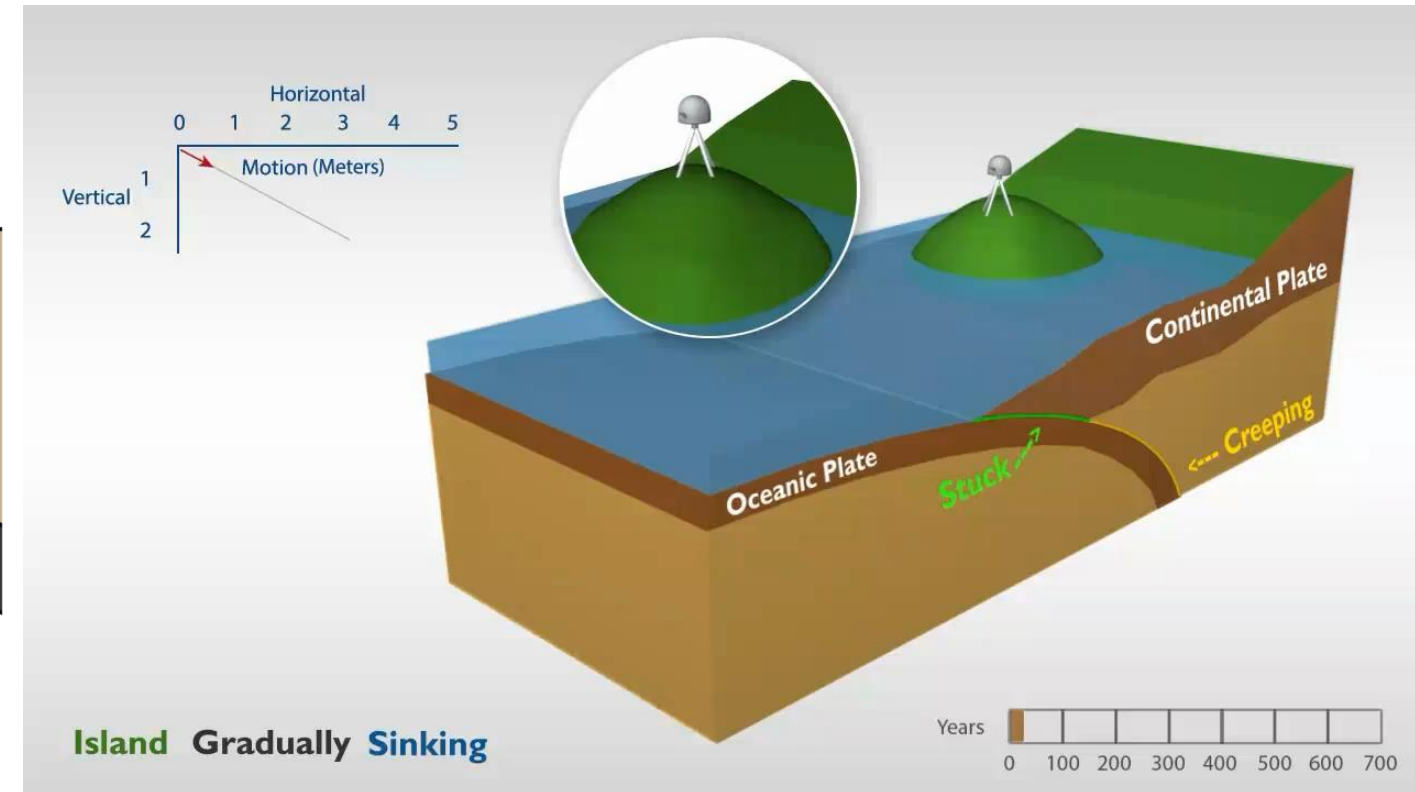
down

Frictionally locked

UNLOADING

SLIPPING

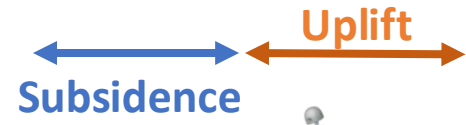
Stress release



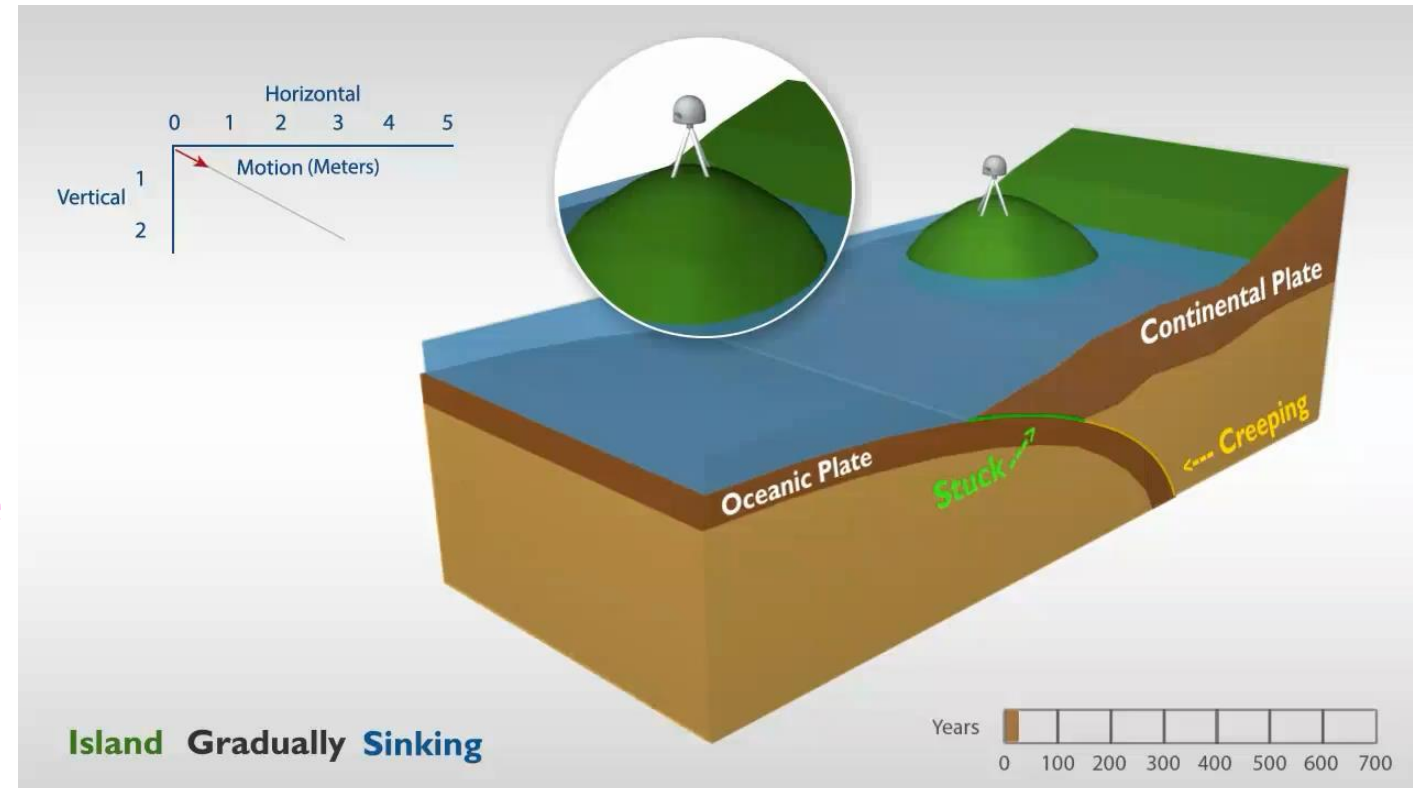
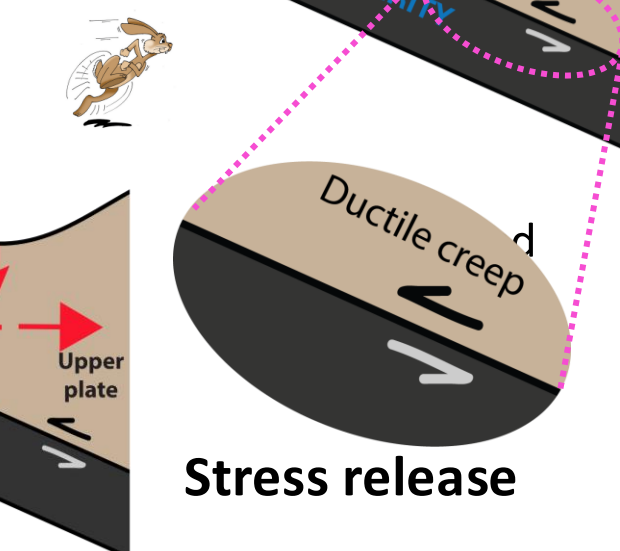
EARTHQUAKE CYCLES IN SUBDUCTION ZONES



Long-term: downgoing plate descends beneath the upper plate in stick-slip fashion.



Interseismic: locked section is “stuck”. Creeping section moves slowly.

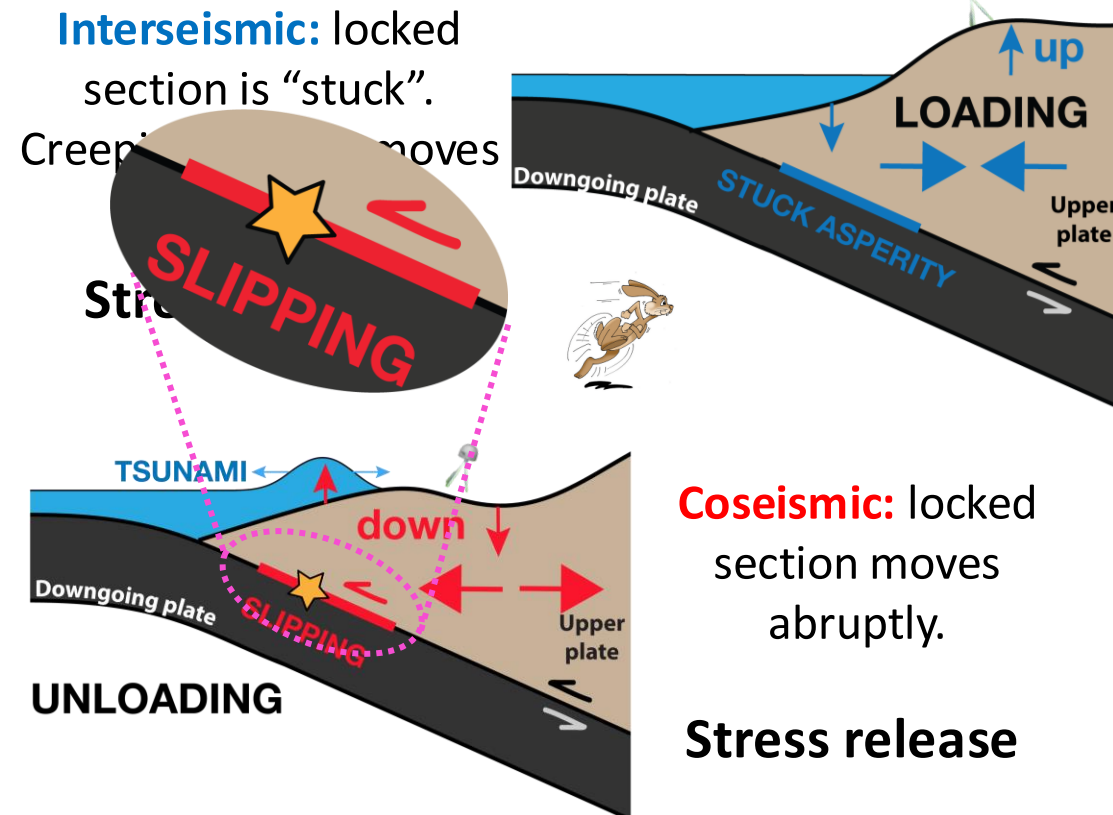


UNLOADING

EARTHQUAKE CYCLES IN SUBDUCTION ZONES



Long-term: downgoing plate descends beneath the upper plate in stick-slip fashion.

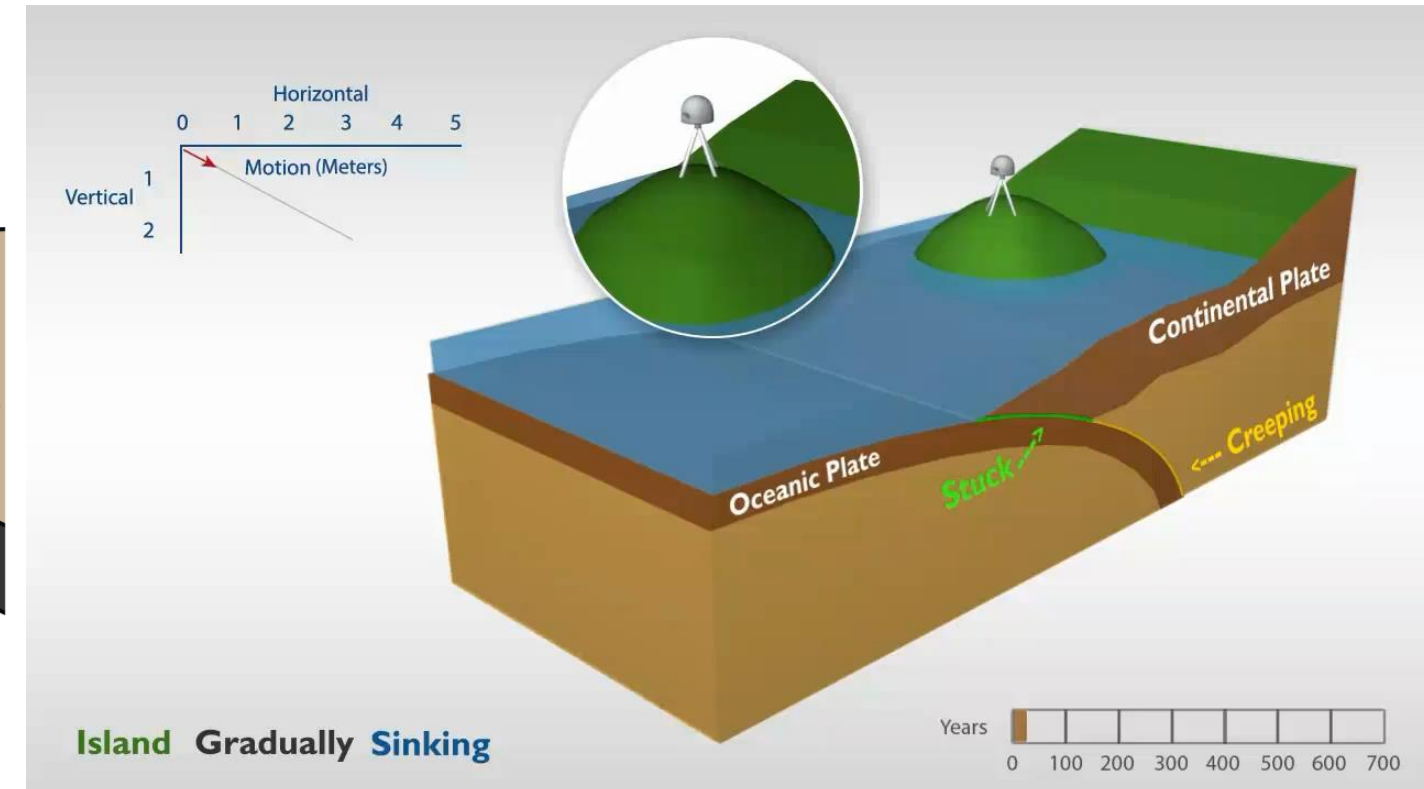


Interseismic: locked section is "stuck".

Creep: plate moves

Coseismic: locked section moves abruptly.

Stress release

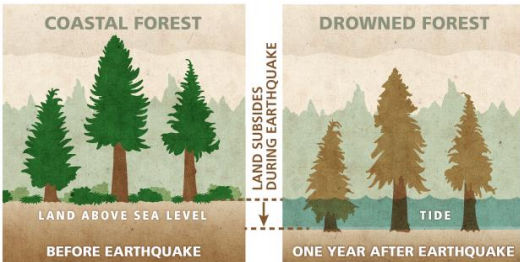


EARTHQUAKE CYCLES IN SUBDUCTION ZONES

long-term subsidence

Cascadia January 26th 1700 megathrust earthquake killed forests along the coast

Coseismic

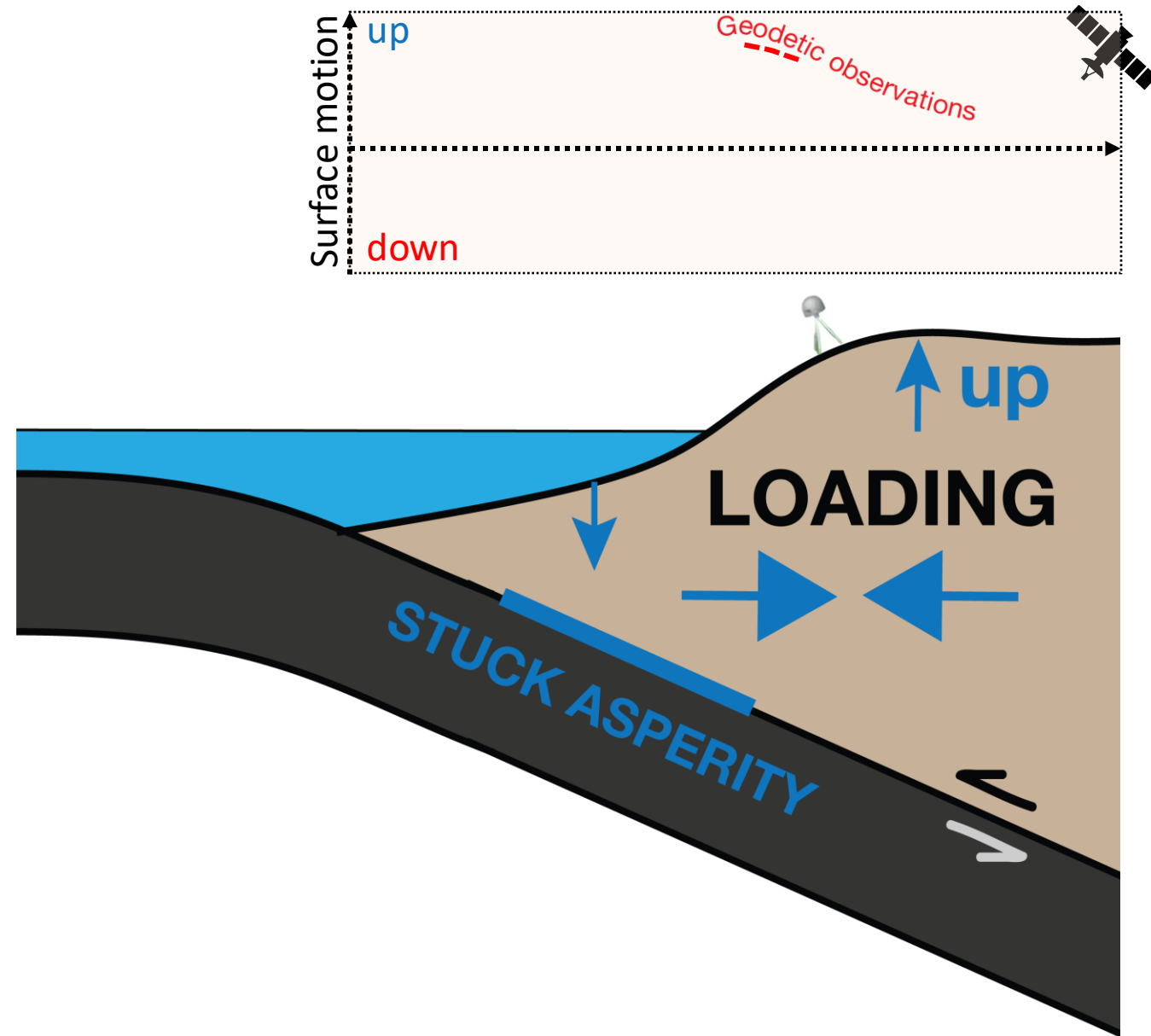


Interseismic



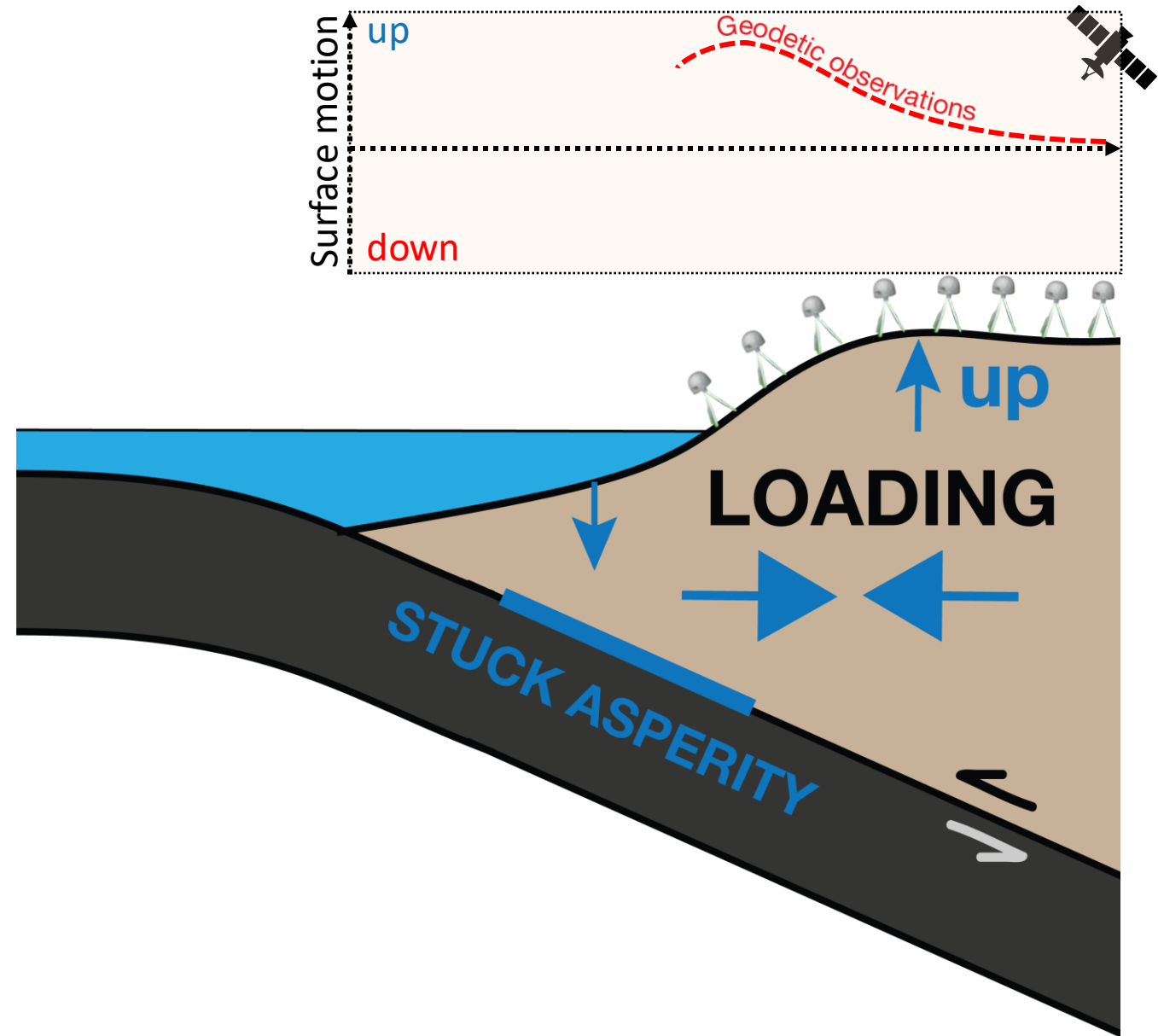
CONSTRAINING MEGATHRUST HAZARD IN SUBDUCTION ZONES

- Deployment of GNSS stations and InSAR data collection have greatly **improved** the **availability** of geodetic data in recent decades.



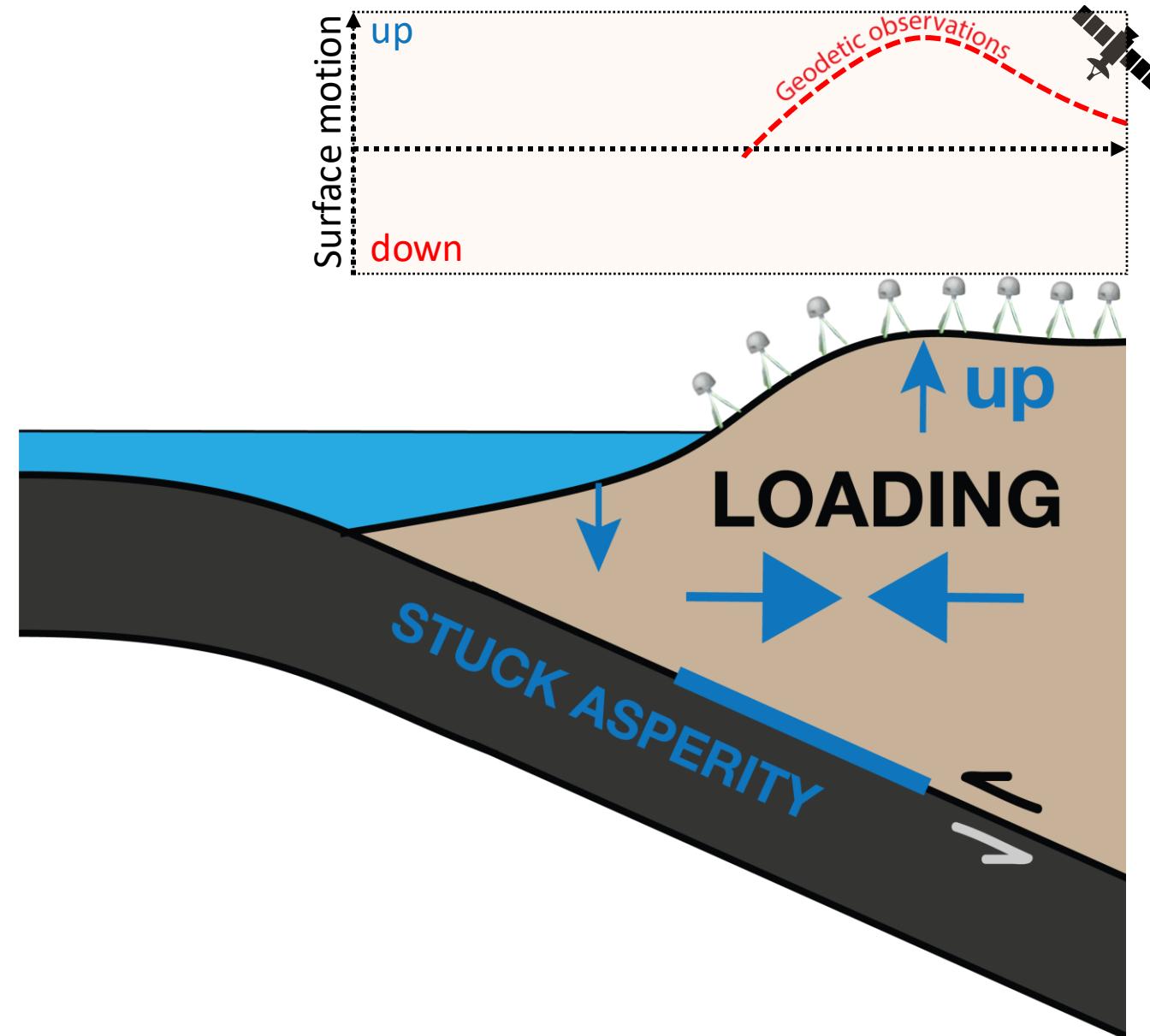
CONSTRAINING MEGATHRUST HAZARD IN SUBDUCTION ZONES

- Deployment of GNSS stations and InSAR data collection have greatly **improved** the **availability** of geodetic data in recent decades.



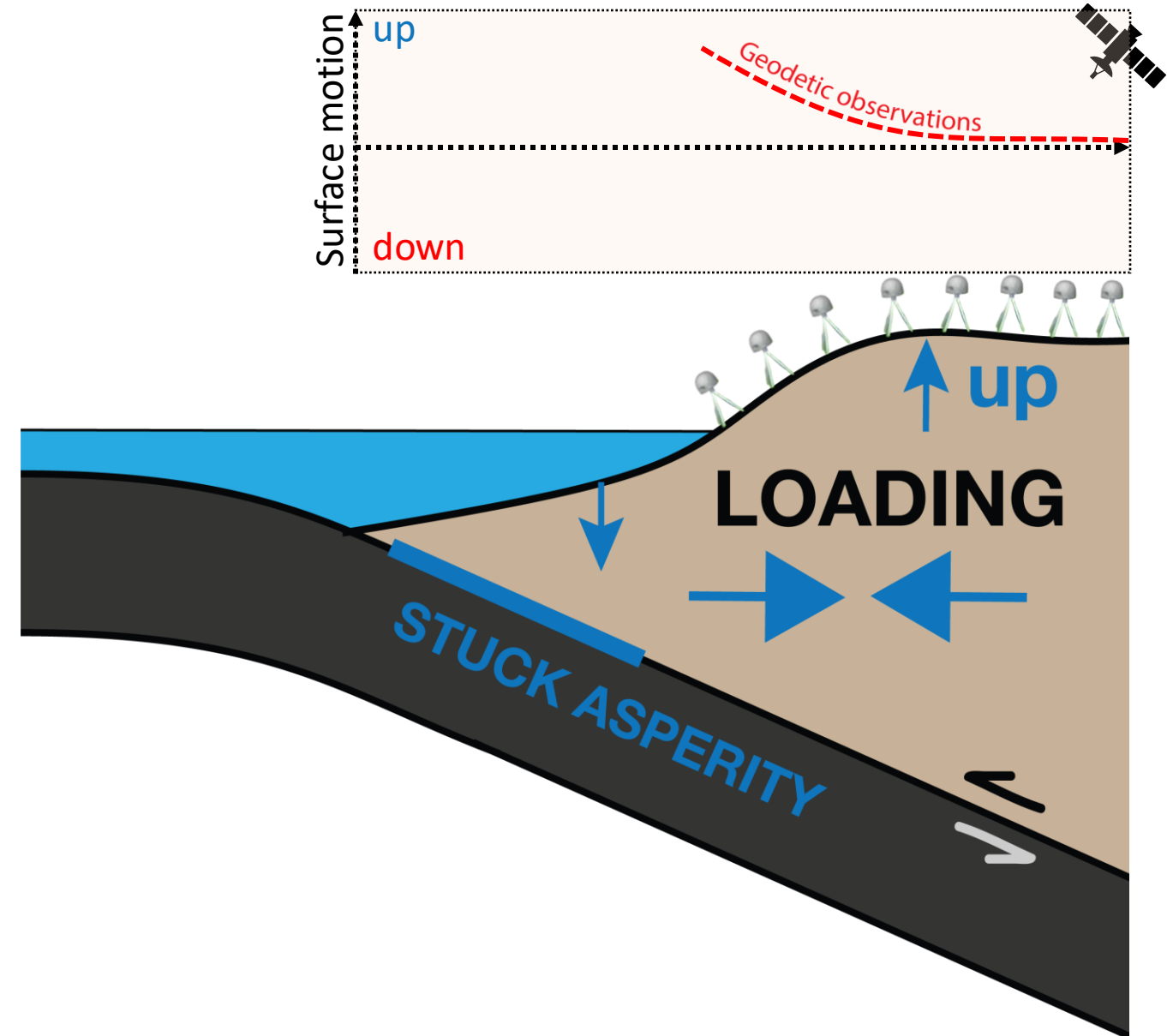
CONSTRAINING MEGATHRUST HAZARD IN SUBDUCTION ZONES

- Deployment of GNSS stations and InSAR data collection have greatly **improved** the **availability** of geodetic data in recent decades.
- It allows to determine the **dimensions and position of locked asperities** in subduction zones with well constrained megathrust geometry.



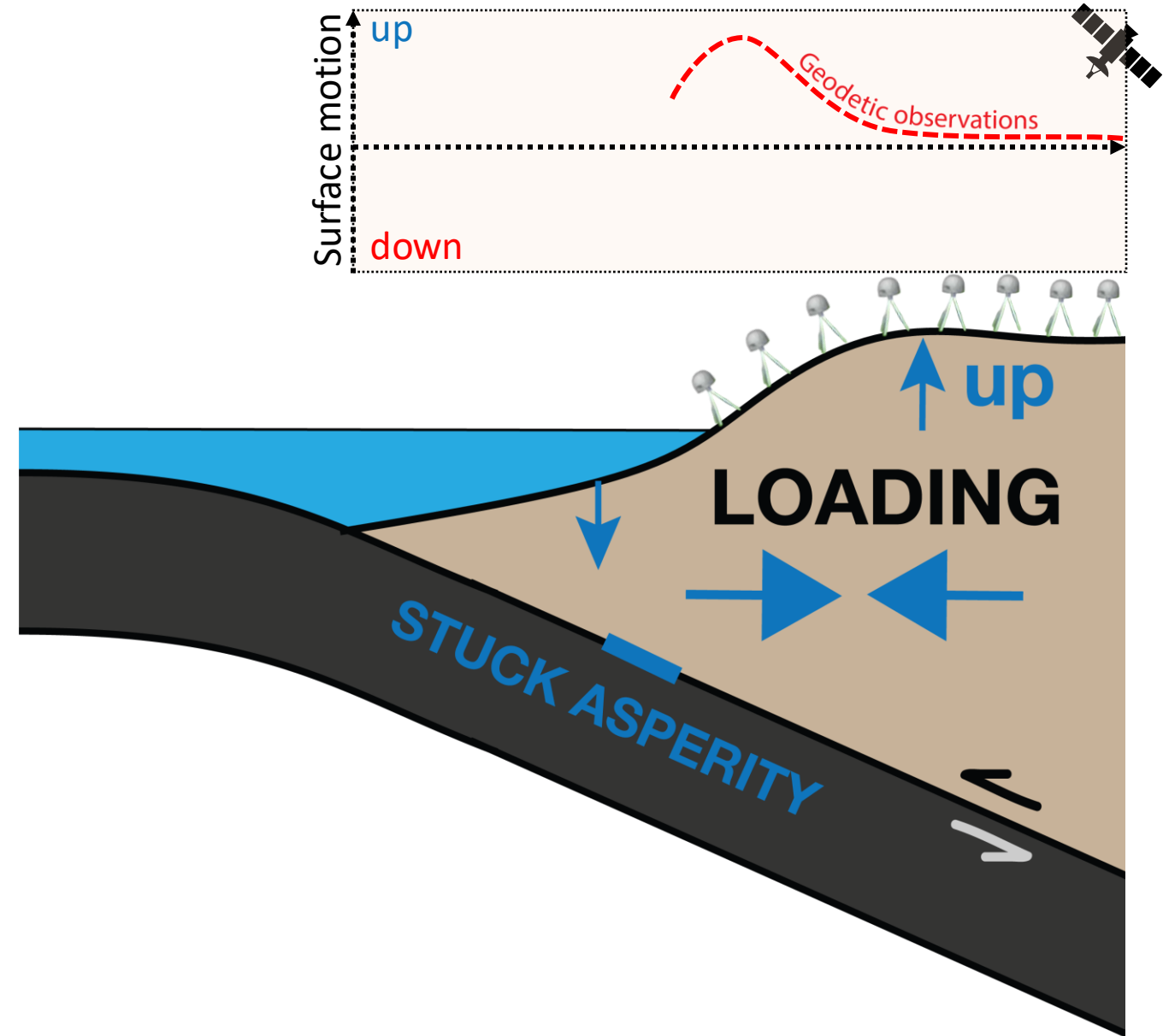
CONSTRAINING MEGATHRUST HAZARD IN SUBDUCTION ZONES

- Deployment of GNSS stations and InSAR data collection have greatly **improved** the **availability** of geodetic data in recent decades.
- It allows to determine the **dimensions and position of locked asperities** in subduction zones with well constrained megathrust geometry.



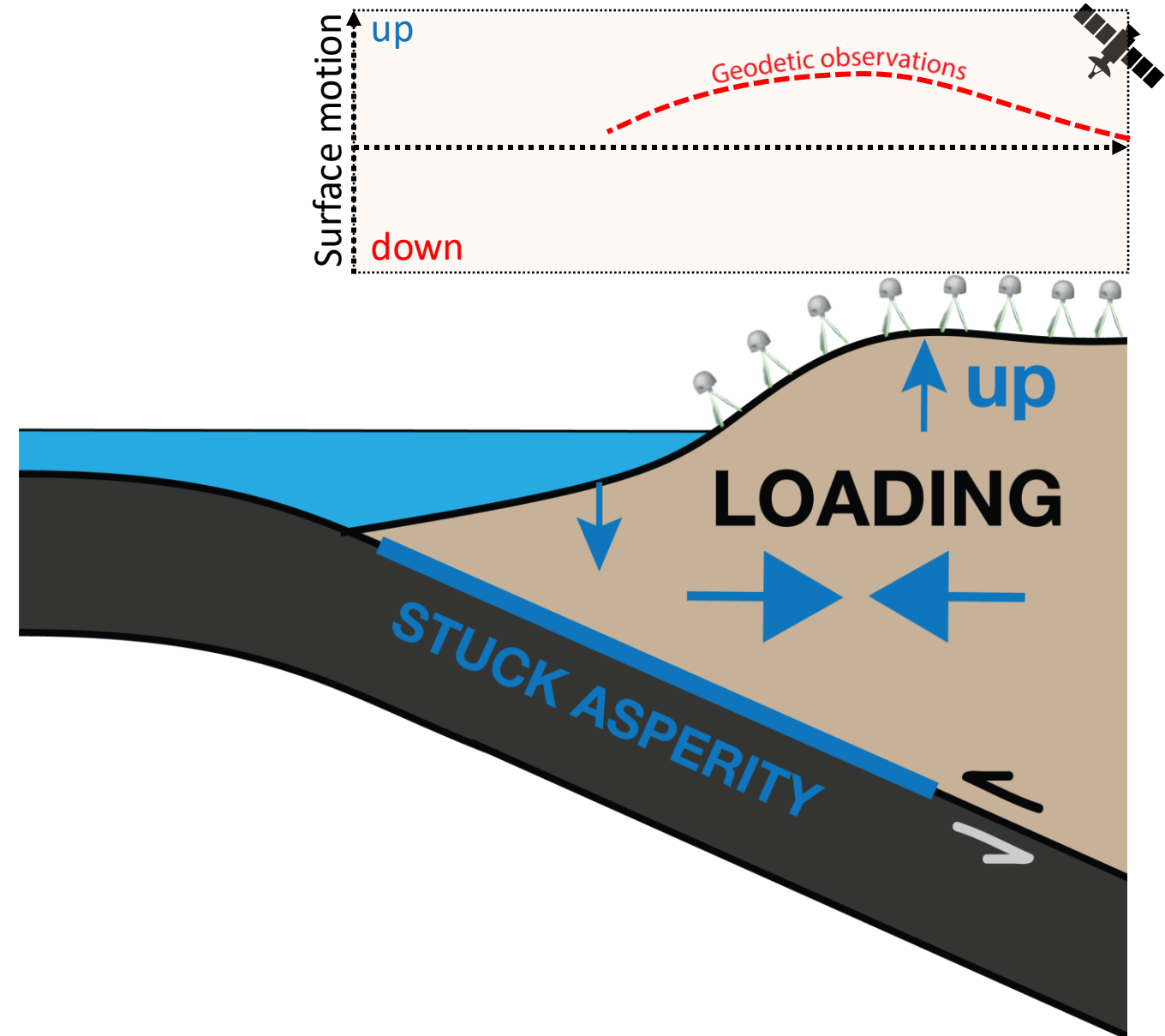
CONSTRAINING MEGATHRUST HAZARD IN SUBDUCTION ZONES

- Deployment of GNSS stations and InSAR data collection have greatly **improved** the **availability** of geodetic data in recent decades.
- It allows to determine the **dimensions and position of locked asperities** in subduction zones with well constrained megathrust geometry.



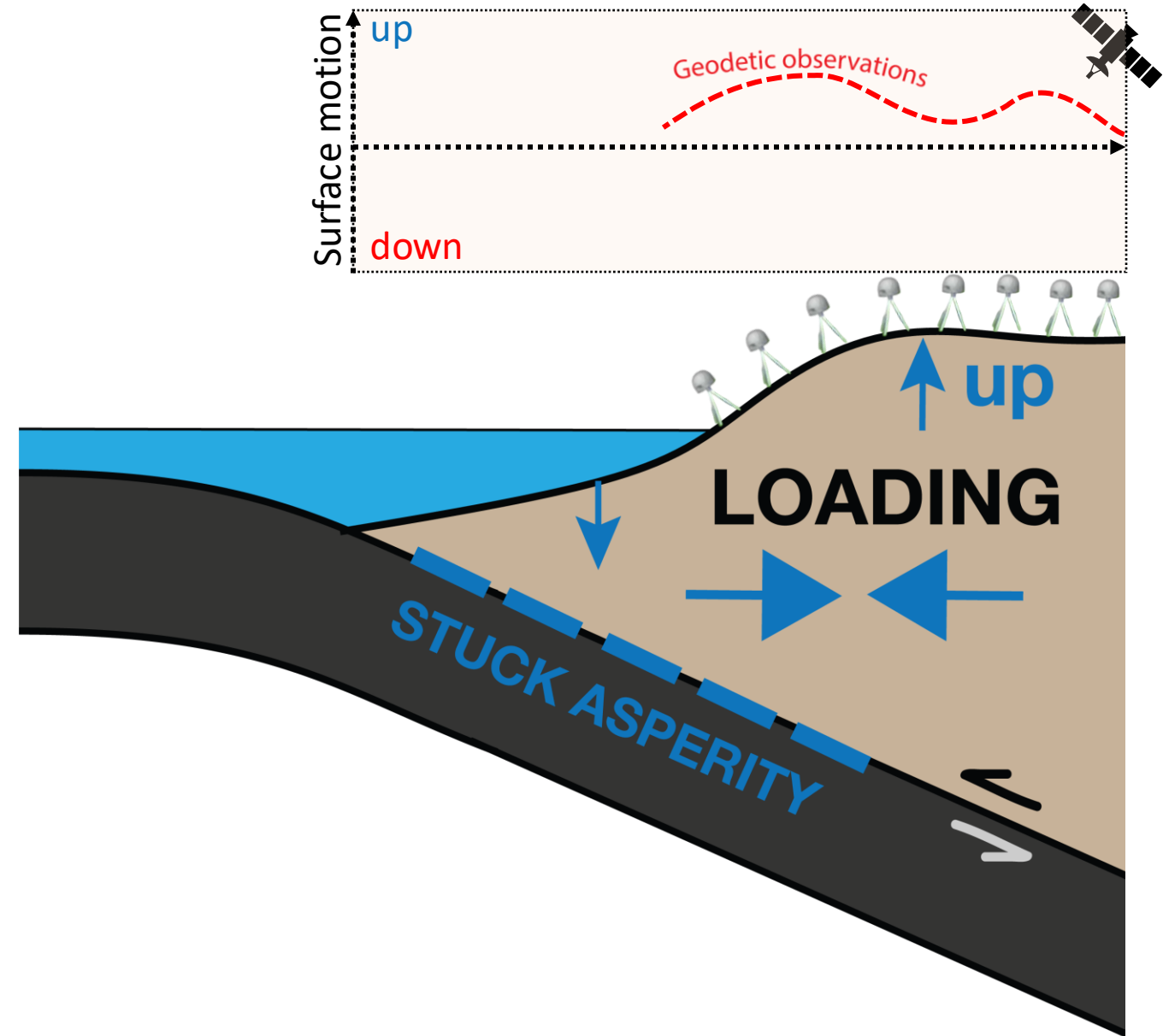
CONSTRAINING MEGATHRUST HAZARD IN SUBDUCTION ZONES

- Deployment of GNSS stations and InSAR data collection have greatly **improved** the **availability** of geodetic data in recent decades.
- It allows to determine the **dimensions and position of locked asperities** in subduction zones with well constrained megathrust geometry.



CONSTRAINING MEGATHRUST HAZARD IN SUBDUCTION ZONES

- Deployment of GNSS stations and InSAR data collection have greatly **improved** the **availability** of geodetic data in recent decades.
- It allows to determine the **dimensions and position of locked asperities** in subduction zones with well constrained megathrust geometry.

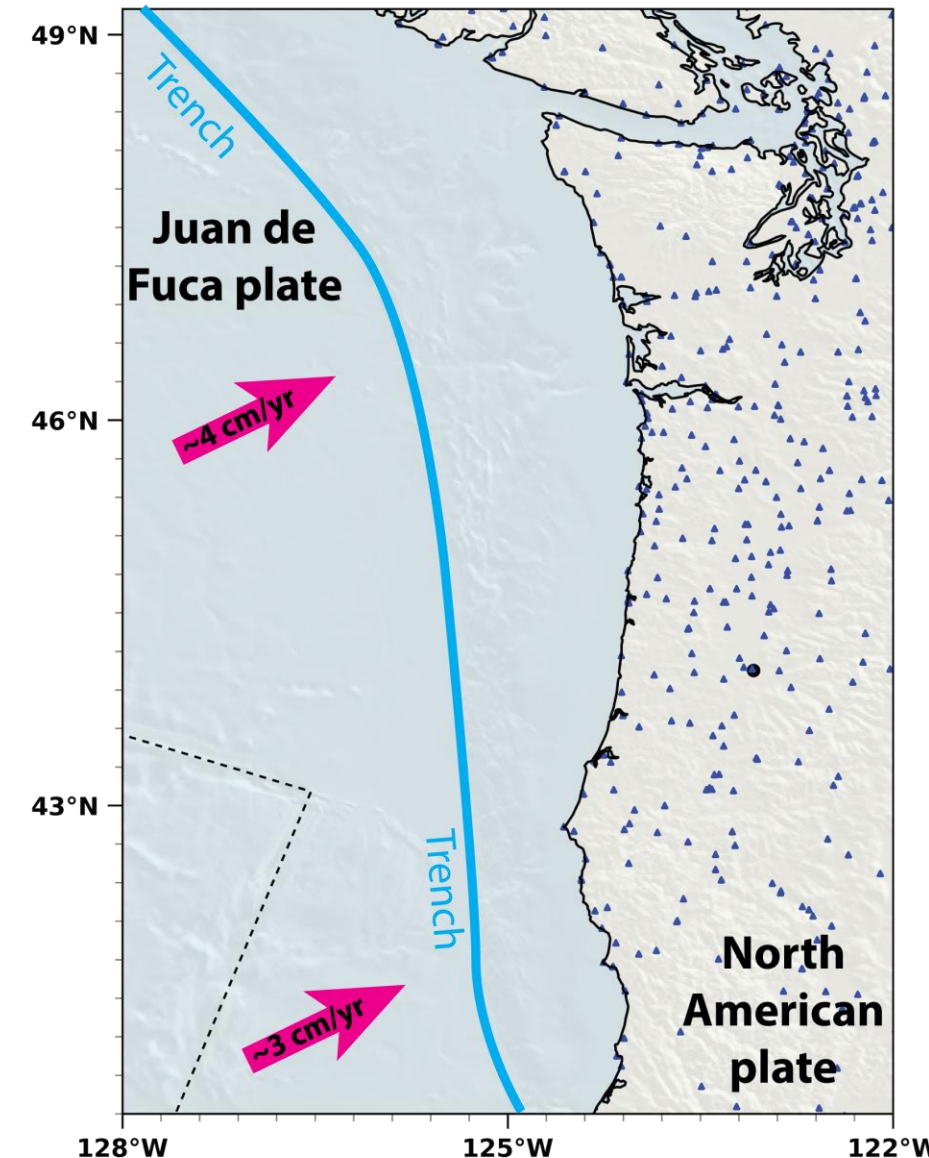


CONSTRAINING MEGATHRUST HAZARD IN SUBDUCTION ZONES

- Deployment of GNSS stations and InSAR data collection have greatly **improved** the **availability of geodetic data** in recent decades.
- It allows to determine the **dimensions and position of locked asperities** in subduction zones with well constrained megathrust geometry.

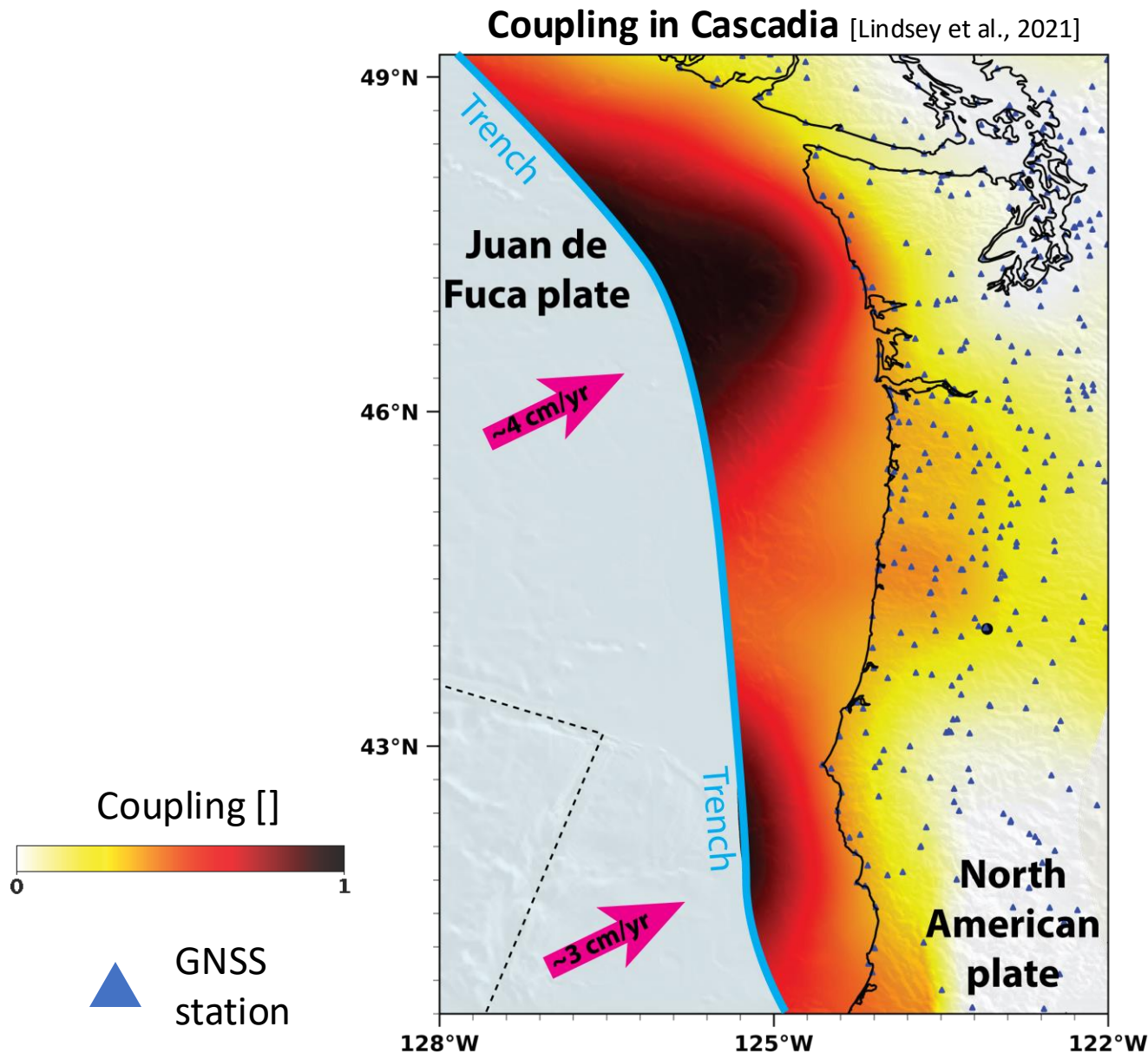


GNSS
station



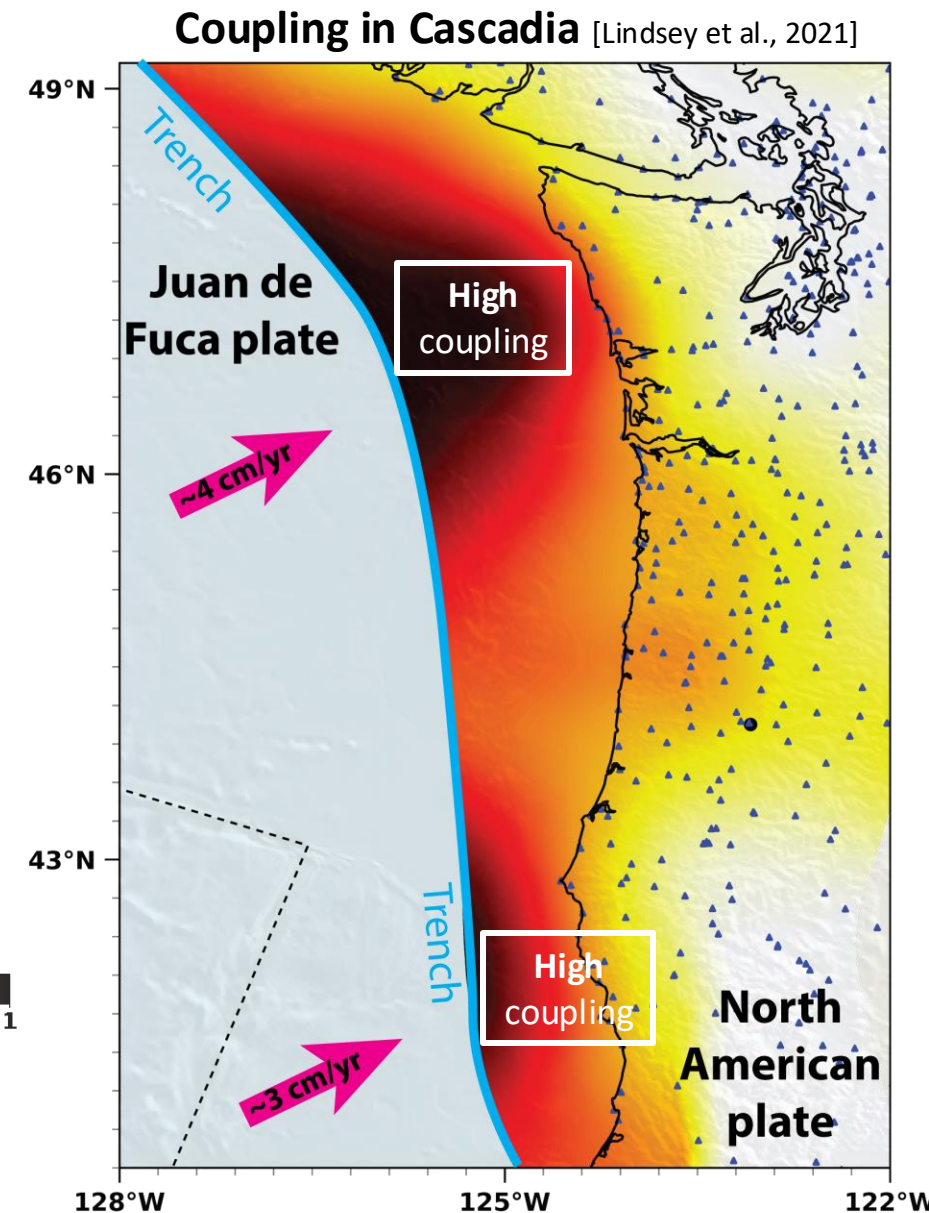
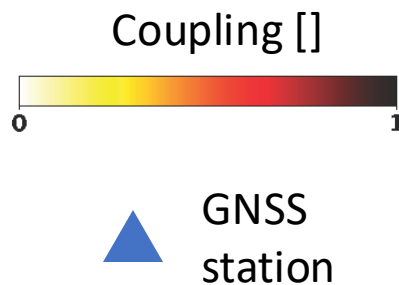
CONSTRAINING MEGATHRUST HAZARD IN SUBDUCTION ZONES

- Locked asperities along the megathrust are often represented using coupling maps.



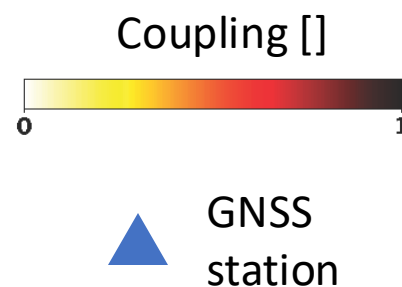
CONSTRAINING MEGATHRUST HAZARD IN SUBDUCTION ZONES

- Locked asperities are often represented using coupling maps.
- Regions with high coupling values are considered locked and stationary.

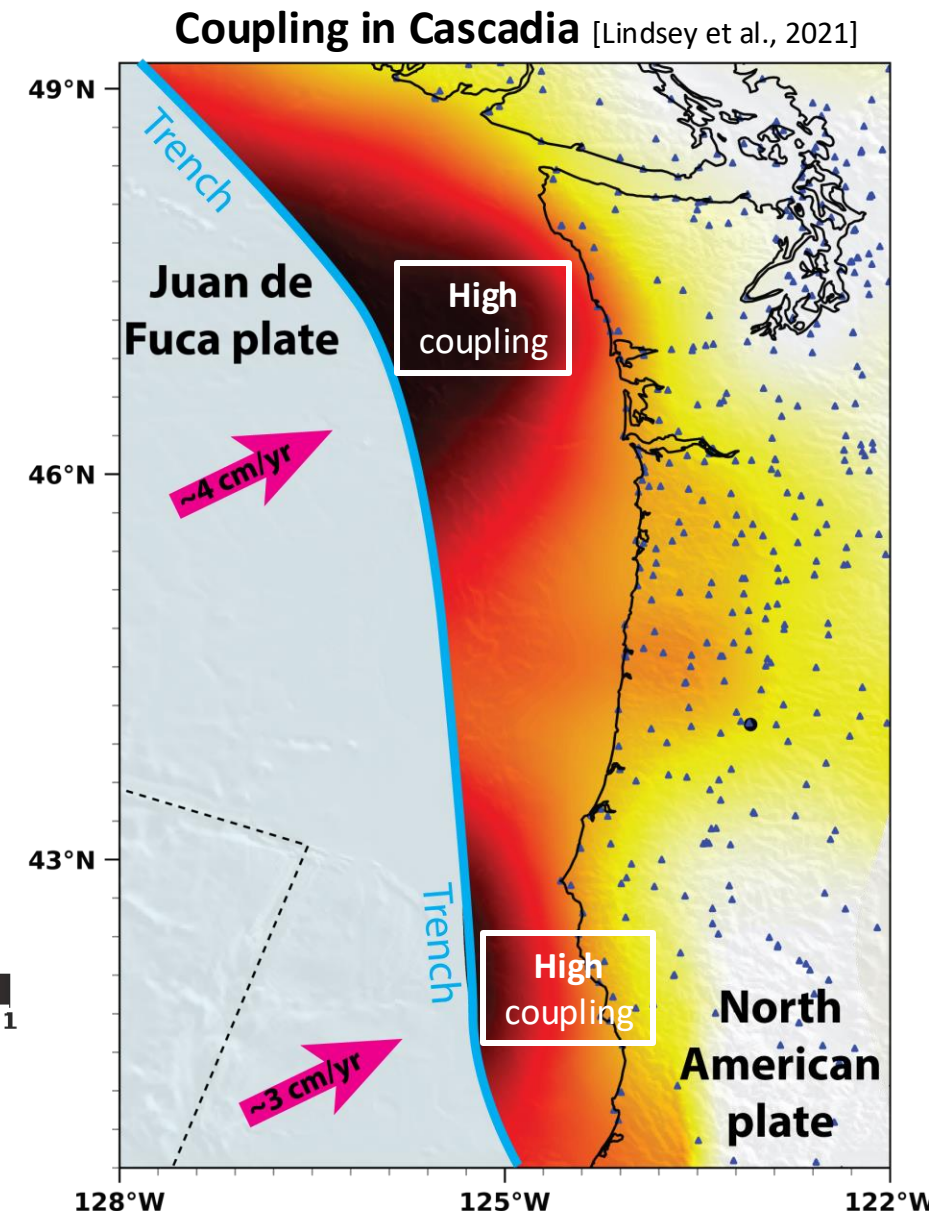


CONSTRAINING MEGATHRUST HAZARD IN SUBDUCTION ZONES

- Locked asperities are often represented using coupling maps.
- Regions with high coupling values are considered locked and stationary.
- These locked regions are believed to accumulate interseismic stresses and are more likely to generate megathrust events.

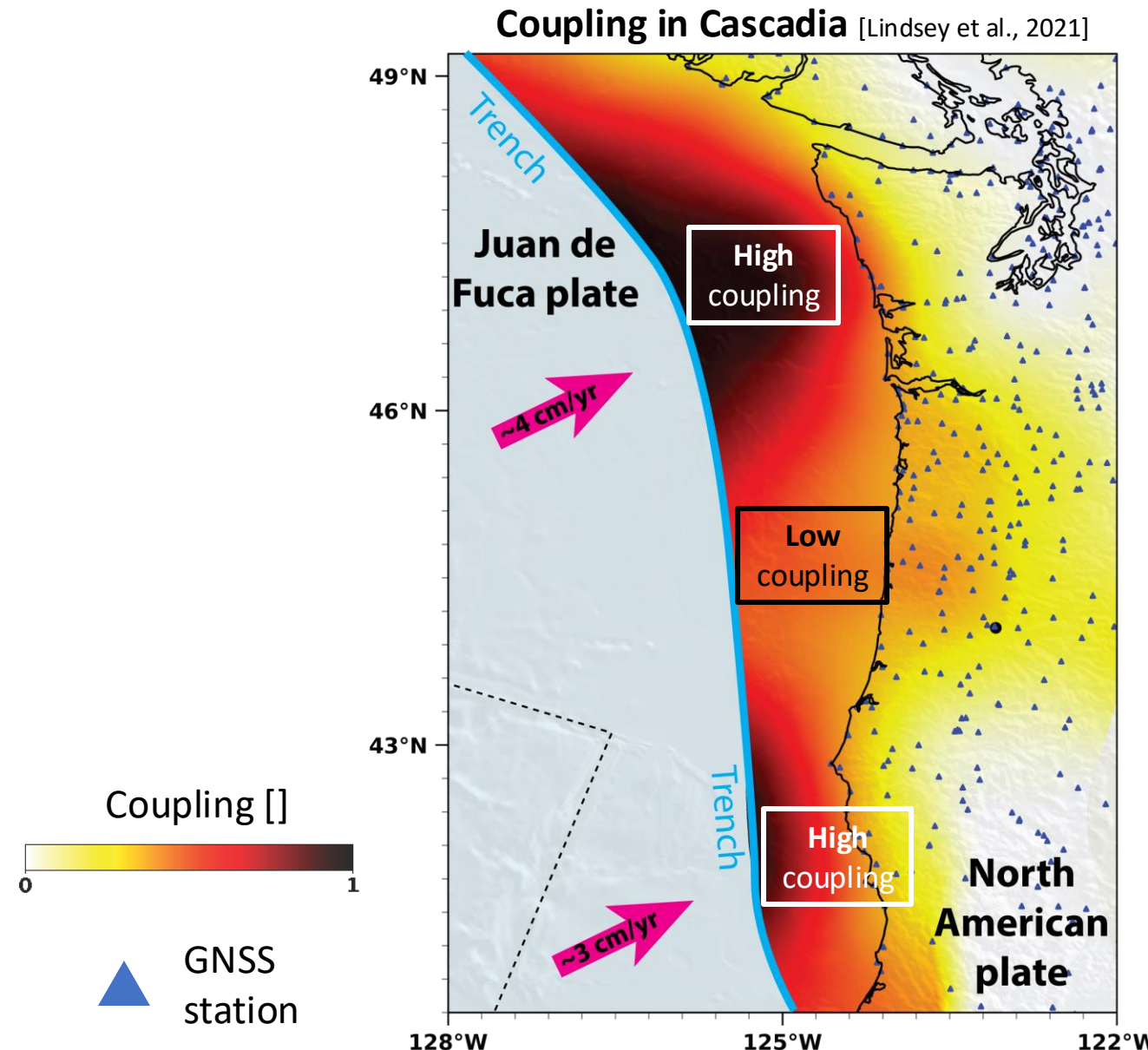


▲ GNSS
station



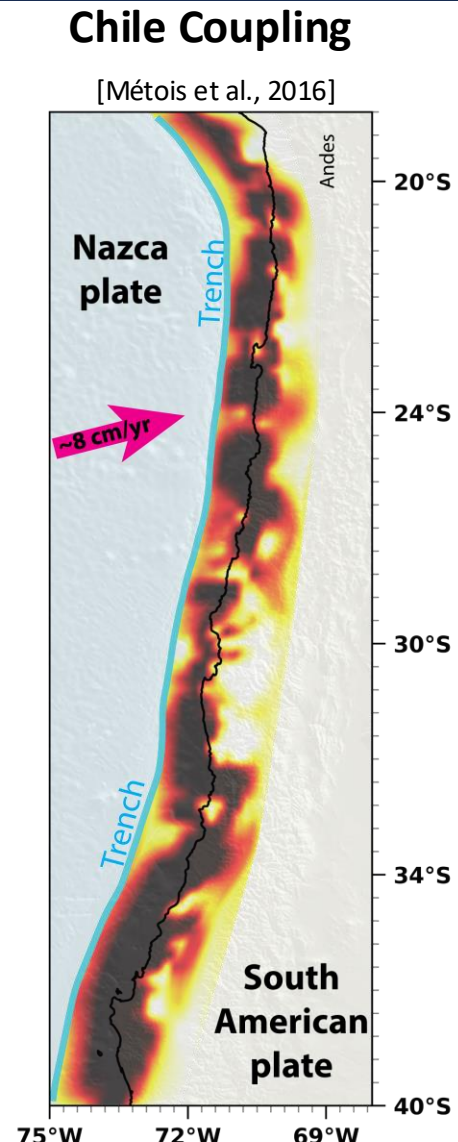
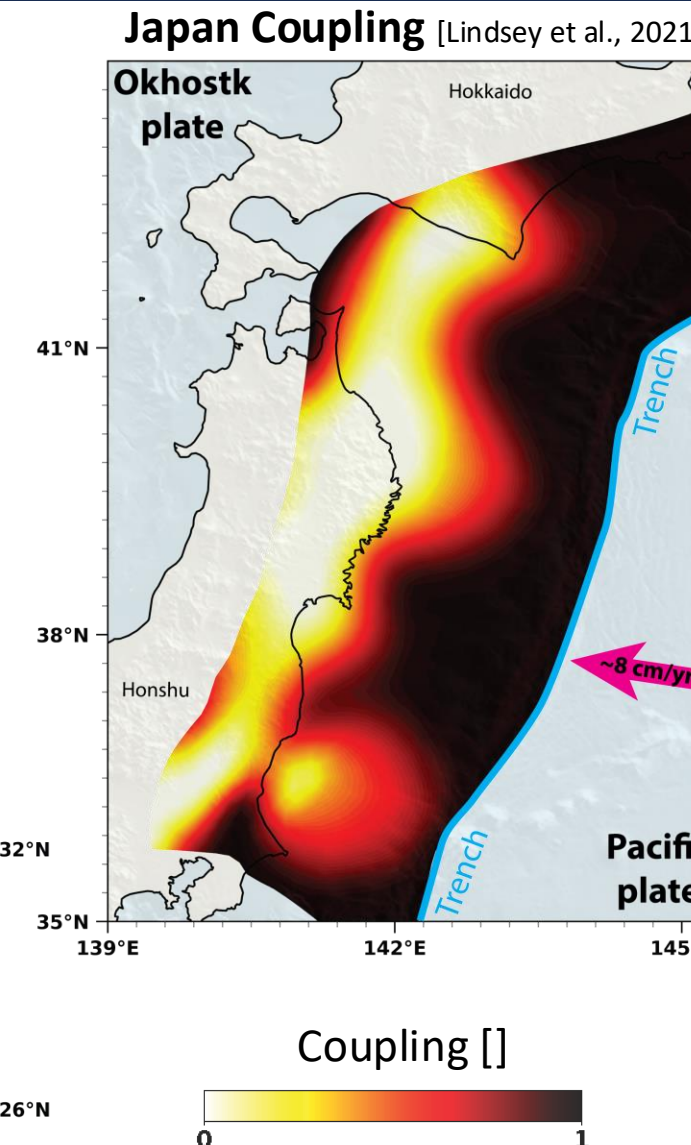
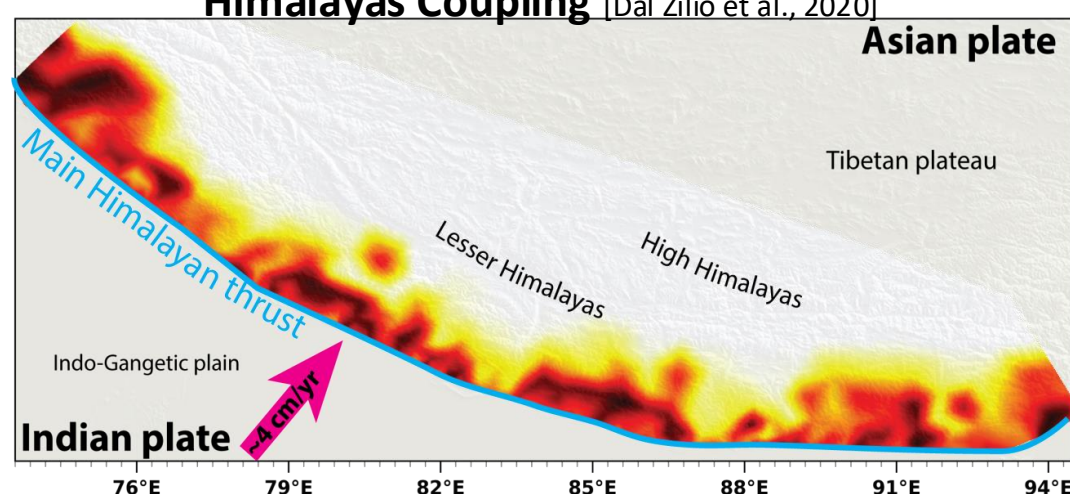
CONSTRAINING MEGATHRUST HAZARD IN SUBDUCTION ZONES

- Locked asperities are often represented using coupling maps.
- Regions with high coupling values are considered locked and stationary.
- These locked regions are believed to accumulate interseismic stress and are more likely to generate megathrust events.
- In contrast, regions with low coupling values are thought to creep during the interseismic period and are less likely to rupture.

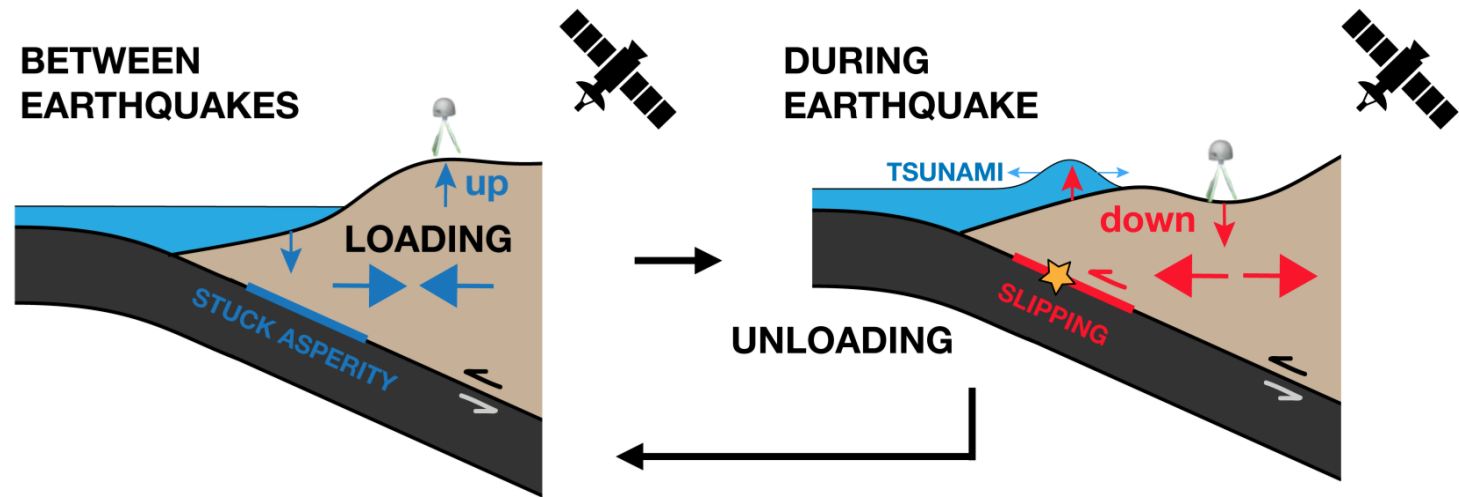
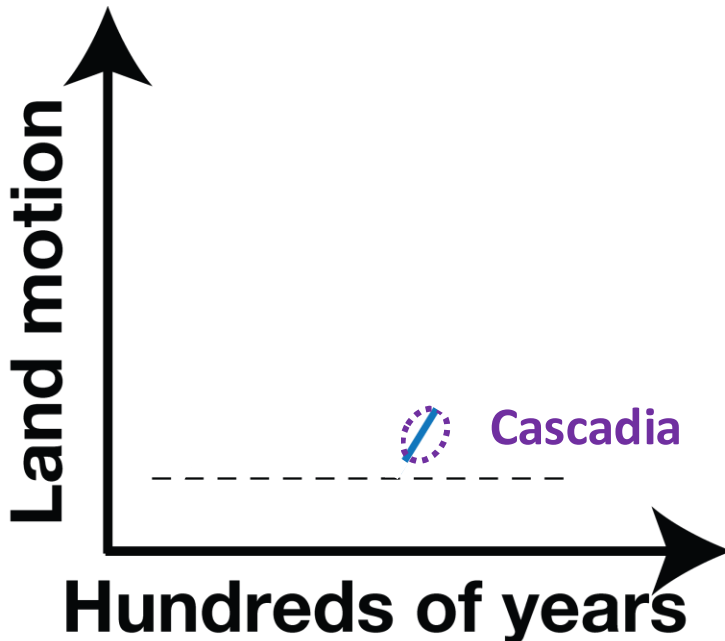


CONSTRAINING MEGATHRUST HAZARD IN SUBDUCTION ZONES

Coupling maps are used to illustrate fault locking variability across **nearly all megathrusts where geodetic data is available.**

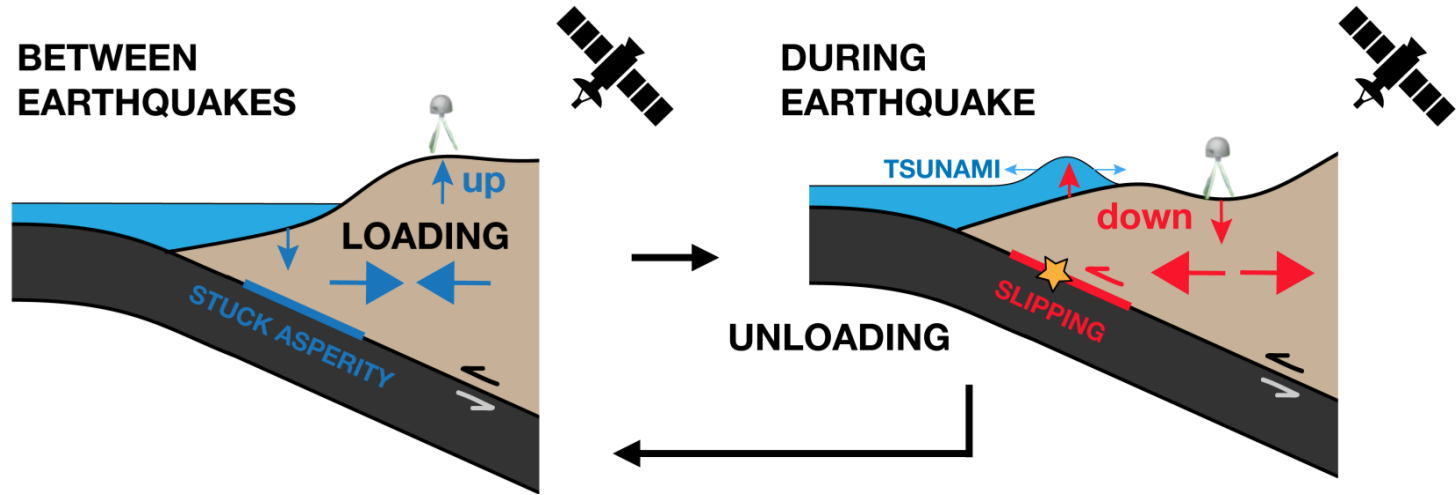
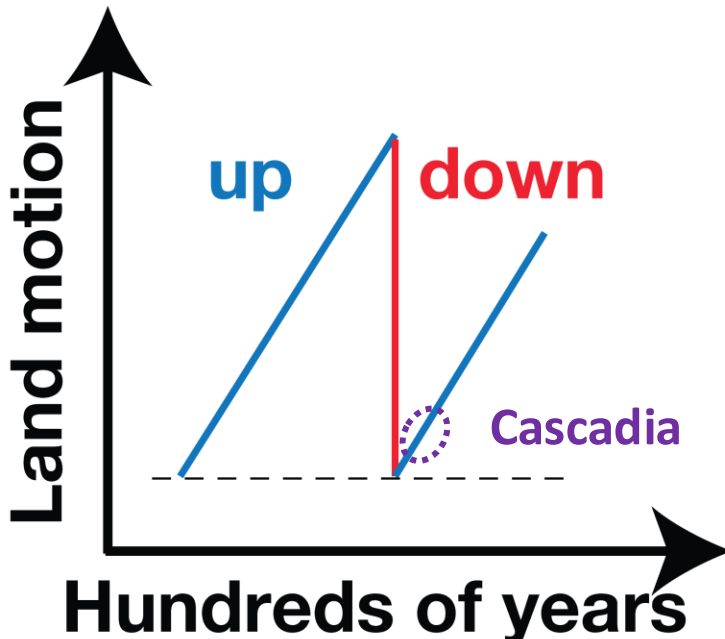


TEMPORAL LIMITATIONS OF GEODETIC DATA COVERAGE



- Geodetic data only captures a **small fraction** of the timescale over which **earthquake cycles operate**.

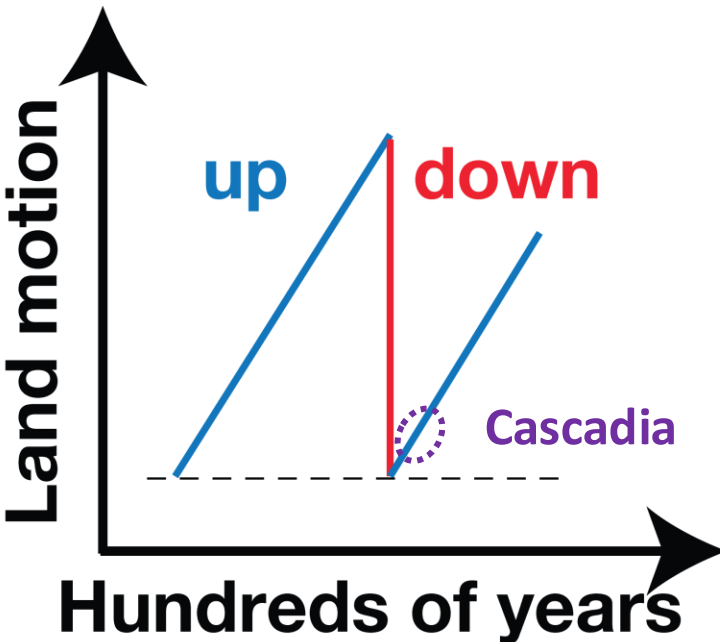
TEMPORAL LIMITATIONS OF GEODETIC DATA COVERAGE



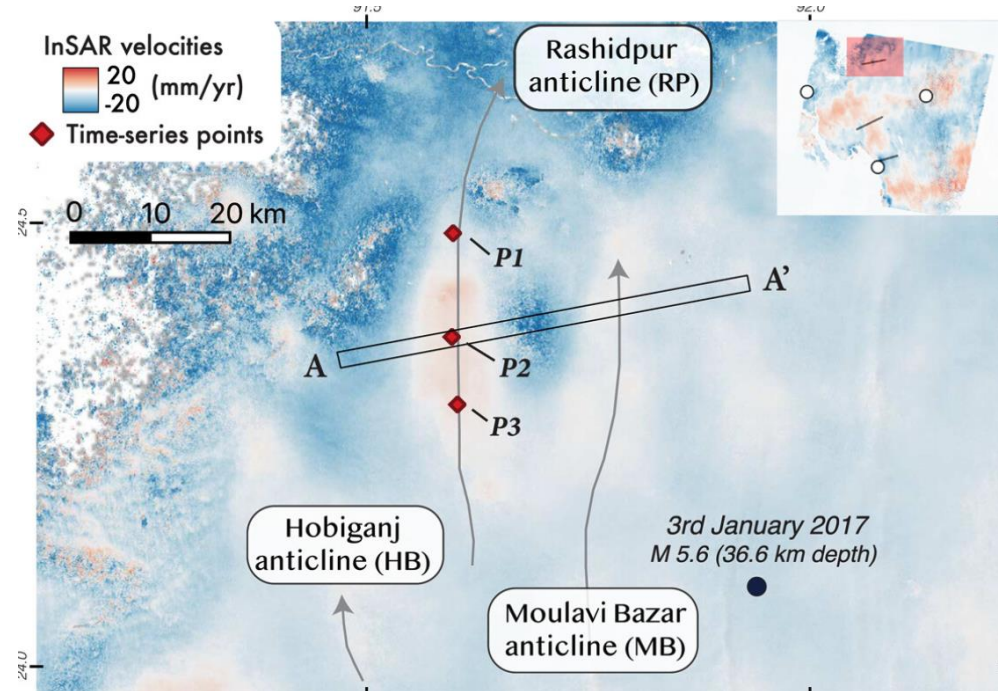
- Geodetic data only captures a **small fraction** of the timescale over which **earthquake cycles operate**.
- The recorded geodetic signal is often **extrapolated** to represent the **entire seismic cycle**.

TEMPORAL LIMITATIONS OF GEODETIC DATA COVERAGE

- Geodetic data captures only a **small fraction** of the timescale over which **earthquake cycles operate**.
- The recorded geodetic signal is often **extrapolated** to represent the **entire seismic cycle**.



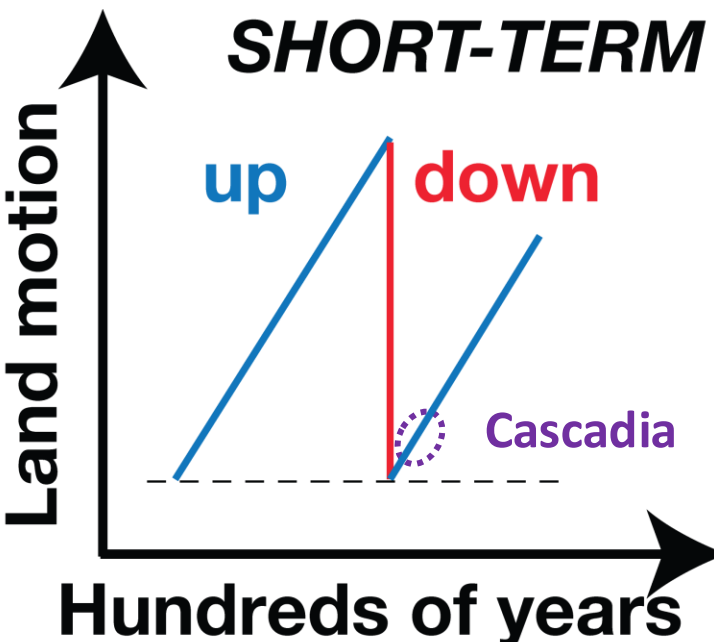
Viscous interseismic uplift of anticlines in the Indo-Burma subduction zone [Chong , Oryan, et al., 2024]



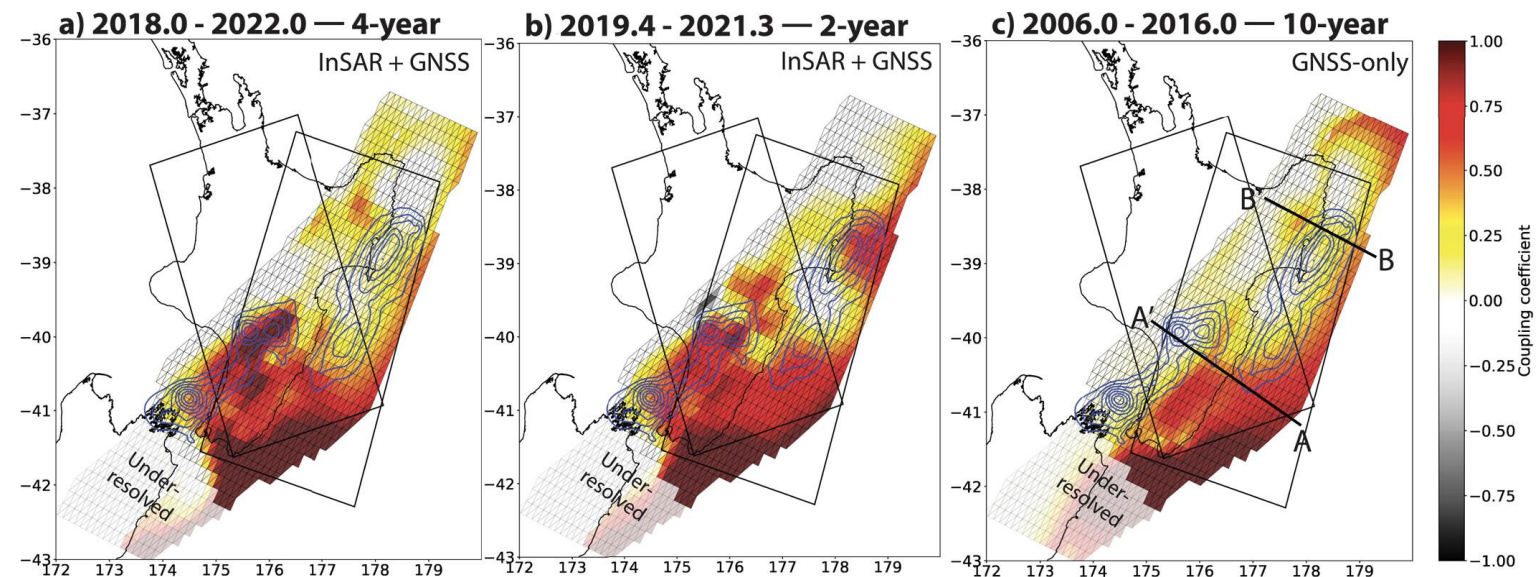
Geodetic observations indicate that the state of **coupling may evolve through time**.

TEMPORAL LIMITATIONS OF GEODETIC DATA COVERAGE

- Geodetic data captures only a **small fraction** of the timescale over which **earthquake cycles operate**.
- The recorded geodetic signal is often **extrapolated** to represent the **entire seismic cycle**.



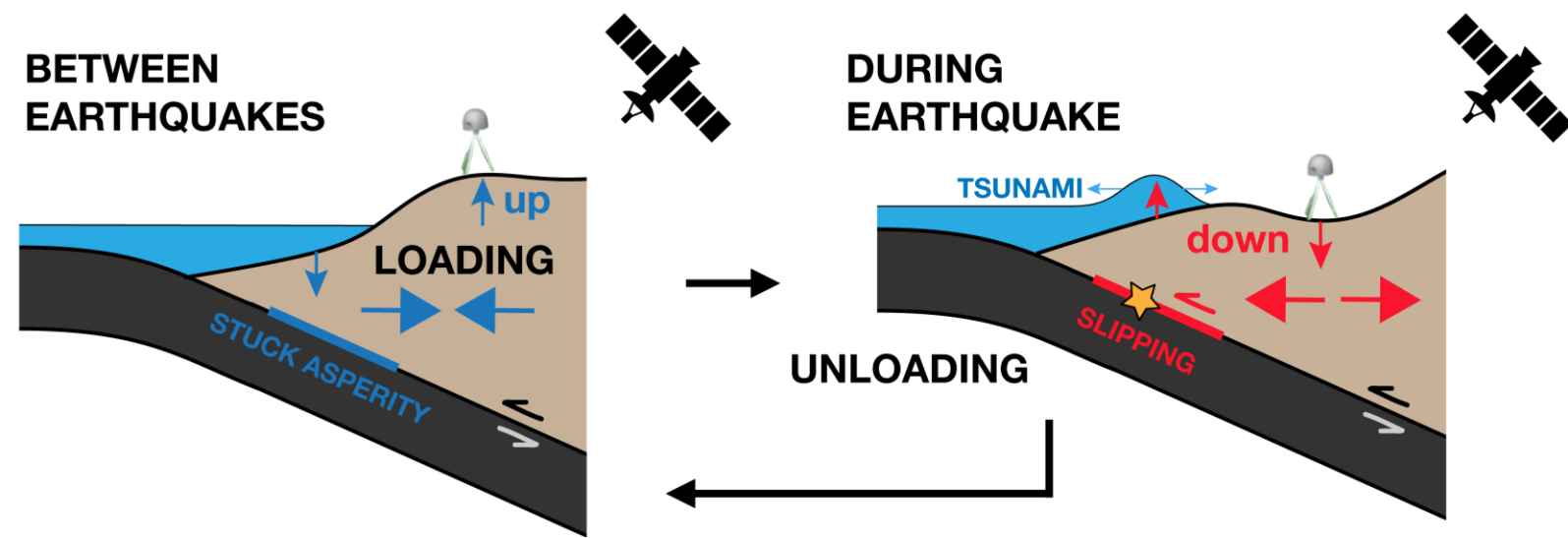
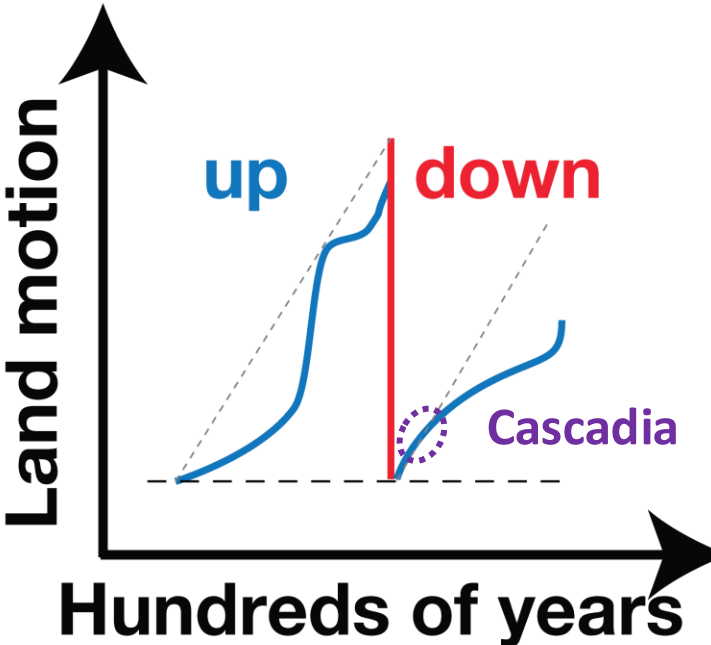
Locking in Hikurangi Subduction Zone variations based on different temporal resolution [Maubant et al., 2023].



Geodetic observations indicate that the state of **coupling may evolve through time**.

TEMPORAL LIMITATIONS OF GEODETIC DATA COVERAGE

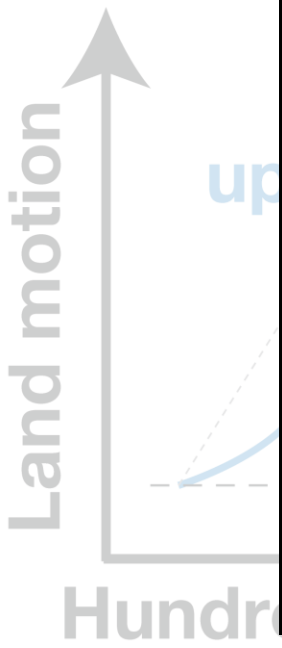
- Geodetic data captures only a **small fraction** of the timescale over which **earthquake cycles operate**.
- The recorded geodetic signal is often **extrapolated** to represent the **entire seismic cycle**.



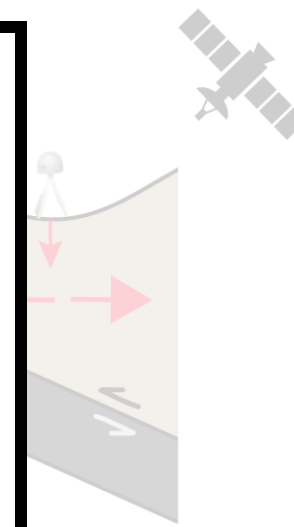
Current geodetic efforts to constrain coupling may be overlooking key deformation components.

TEMPORAL LIMITATIONS OF GEODETIC DATA COVERAGE

- Geodetic data captures only a small fraction over which they operate.
- The recorded data often extrapolates the entire area.

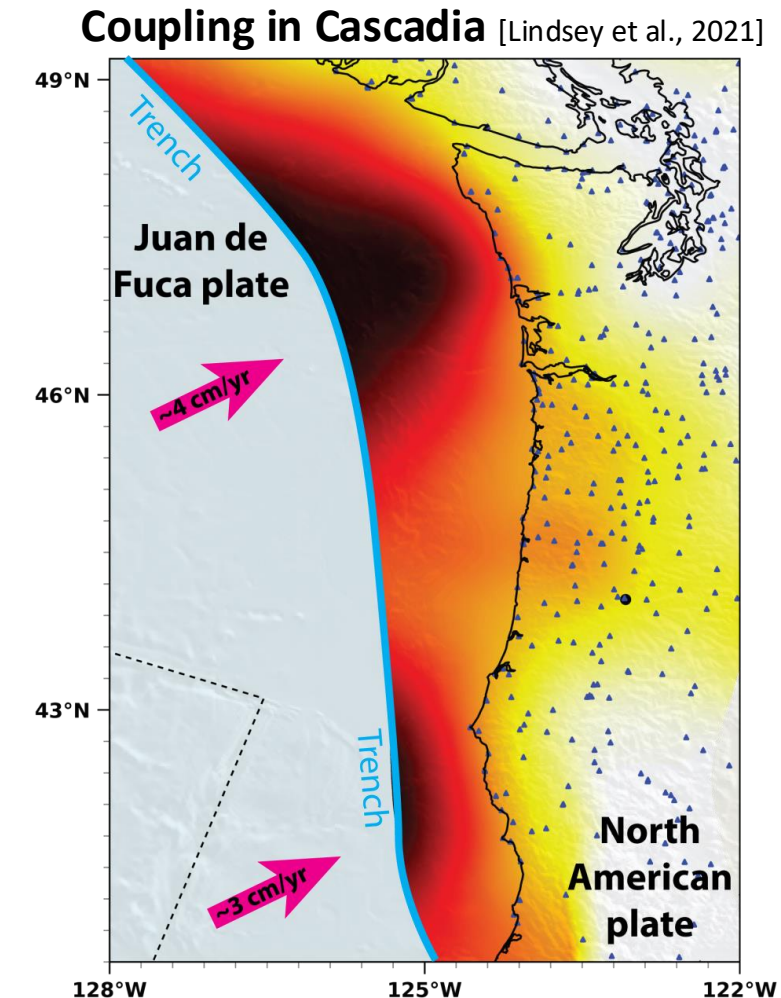
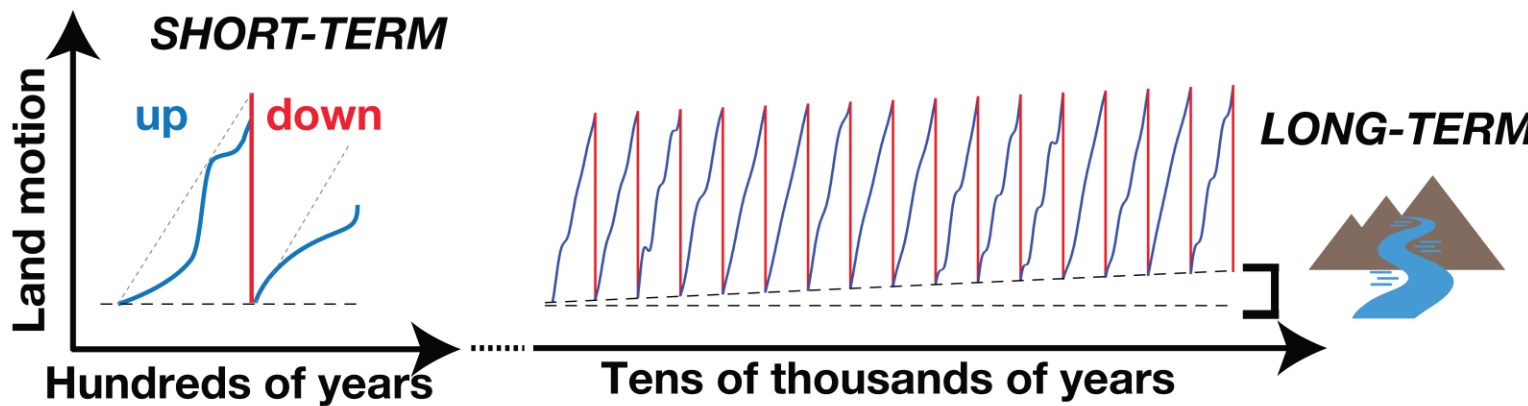


Traversing the Sun Koshi River, Nepal

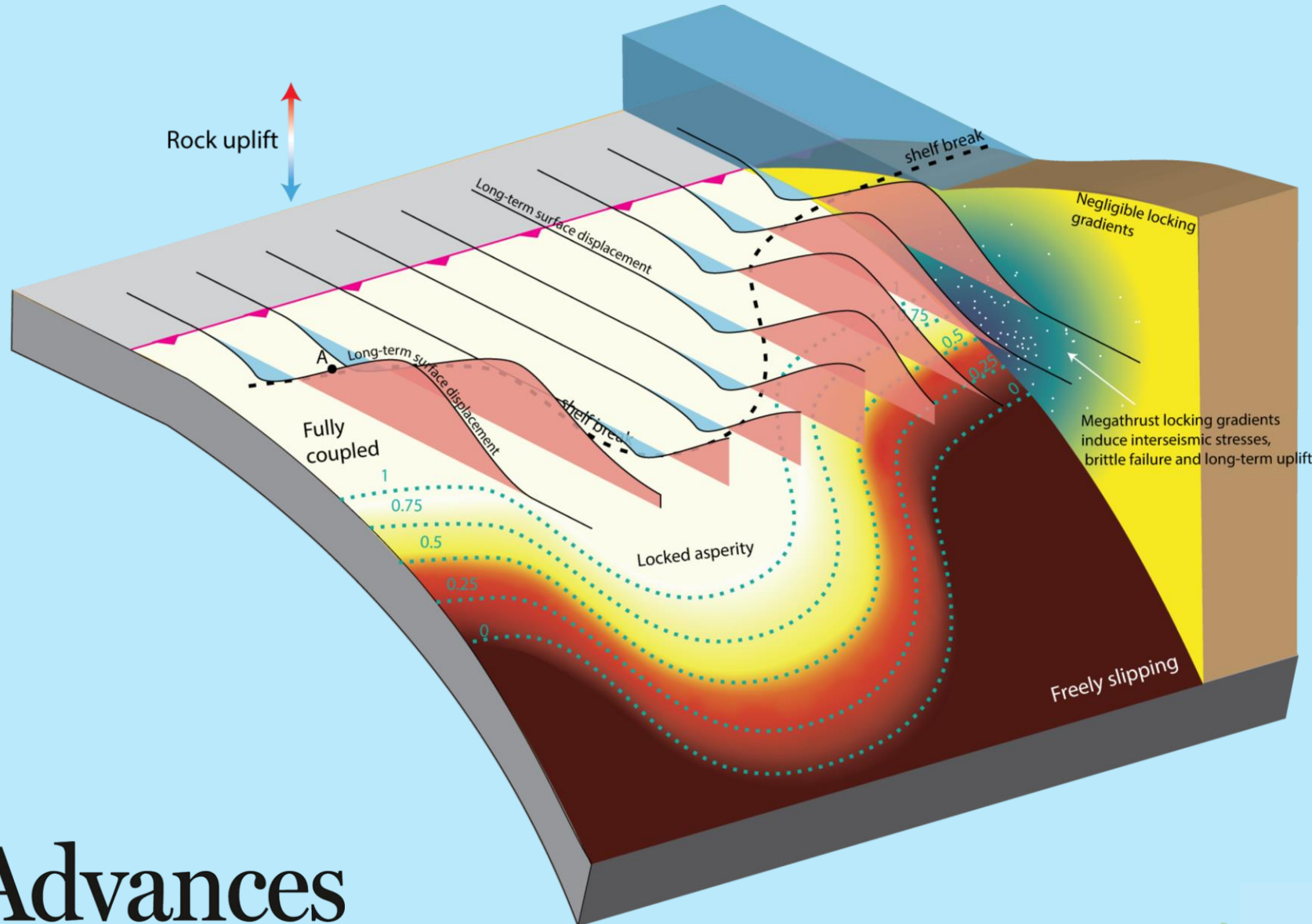


KEY POINTS SO FAR

- Geodetic documentation of upper plate deformation help constrain the hazard associated with megathrust earthquakes.
- Geodetic data captures only a **small fraction** of the timescale over which **earthquake cycles operate**.
- **Landscapes record deformation** on time-scales of **hundreds of thousands of years** and could point to the **persistent plate locking**.

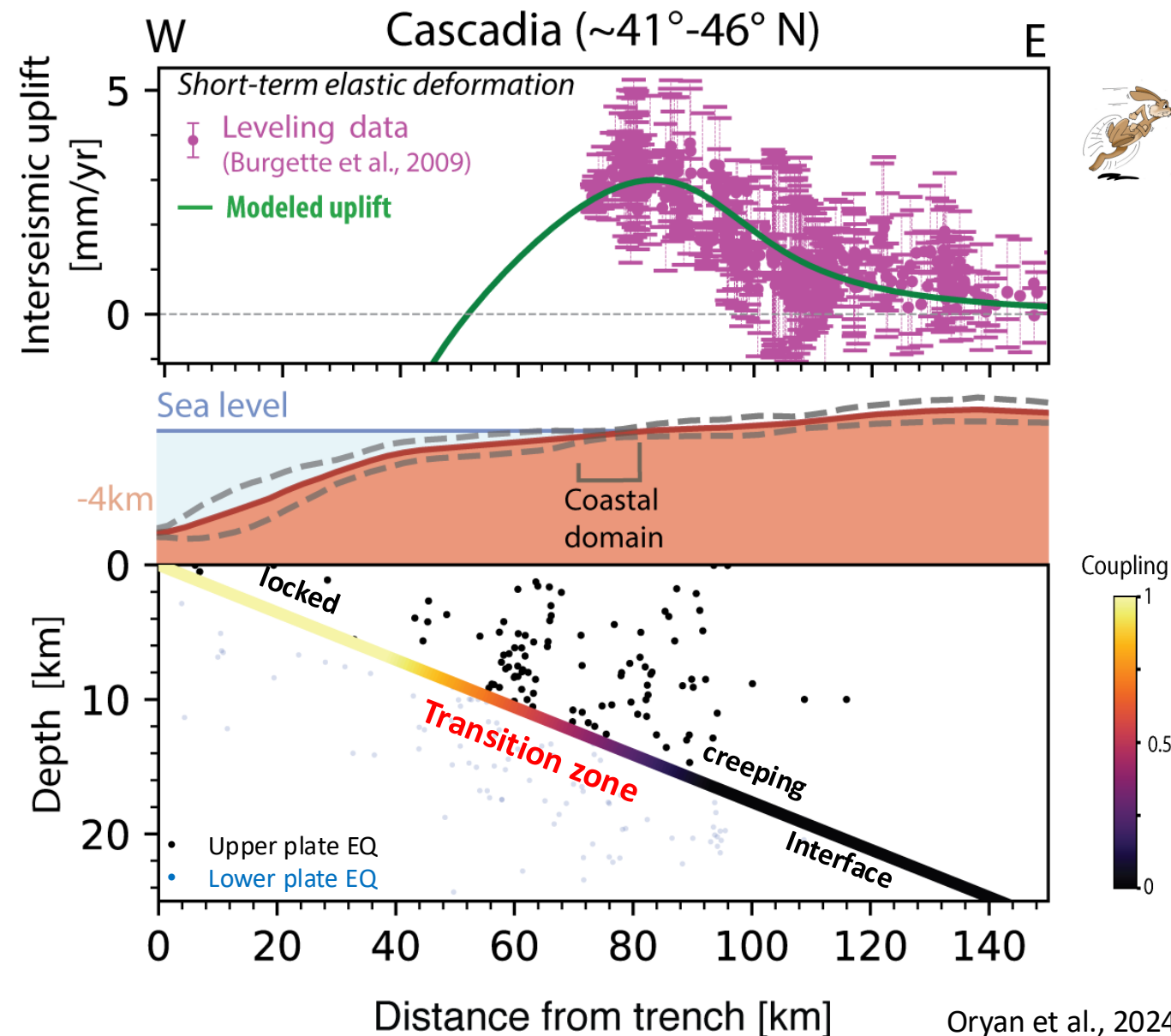


Section 2 - Fingerprints of Megathrust Locking in Subduction Landscapes



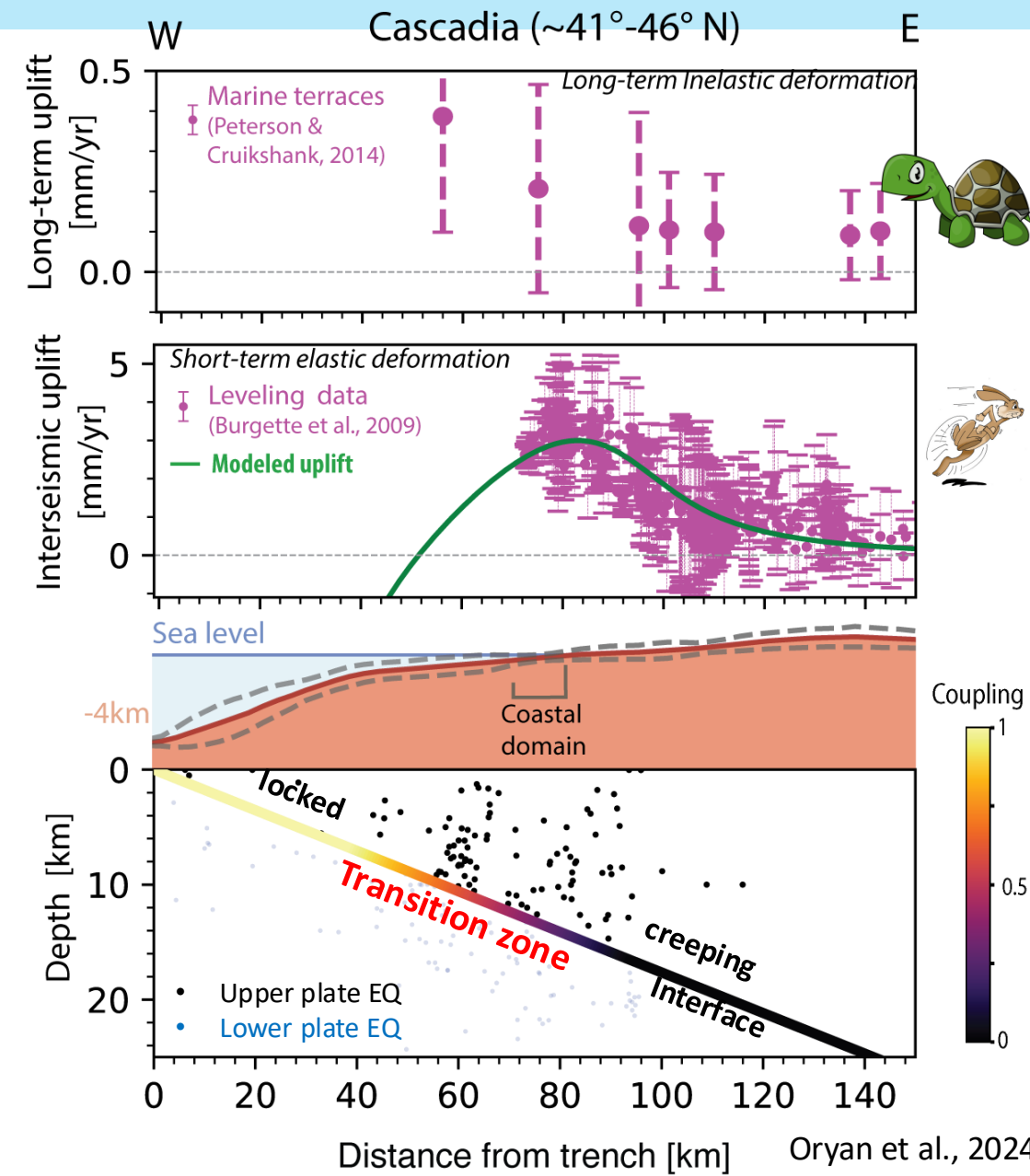
SHORT-TERM DEFORMATION IN CASCADIA

- Short-term (**geodetic**) uplift shows a peak above the transition zone.



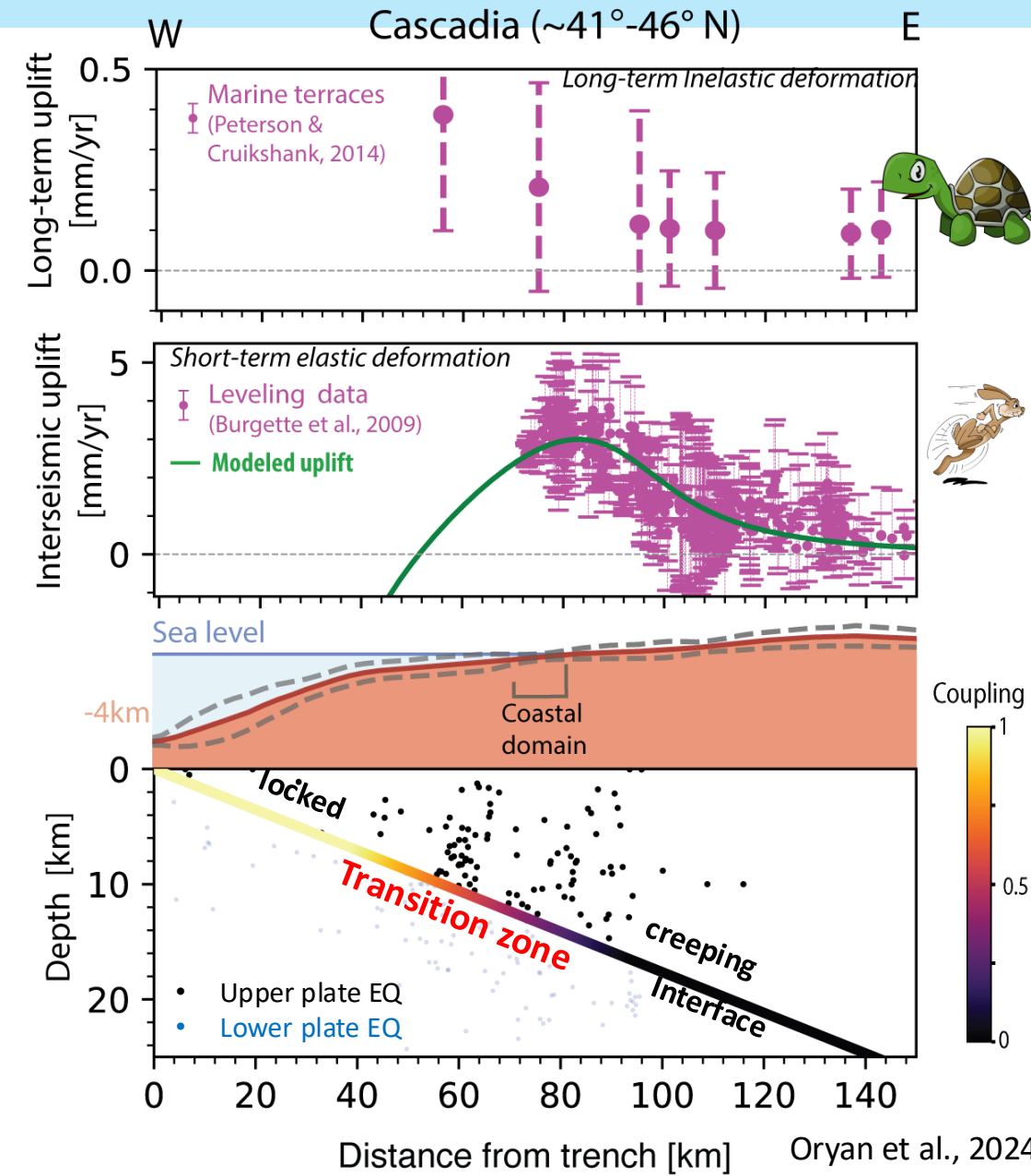
SHORT- AND LONG-TERM DEFORMATION IN CASCADIA

- **Short-term (geodetic) uplift** shows a peak above the transition zone.
- **Long-term (geomorphic) uplift** aligns with the short-term deformation, peaking above the transition zone.



SHORT- AND LONG-TERM DEFORMATION IN CASCADIA

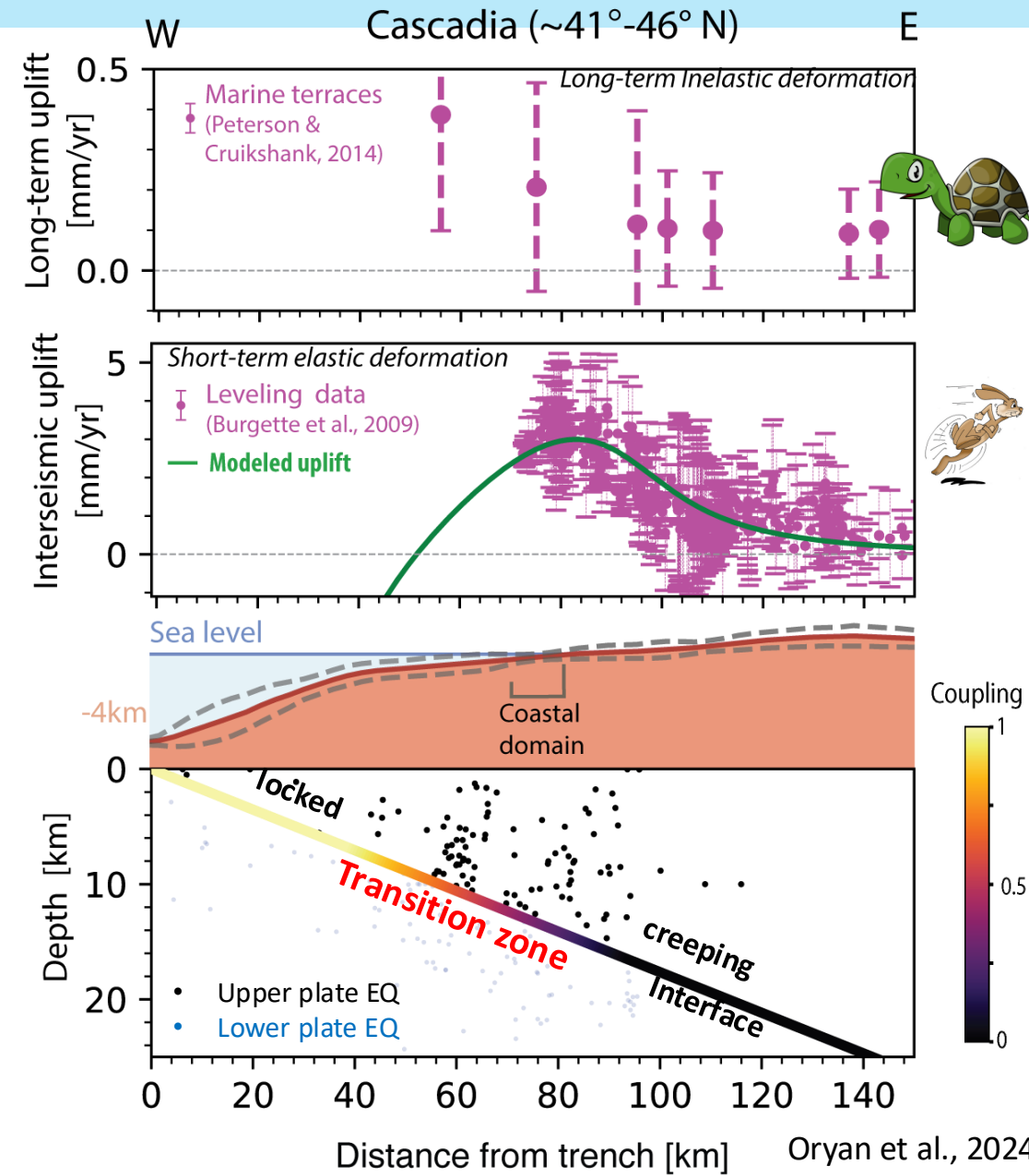
- **Short-term (geodetic) uplift** shows a peak above the transition zone.
- **Long-term (geomorphic) uplift** aligns with the short-term deformation, peaking above the transition zone.
- **Upper plate seismicity** is concentrated above the transition zone.



SHORT- AND LONG-TERM DEFORMATION IN CASCADIA

- **Short-term (geodetic) uplift** shows a peak above the transition zone.
- **Long-term (geomorphic) uplift** aligns with the short-term deformation, peaking above the transition zone.
- **Upper plate seismicity** is concentrated above the transition zone.

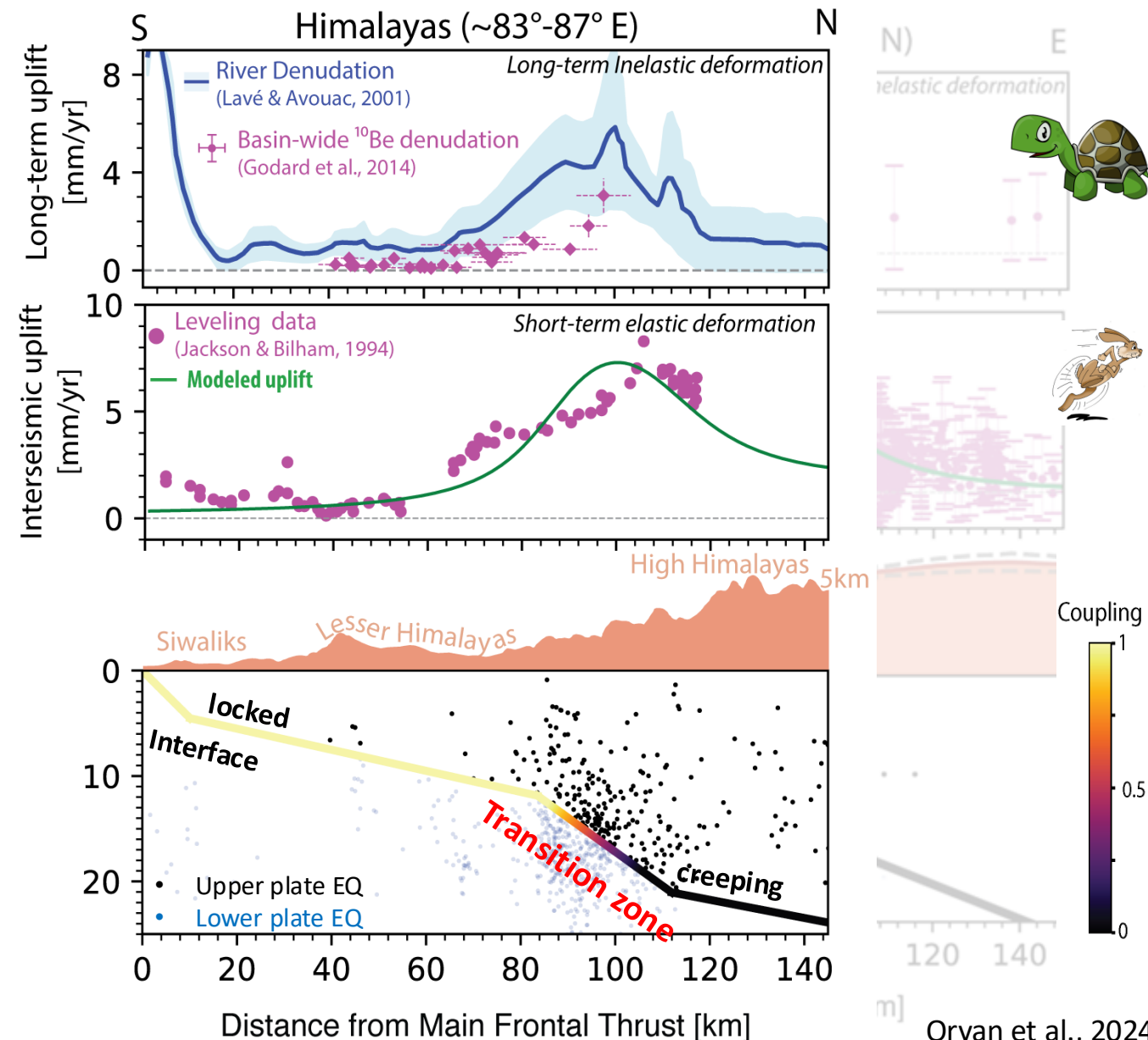
Short- (geodetic) and Long-term (geomorphic) deformation coincide.



SHORT- AND LONG-TERM DEFORMATION IN HIMALYAS

- **Short-term (geodetic) uplift** shows a peak above the transition zone.
- **Long-term (geomorphic) uplift** aligns with the short-term deformation, peaking above the transition zone.
- **Upper plate seismicity** is concentrated above the transition zone.

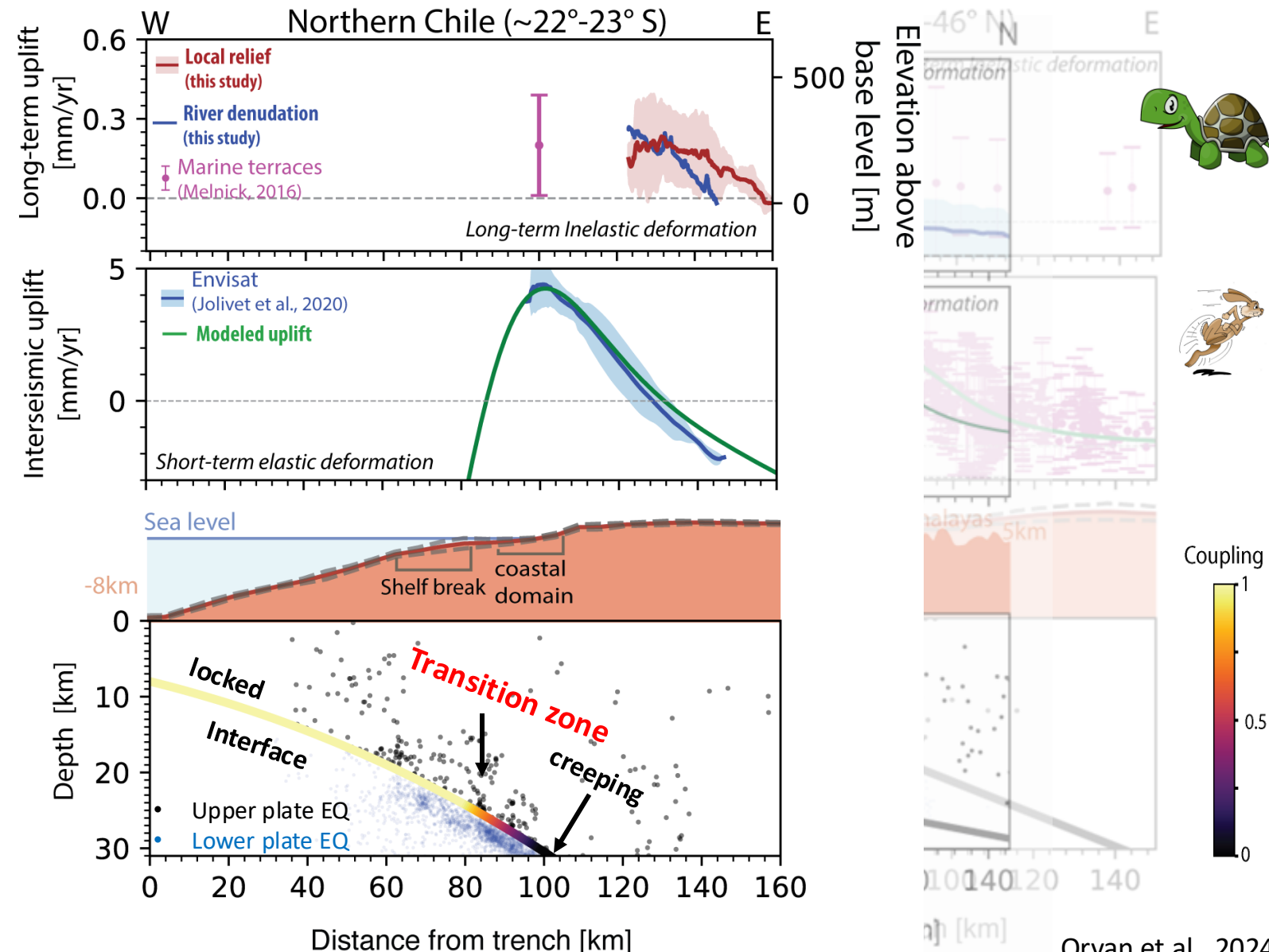
Short- (geodetic) and Long-term (geomorphic) deformation coincide.



SHORT- AND LONG-TERM DEFORMATION IN CHILE

- **Short-term (geodetic) uplift** shows a peak above the transition zone.
- **Long-term (geomorphic) uplift** aligns with the short-term deformation, peaking above the transition zone.
- **Upper plate seismicity** is concentrated above the transition zone.

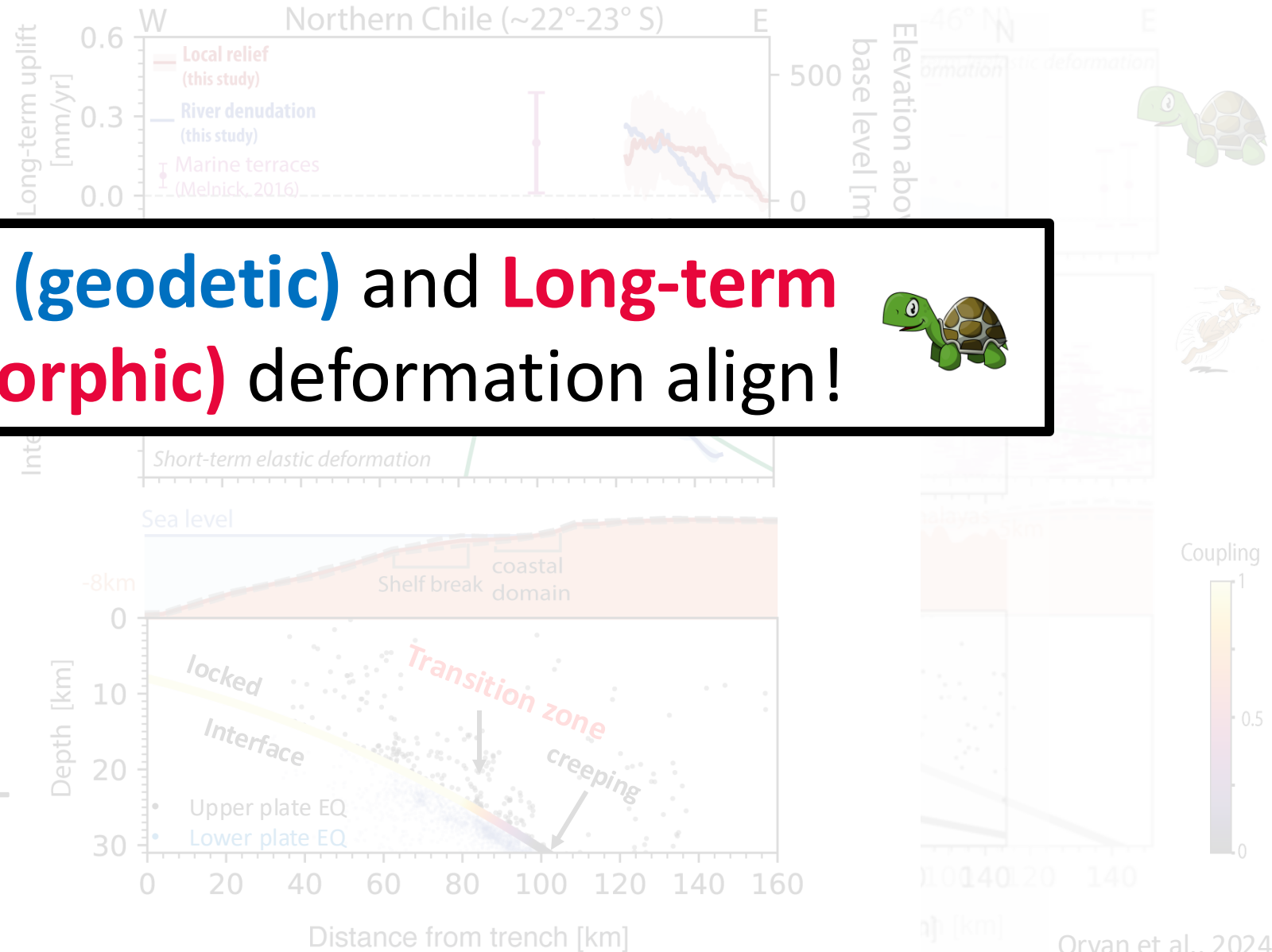
Short- (geodetic) and Long-term (geomorphic) deformation coincide.



SHORT- AND LONG-TERM DEFORMATION IN CHILE

- Short-term (elastic) uplift shows a peak above the transition zone.
- Long-term aligns with deformation the transition
- Upper plate seismicity (inelastic) is concentrated above the transition zone.

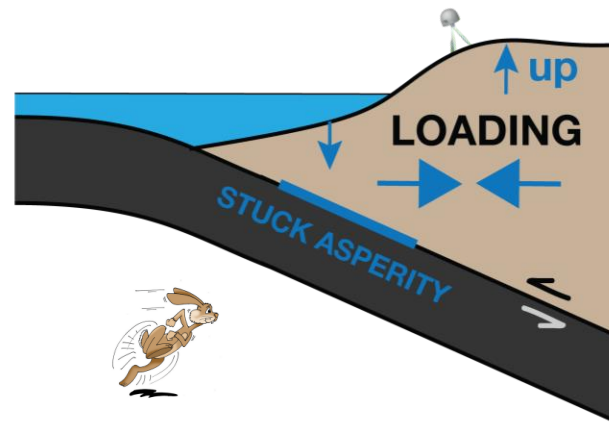
Short- (elastic) and Long-term (inelastic) deformation coincide.



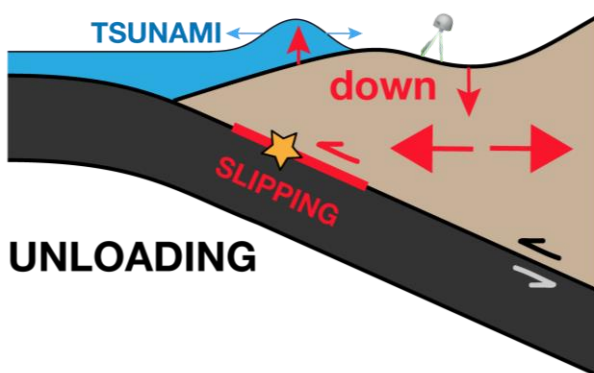
ELASTIC EARTHQUAKE CYCLES IN SUBDUCTION ZONES



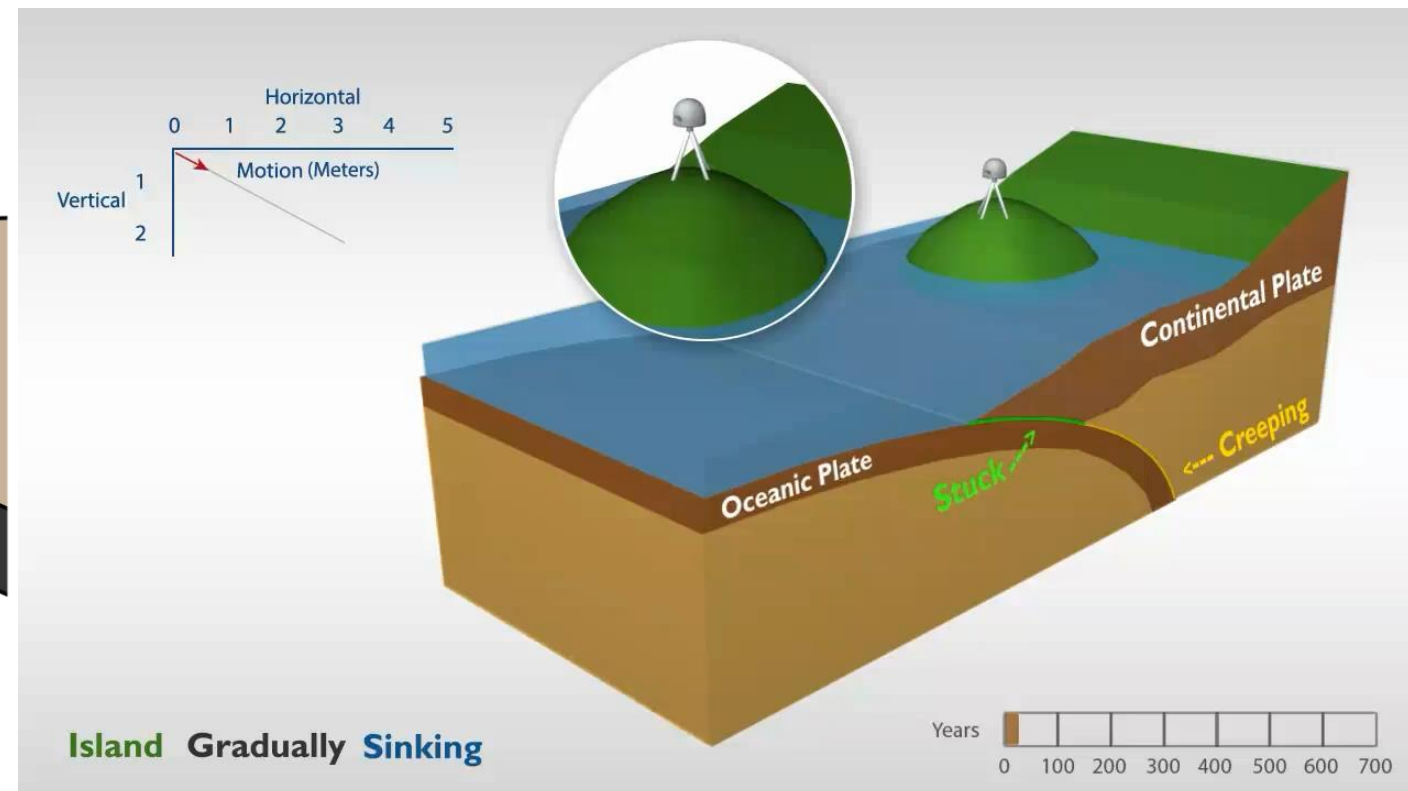
Long-term: downgoing plate descends beneath the upper plate in stick-slip fashion.



Interseismic: locked section is “stuck”. Creeping section moves slowly. Upper plate deform **elastically**



Coseismic: locked section moves abruptly. Upper plate deform **elastically** in an opposite sense.

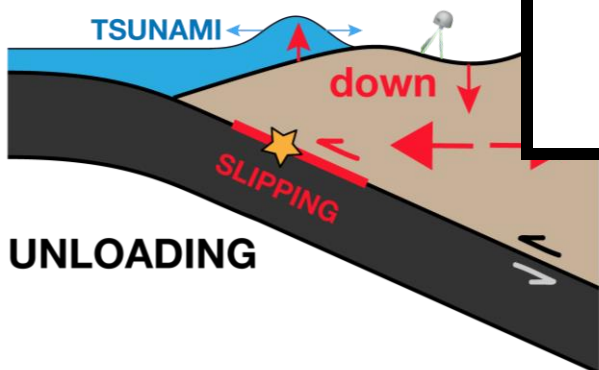


ELASTIC EARTHQUAKE CYCLES IN SUBDUCTION ZONES



Long-term: downgoing plate descends beneath the upper plate in stick-slip fashion

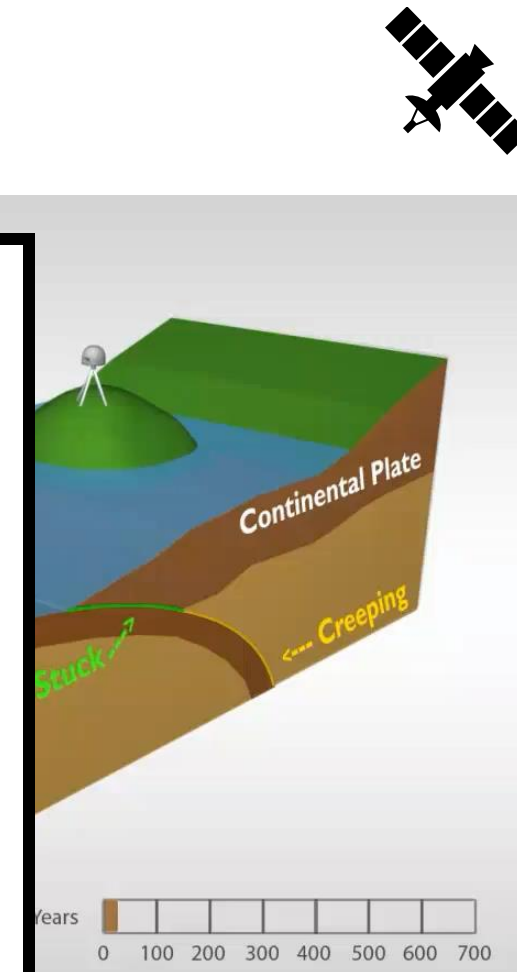
Interseismic: locked section is “stuck”. Creeping section moves slowly. Upper plate deform **elastically**



Elastic deformation is reversible



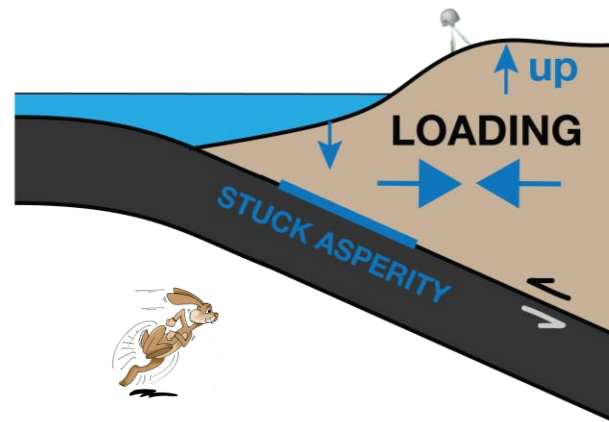
plate deform **elastically** in an opposite sense.



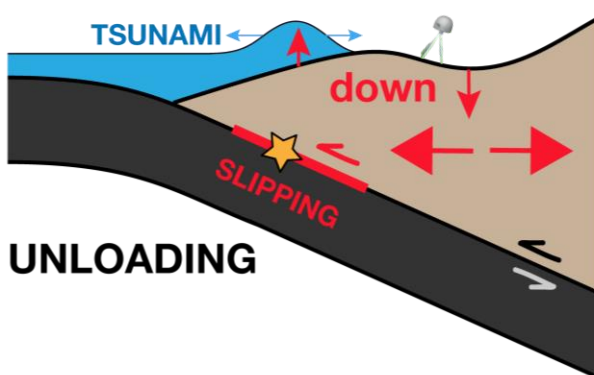
ELASTIC EARTHQUAKE CYCLES IN SUBDUCTION ZONES



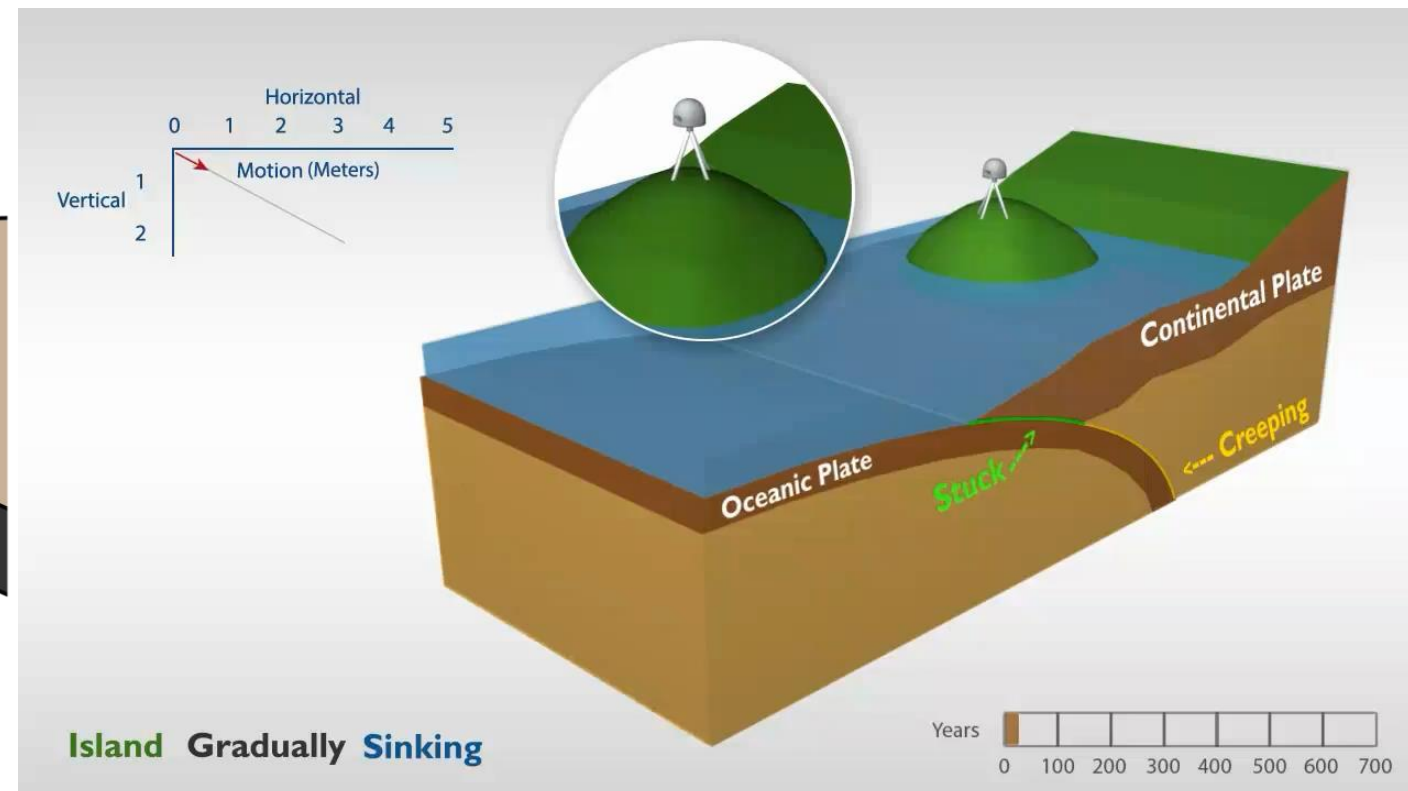
Long-term: downgoing plate descends beneath the upper plate in stick-slip fashion.



Interseismic: locked section is “stuck”. Creeping section moves slowly. Upper plate deform **elastically**



Coseismic: locked section moves abruptly. Upper plate deform **elastically** in an opposite sense.

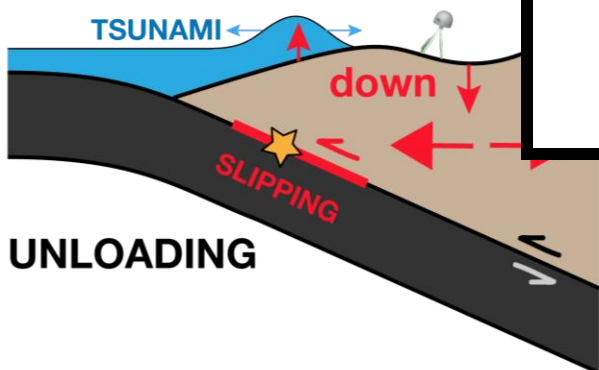


ELASTIC EARTHQUAKE CYCLES IN SUBDUCTION ZONES



Long-term: downgoing plate descends beneath the upper plate in stick-slip fashion

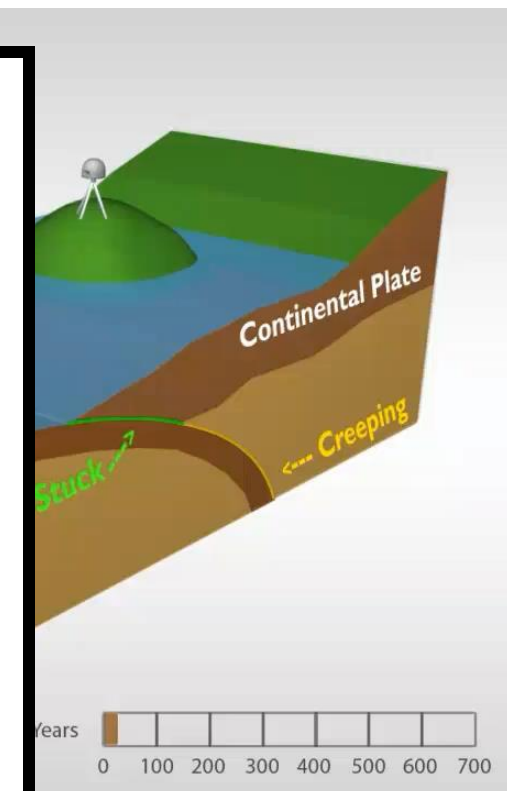
Interseismic: locked section is “stuck”. Creeping section moves slowly. Upper plate deform **elastically**



Plastic deformation is **permanent/irreversible**



plate deform **elastically** in an opposite sense.



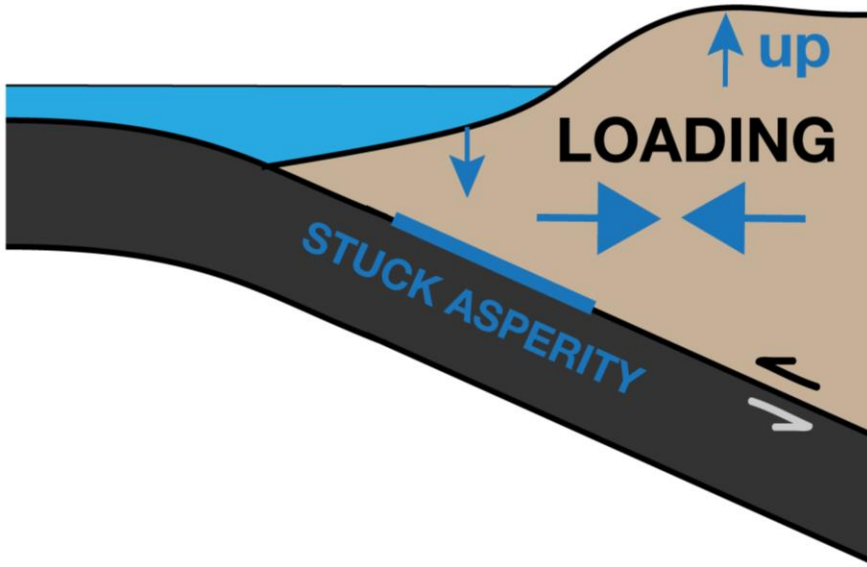
HOW INTERSEISMIC FAULT LOCKING IMPRINTS SUBDUCTION LANDSCPES ?



HOW INTERSEISMIC FAULT LOCKING IMPRINTS SUBDUCTION LANDSCPES ?

Bending

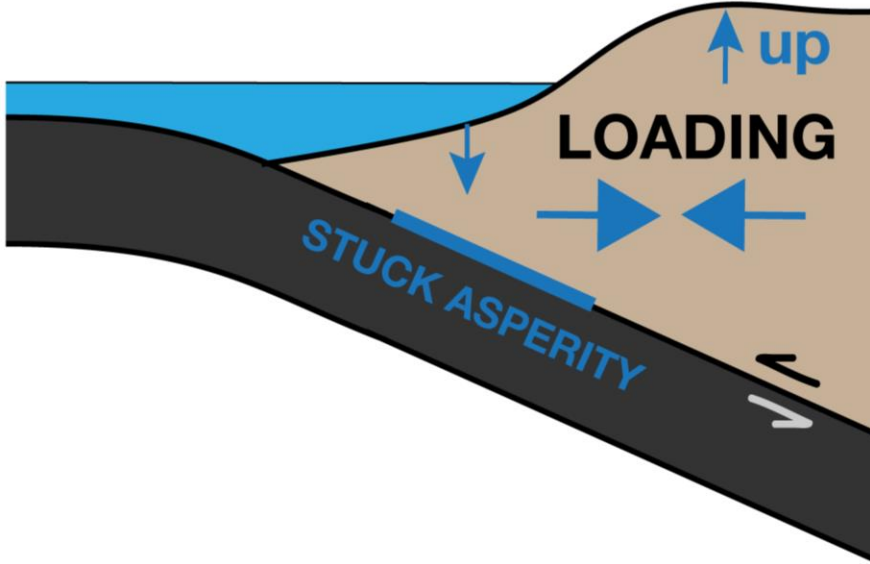
BETWEEN
EARTHQUAKES



HOW INTERSEISMIC FAULT LOCKING IMPRINTS SUBDUCTION LANDSCPES ?

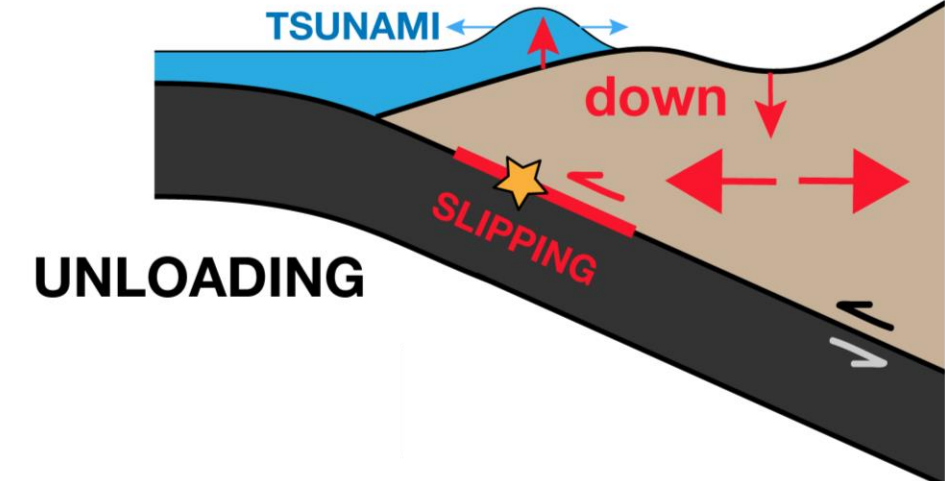
Bending

BETWEEN
EARTHQUAKES



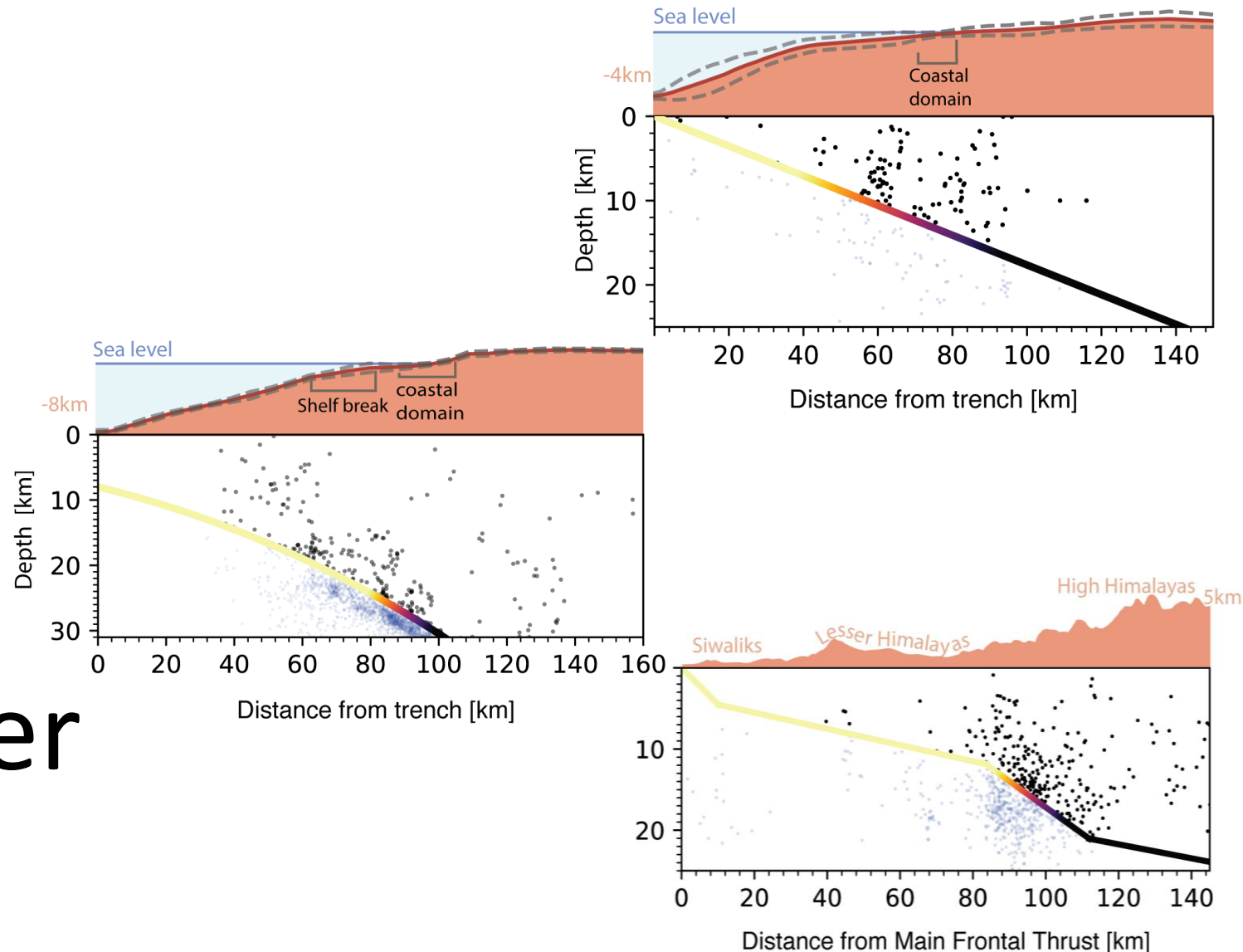
Unbending

DURING
EARTHQUAKE



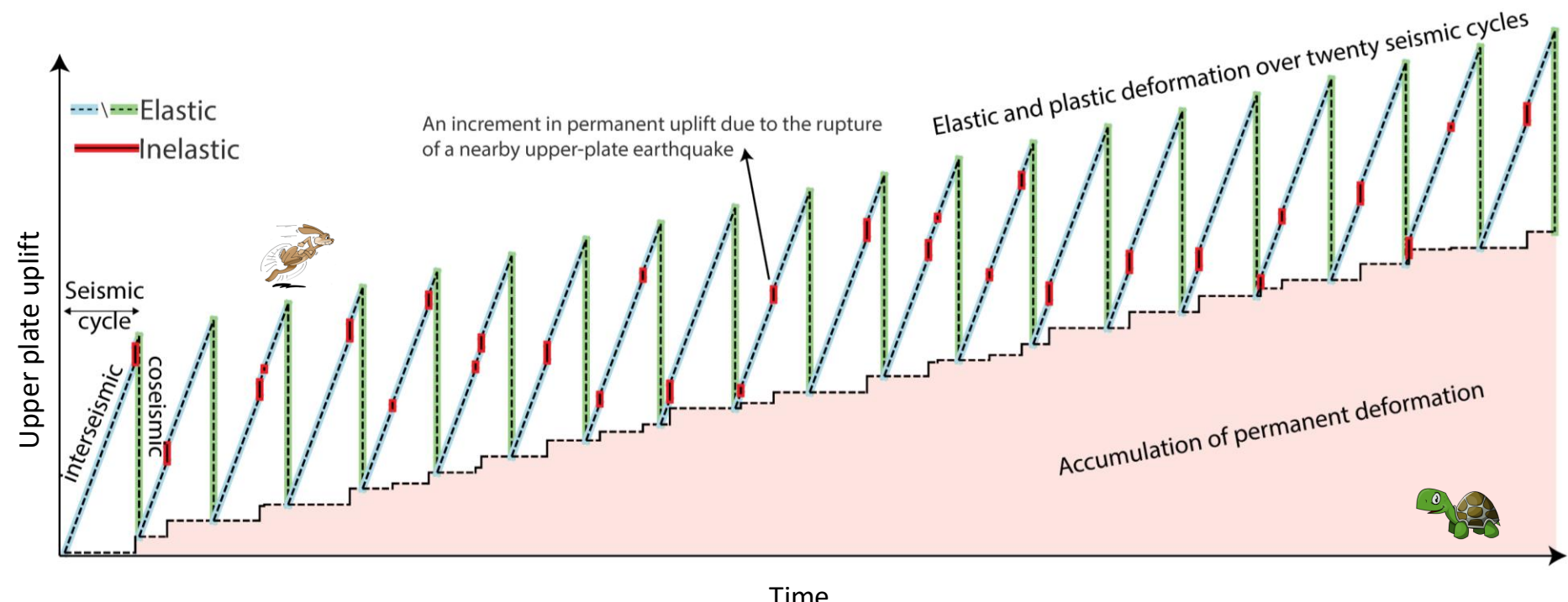
HOW INTERSEISMIC FAULT LOCKING IMPRINTS SUBDUCTION LANDSCPES ?

Upper plate
interseismic
earthquakes
permanently
shape the upper
plate.



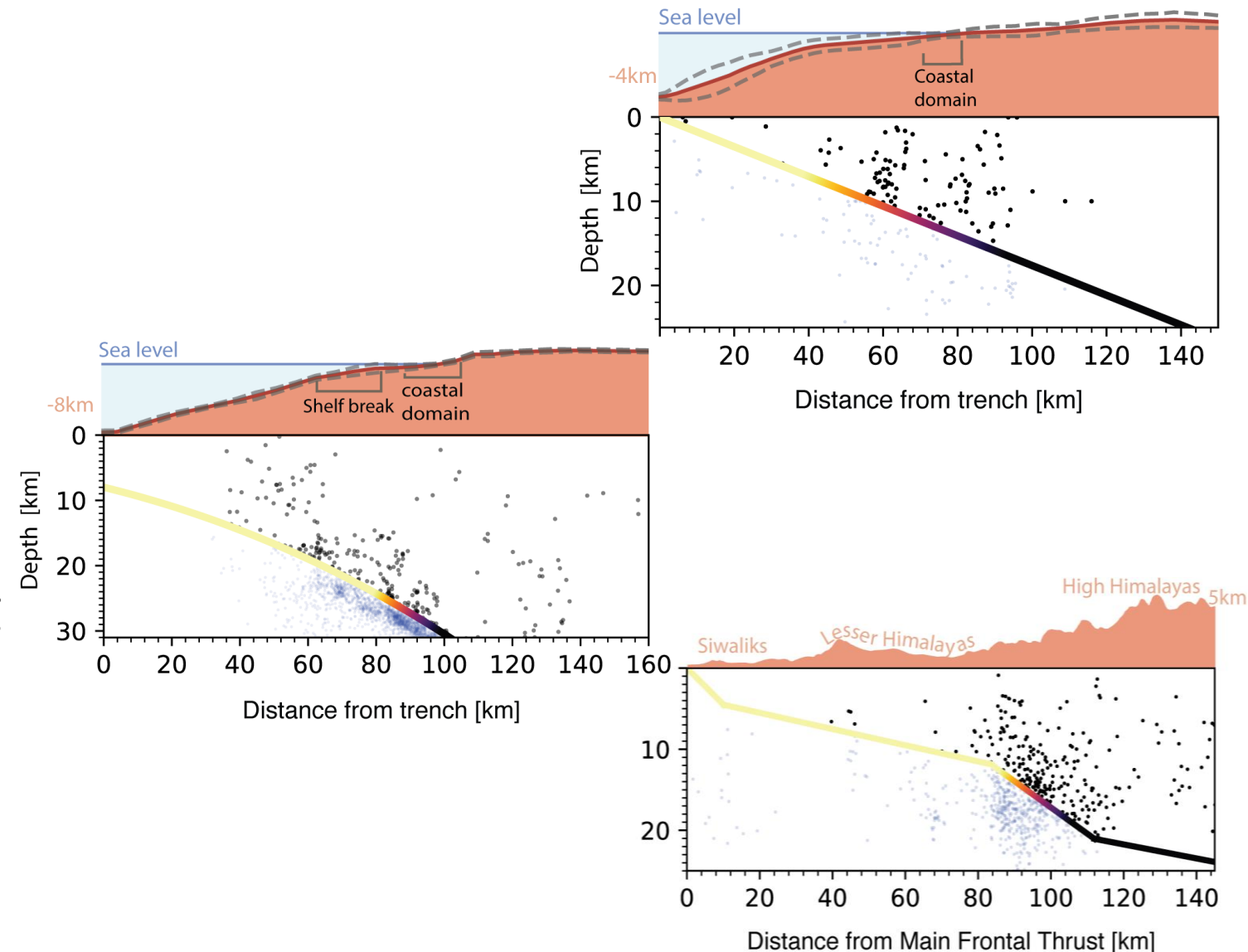
HOW INTERSEISMIC FAULT LOCKING IMPRINTS SUBDUCTION LANDSCPES ?

- **Interseismic upper plate stresses** induced by locking gradients push parts of the upper plate to **failure** generating overriding plate earthquakes.
- Repeated **failure** over multiple earthquake cycles explains the overlap between short- and long-term deformation.



MODELING INTERSEISMIC INELASTIC DEFORMATION ACROSS UPPER PLATES

- Current interseismic recorded seismicity represents a **snapshot of the long-term processes** that gradually shape topography.
- We extend the upper plate seismic record by generating upper plate earthquakes, **representing the complete signature of earthquake cycles.**



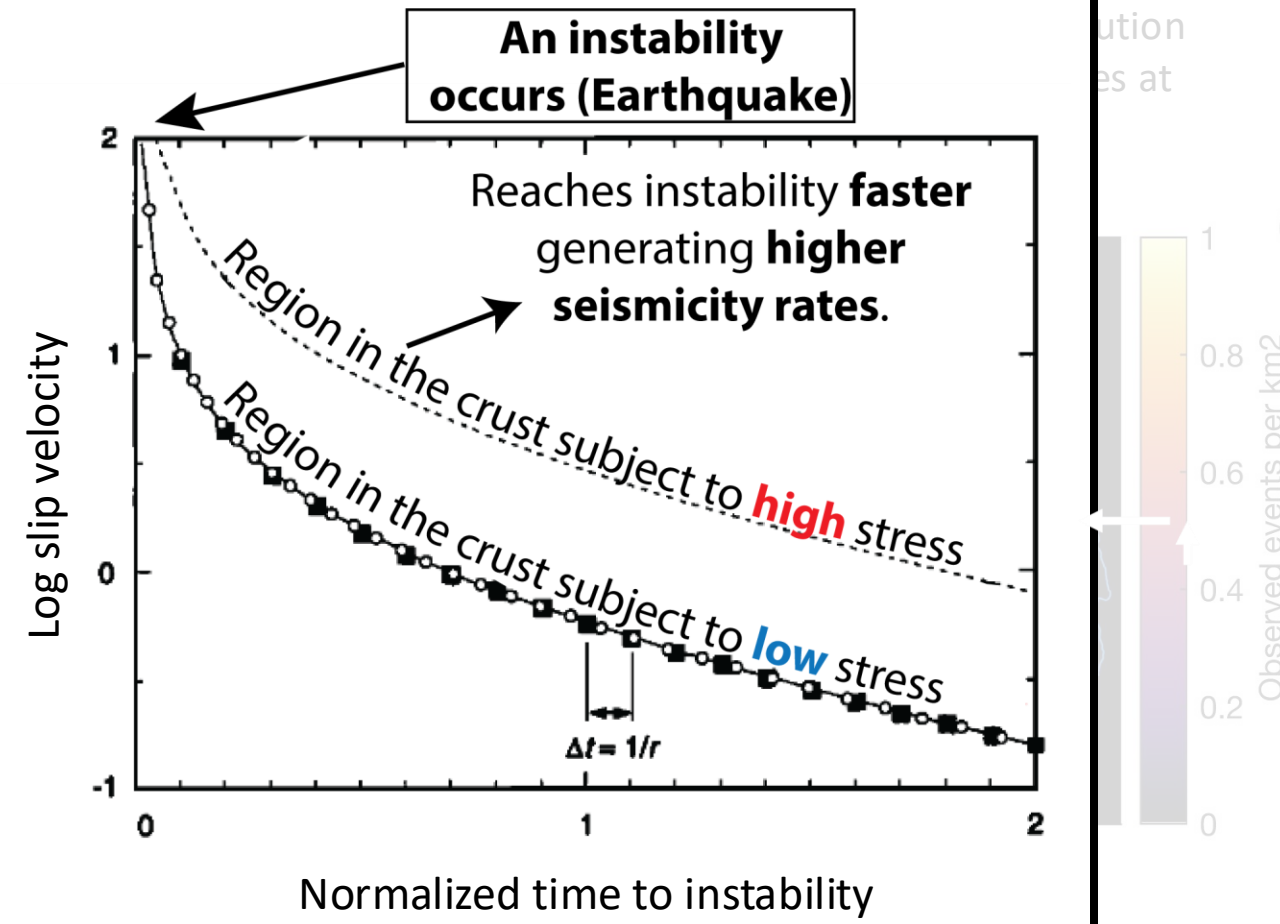
MODELING INTERSEISMIC INELASTIC DEFORMATION ACROSS UPPER PLATES

- We apply it with stress
- The Dieterich approach models the crust as a series of independent nucleation points governed by rate-and-state friction, progressing toward instability.
- Higher stressing rate will reduce the time to reach instability.

Underlying assumption:

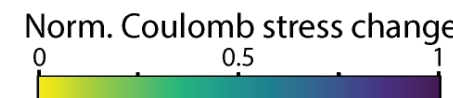
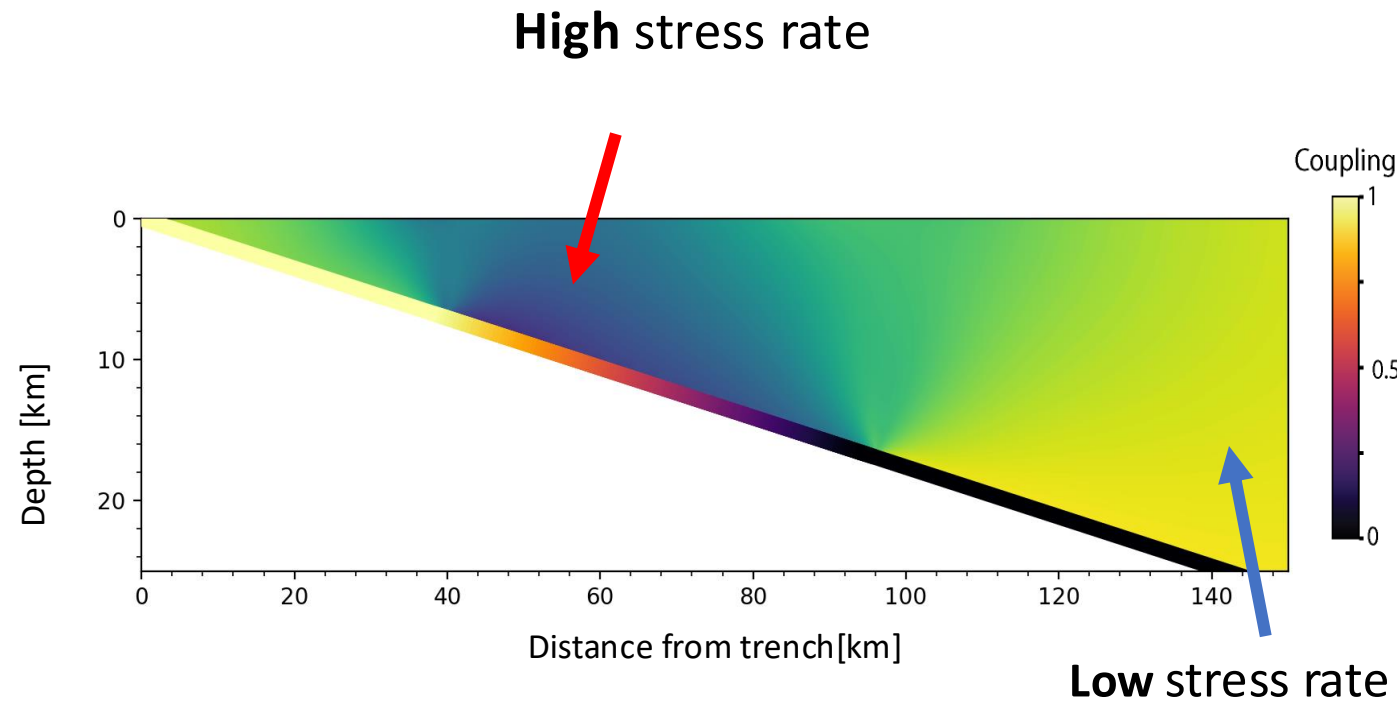
The state variable, θ , in rate-and-state friction follows $\theta\dot{\delta} \gg 1$ so $\theta = \theta_0 \exp(-\frac{\delta}{D_c})$ and as such the slip velocity:

$$\dot{\delta} = \left\{ \left[\frac{1}{\dot{\delta}_0} + \frac{H\sigma_n}{\dot{\tau}} \right] \exp\left(-\frac{\dot{\tau}t}{A\sigma_n}\right) - \frac{H\sigma_n}{\dot{\tau}} \right\}^{-1}.$$



MODELING INTERSEISMIC INELASTIC DEFORMATION ACROSS UPPER PLATES

- Compute the stress rate imparted by **locking gradients**.
- **Populate millions of synthetic earthquakes** spanning thousands of years and dozens of seismic cycles according to the **stress rate**.
- Estimate **cumulative long-term surface displacement** from the synthetic seismic events using the Okada solution.

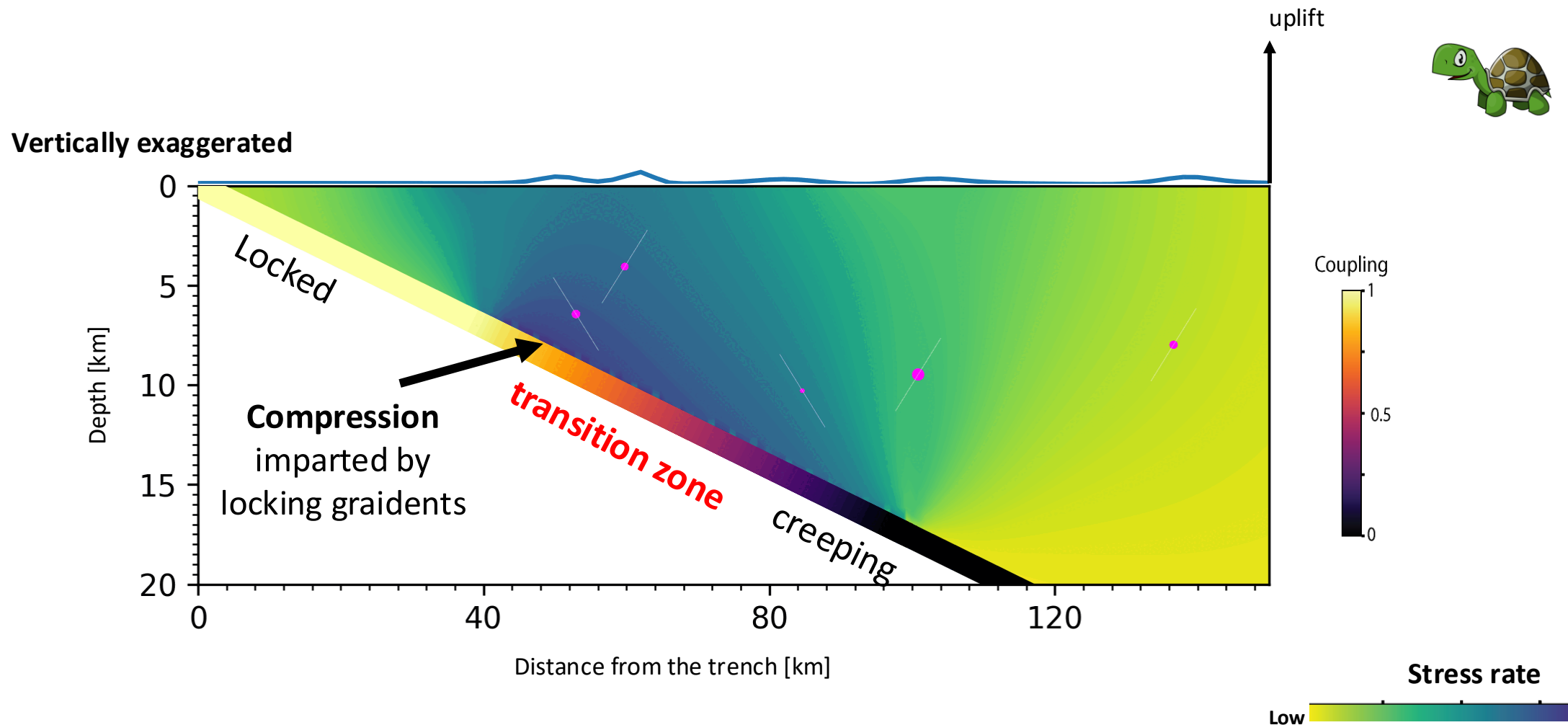


stress rate = Coulomb stress change assuming optimally orientated thrust faults (30°)

MODELING INTERSEISMIC INELASTIC DEFORMATION ACROSS UPPER PLATES

10 degree dip, fully locked to 40km

Uplift during three seismic cycles producing average **long-term** rate of 0.1 mm/yr



MODELING INTERSEISMIC INELASTIC DEFORMATION ACROSS UPPER PLATES

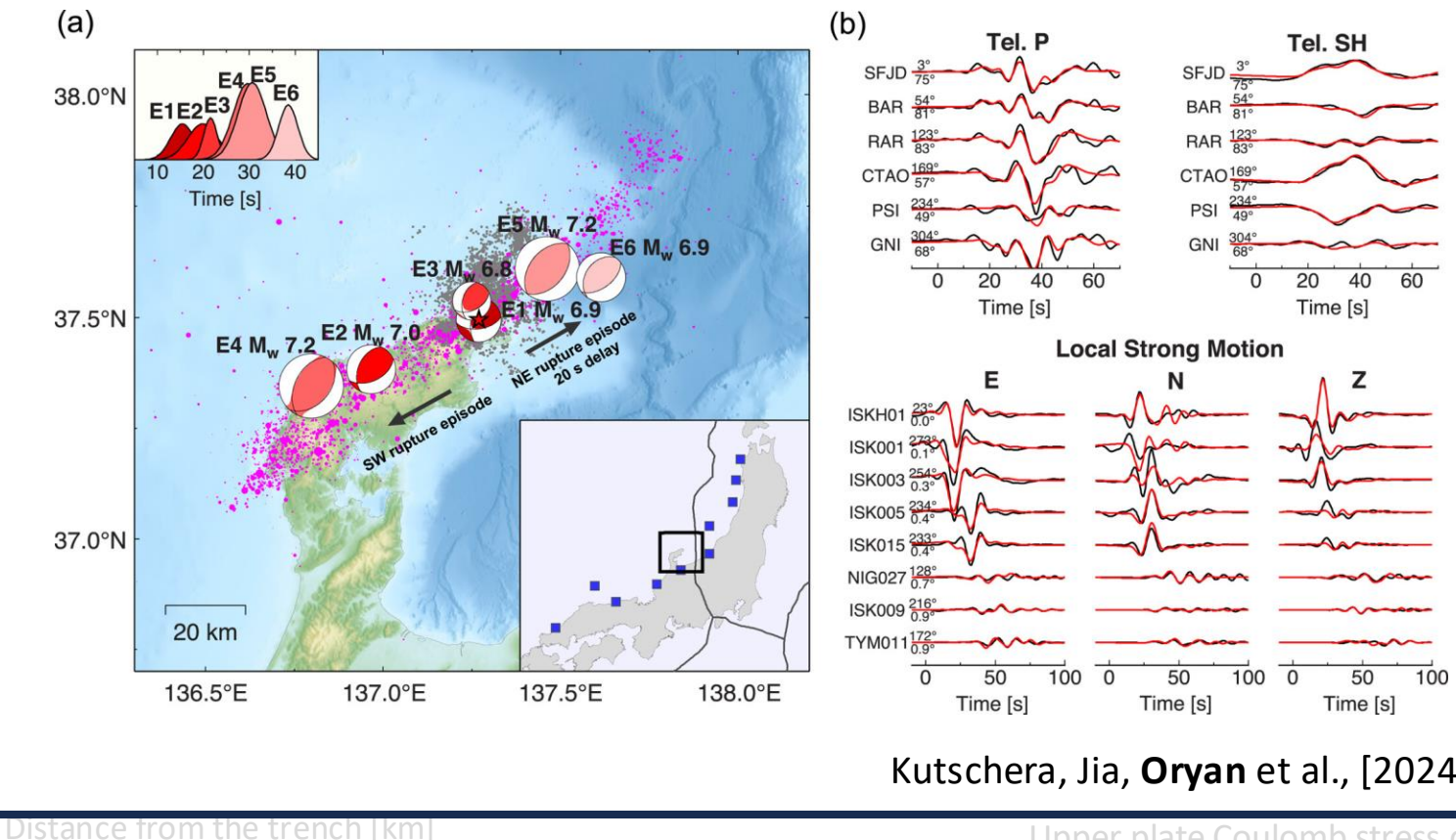
10 degree dip, f
locked to 40km

Vertically

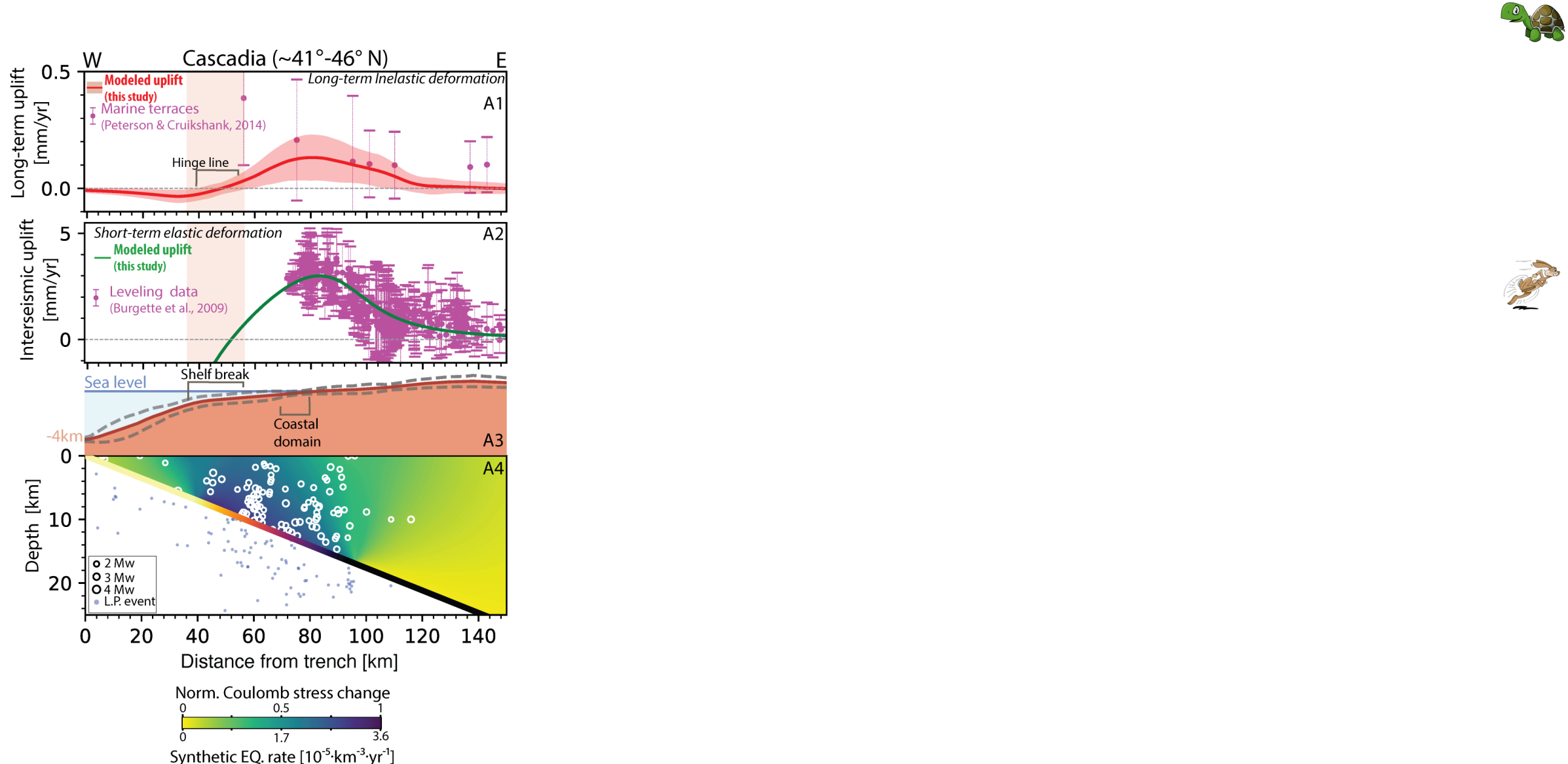
Depth [km]

Bayesian inversion of seismic data is used to generate earthquakes and estimate the surface deformation for the **2024 Noto earthquake.**

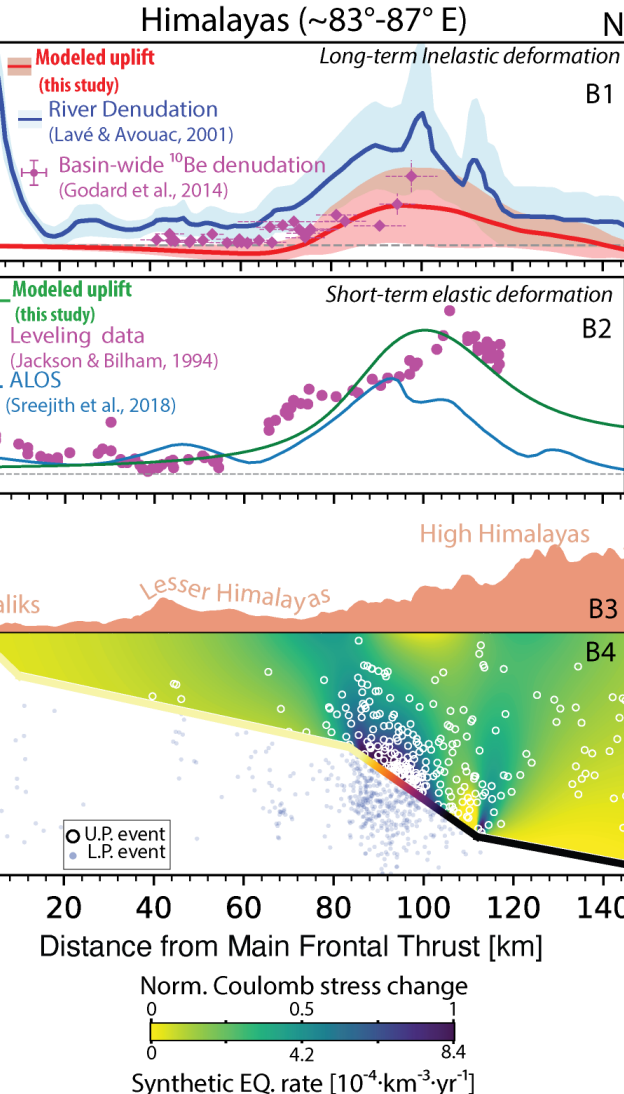
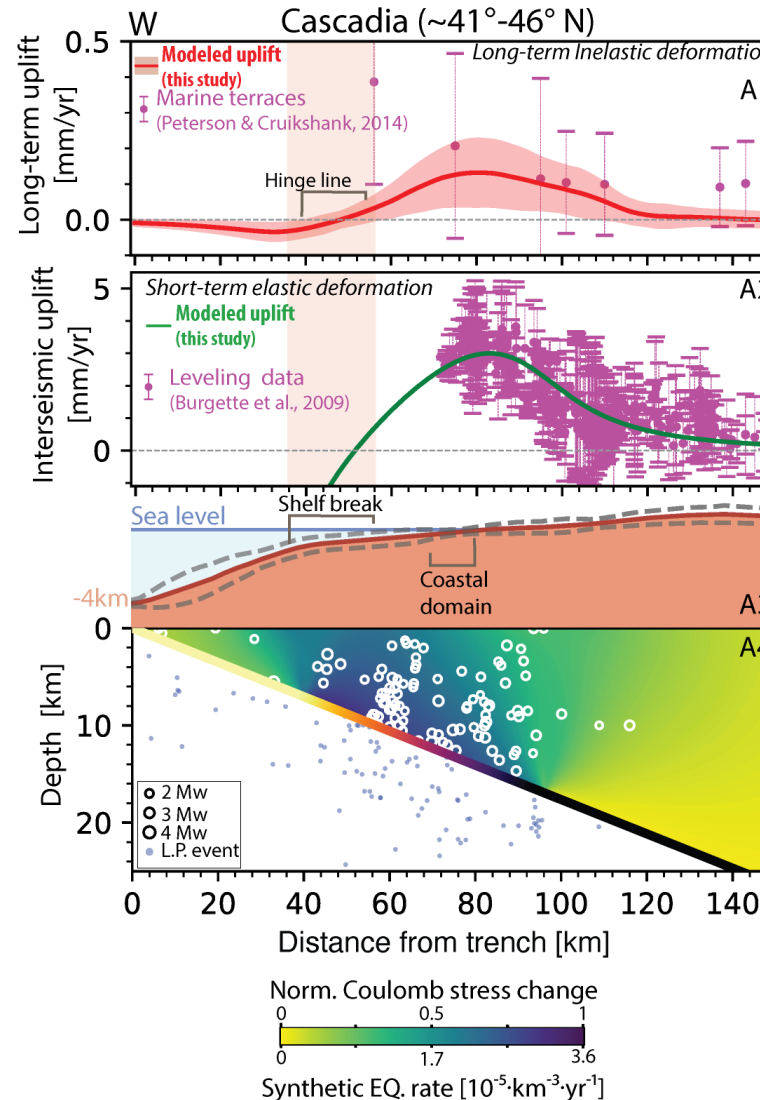
The approach of generating multiply synthetic **events** based on a probability density function has been utilized in other studies.



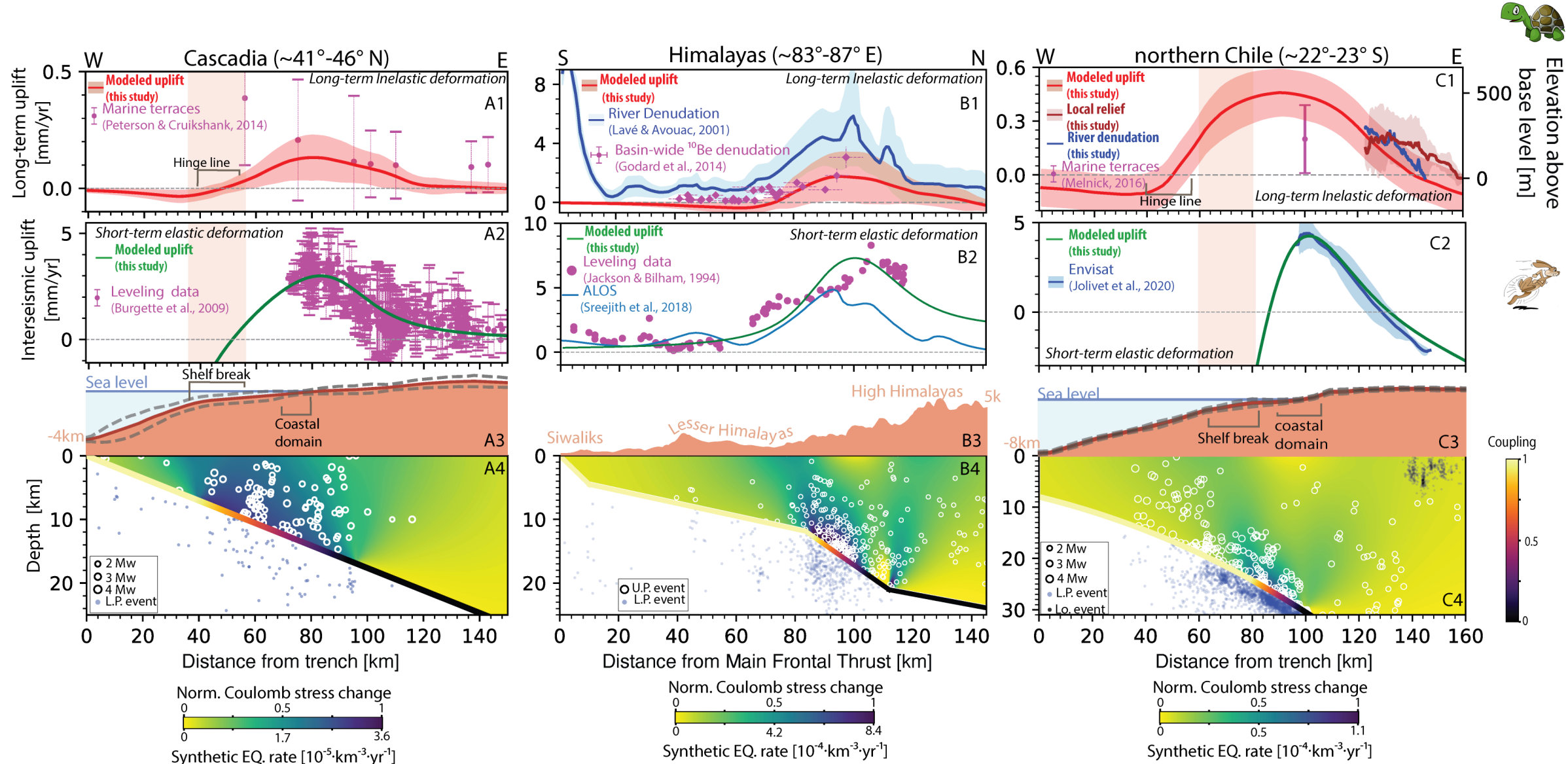
DEFORMATION IN CASCADIA, HIMALYAS AND CHILE



DEFORMATION IN CASCADIA, HIMALYAS AND CHILE

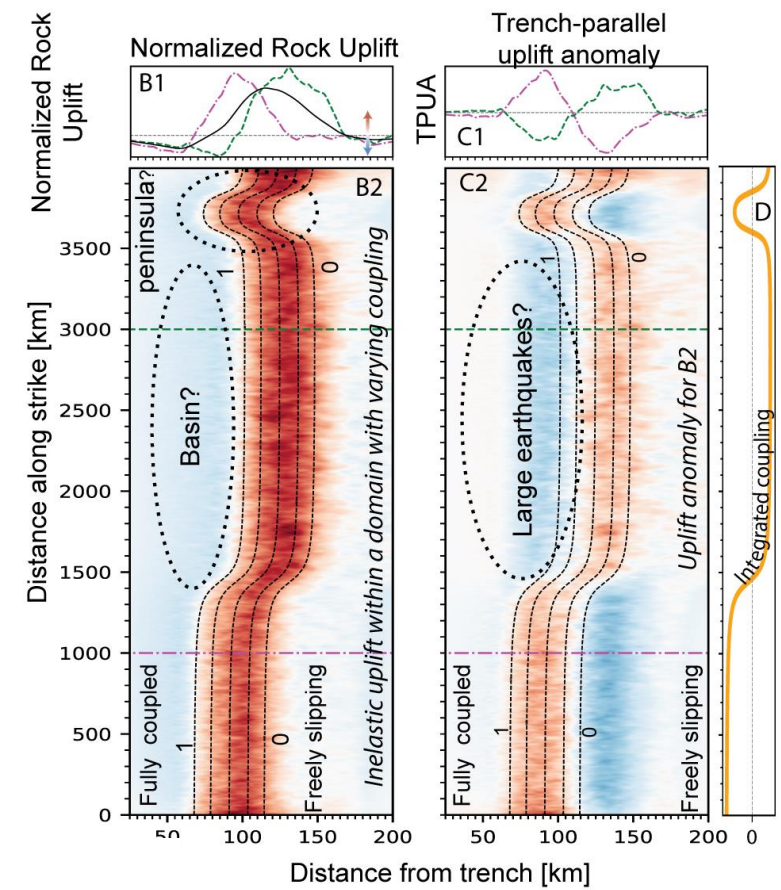
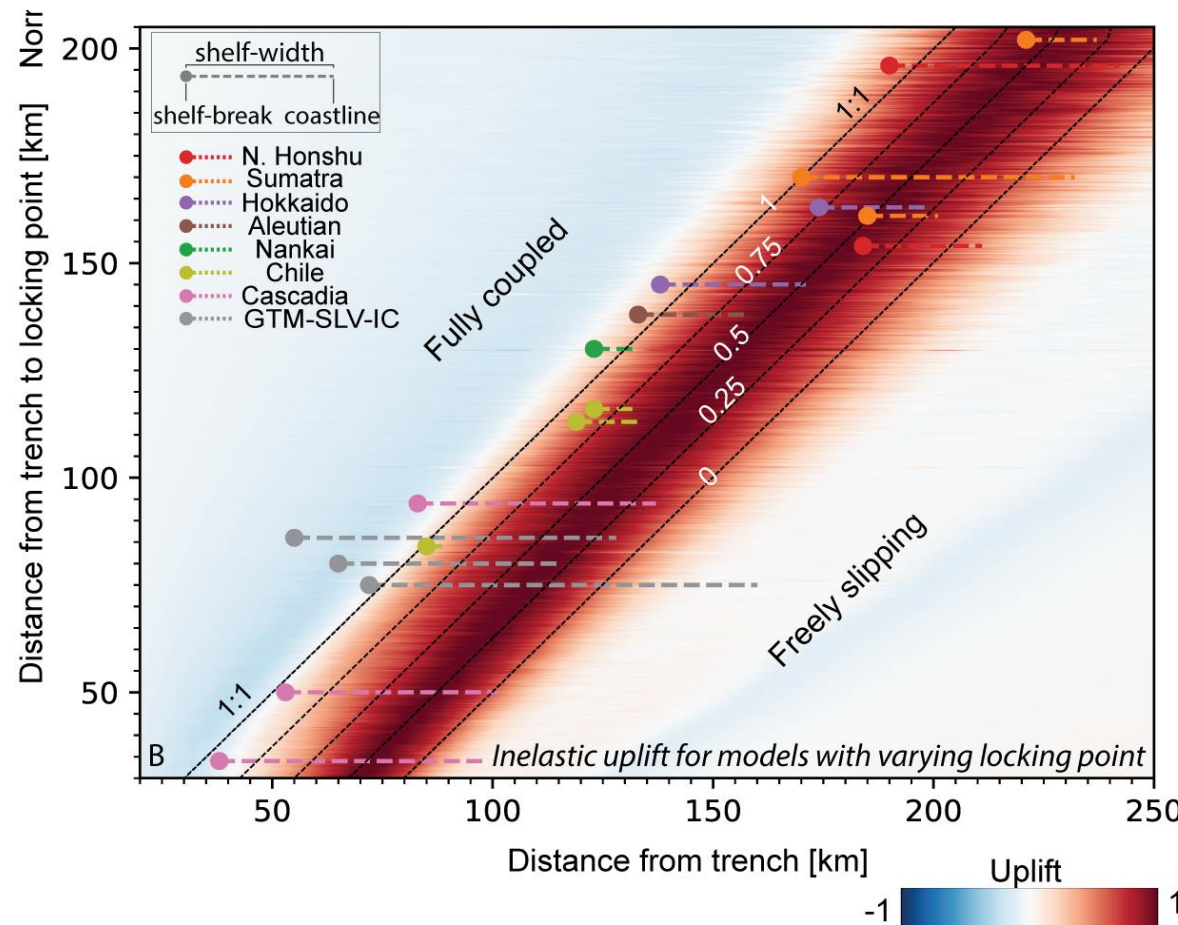


DEFORMATION IN CASCADIA, HIMALYAS AND CHILE



MODELING GLOBAL TRENDS IN SUBDUCTION LANDSCAPES

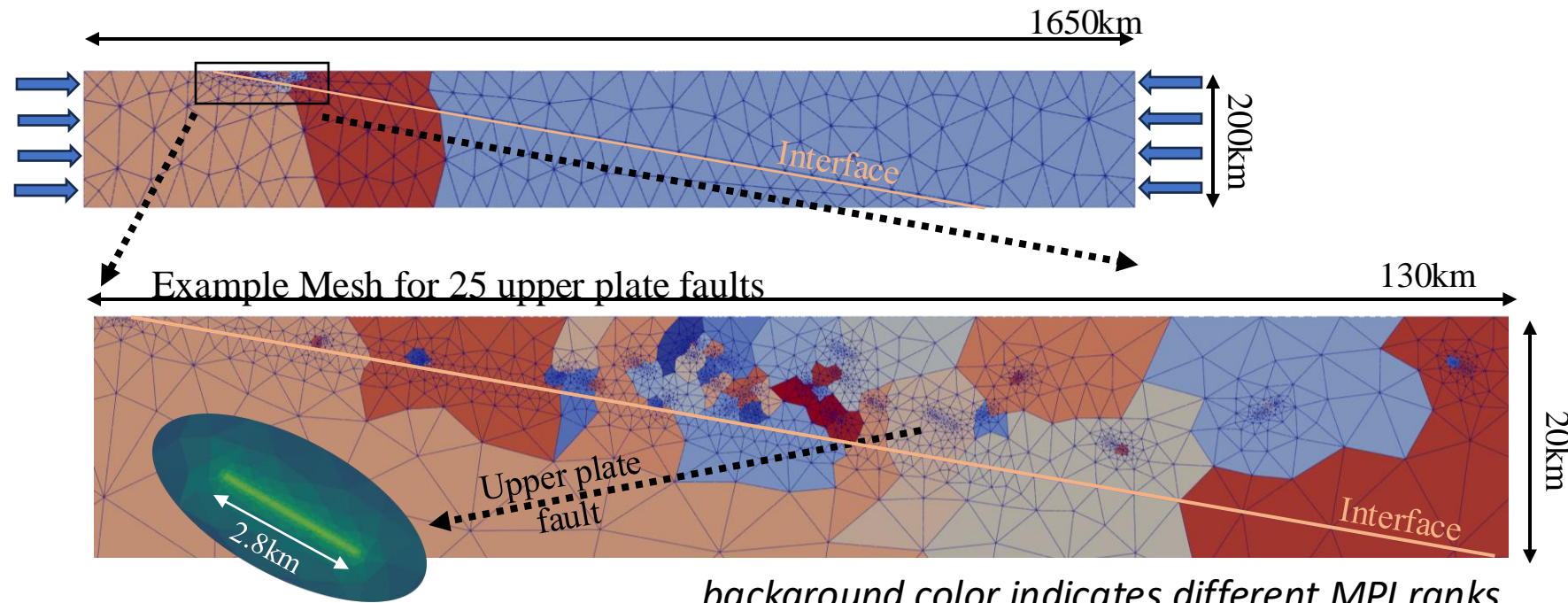
Our model also explains first-order observations of the correlations found between long-term fields such as **gravity anomalies**, **shelf breaks**, and **peninsulas** with short term processes like **megathrust earthquakes** and **fault locking**.



MODELING INTERSEISMIC INELASTIC DEFORMATION ACROSS UPPER PLATES

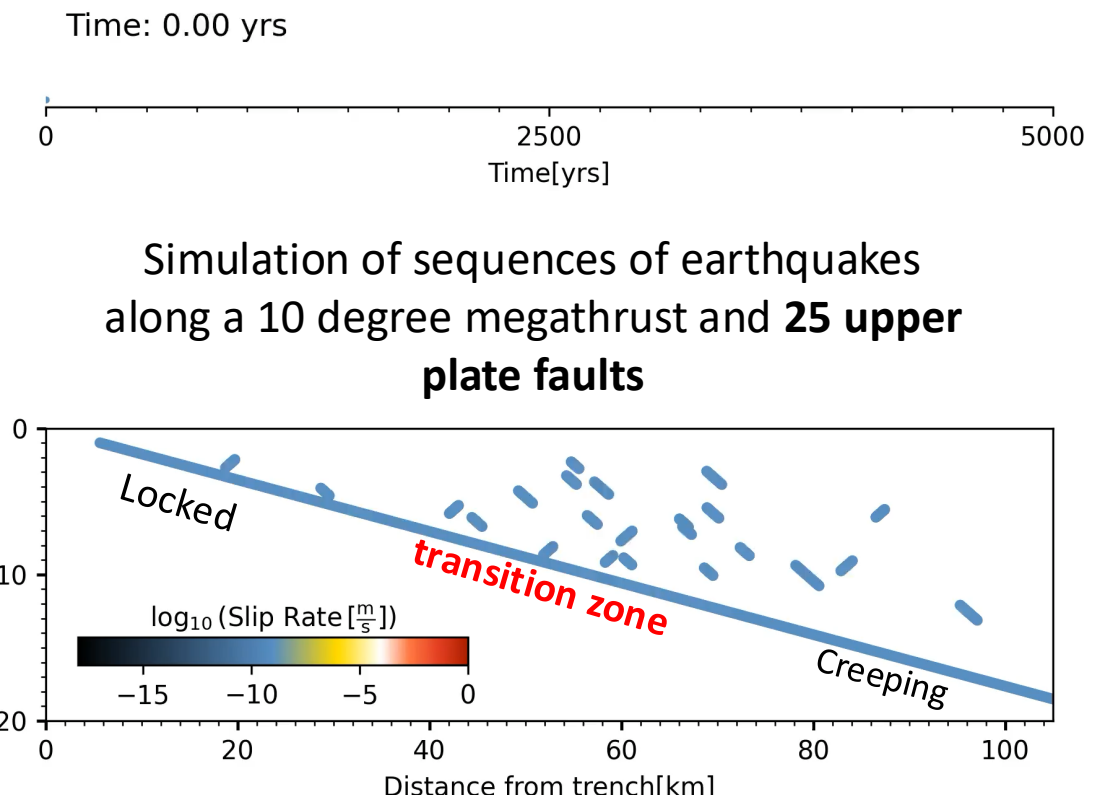
- Simulations of megathrust cycles combined with discrete, randomly distributed upper plate faults governed by rate-and-state friction laws provide a comprehensive and realistic physics base numerical model of the problem.

Unstructured triangular mesh used to model **megathrust and upper plate faults** using Discontinuous Galerkin method



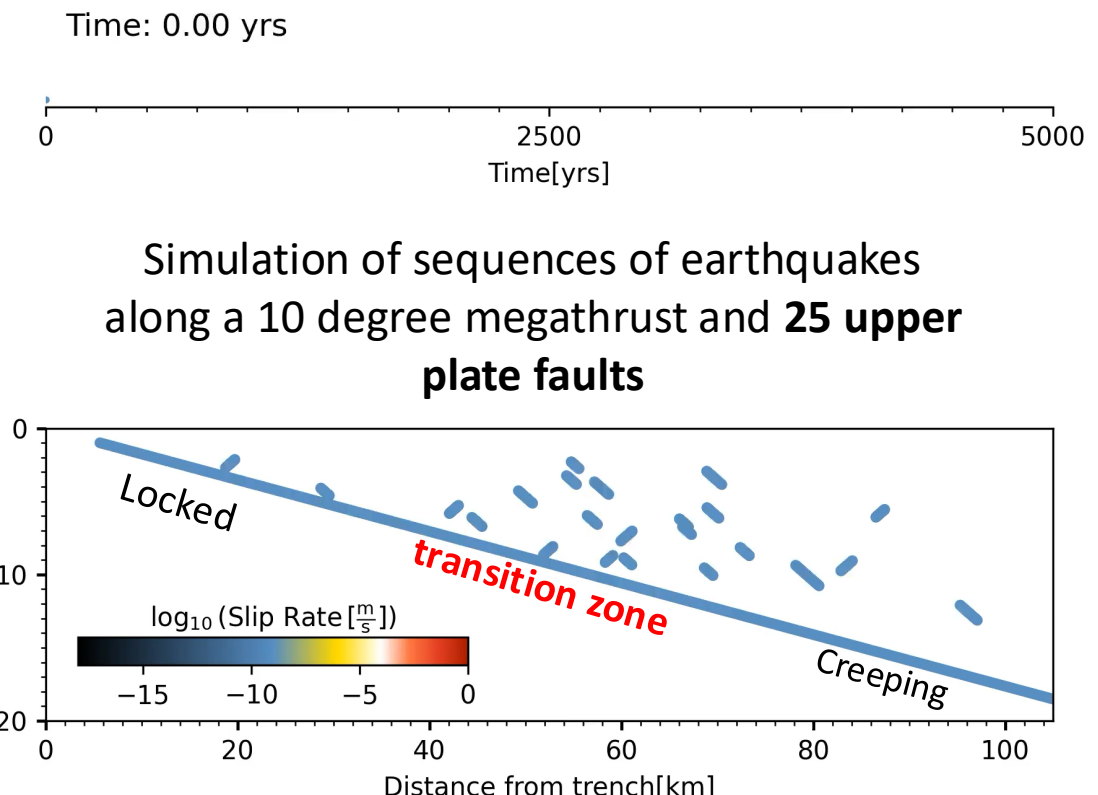
MODELING INTERSEISMIC INELASTIC DEFORMATION ACROSS UPPER PLATES

- Simulations of seismic cycles along a megathrust fault, combined with discrete, randomly distributed upper plate faults governed by rate-and-state friction laws, reveal that:
 - Upper plate faults can **fail interseismically** and generate earthquakes.



MODELING INTERSEISMIC INELASTIC DEFORMATION ACROSS UPPER PLATES

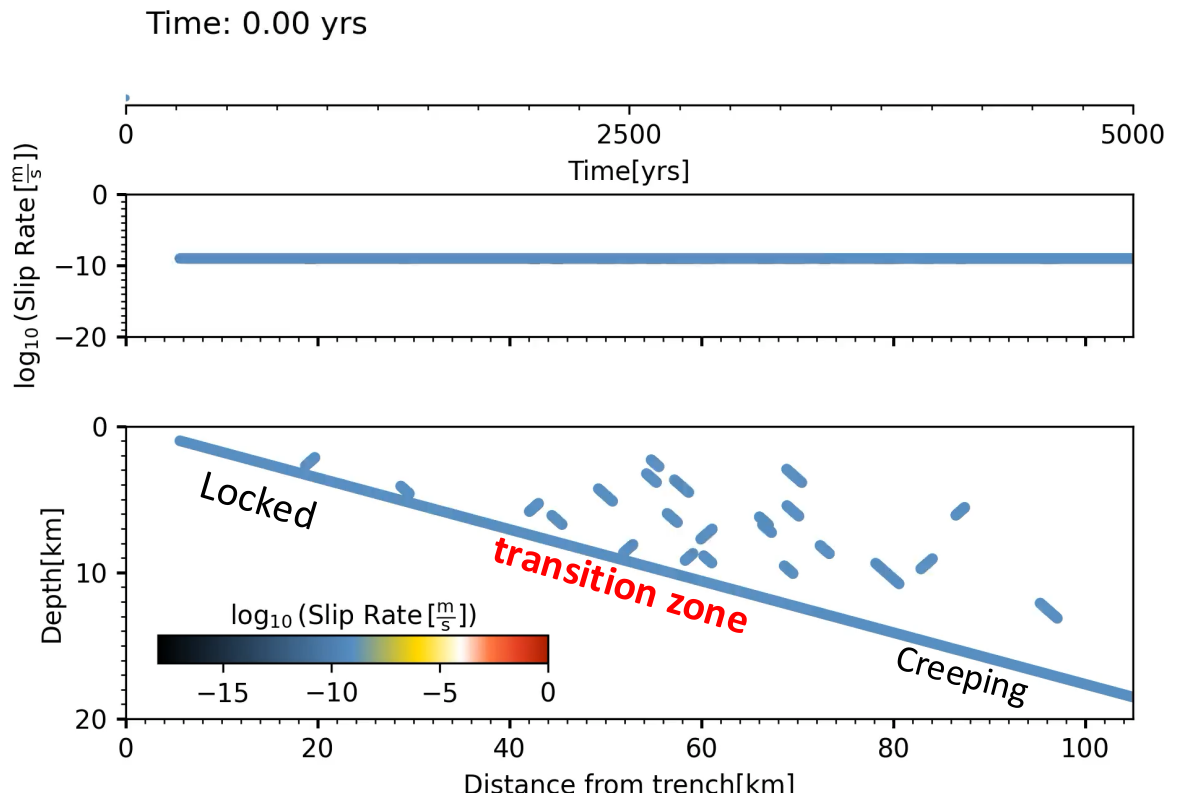
- Simulations of seismic cycles along a megathrust fault, combined with discrete, randomly distributed upper plate faults governed by rate-and-state friction laws, reveal that:
 - Upper plate faults can **fail interseismically** and generate earthquakes.



MODELING INTERSEISMIC INELASTIC DEFORMATION ACROSS UPPER PLATES

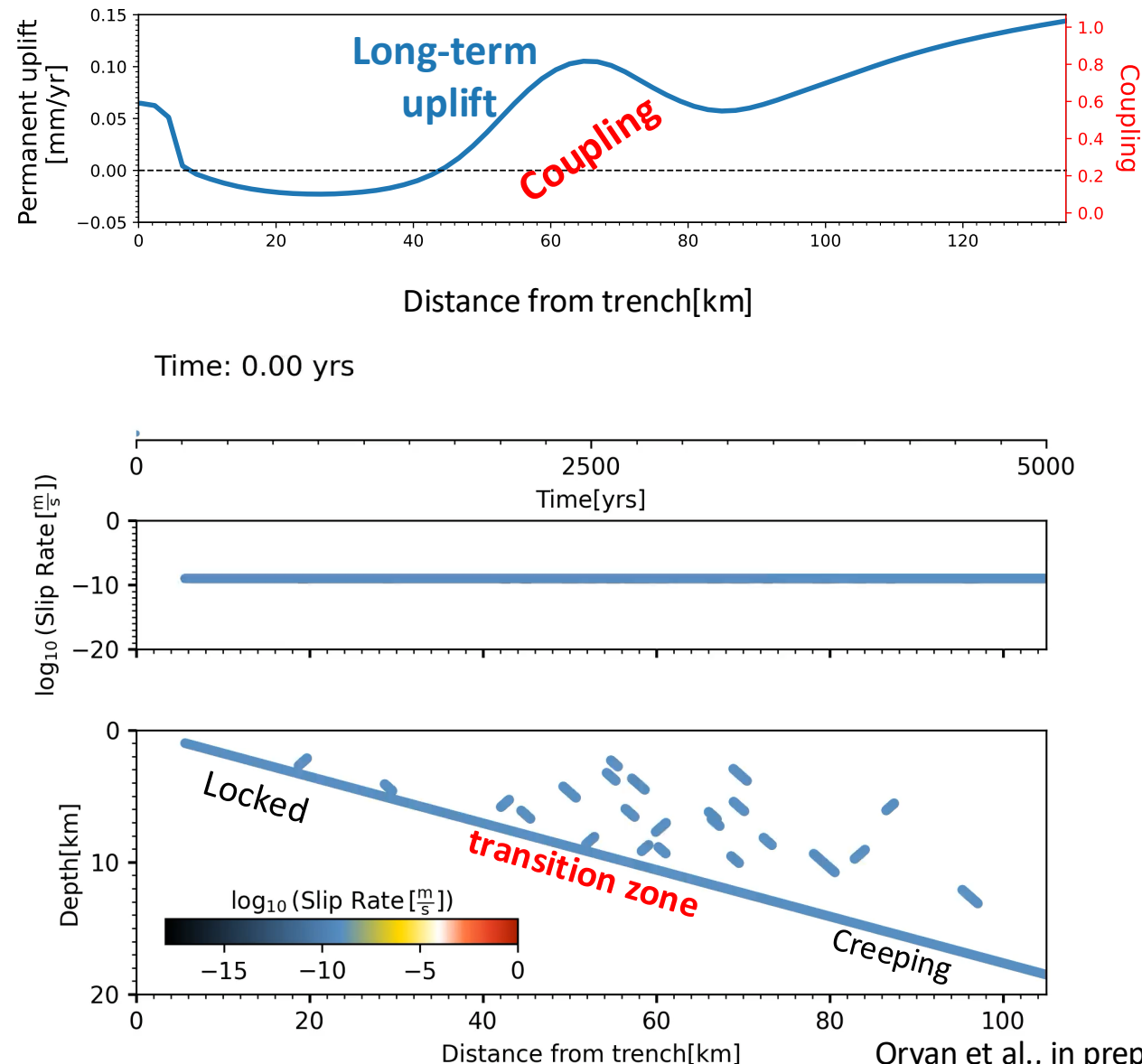
- Simulations of seismic cycles along a megathrust fault, combined with discrete, randomly distributed upper plate faults governed by rate-and-state friction laws, reveal that:
 - Upper plate faults can fail **interseismically** and generate earthquakes.

Simulation of sequences of earthquakes along a 10 degree megathrust and **25 upper plate faults**



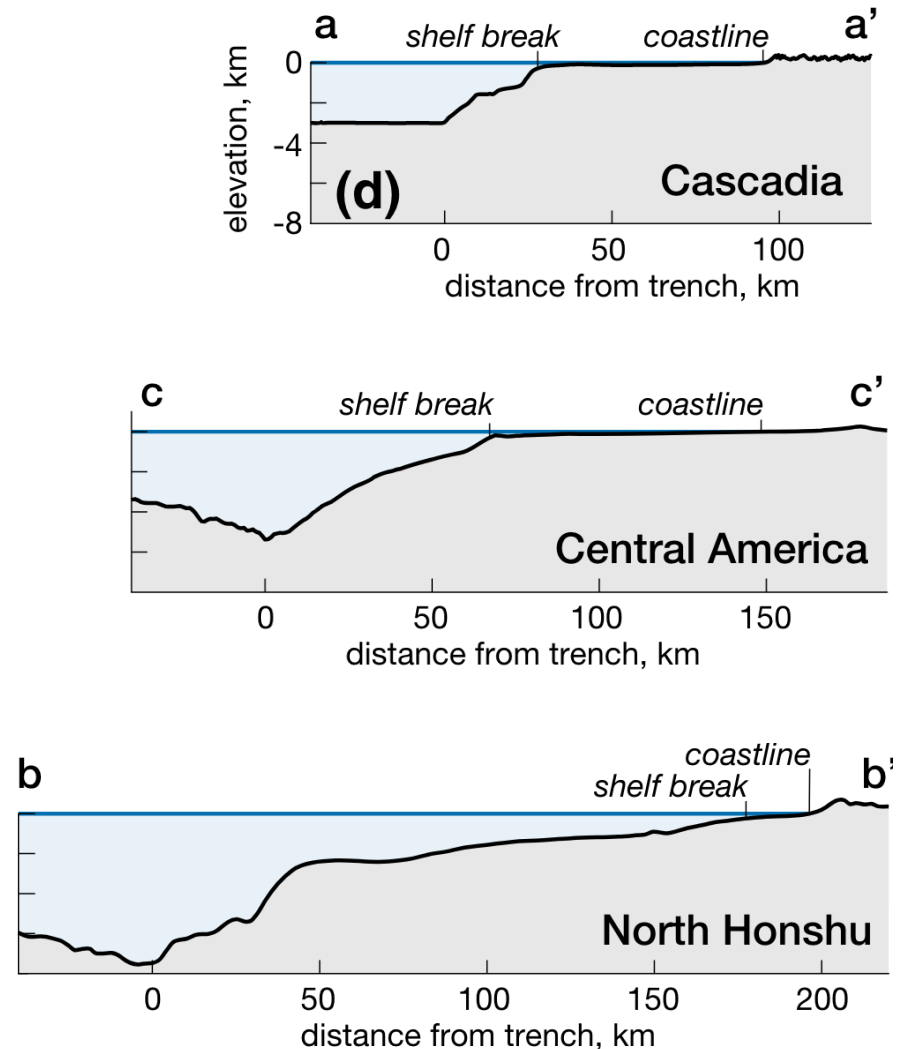
MODELING INTERSEISMIC INELASTIC DEFORMATION ACROSS UPPER PLATES

- Simulations of seismic cycles along a megathrust fault, combined with discrete, randomly distributed upper plate faults governed by rate-and-state friction laws, reveal that:
 - Upper plate faults can **fail interseismically** and generate earthquakes.
 - **Permanent uplift**, observed after four seismic cycles, **peaks above the transition zone**.



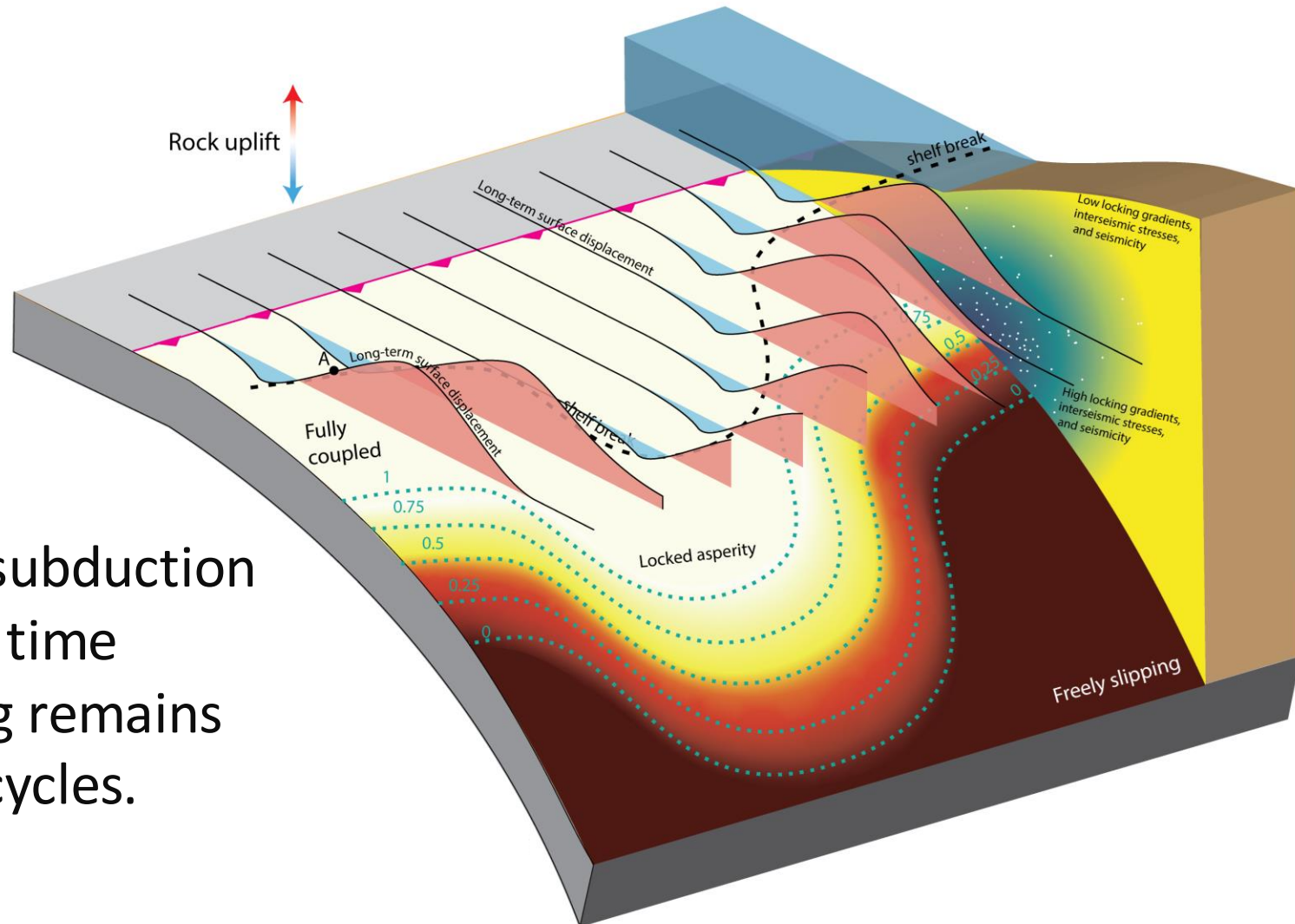
IMPLICATIONS FOR LONG-TERM PLATE COUPLING

- Our results imply that the downdip pattern of megathrust locking tends to **remain steady over hundreds of thousands of years**.
- Could the absence of a landscape signature indicative of **frequent changes in megathrust coupling**?

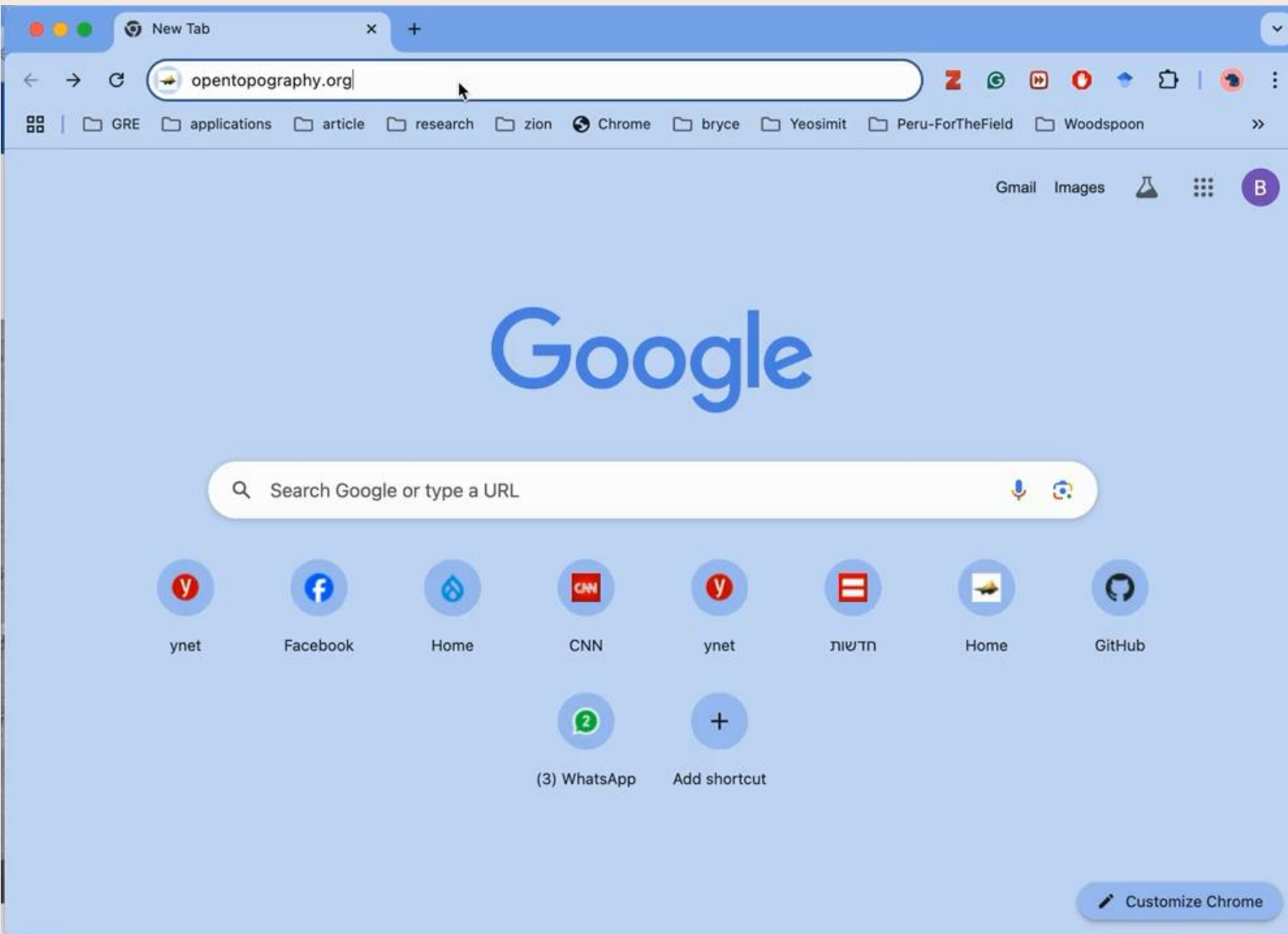


KEY POINTS SO FAR

- Variations in the degree of **megathrust locking** generate increments of **non-recoverable brittle deformation** within the overriding plate.
- This is expressed primarily as interseismic **upper plate seismicity**.
- Over time, this process **imprints** subduction landscapes one seismic cycle at a time
- This hints that megathrust locking remains stable over multiple earthquake cycles.

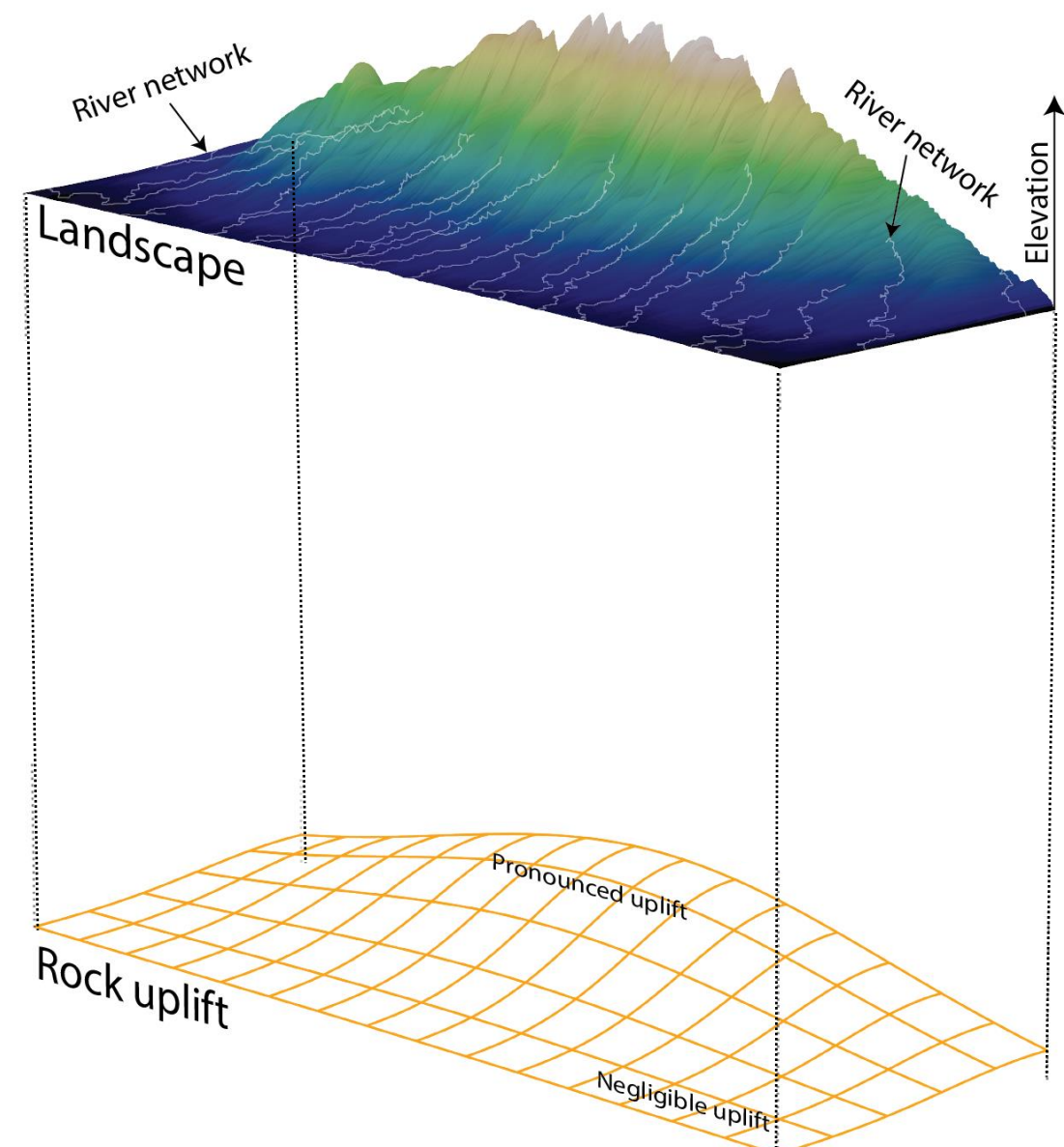


Section 3 - Inferring Long-Term Tectonic Uplift from Bayesian Inversion of Landscapes



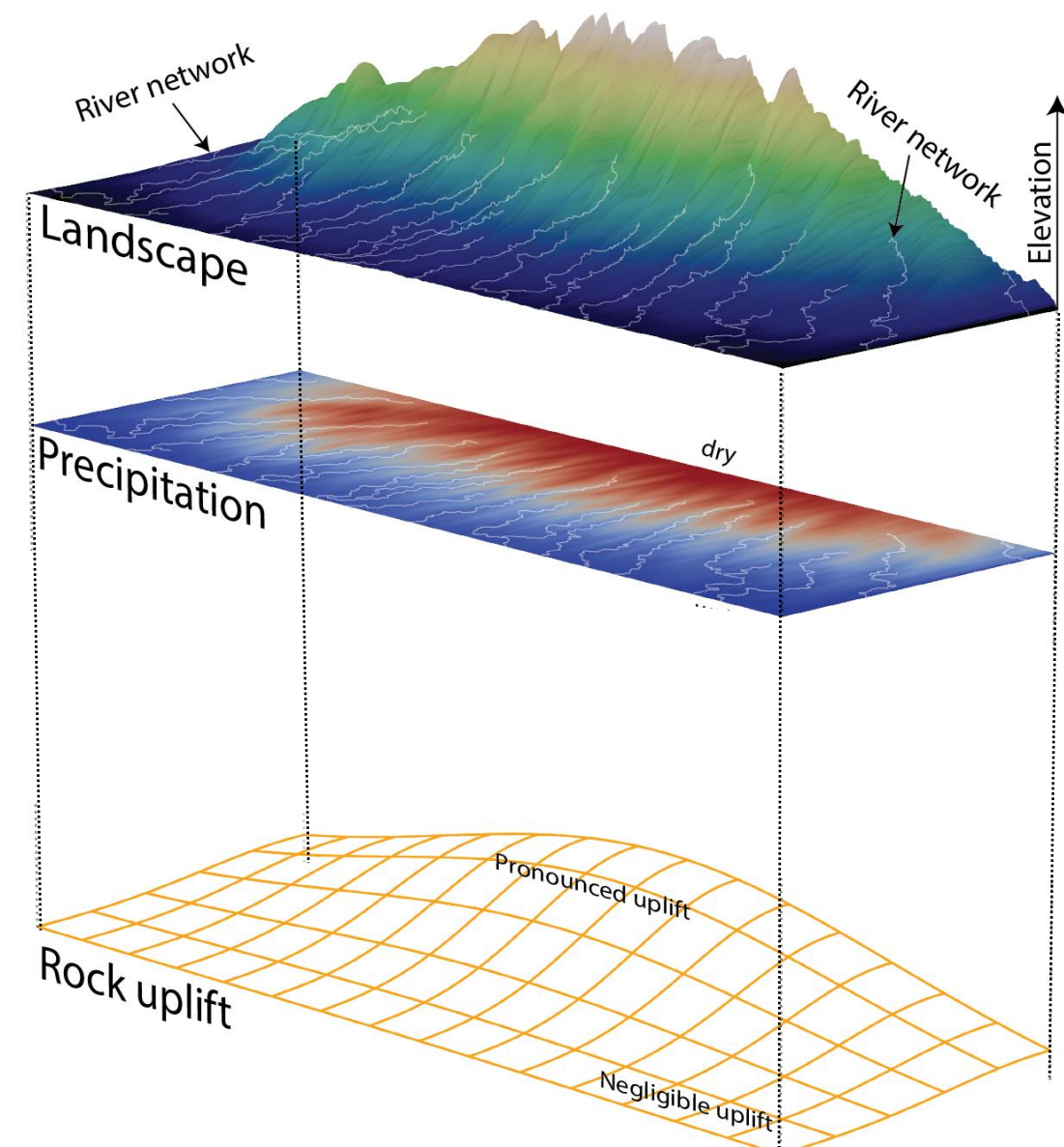
INFERRING LONG-TERM TECTONIC UPLIFT FROM BAYESIAN INVERSION OF LANDSCAPES

- Landscapes encode the forcing of **tectonic uplift**



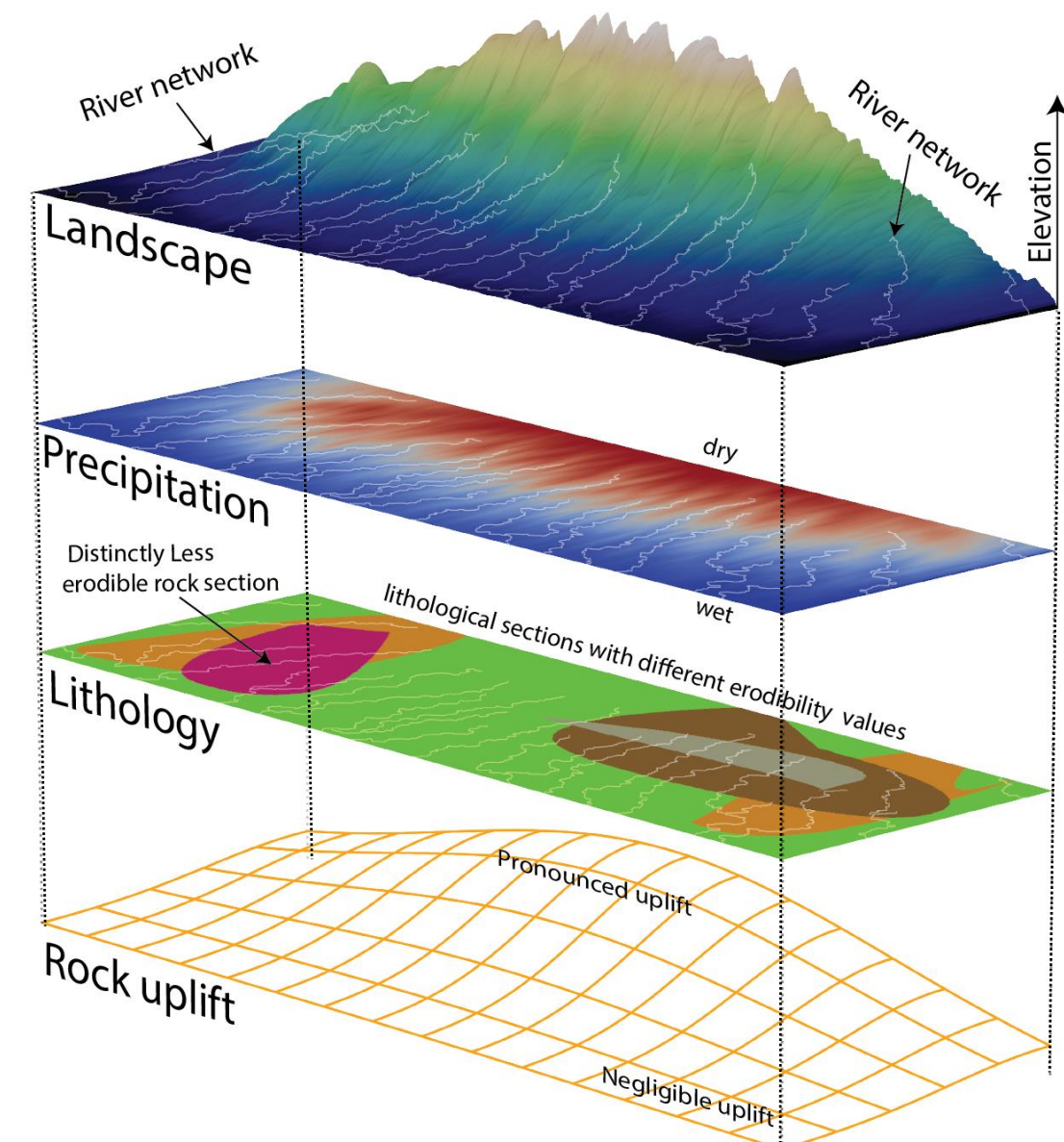
INFERRING LONG-TERM TECTONIC UPLIFT FROM BAYESIAN INVERSION OF LANDSCAPES

- Landscapes encode the combined forcing of **tectonic uplift** and erosion driven by **climate**



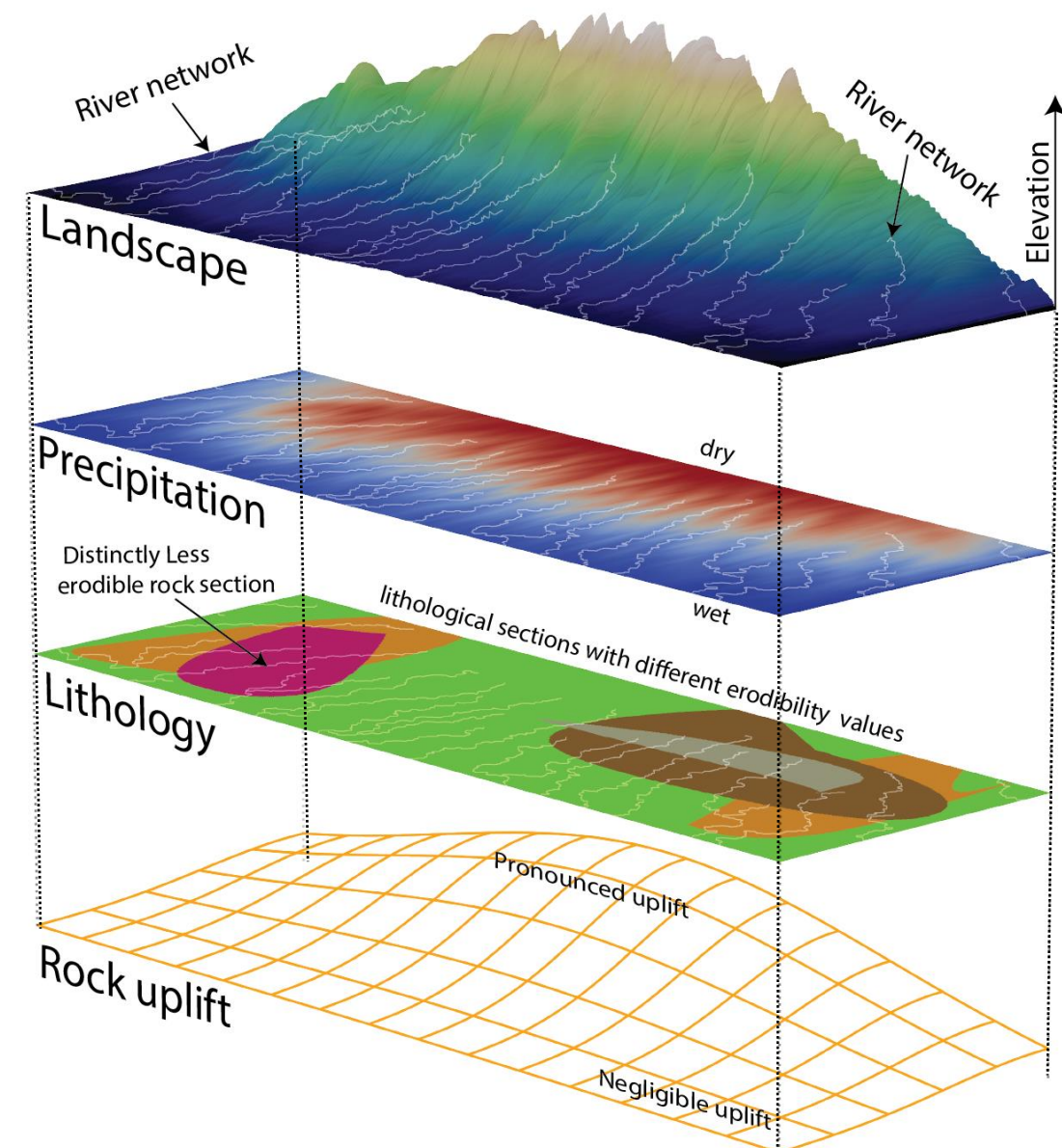
INFERRING LONG-TERM TECTONIC UPLIFT FROM BAYESIAN INVERSION OF LANDSCAPES

- Landscapes encode the combined forcing of **tectonic uplift** and erosion driven by **climate** and **rock erodibility**.

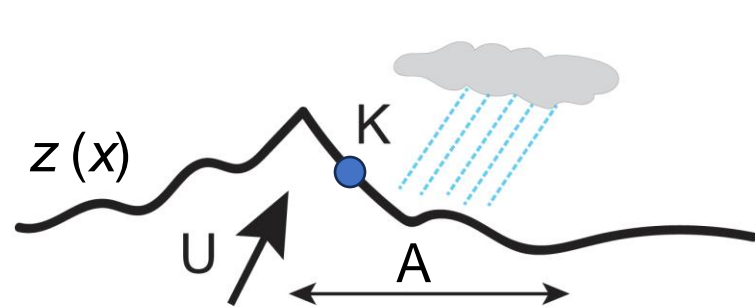


INFERRING LONG-TERM TECTONIC UPLIFT FROM BAYESIAN INVERSION OF LANDSCAPES

- Landscapes encode the combined forcing of **tectonic uplift** and erosion driven by **climate** and **rock erodibility**.
- Disentangling their contributions is essential for using landscapes as quantitative records of crustal deformation.



RIVER INCISION AT STEADY STATE



$$U(X) \uparrow = \downarrow K(x)A^m(x)S^n(x)$$

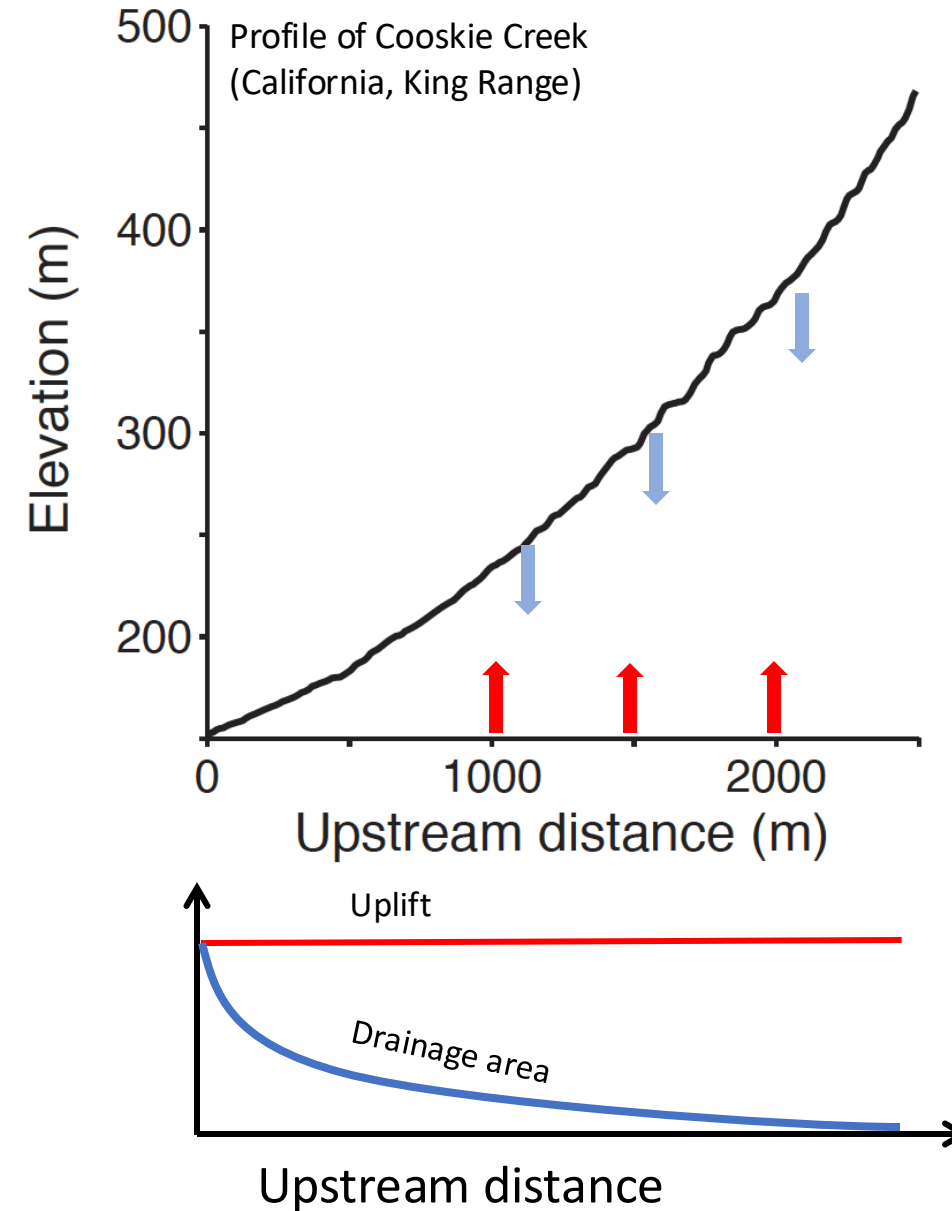
Tectonic
uplift

Local incision rate
(faster for steeper
slope S , with more
water flowing and
larger erodibility)

Parameters:

- erodibility (K)
- drainage area (A)
- exponents (m, n)

RIVER INCISION AT STEADY STATE



$$U(X) \uparrow = \downarrow K(x)A^m(x)S^n(x)$$

Tectonic
uplift

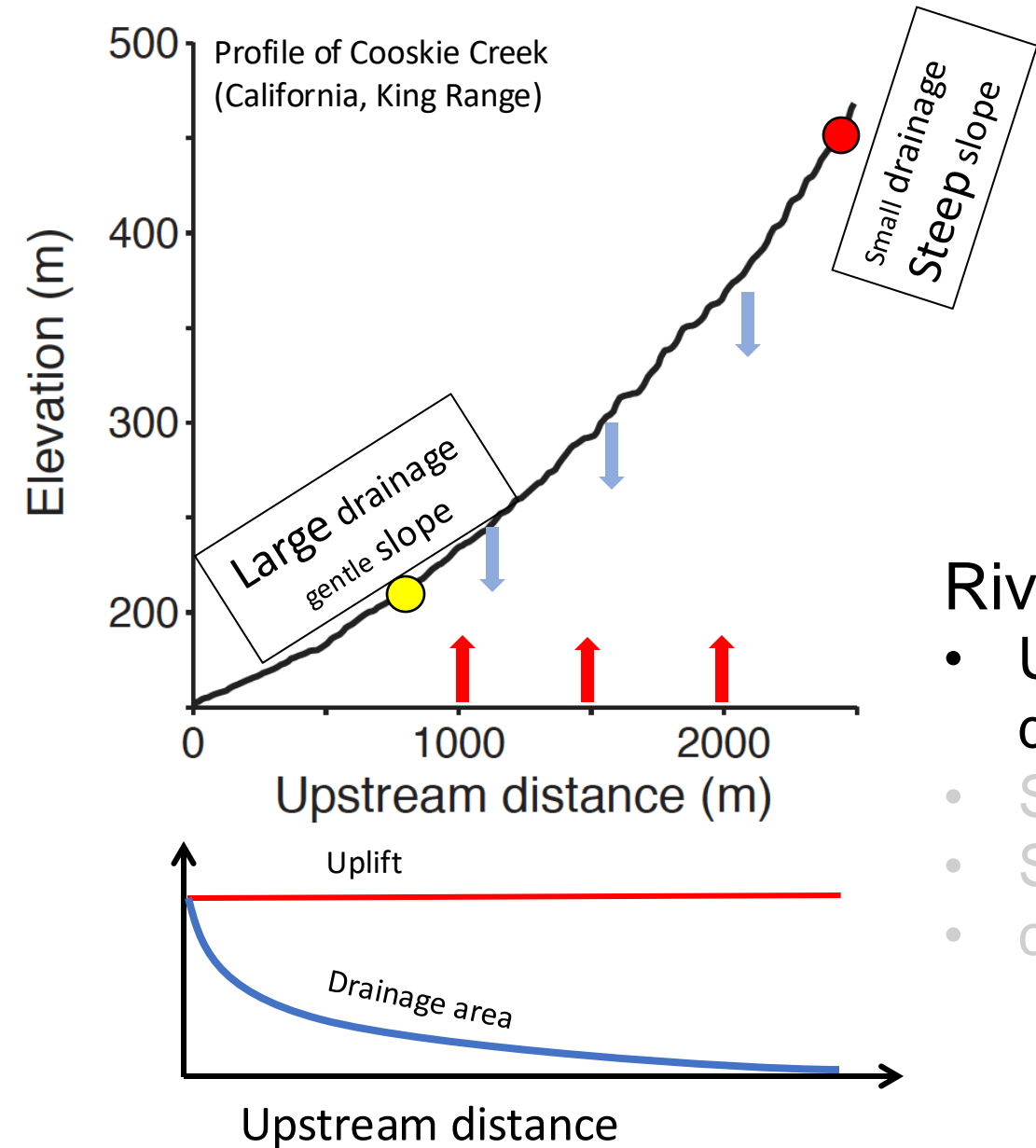
- River concavity reflects:
- Upstream decrease in drainage area
 - Shape of uplift
 - Spatially variable erodibility
 - climate

Local incision rate
(faster for steeper slope S , with more water flowing and larger erodibility)

Parameters:

- erodibility (K)
- drainage area (A)
- exponents (m, n)

RIVER INCISION AT STEADY STATE



$$U(X) \uparrow = K(x)A^m(x)S^n(x) \downarrow$$

Tectonic uplift

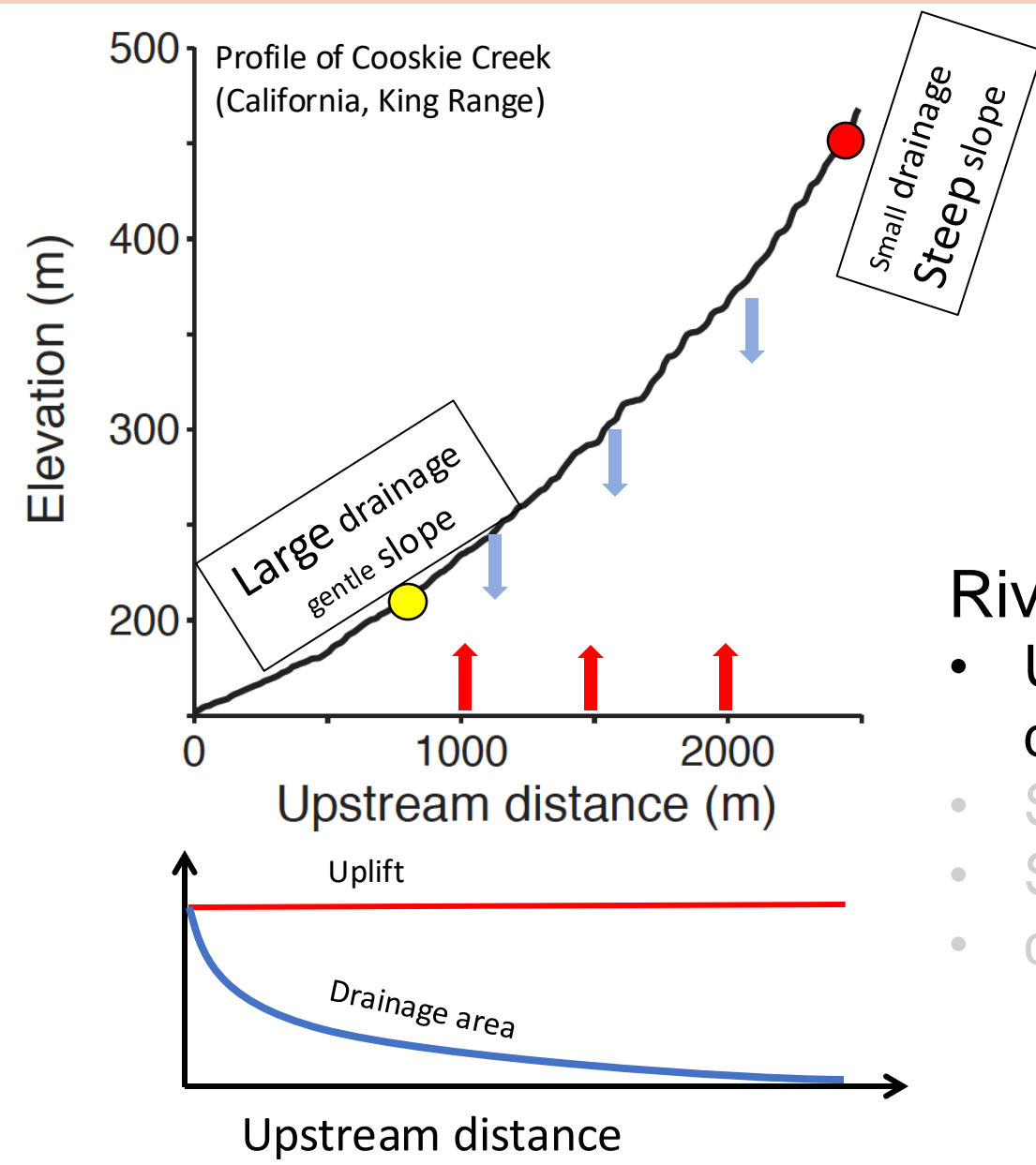
- River concavity reflects:
- Upstream decrease in drainage area
 - Shape of uplift
 - Spatially variable erodibility
 - climate

Local incision rate
(faster for steeper slope S , with more water flowing and larger erodibility)

Parameters:

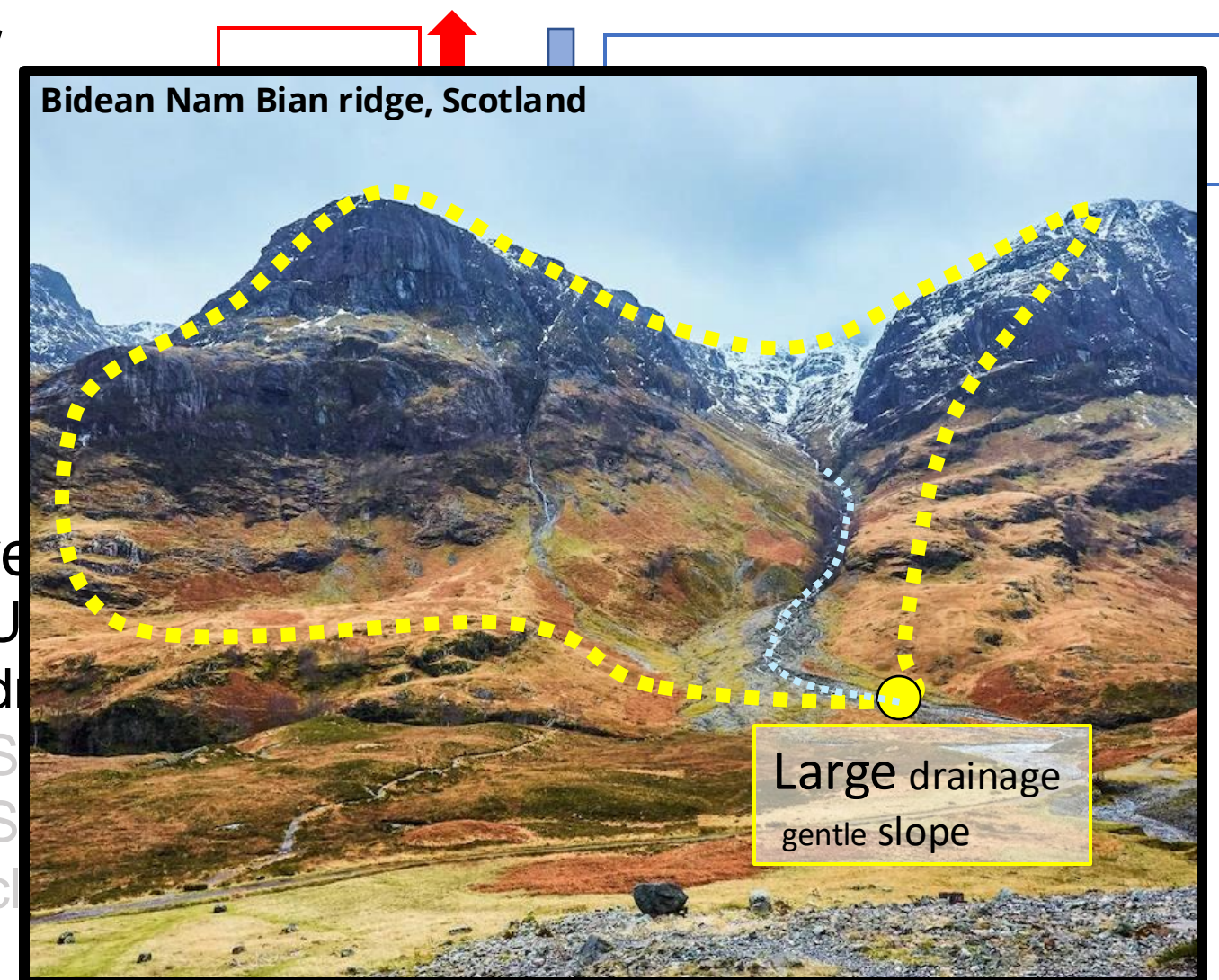
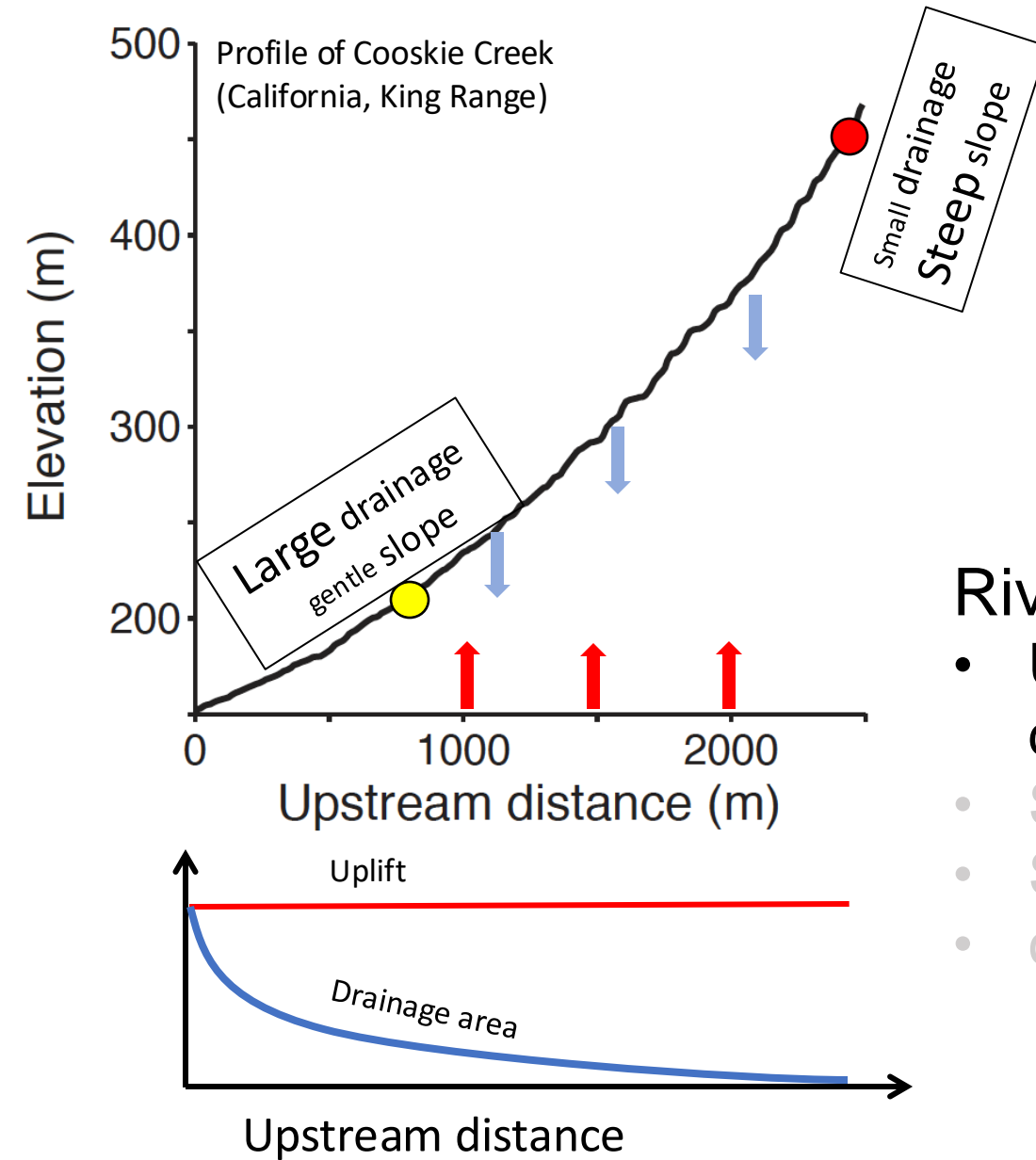
- erodibility (K)
- drainage area (A)
- exponents (m, n)

RIVER INCISION AT STEADY STATE

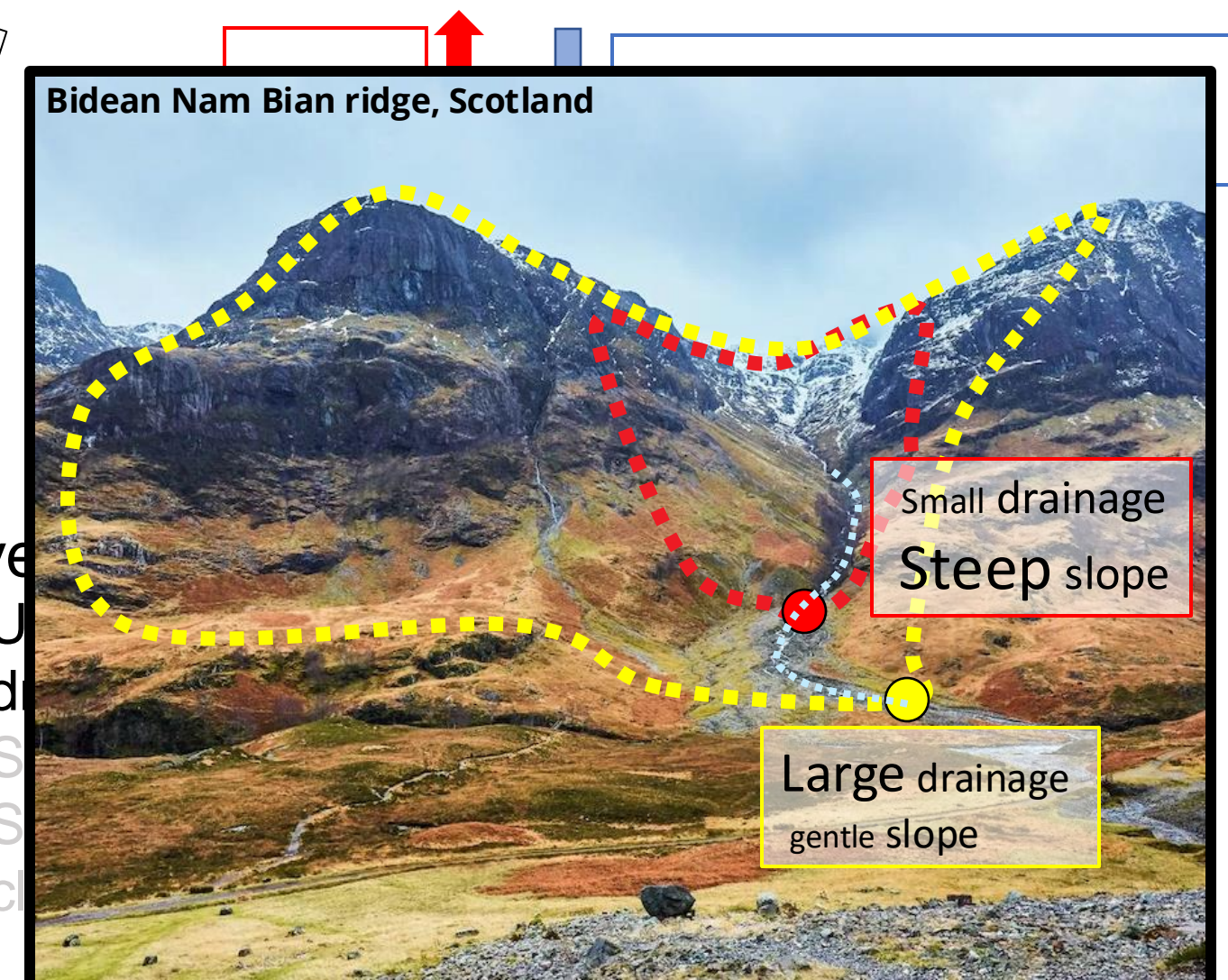
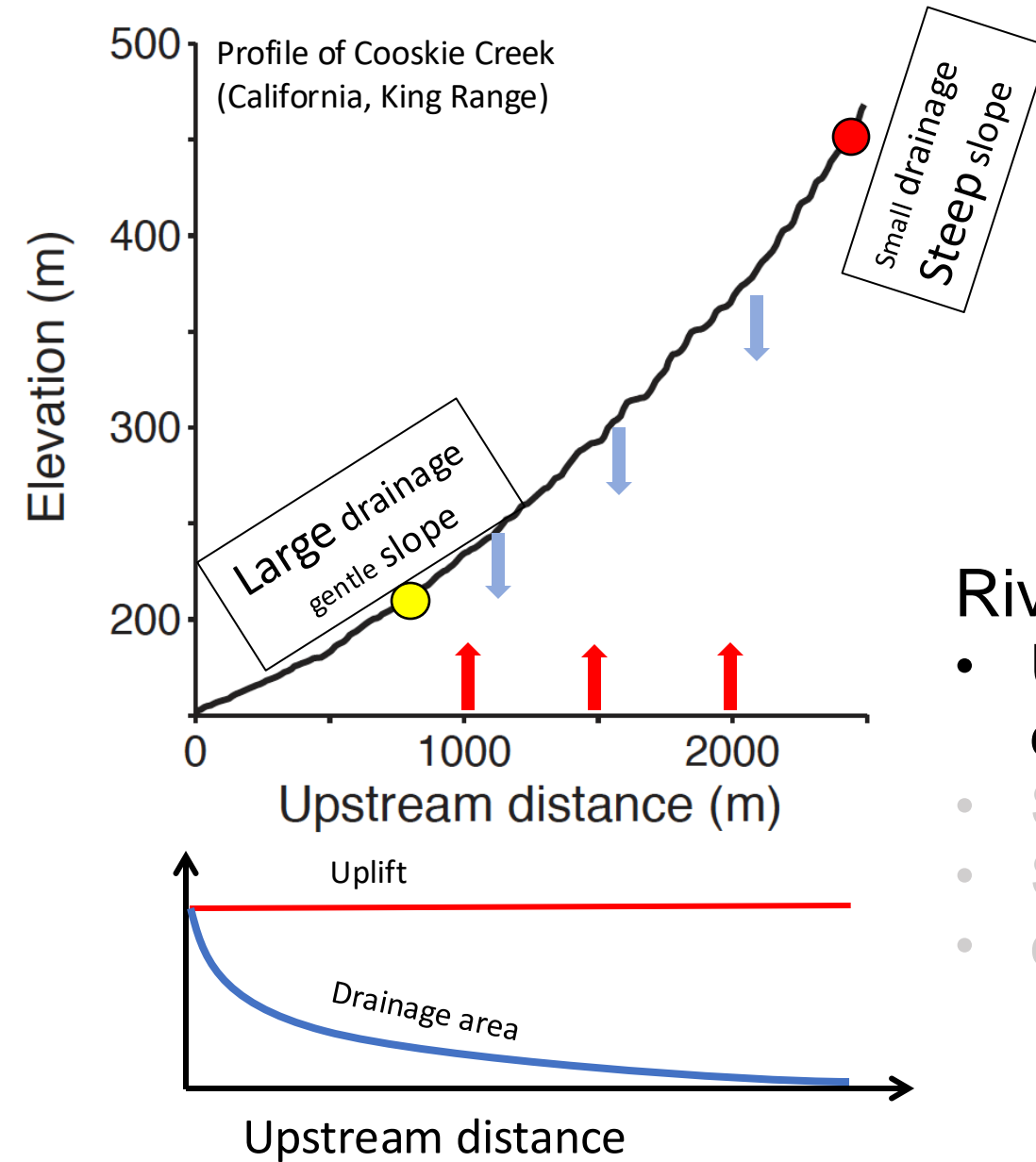


- River
- Uplift
- Drainage area
- Steep slope
- Gentle slope
- Large drainage
- Small drainage

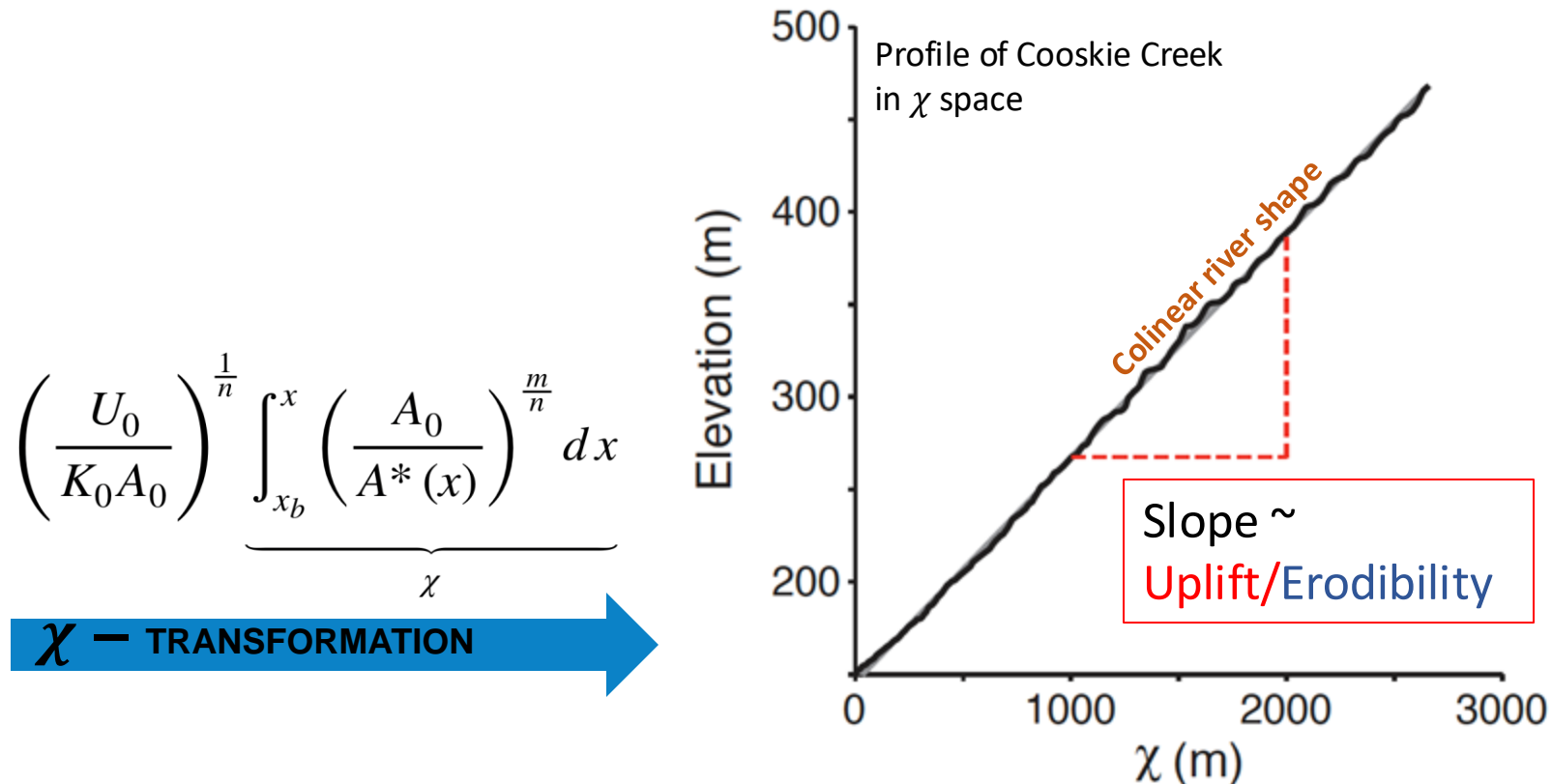
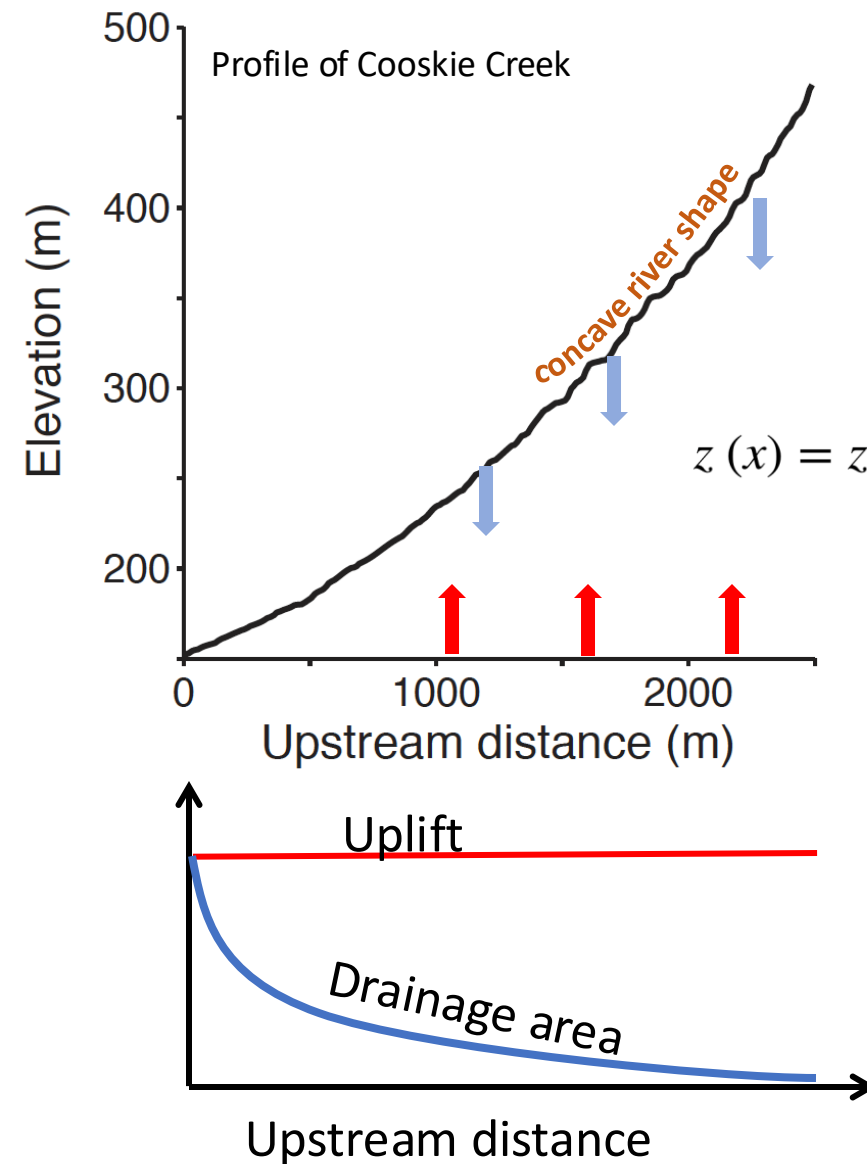
RIVER INCISION AT STEADY STATE



RIVER INCISION AT STEADY STATE

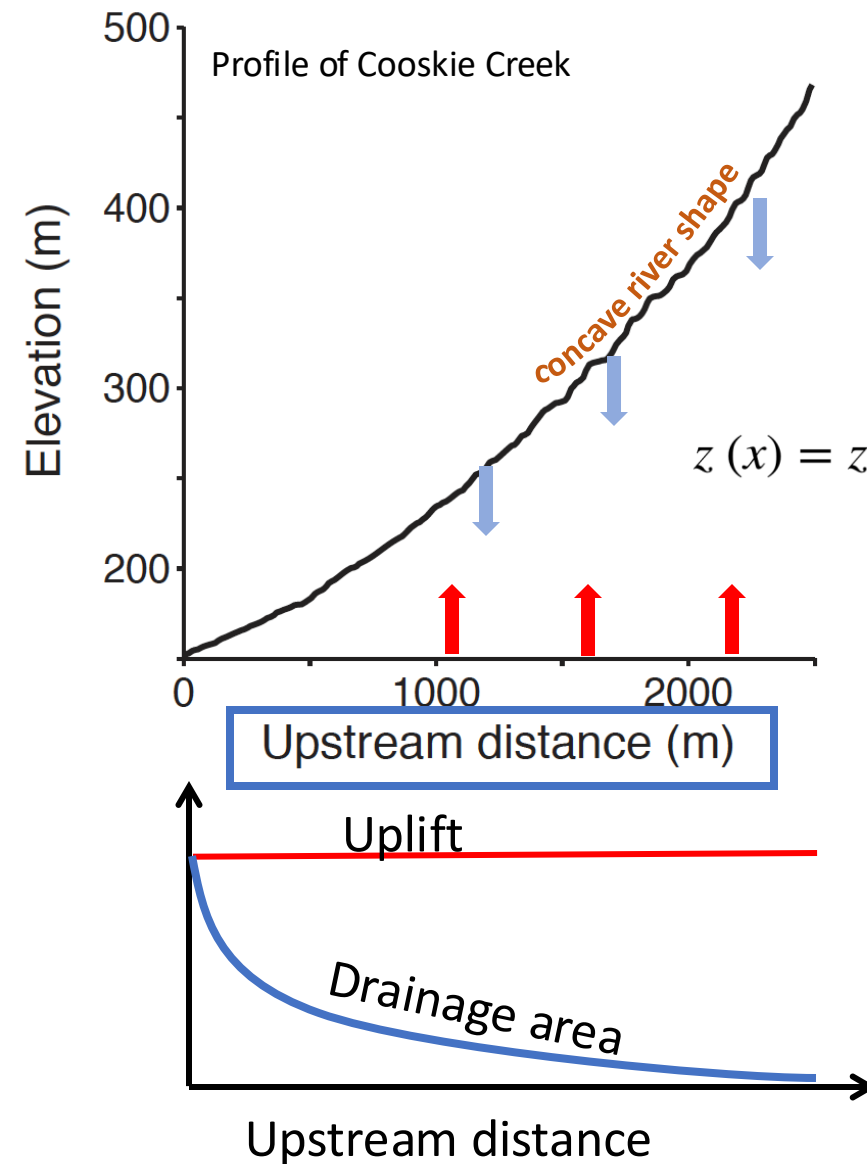


χ – TRANSFORMATION OF RIVERS



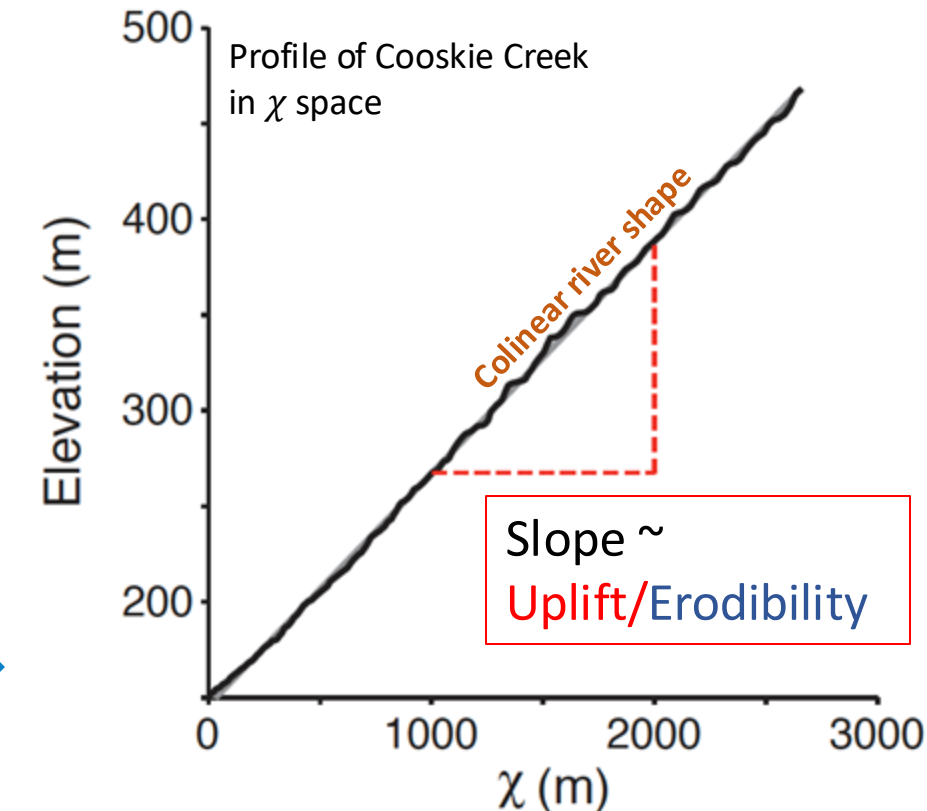
Corrects for upstream decrease in drainage area while assuming uniform spatial uplift

χ – TRANSFORMATION OF RIVERS



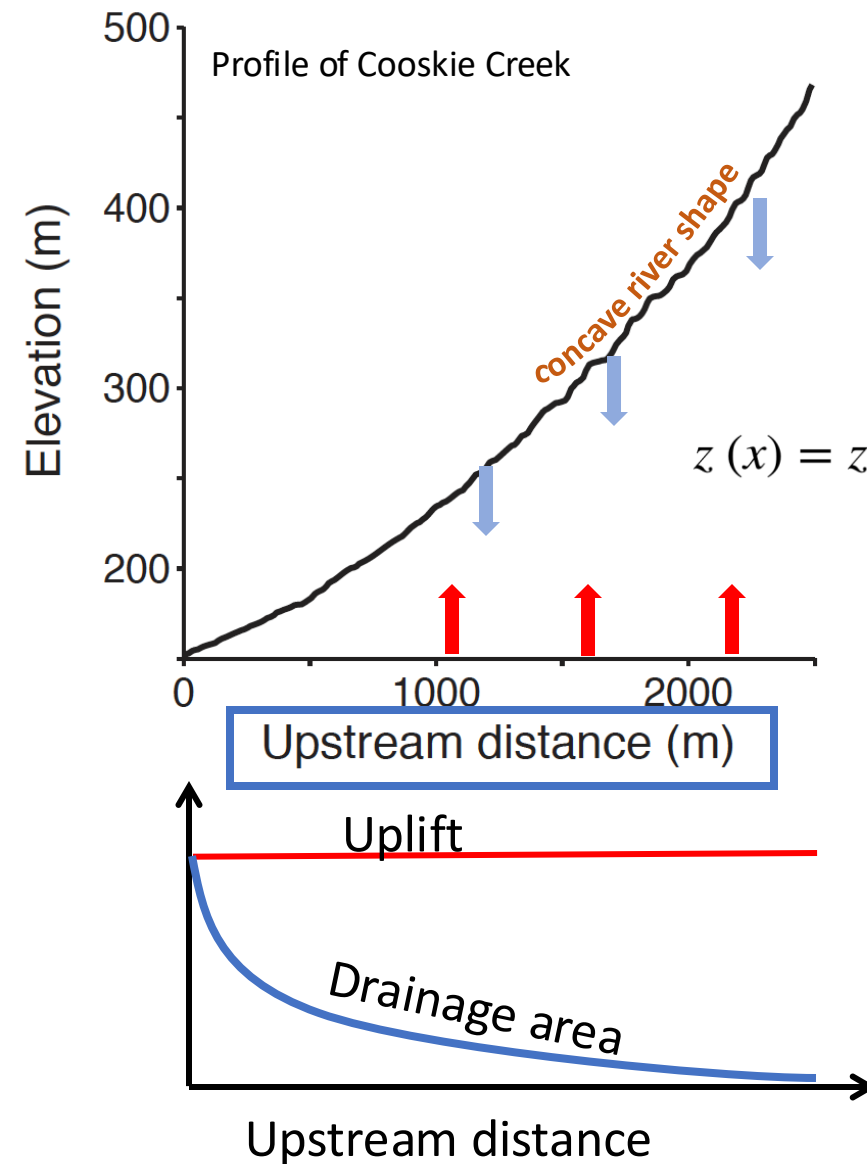
$$z(x) = z_b + \left(\frac{U_0}{K_0 A_0} \right)^{\frac{1}{n}} \underbrace{\int_{x_b}^x \left(\frac{A_0}{A^*(x)} \right)^{\frac{m}{n}} dx}_{\chi}$$

χ – TRANSFORMATION



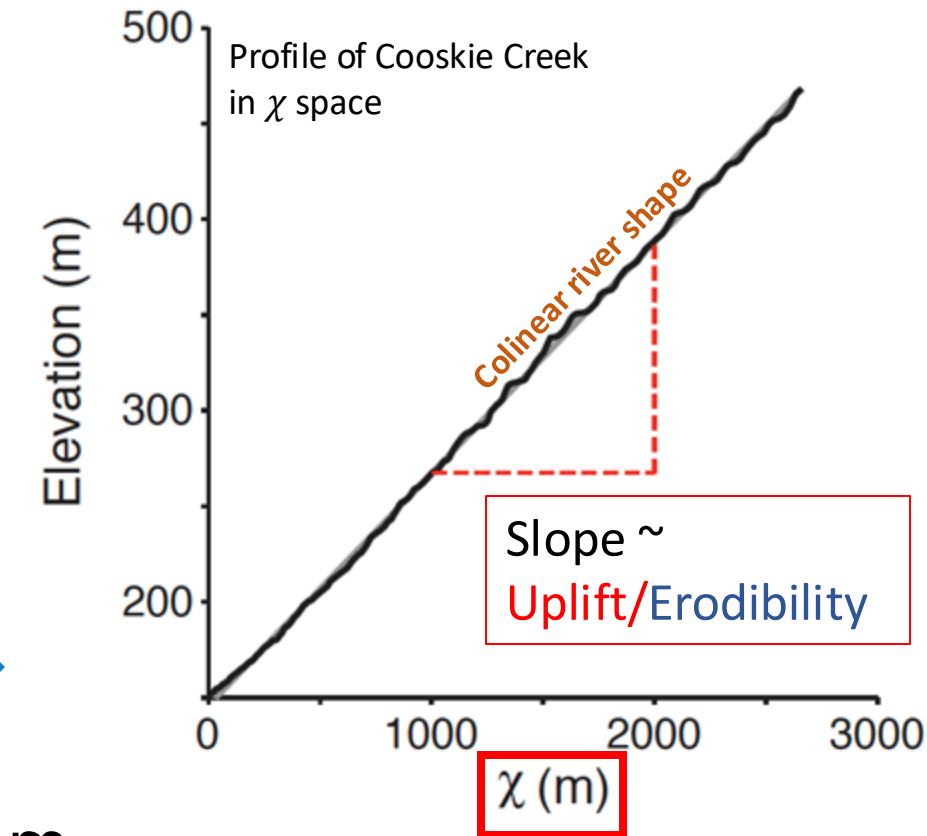
Corrects for upstream decrease in drainage area while assuming uniform spatial uplift

χ – TRANSFORMATION OF RIVERS



$$z(x) = z_b + \left(\frac{U_0}{K_0 A_0} \right)^{\frac{1}{n}} \int_{x_b}^x \left(\frac{A_0}{A^*(x)} \right)^{\frac{m}{n}} dx$$

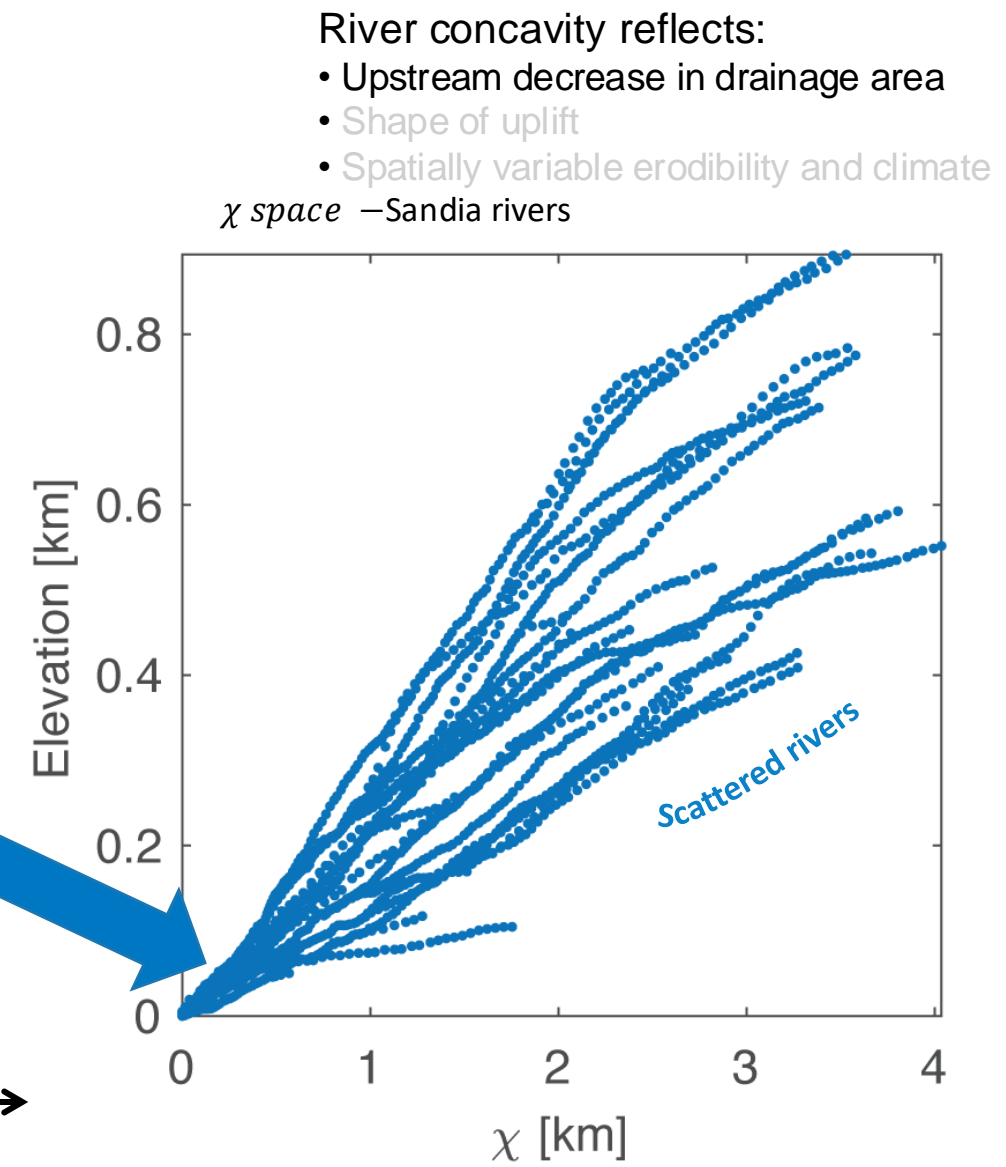
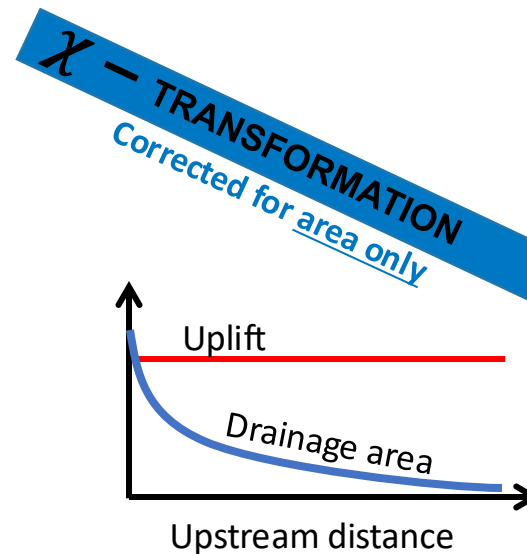
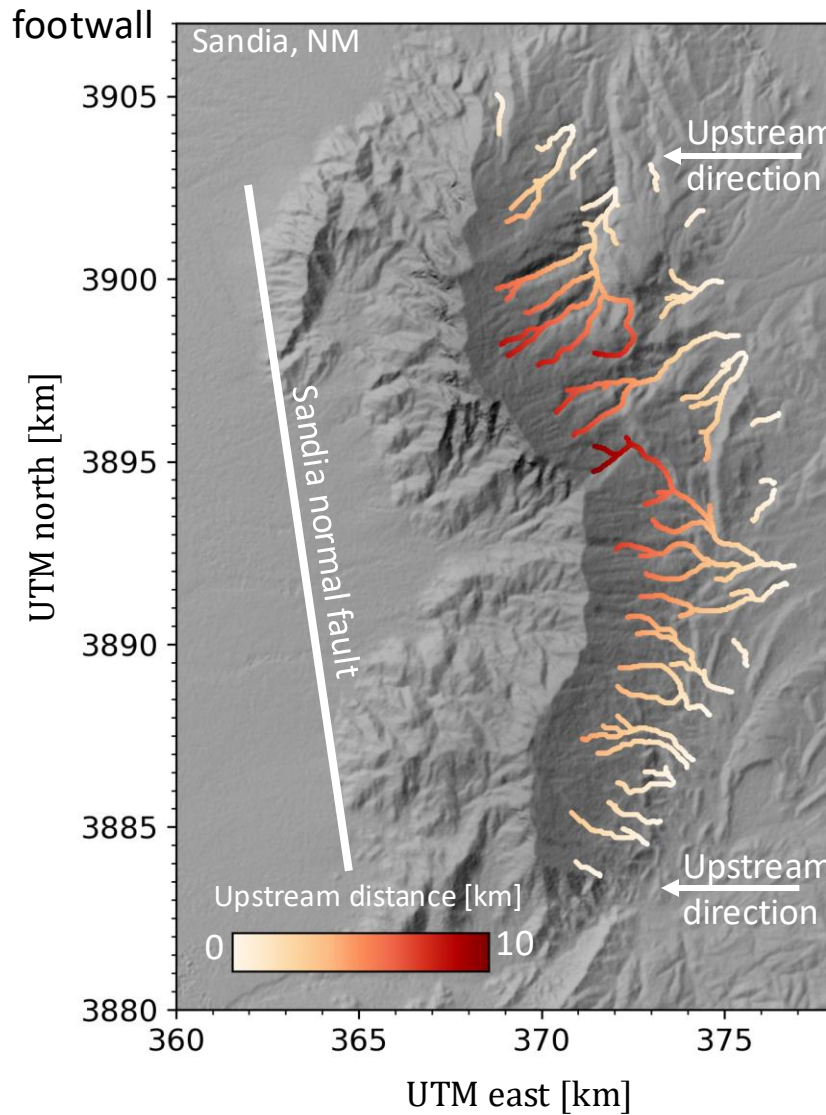
χ – TRANSFORMATION



Corrects for upstream decrease in drainage area while assuming uniform spatial uplift

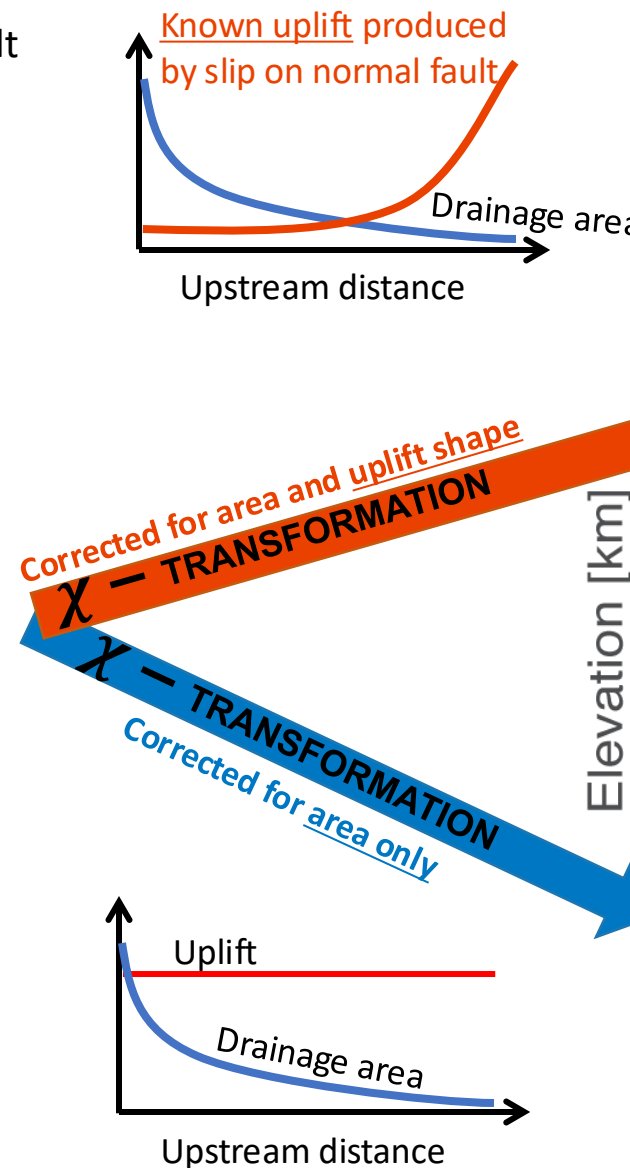
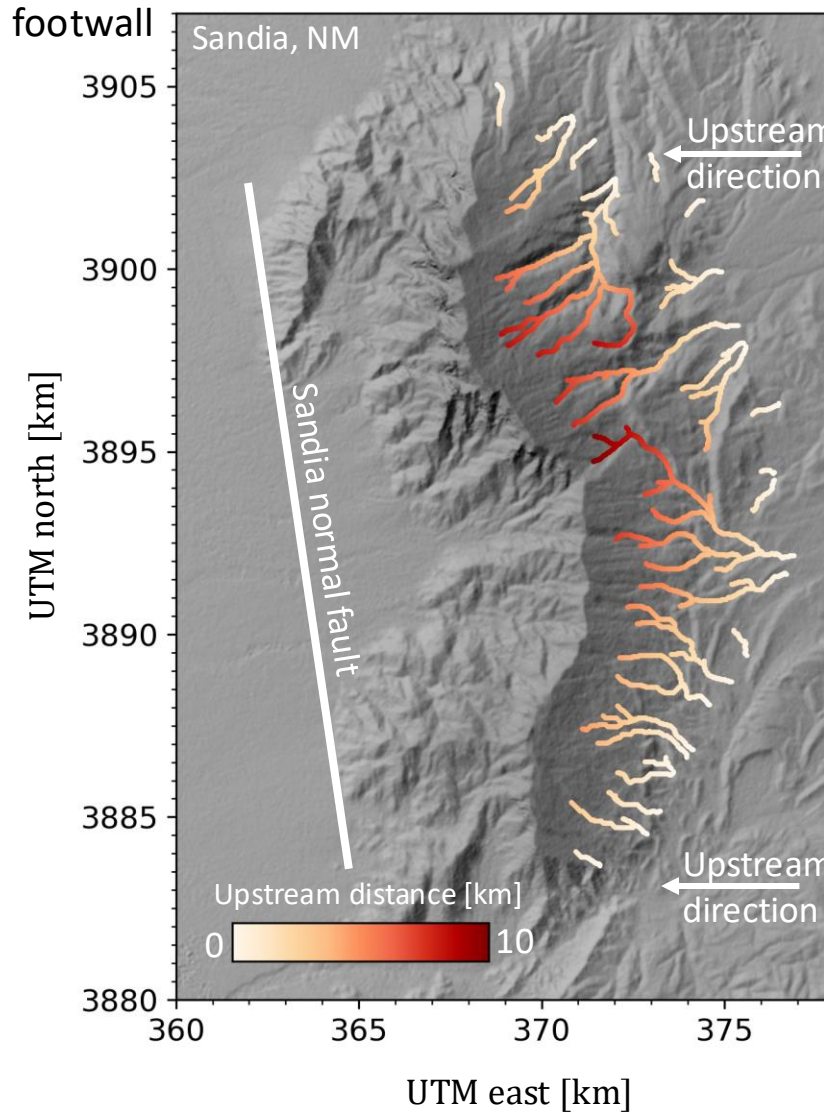
χ - TRANSFORMATION OF RIVER PROFILES IN SANDIA

Application to simple tectonic settings - normal fault



χ - TRANSFORMATION OF RIVER PROFILES IN SANDIA

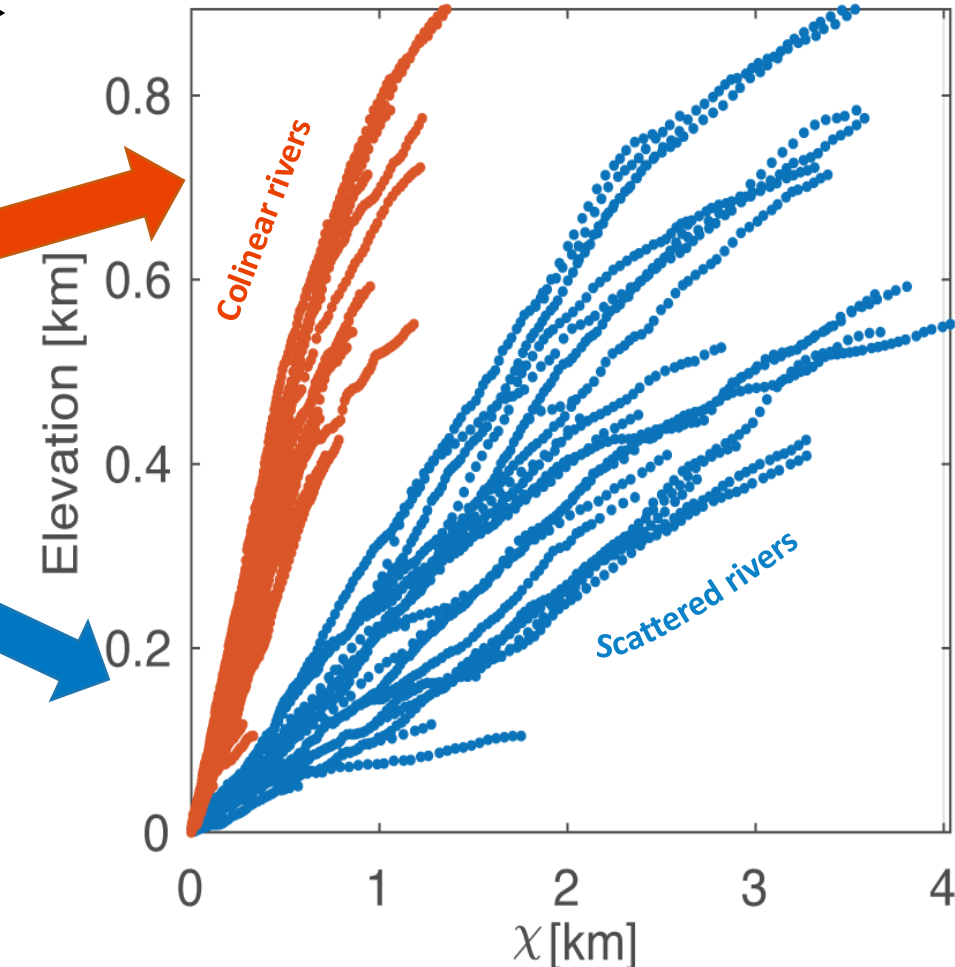
Application to simple tectonic settings - normal fault



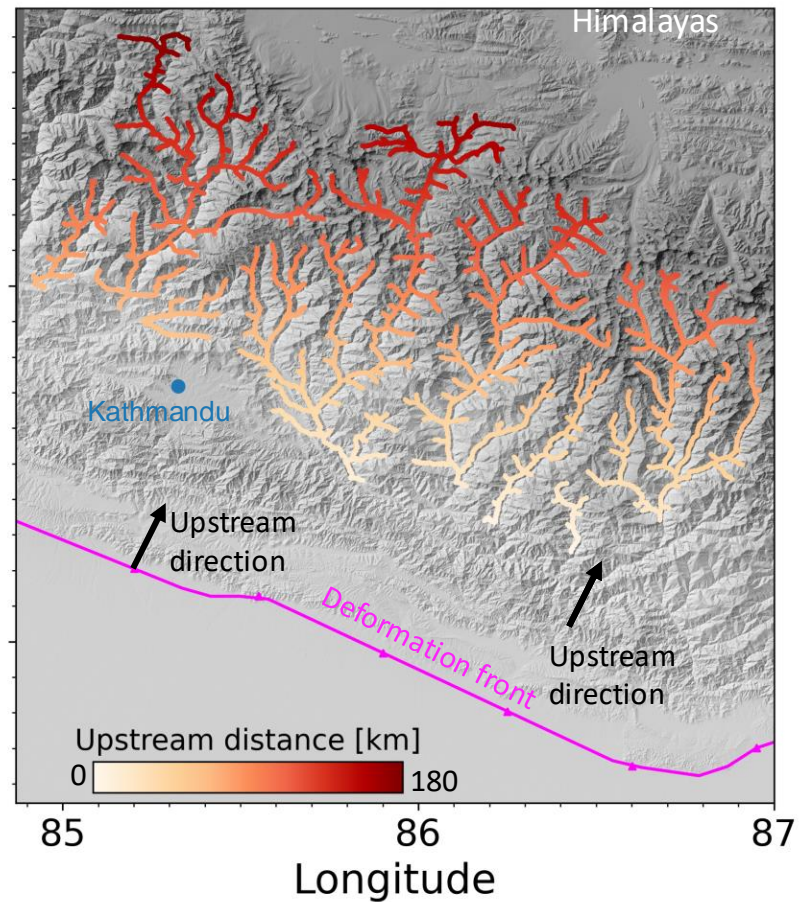
River concavity reflects:

- Upstream decrease in drainage area
- Shape of uplift
- Spatially variable erodibility and climate

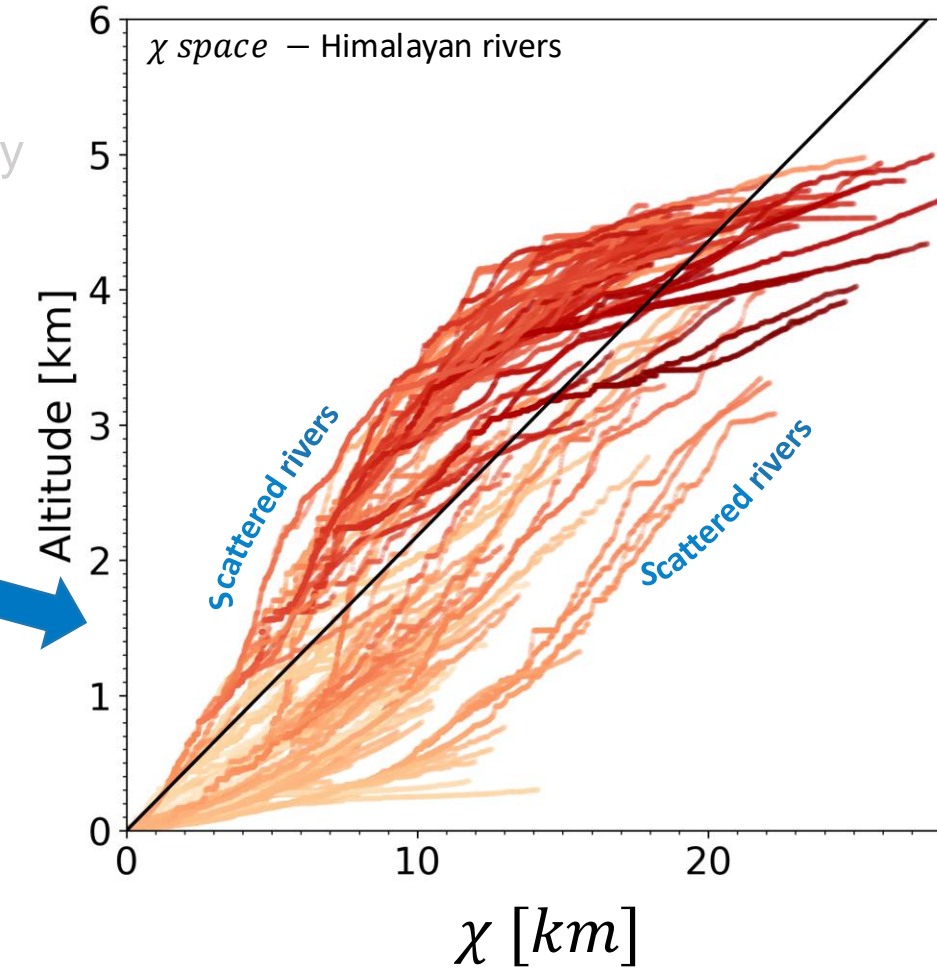
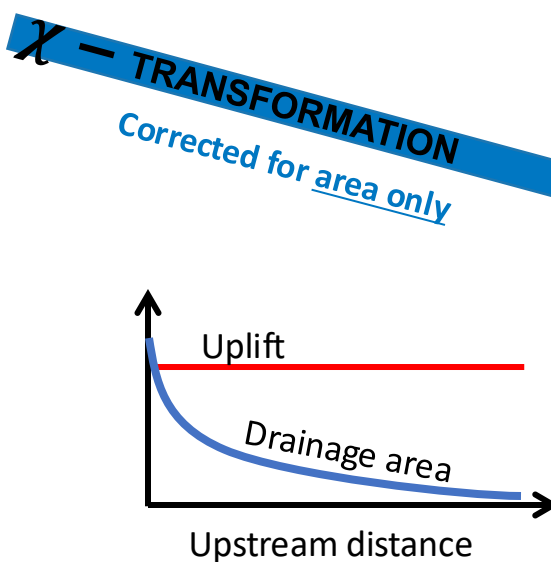
χ space – Sandia rivers



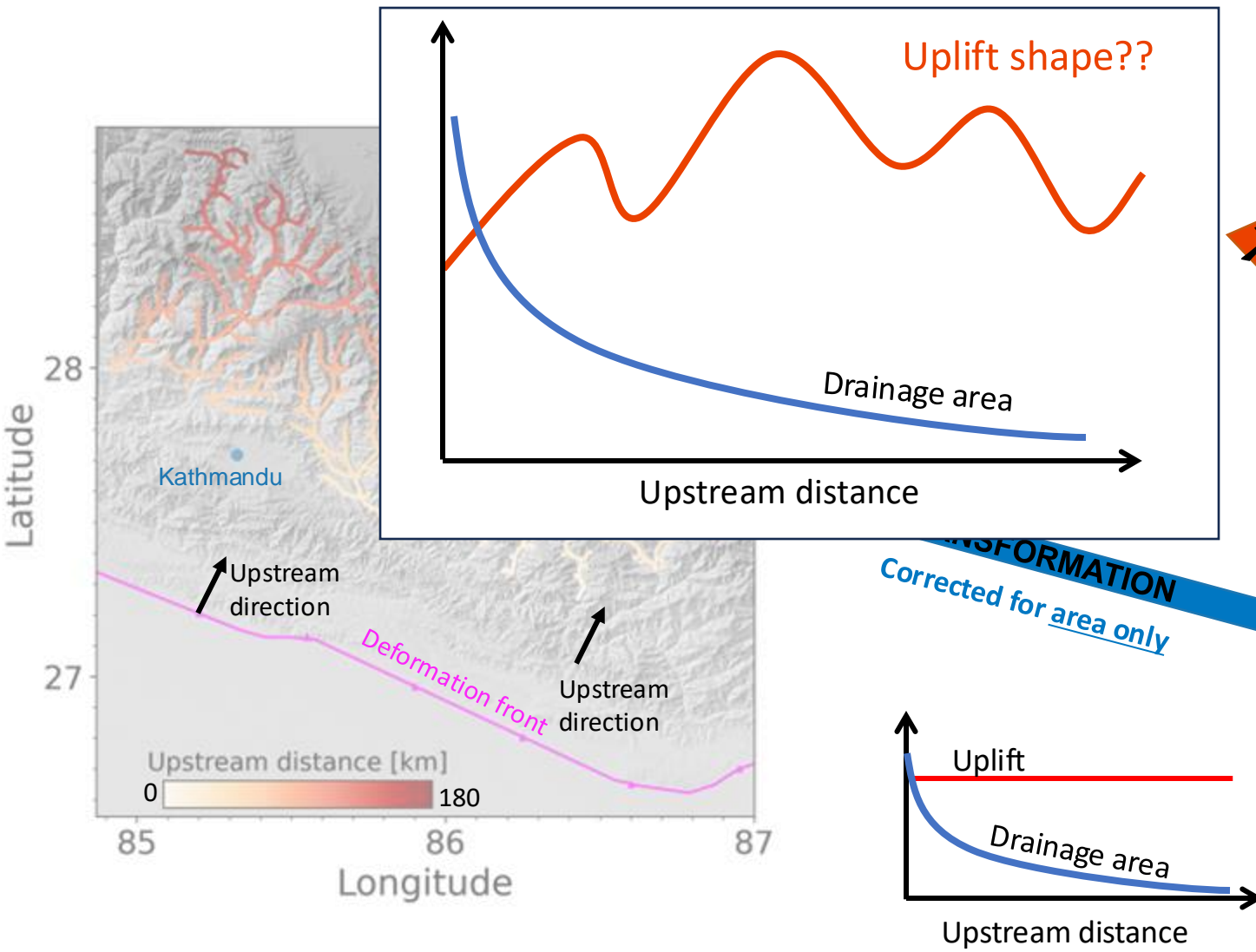
χ – TRANSFORMATION OF RIVER PROFILES IN THE HIMALAYAS



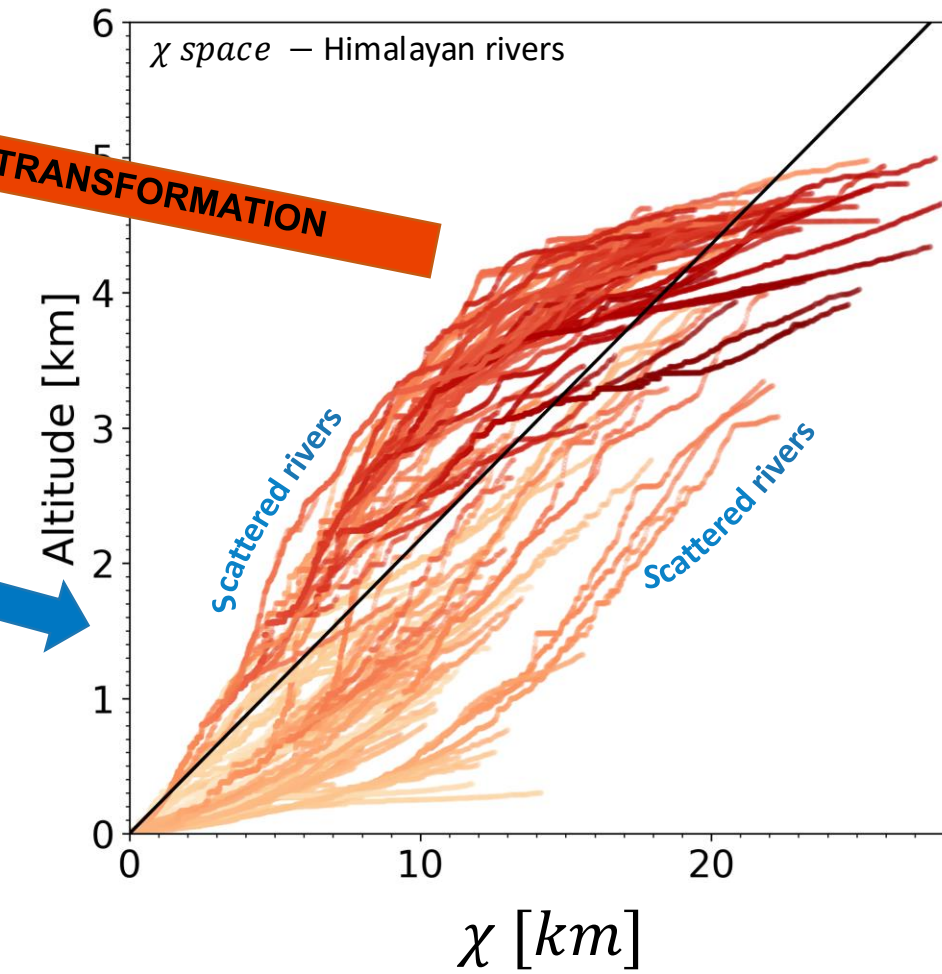
- River concavity reflects:
- Upstream decrease in drainage area
 - Shape of uplift
 - Spatially variable erodibility
 - climate



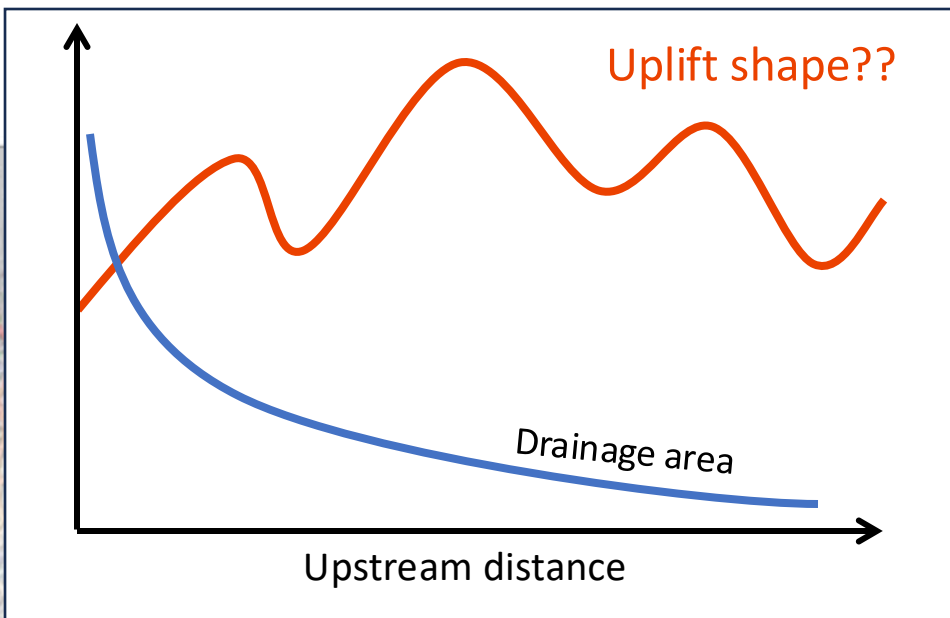
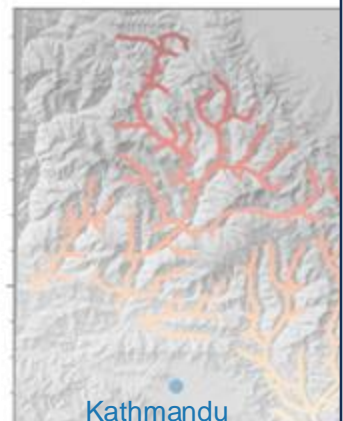
χ – TRANSFORMATION OF RIVER PROFILES IN THE HIMALAYAS



Invert for uplift shape that minimize rivers scatteredness



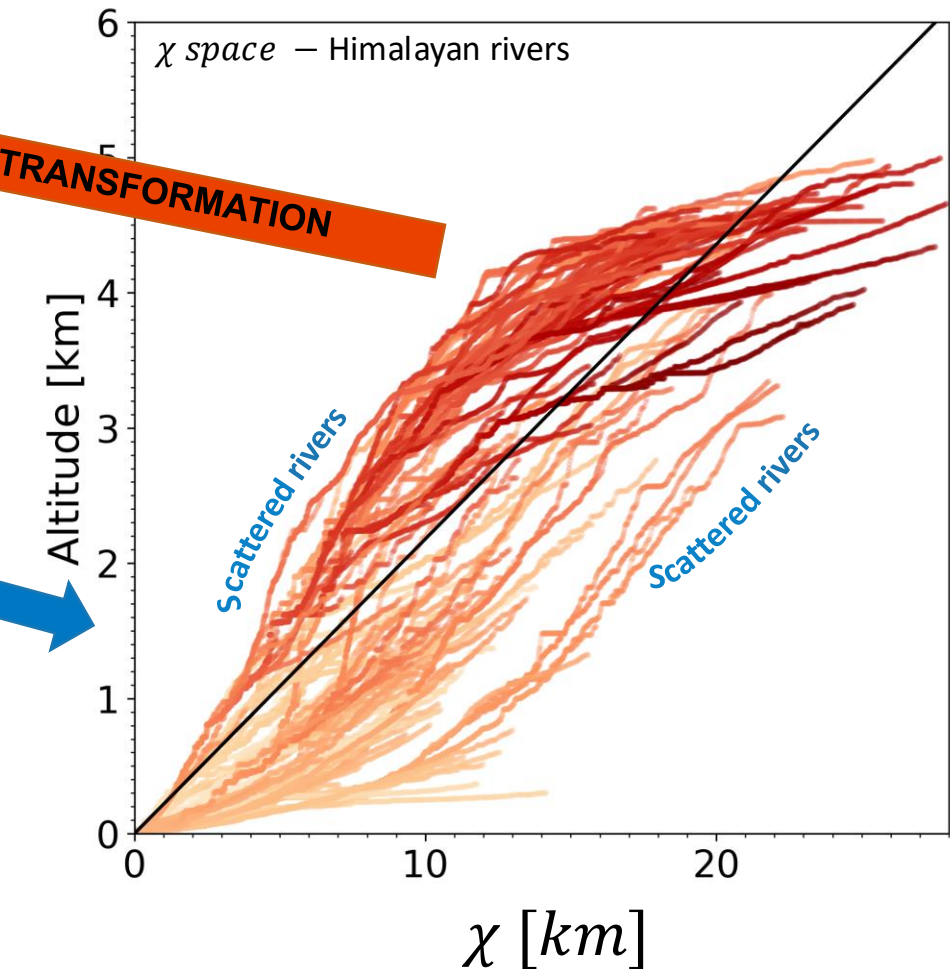
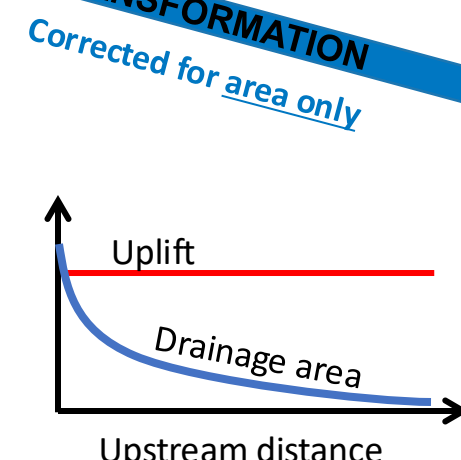
χ – TRANSFORMATION OF RIVER PROFILES IN THE HIMALAYAS



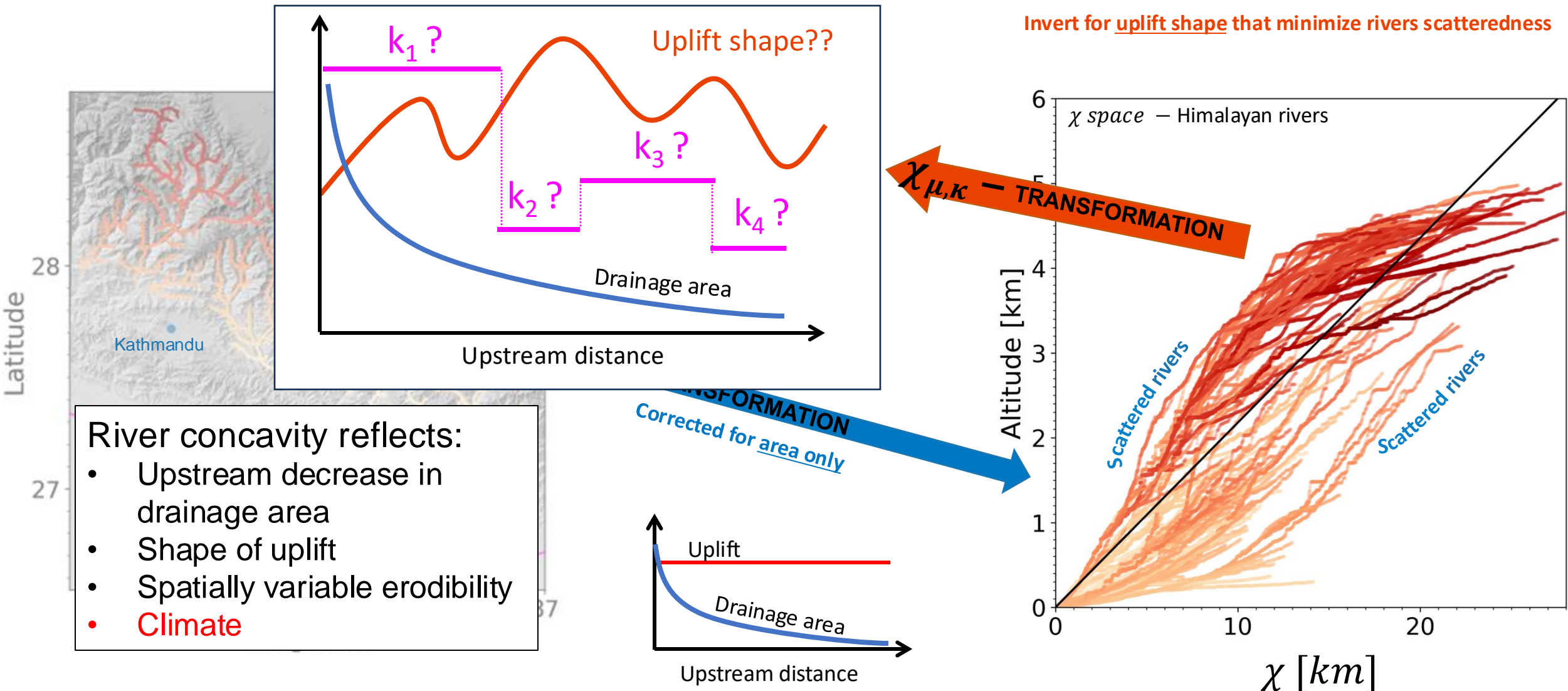
Invert for uplift shape that minimize rivers scatteredness

River concavity reflects:

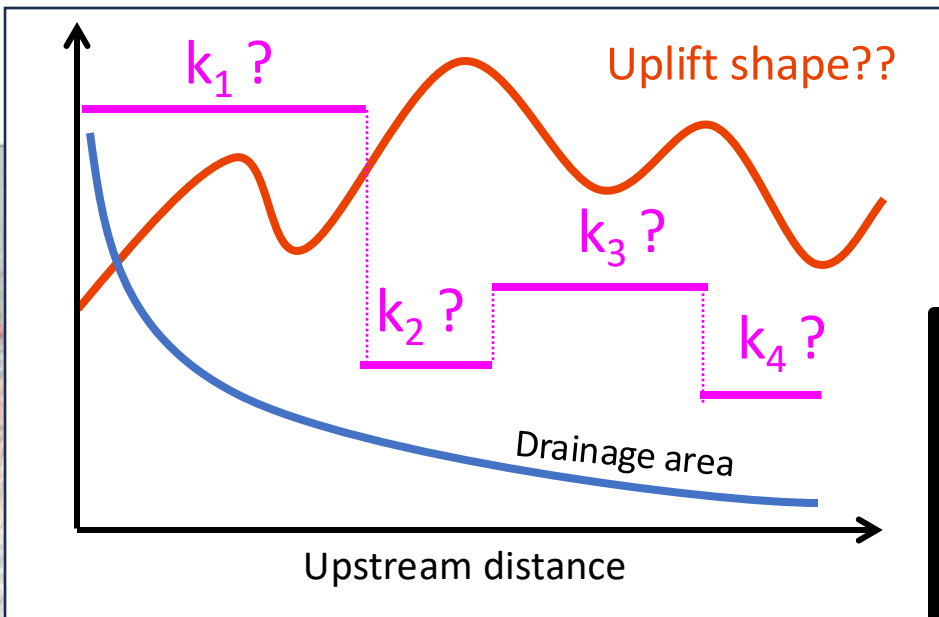
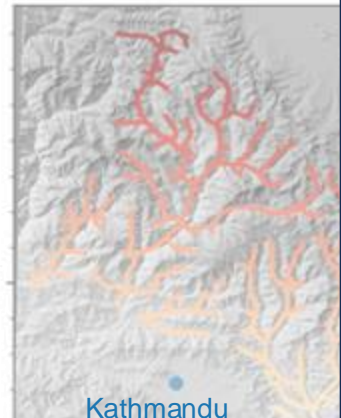
- Upstream decrease in drainage area
- Shape of uplift
- Spatially variable erodibility
- Climate



χ – TRANSFORMATION OF RIVER PROFILES IN THE HIMALAYAS

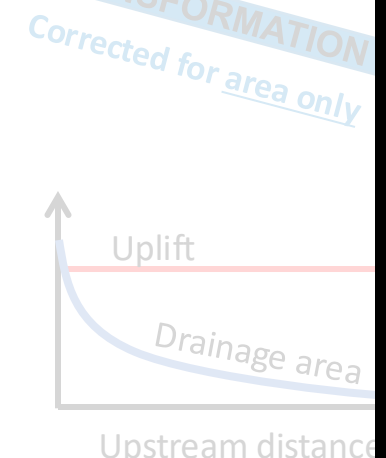


χ – TRANSFORMATION OF RIVER PROFILES IN THE HIMALAYAS

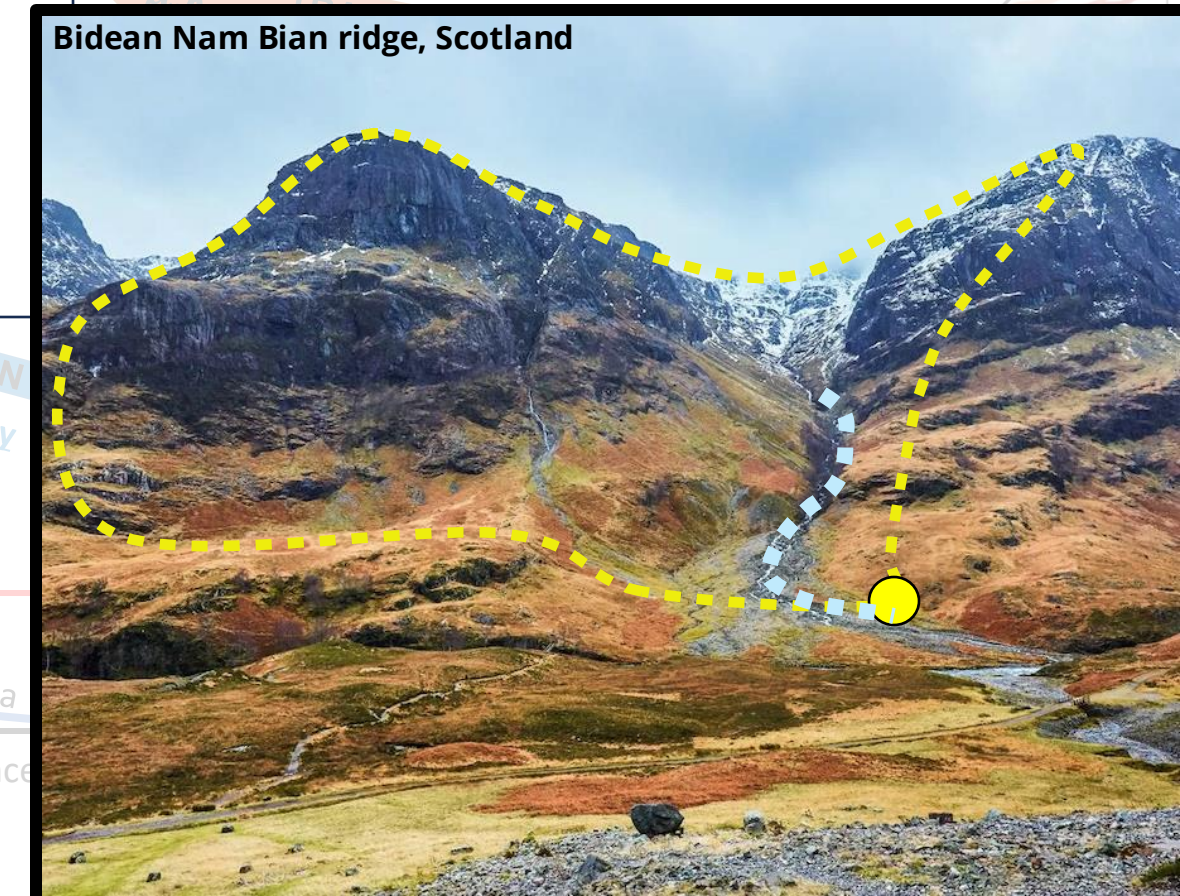


River concavity reflects:

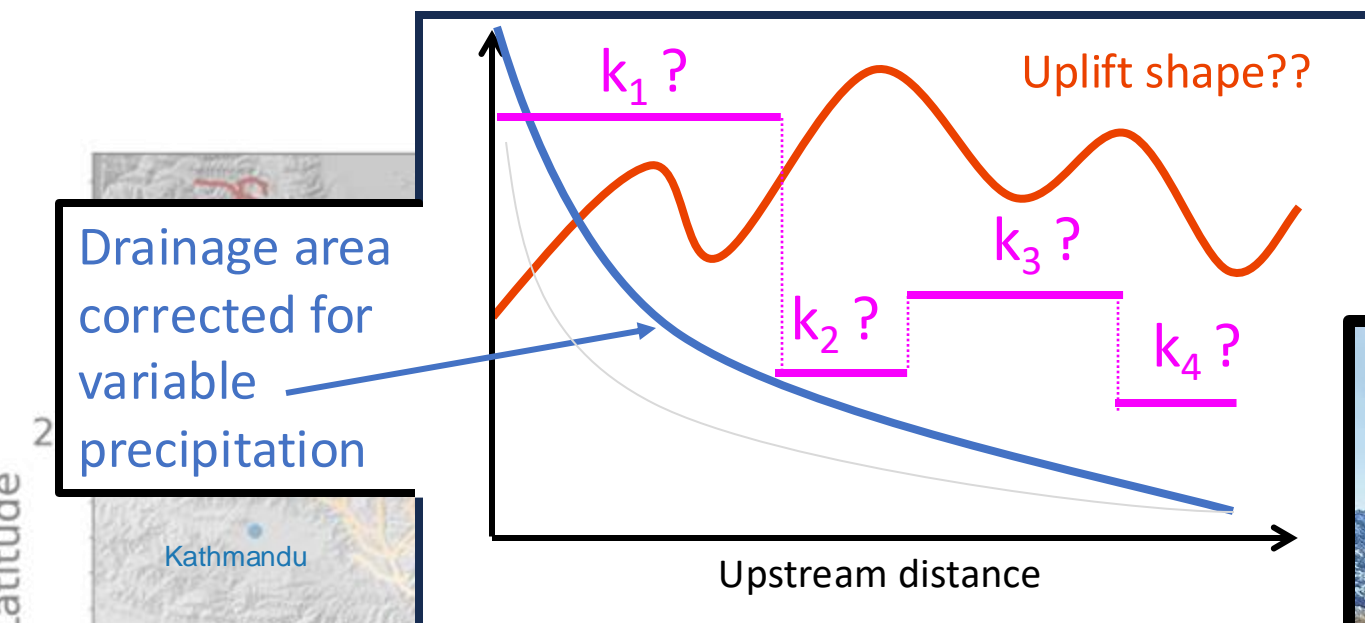
- Upstream decrease in drainage area
- Shape of uplift
- Spatially variable erodibility
- Climate



Invert for uplift shape that minimize rivers scatteredness

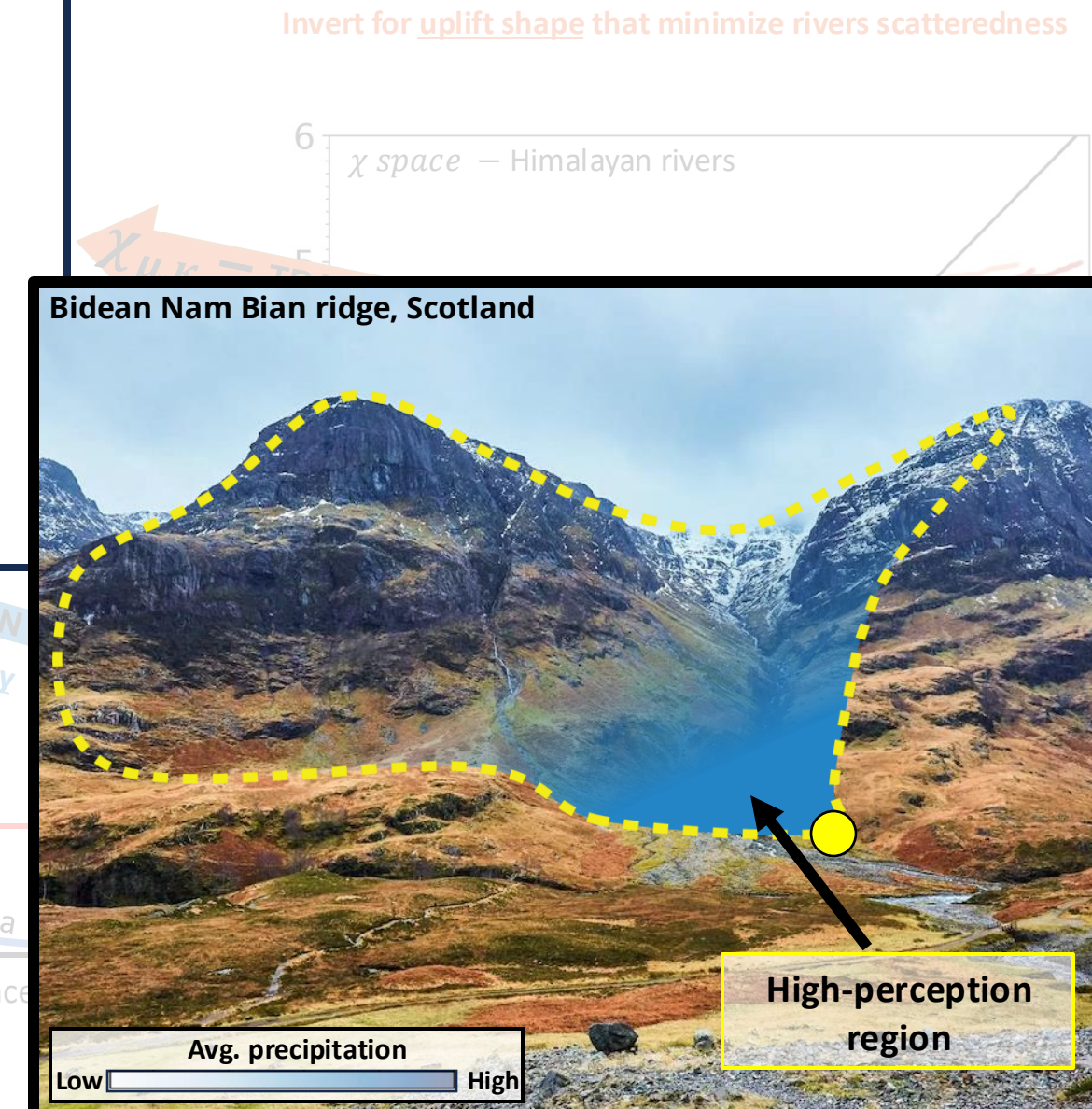
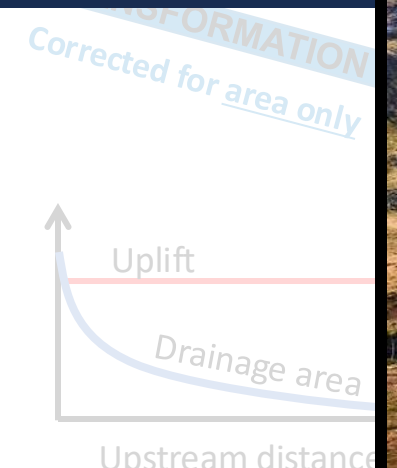


$\chi_{u,k}$ – TRANSFORMATION OF RIVER PROFILES IN THE HIMALAYAS

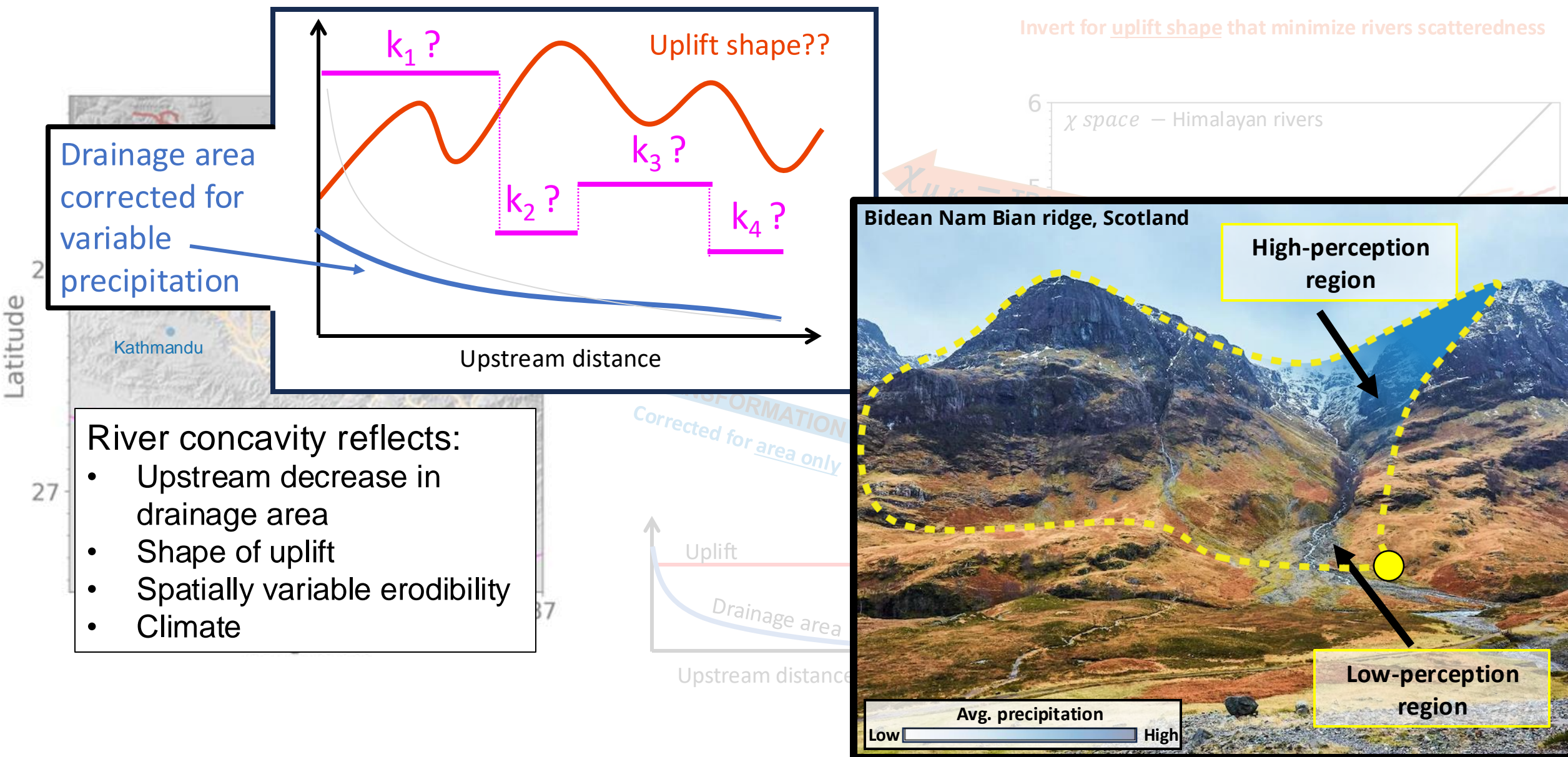


River concavity reflects:

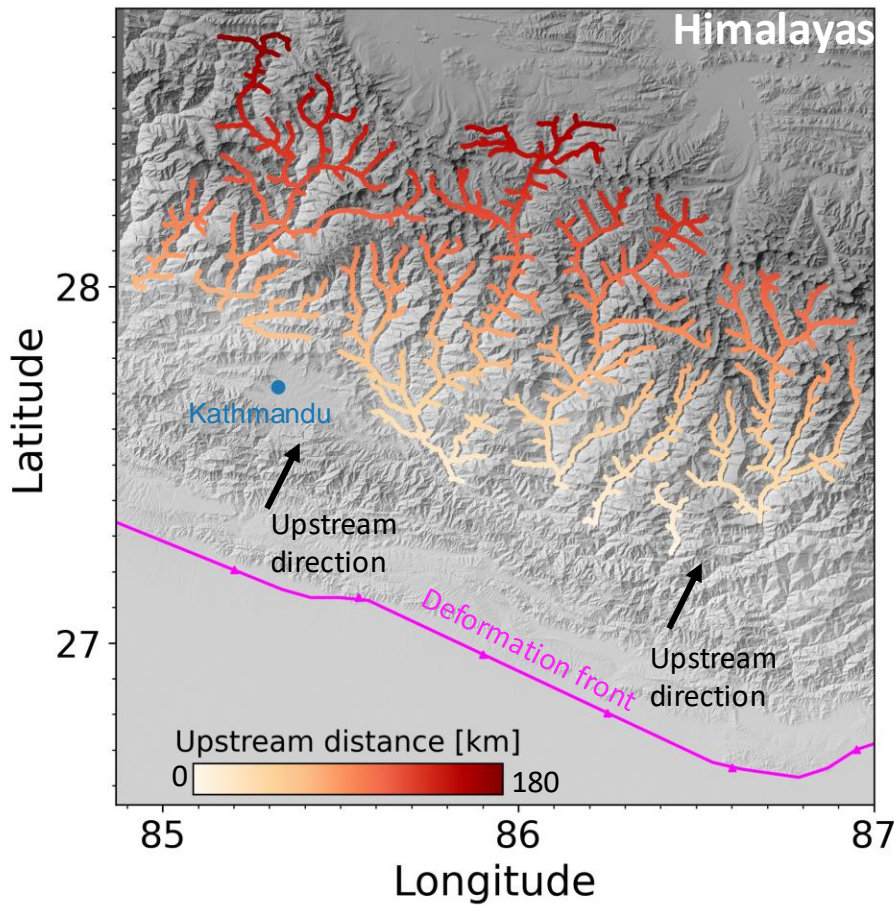
- Upstream decrease in drainage area
- Shape of uplift
- Spatially variable erodibility
- Climate



$\chi_{u,k}$ – TRANSFORMATION OF RIVER PROFILES IN THE HIMALAYAS

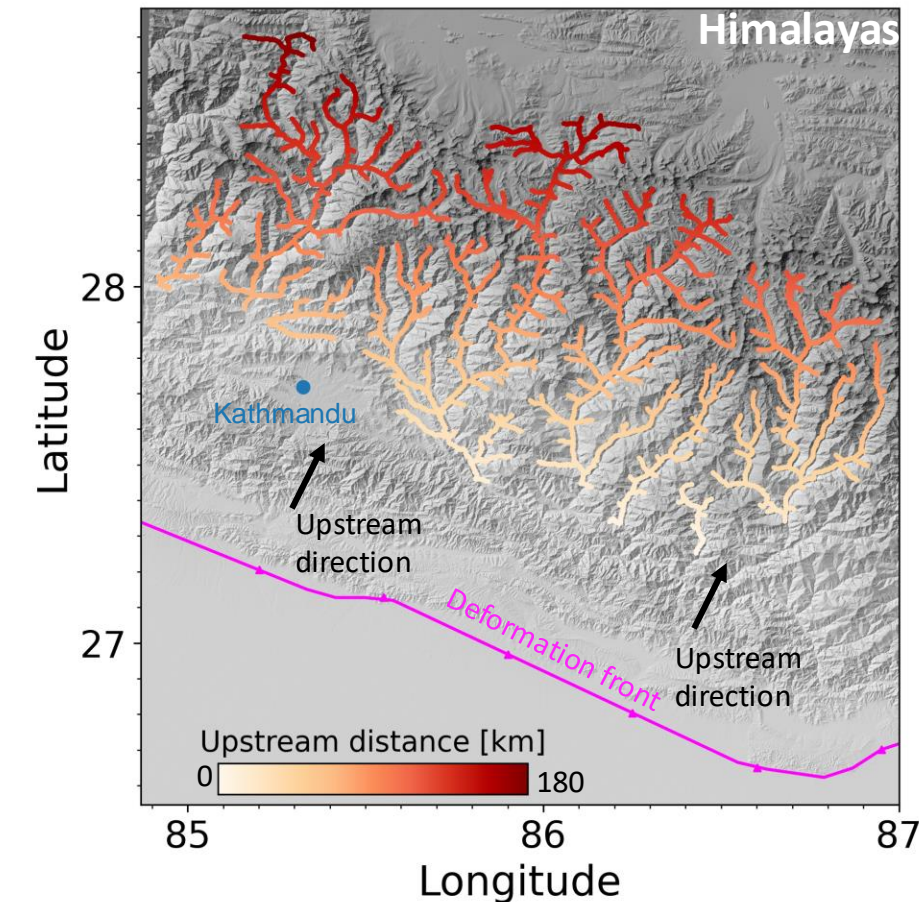
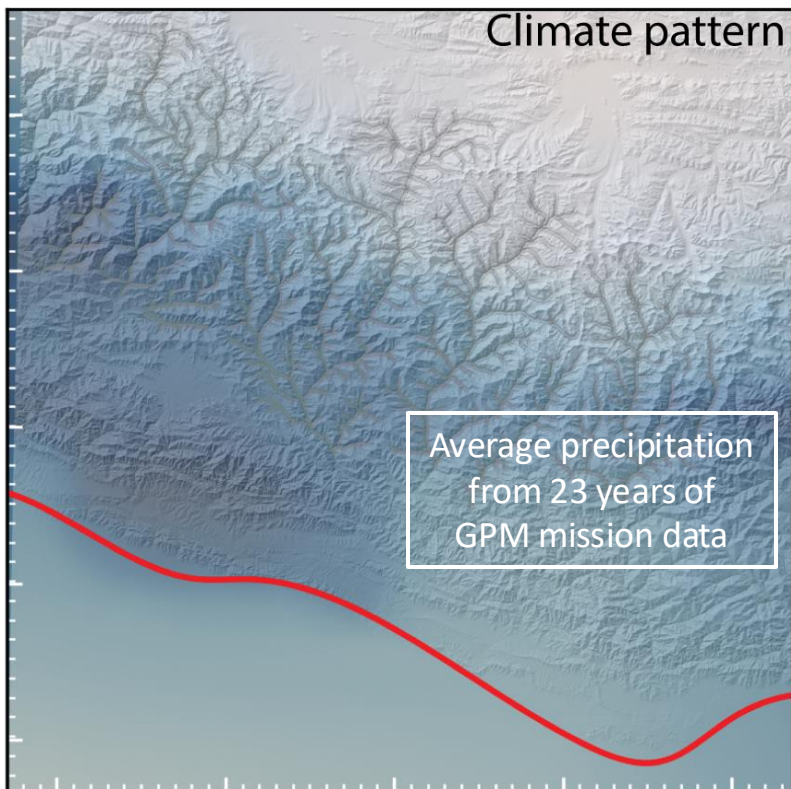
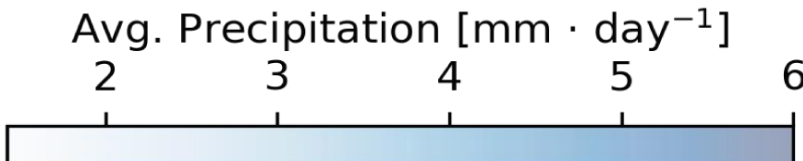


INVERTING HIMALAYAS USING $\chi_{u,k}$ TRANSFORMATION



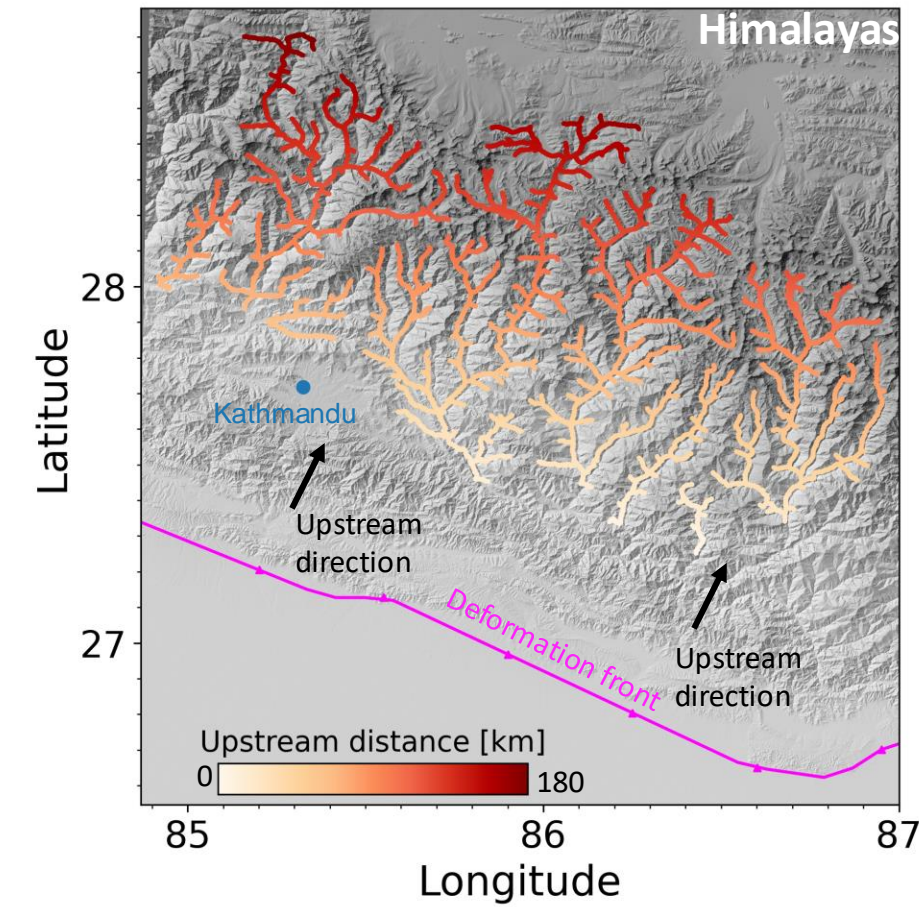
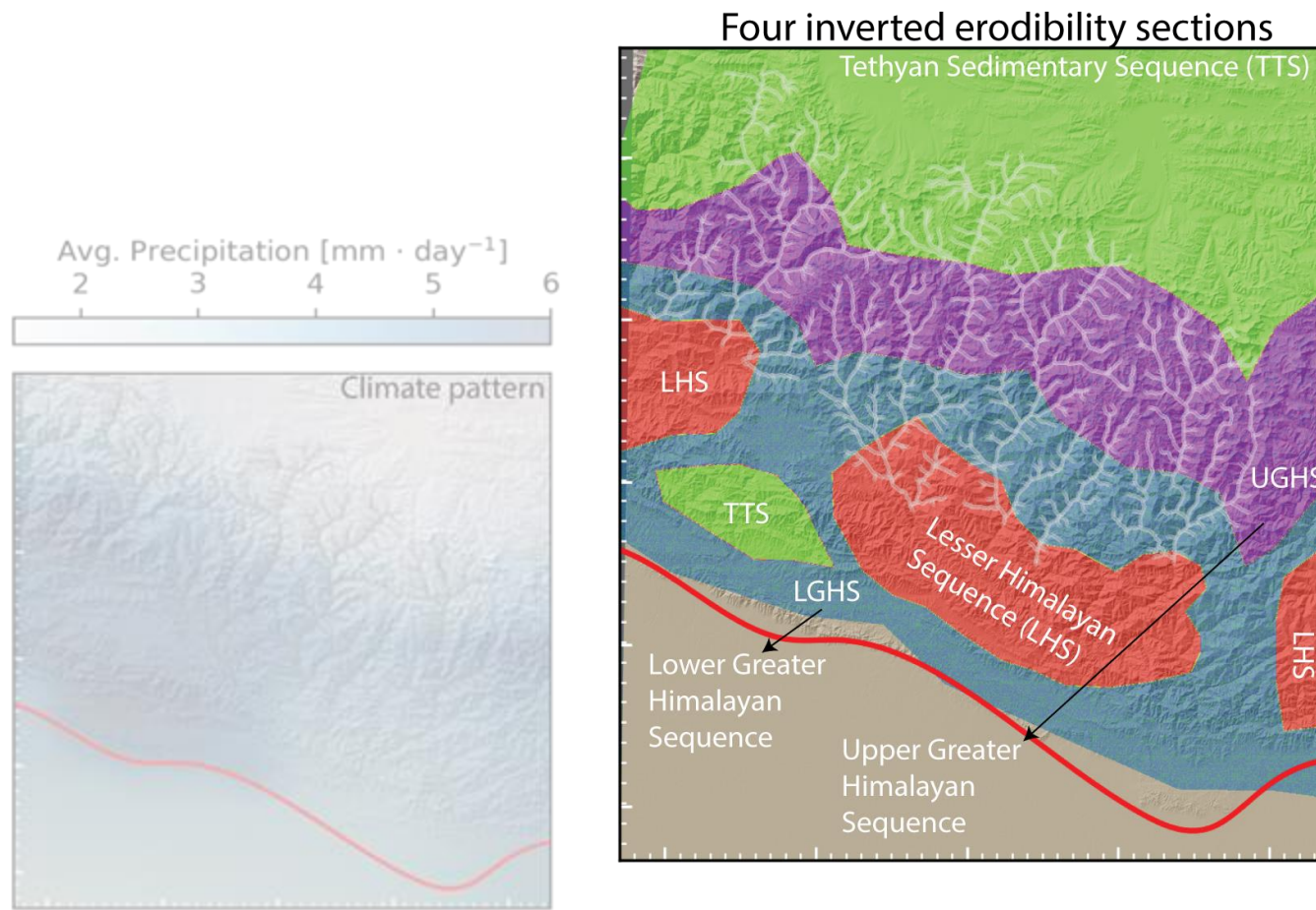
INVERTING HIMALAYAS USING $\chi_{u,k}$ TRANSFORMATION

1. Download a DEM and compute drainage area corrected for climate.



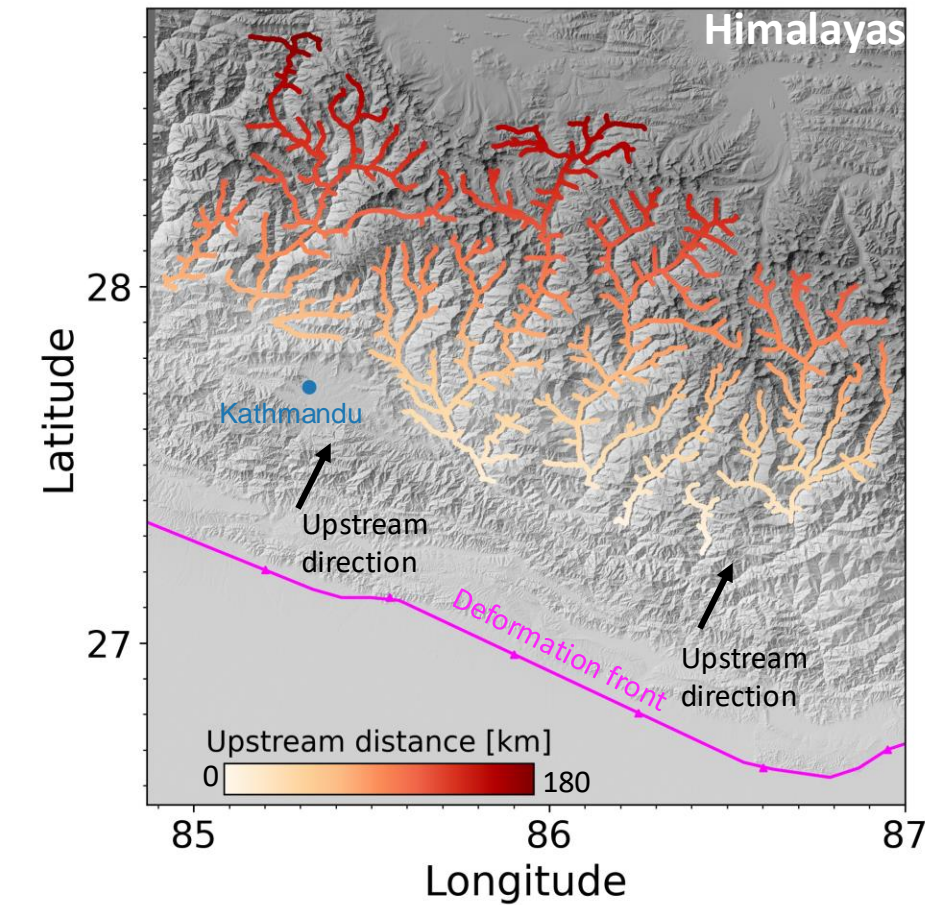
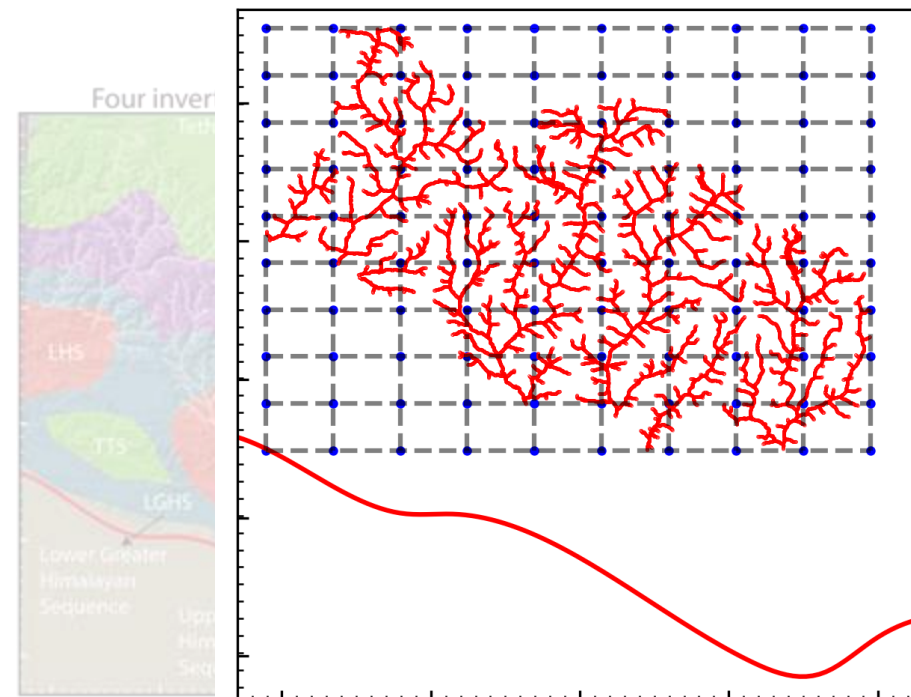
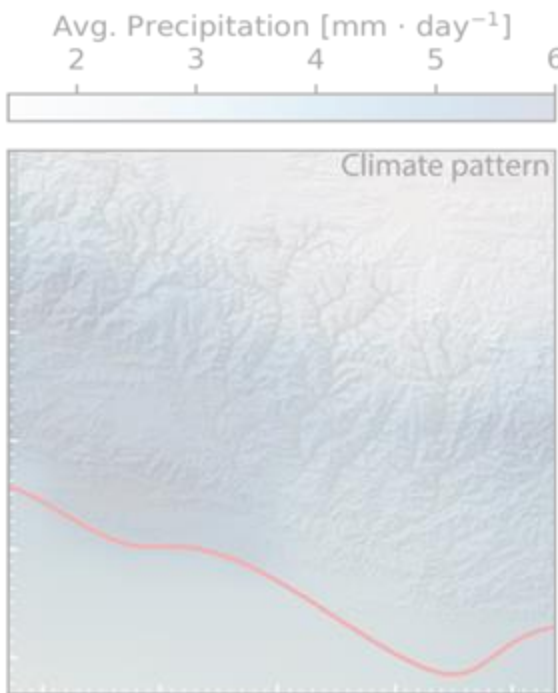
INVERTING HIMALAYAS USING $\chi_{u,k}$ TRANSFORMATION

1. Download a DEM and compute drainage area corrected for climate.
2. Map the spatial distribution of major lithological sections for piecewise rock erodibility values.



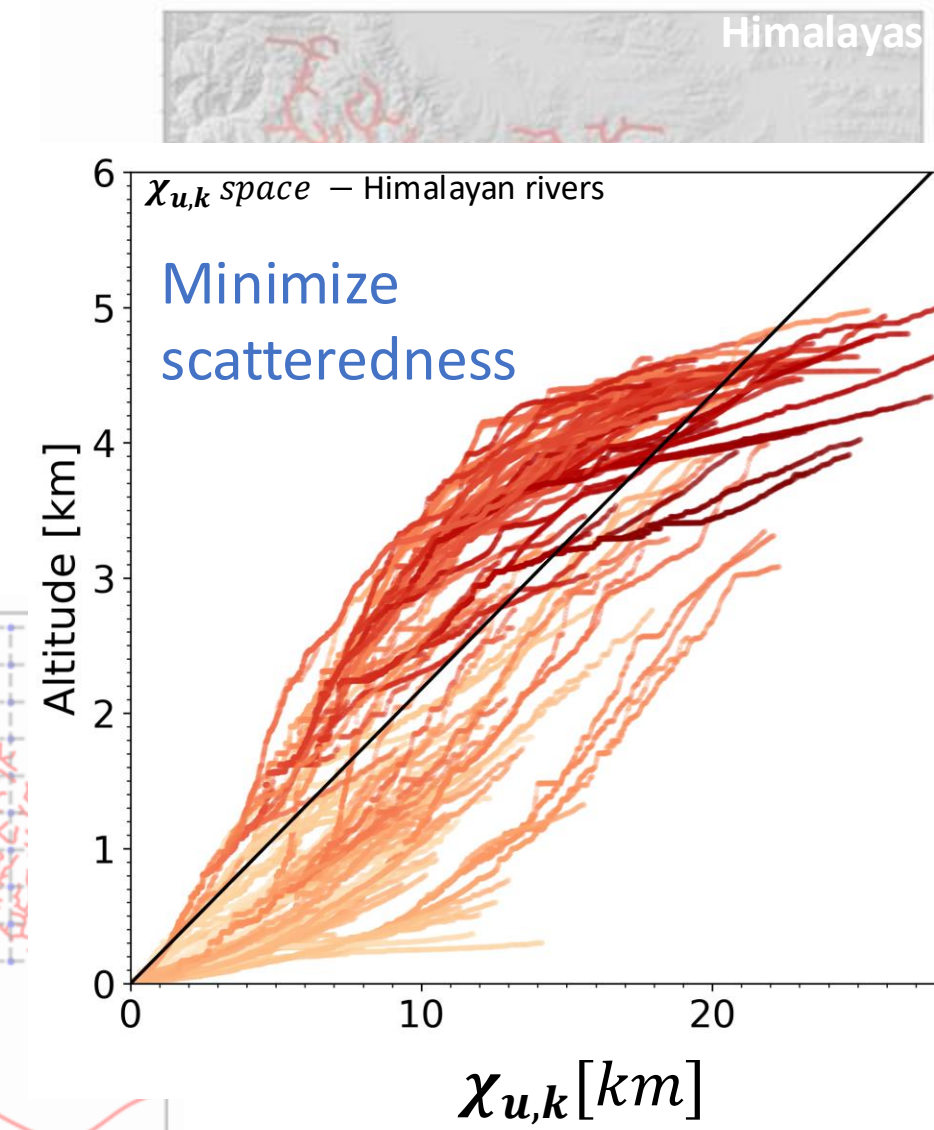
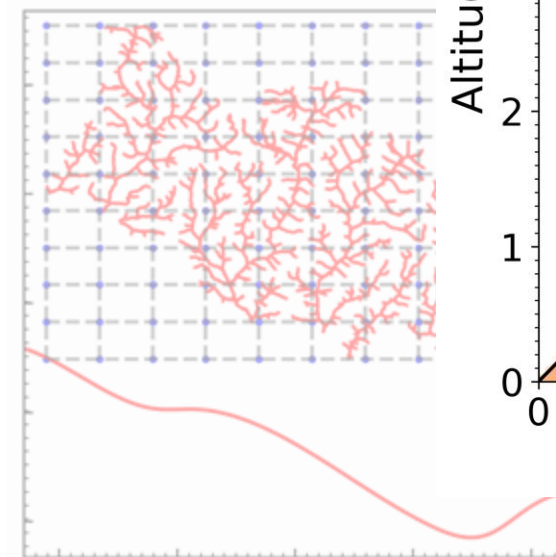
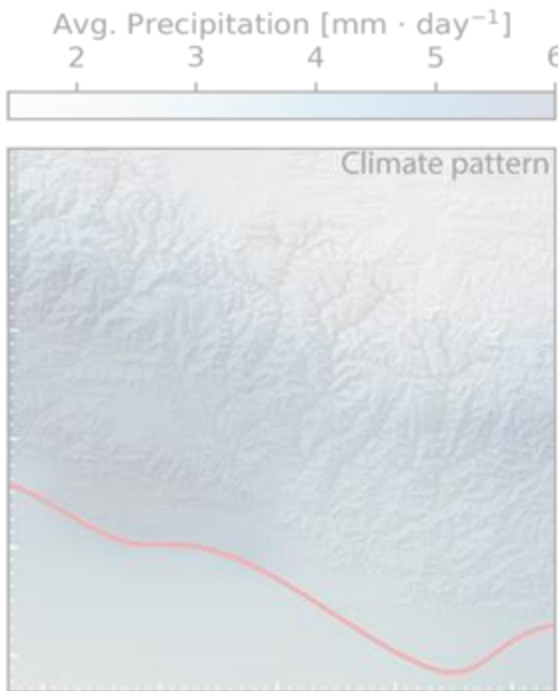
INVERTING HIMALAYAS USING $\chi_{u,k}$ TRANSFORMATION

1. Download a DEM and compute drainage area corrected for climate.
2. Map the spatial distribution of major lithological sections for piecewise rock erodibility values.
3. Describe 2D uplift surface using interpolating B-spline functions extending across the river network.



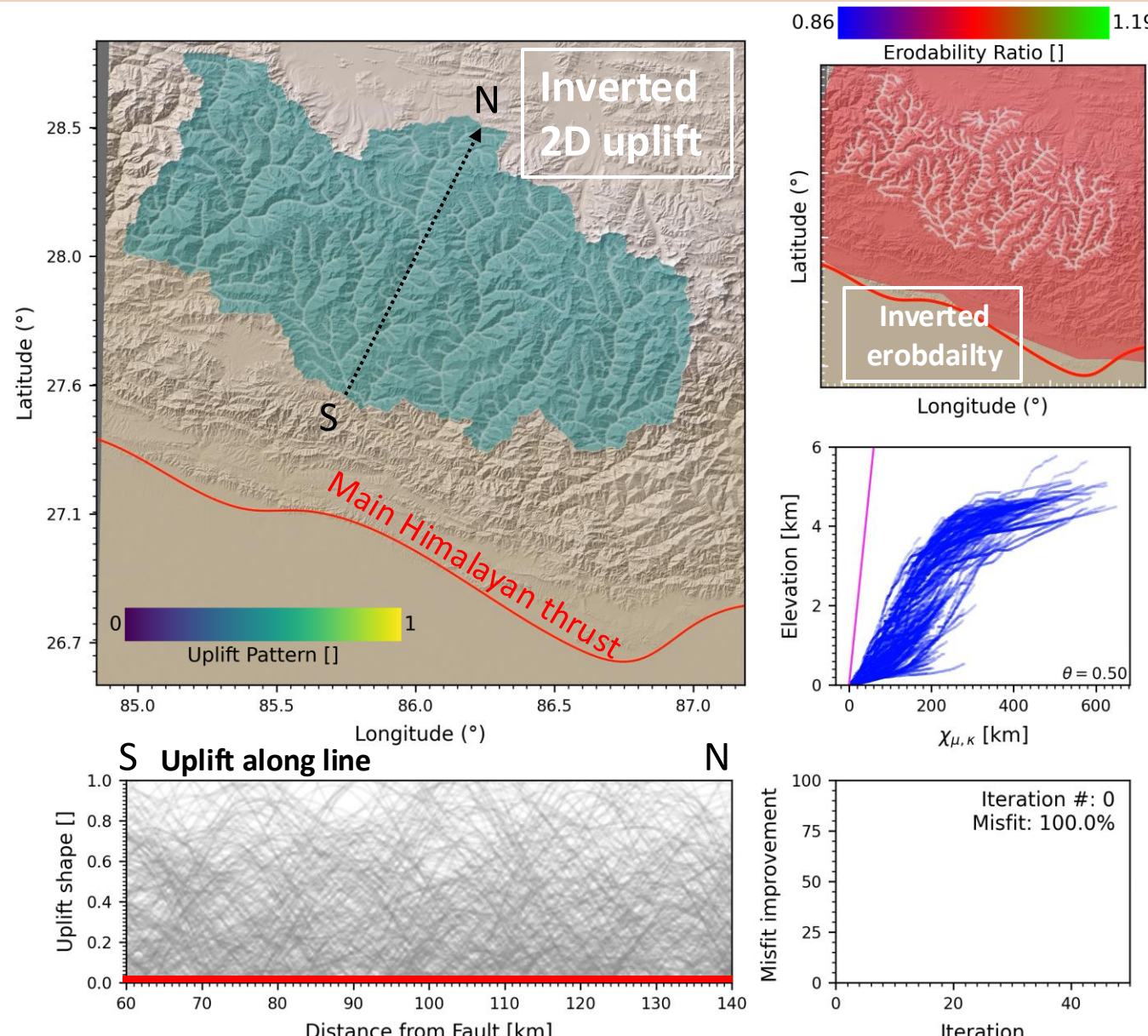
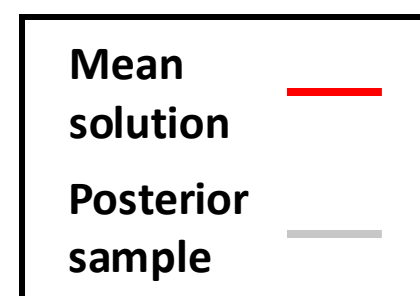
INVERTING HIMALAYAS USING $\chi_{u,k}$ TRANSFORMATION

1. Download a DEM and compute drainage area corrected for climate.
2. Map the spatial distribution of major lithological sections for piecewise rock erodibility values.
3. Describe 2D uplift surface using interpolating B-spline functions extending across the river network.
4. Invert for uplift and erodibility values minimizing $\chi_{u,k}$.



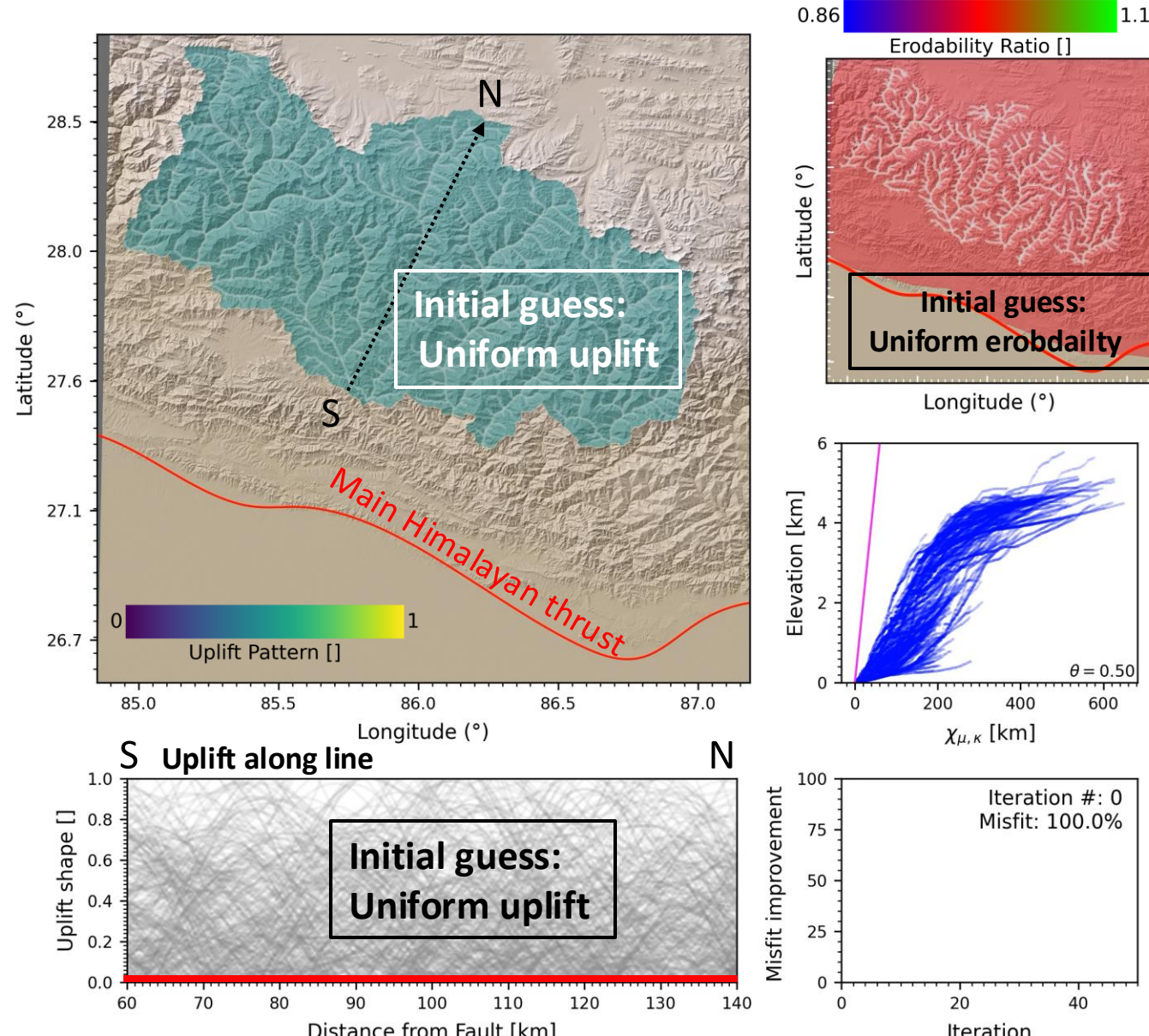
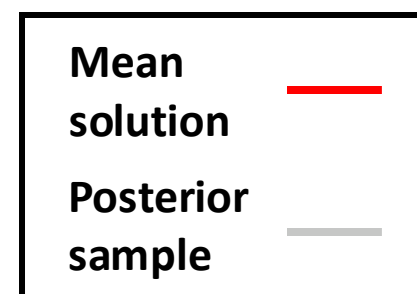
INVERTING HIMALAYAS USING $\chi_{u,k}$ TRANSFORMATION

- Inversion of 120,000 river nodes spanning 18,000km² using Bayesian Quasi-Newton inversion method.
- Inverting for 144 parameters describing the uplift pattern and 4 erodibility values that best linearizes river profiles in $\chi_{u,k}$ space.



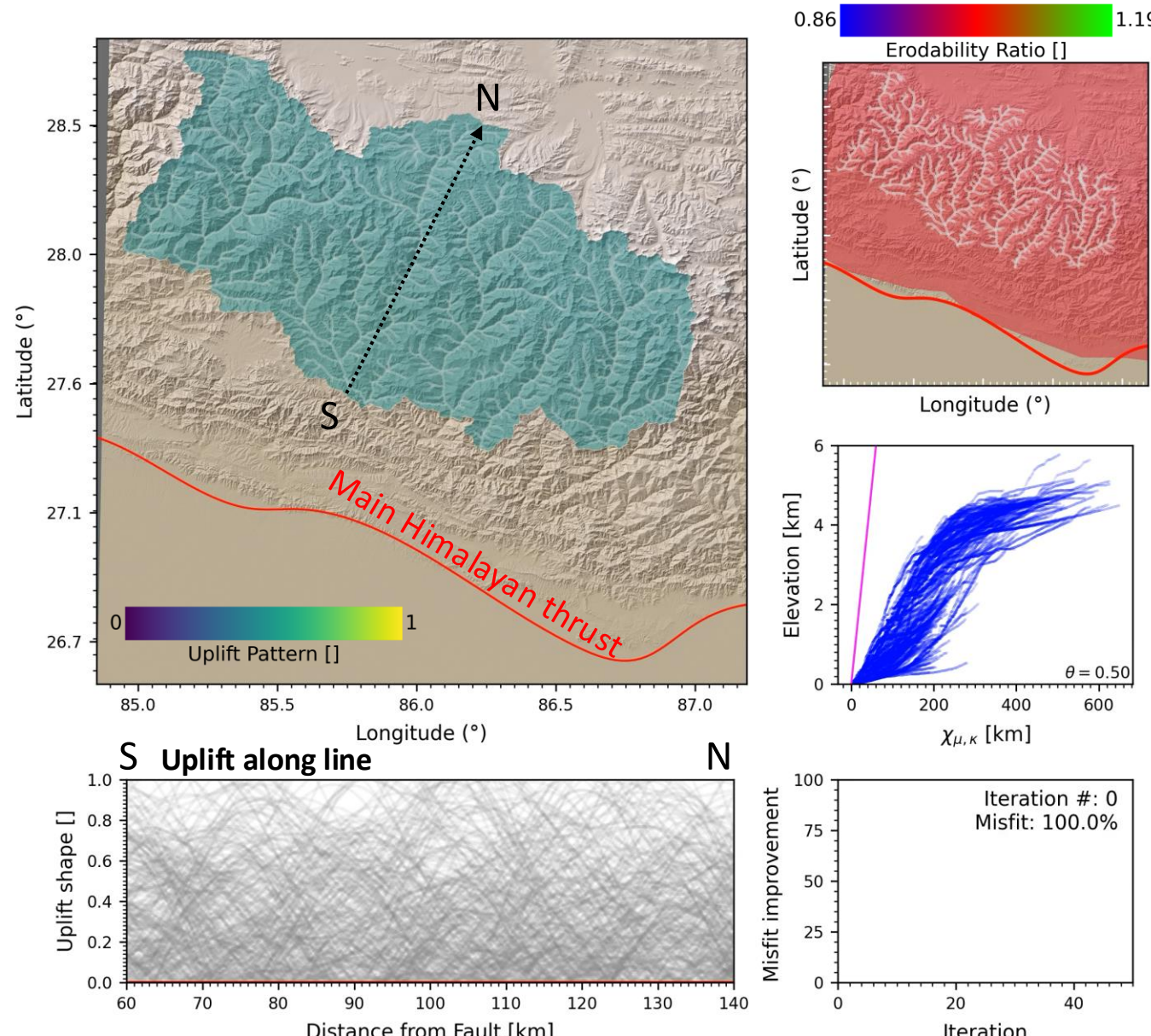
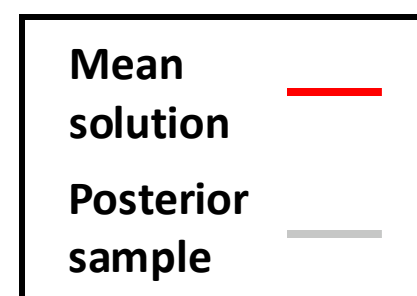
INVERTING HIMALAYAS USING $\chi_{u,k}$ TRANSFORMATION

- Inversion of 120,000 river nodes spanning 18,000km² using Bayesian Quasi-Newton inversion method.
- Inverting for 144 parameters describing the uplift pattern and 4 erodibility values that best linearizes river profiles in $\chi_{u,k}$ space.



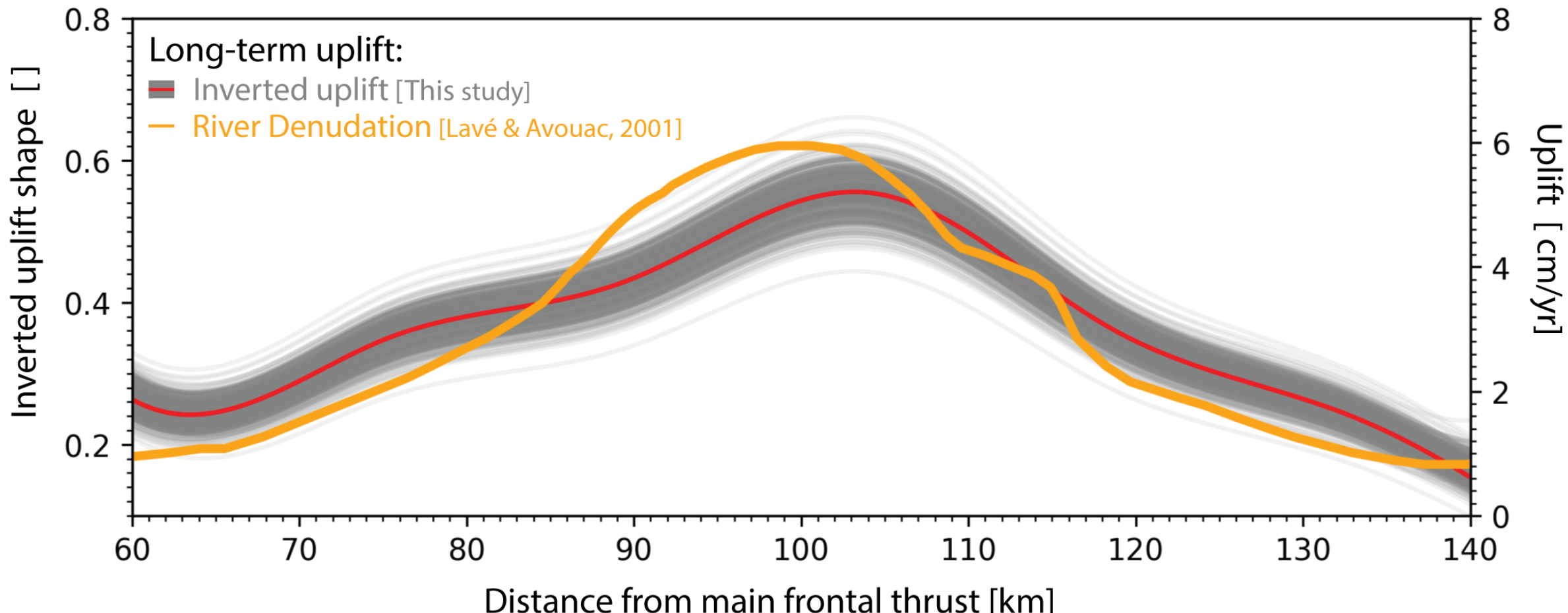
INVERTING HIMALAYAS USING $\chi_{u,k}$ TRANSFORMATION

- Inversion of 120,000 river nodes spanning 18,000km² using Bayesian Quasi-Newton inversion method.
- Inverting for 144 parameters describing the uplift pattern and 4 erodibility values that best linearizes river profiles in $\chi_{u,k}$ space.



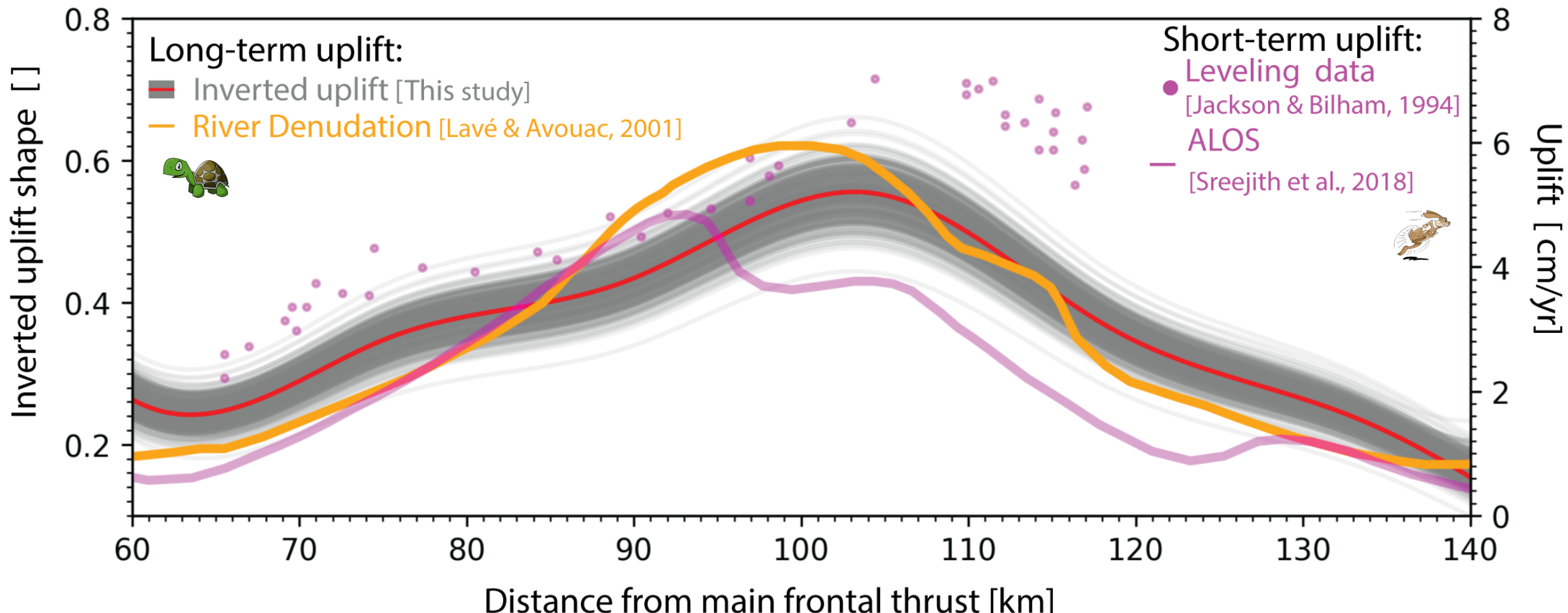
RETRIEVED UPLIFT PATTERN RESEMBLE PREVIOUS ESTIMATES

- Inferred long-term uplift matches denudation rates.



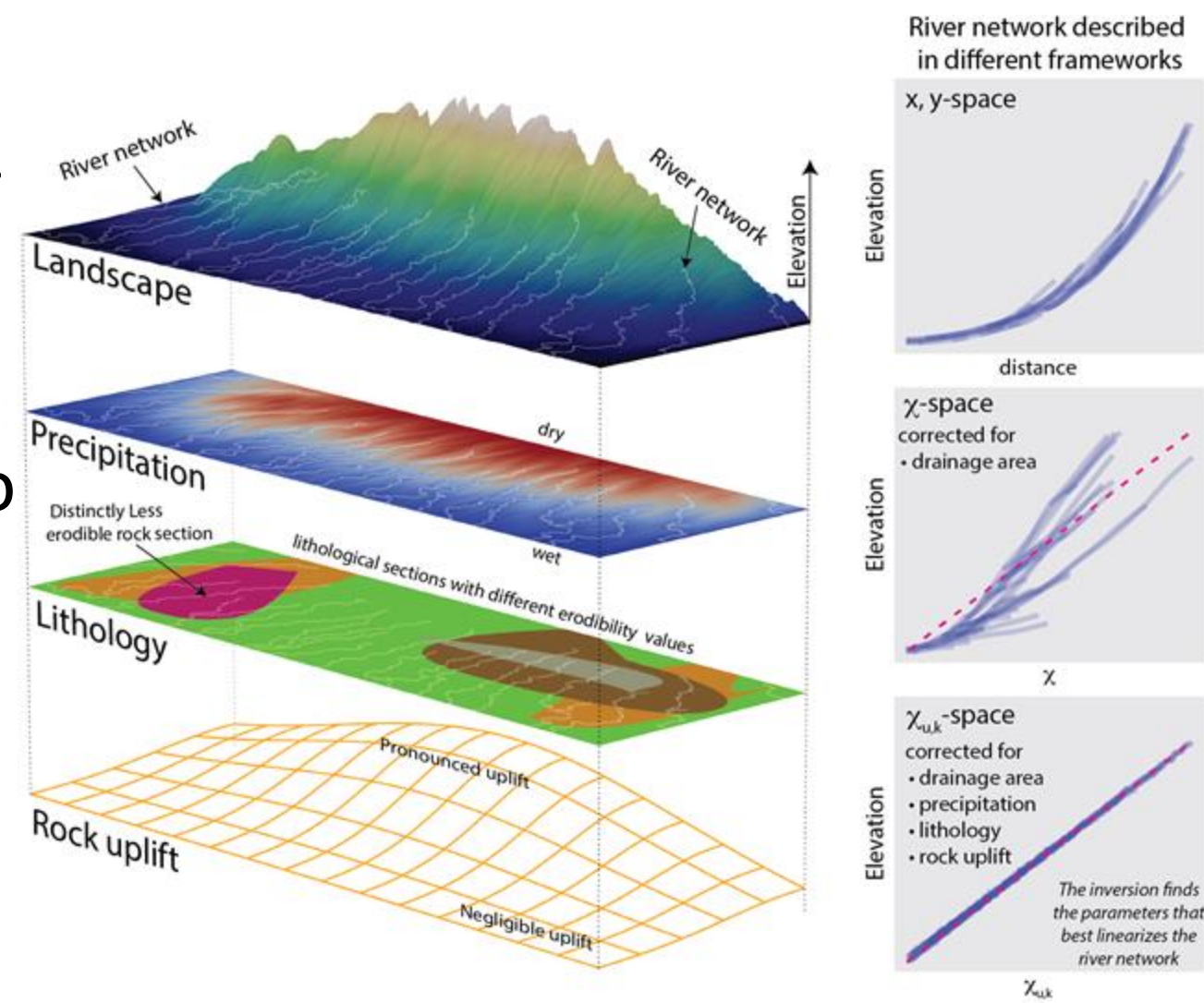
RETRIEVED UPLIFT PATTERN RESEMBLE PREVIOUS ESTIMATES

- Inferred long-term uplift matches denudation rates.
- Uplift shape is comparable with shape of short term interseismic uplift.



KEY POINTS SO FAR

- Inversion in $\chi_{u,k}$ space can disentangle the contributions of tectonics, climate and erodibility from landscapes.
- This approach opens the door to leveraging time-averaged signals preserved in landscapes to infer crustal deformation resulting from earthquake cycles.

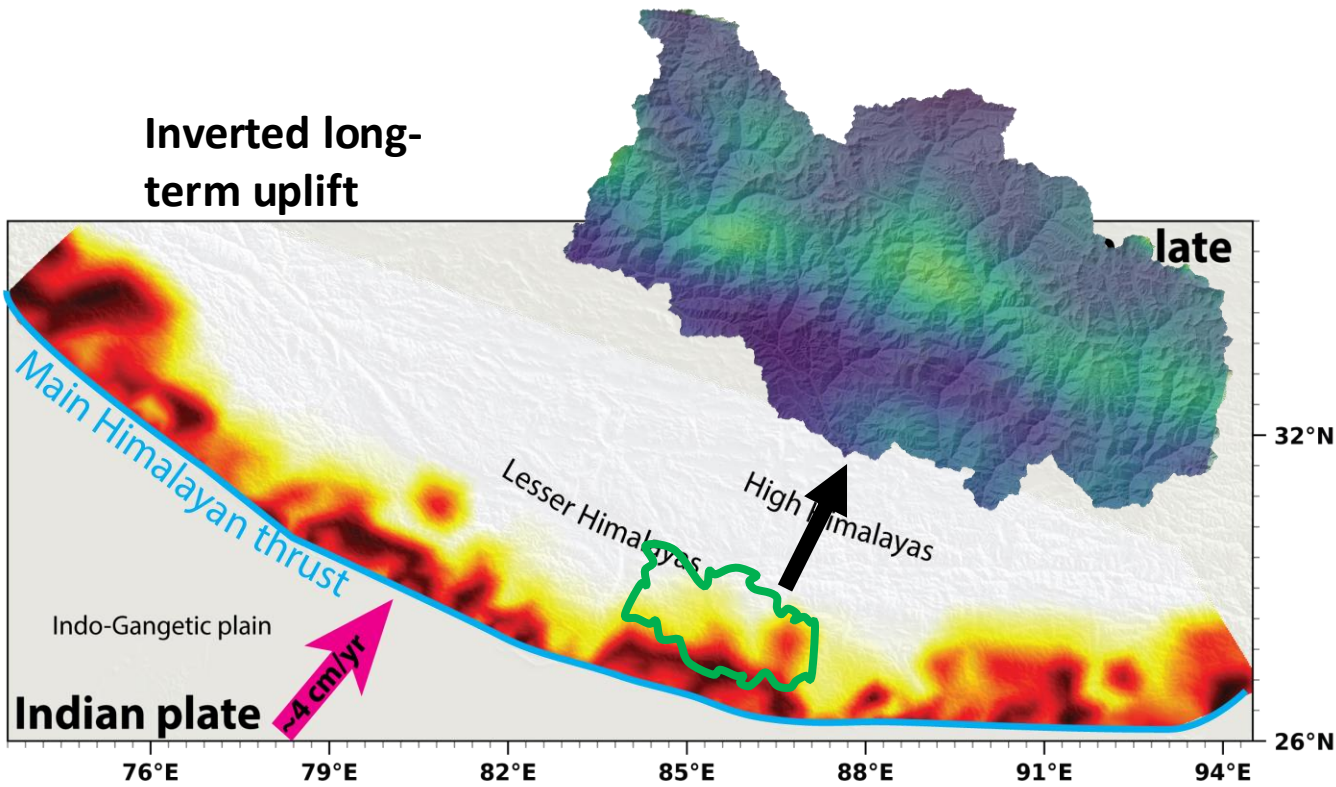


Section 4 – Research Program at Dartmouth



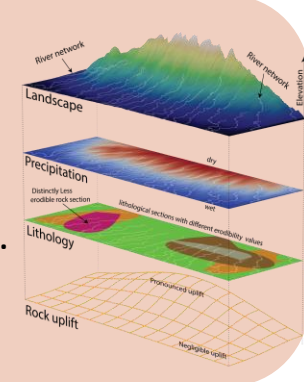
INVERTING LANDSCAPES FOR PERSISTENT PLATE LOCKING

- My group will use the frameworks described in sections 2 and 3 to **invert forearc landscapes for long-term megathrust coupling**.

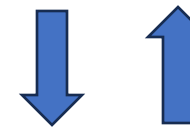


Observational data

Inferring Long-Term Tectonic Uplift from Bayesian Inversion of Landscapes [Oryan et al. in review]

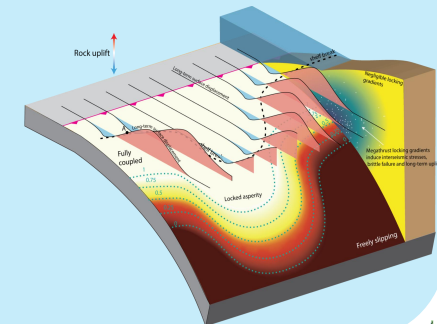


Landscape $\xrightarrow{\hspace{1cm}}$ Long-term Uplift



Forward model

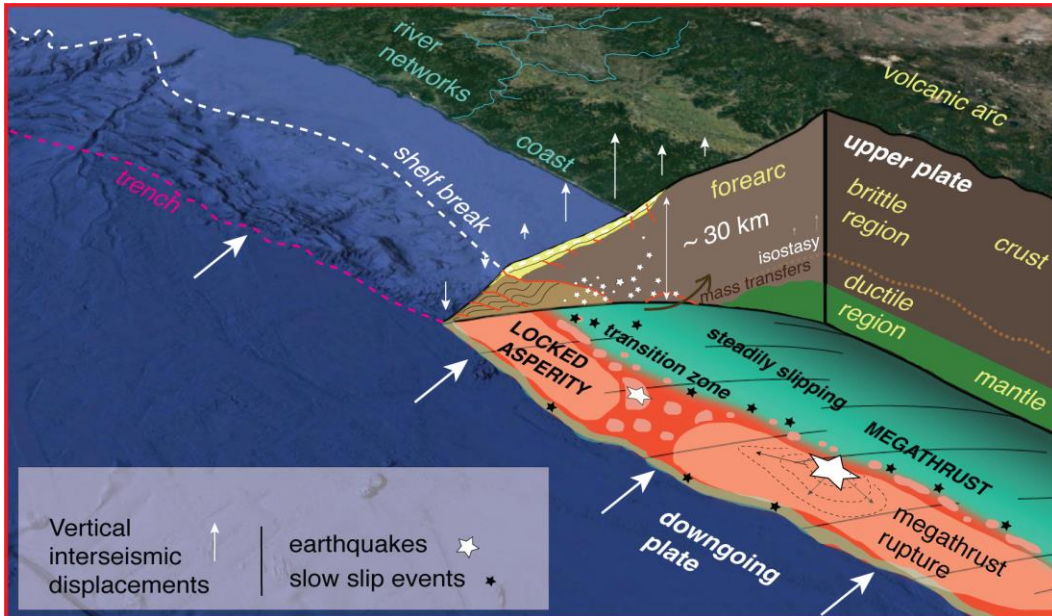
Fingerprints of Megathrust Locking in Subduction Landscapes [Oryan et al., 2024]



Coupling $\xrightarrow{\hspace{1cm}}$ Long-term Uplift

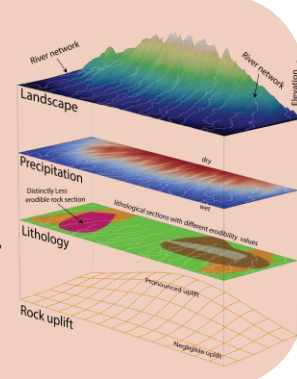
INVERTING LANDSCAPES FOR PERSISTENT PLATE LOCKING

- My group will use the frameworks described in sections 2 and 3 to **invert forearc landscapes for long-term megathrust coupling**.

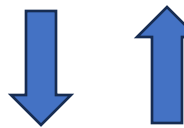


Observational data

Inferring Long-Term Tectonic Uplift from Bayesian Inversion of Landscapes [Oryan et al. in review]

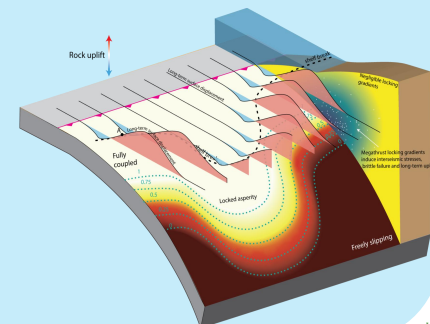


Landscape $\xrightarrow{\hspace{1cm}}$ Long-term Uplift



Forward model

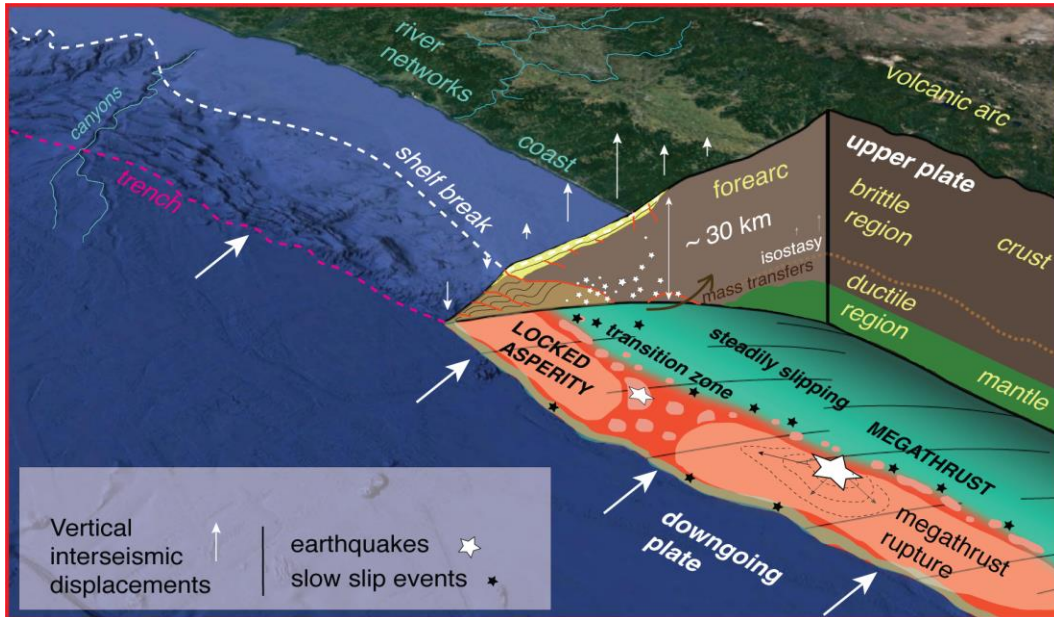
Fingerprints of Megathrust Locking in Subduction Landscapes [Oryan et al., 2024]



Coupling $\xrightarrow{\hspace{1cm}}$ Long-term Uplift

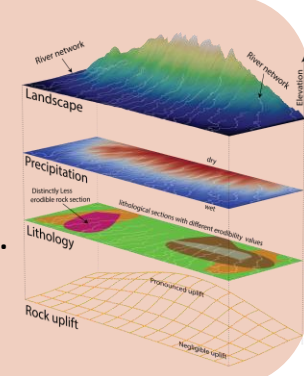
INVERTING LANDSCAPES FOR PERSISTENT PLATE LOCKING

- My group will use the frameworks described in sections 2 and 3 to **invert forearc landscapes for long-term megathrust coupling**.
- We will strive to expand our observational record and use **submarine canyons**.

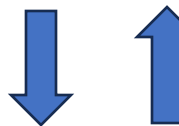


Observational data

Inferring Long-Term Tectonic Uplift from Bayesian Inversion of Landscapes [Oryan et al. in review]

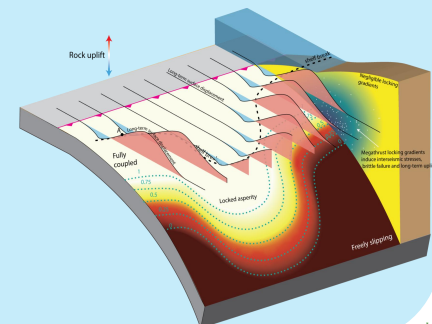


Landscape $\xrightarrow{\hspace{1cm}}$ Long-term Uplift



Forward model

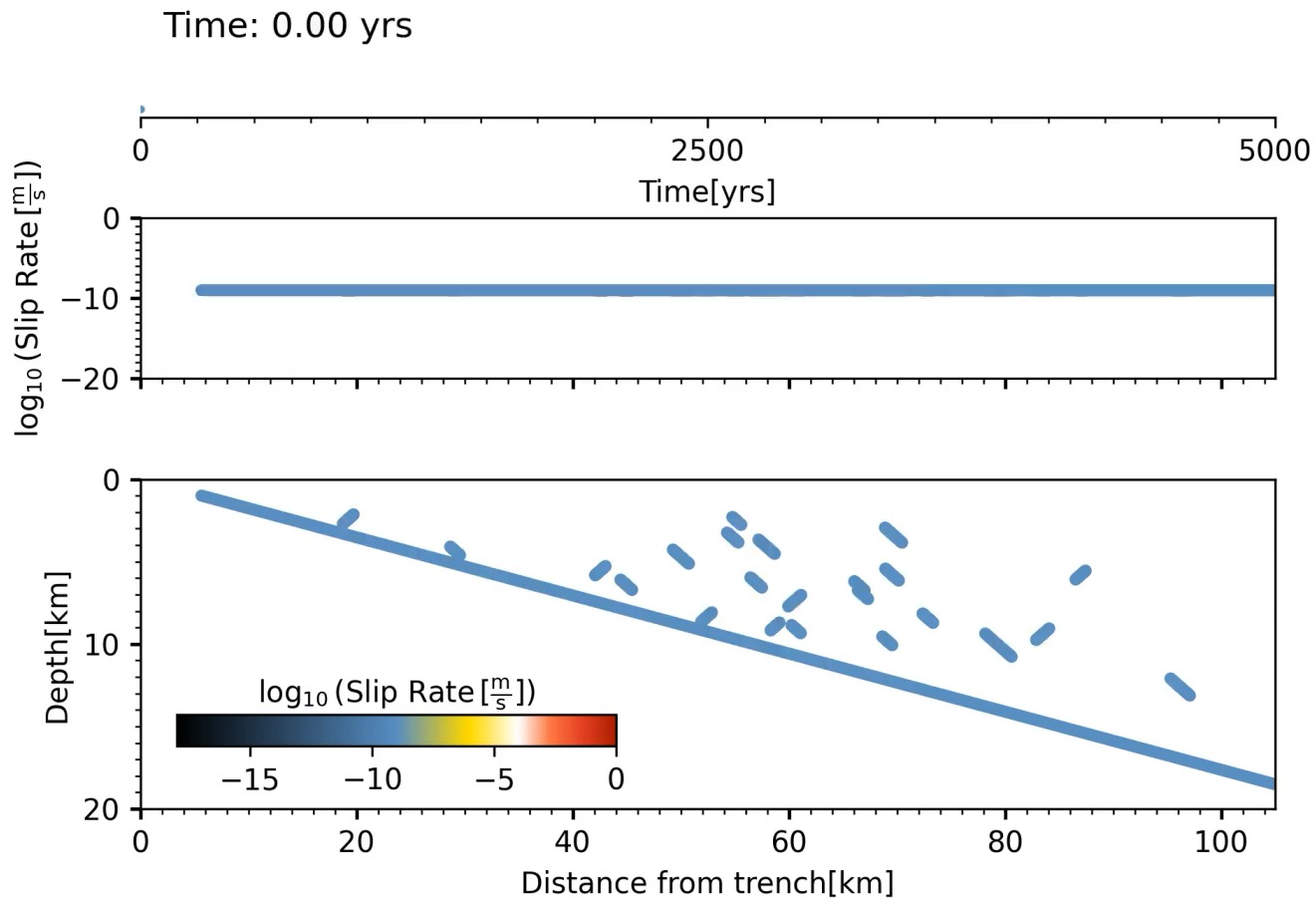
Fingerprints of Megathrust Locking in Subduction Landscapes [Oryan et al., 2024]



Coupling $\xrightarrow{\hspace{1cm}}$ Long-term Uplift

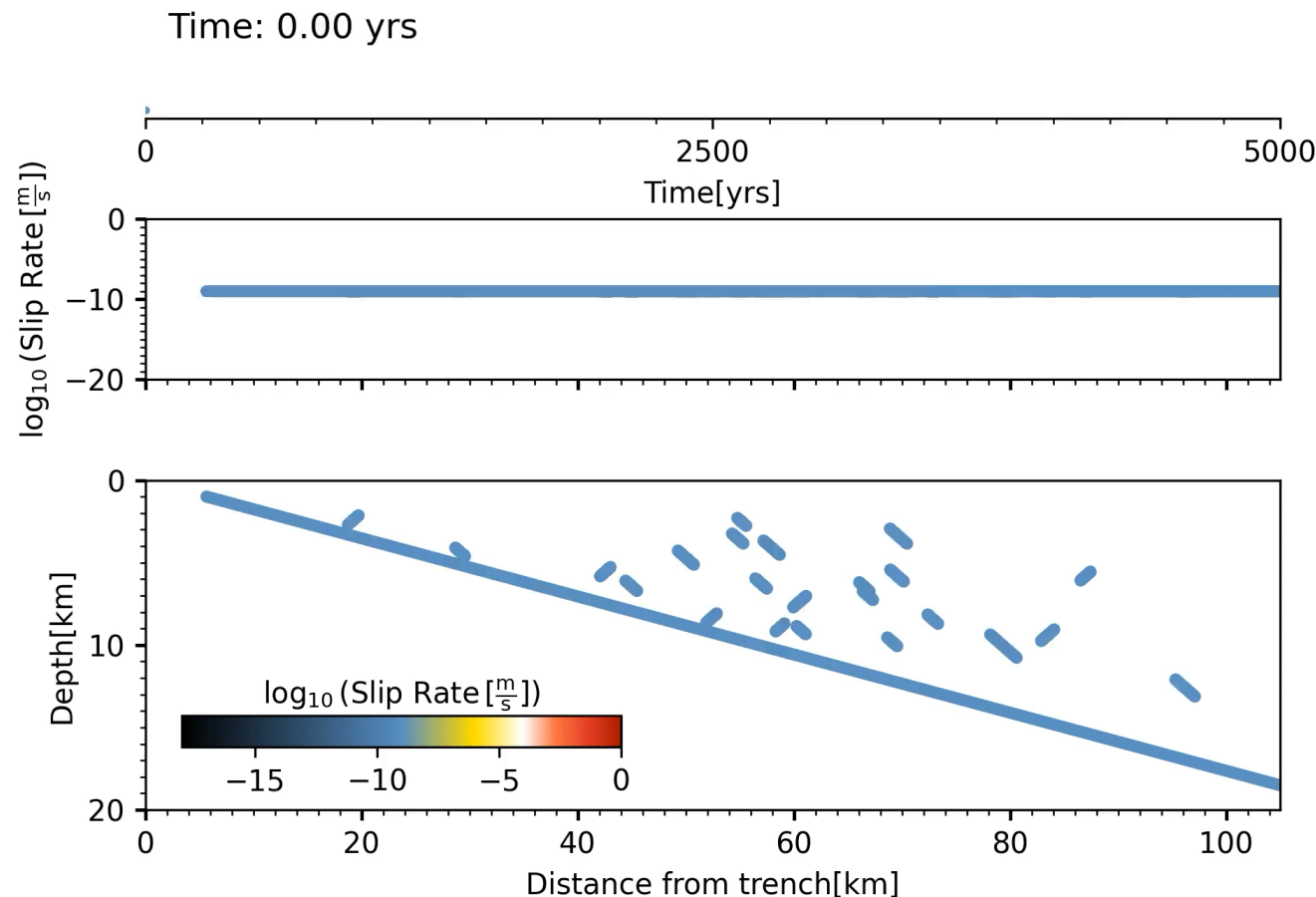
THE ENERGY BUGDET OF EARTHQUAKE CYCLES

- **Unraveling Energy Distribution in Subduction Zones:** We will study the rheological properties that govern the balance between elastic deformation (fueling earthquakes) and inelastic strain (shaping subduction zone landscapes).



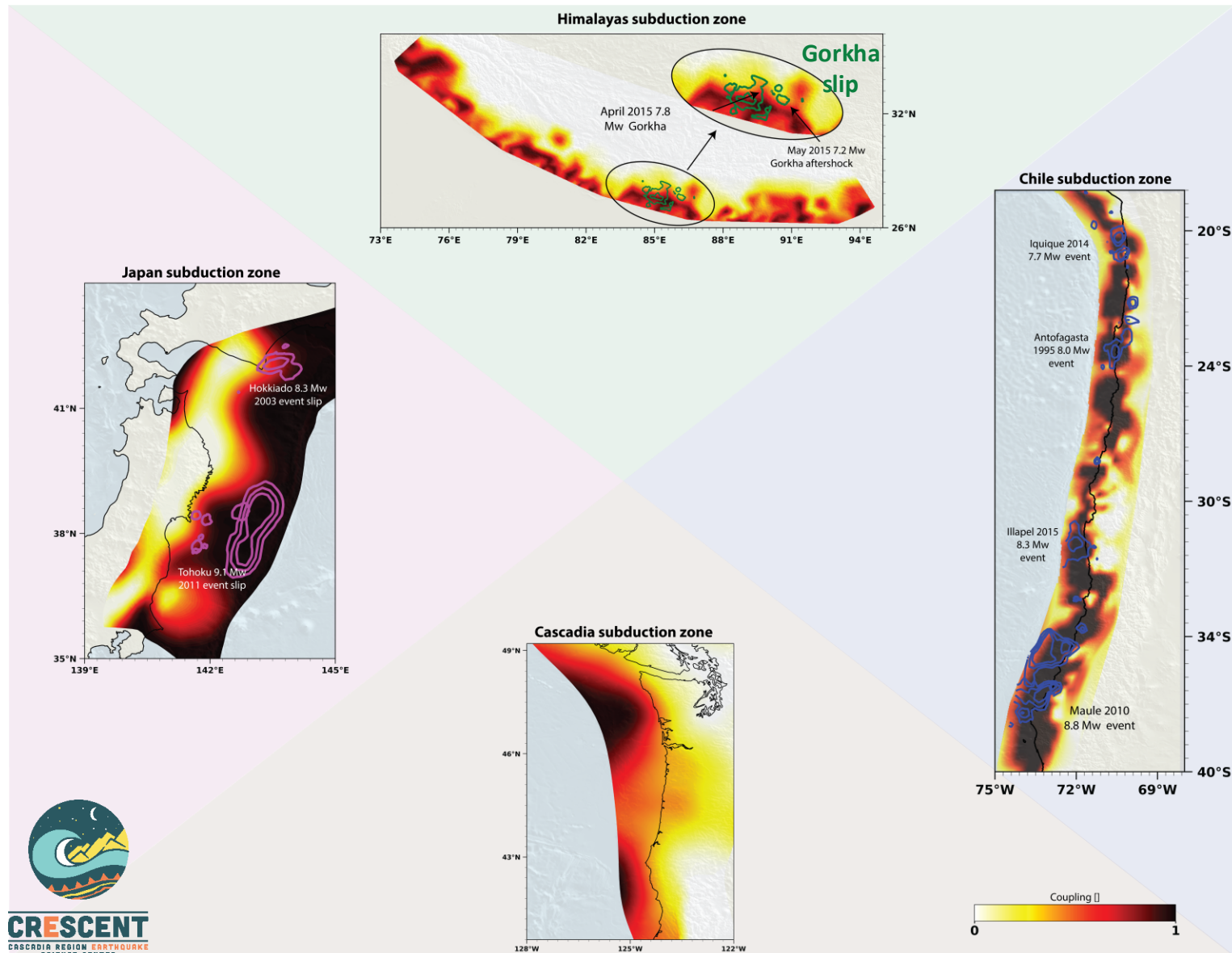
THE ENERGY BUGDET OF EARTHQUAKE CYCLES

- **Unraveling Energy Distribution in Subduction Zones:** We will study the rheological properties that govern the balance between elastic deformation (fueling earthquakes) and inelastic strain (shaping subduction zone landscapes).
- **Investigating Seismic Cycle Dynamics:** Using SEAS simulations, my group will explore how non-recoverable strain accumulation in the overriding plate impacts earthquake dynamics and the coseismic period.

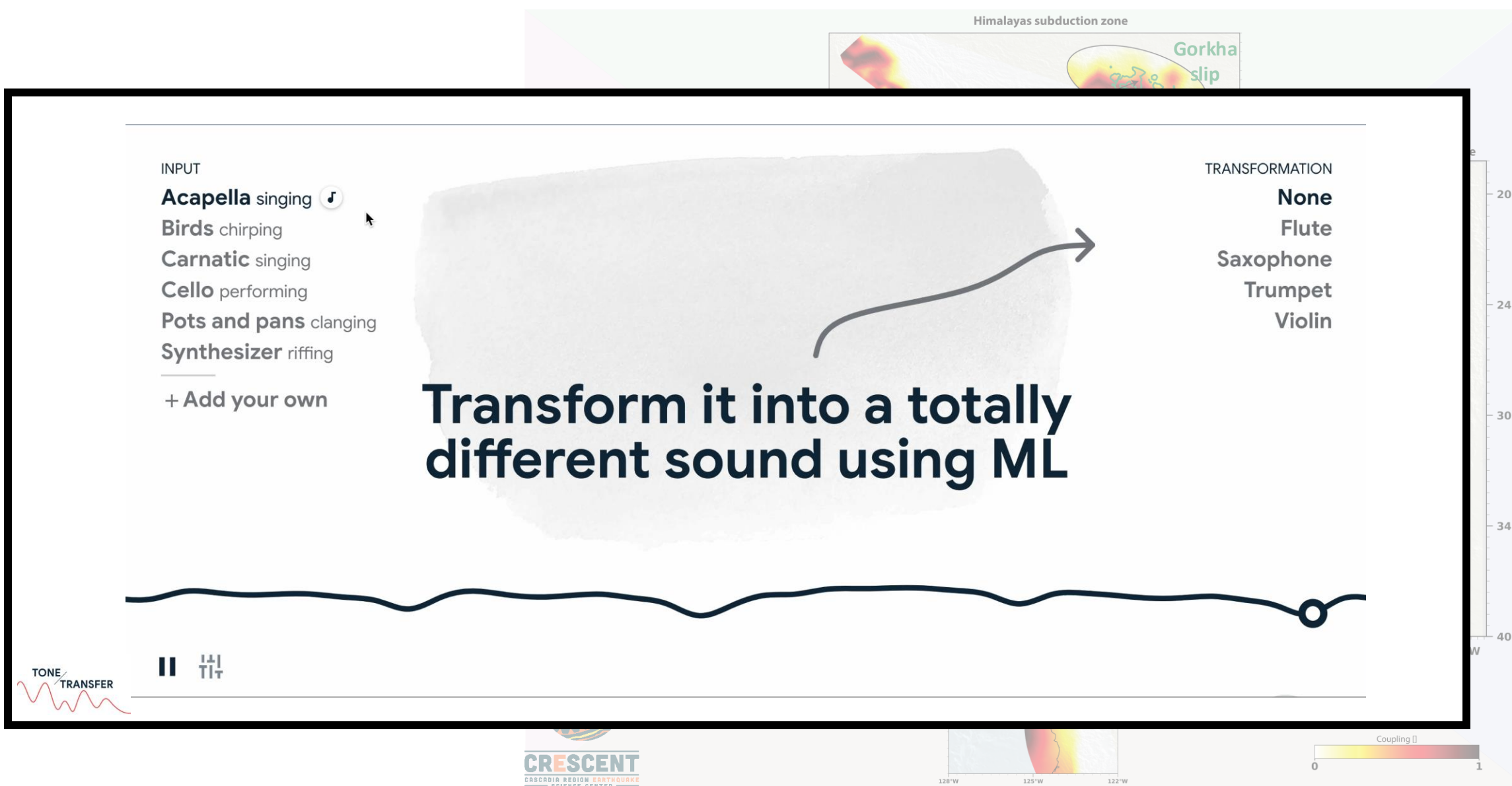


UNIFYING MEGATHRUSTS FAULTS USING OPTIMAL TRANSPORT AND MACHINE LEARNING TOOLS

- Seismo-geodetic observations span decades at each subduction zone.

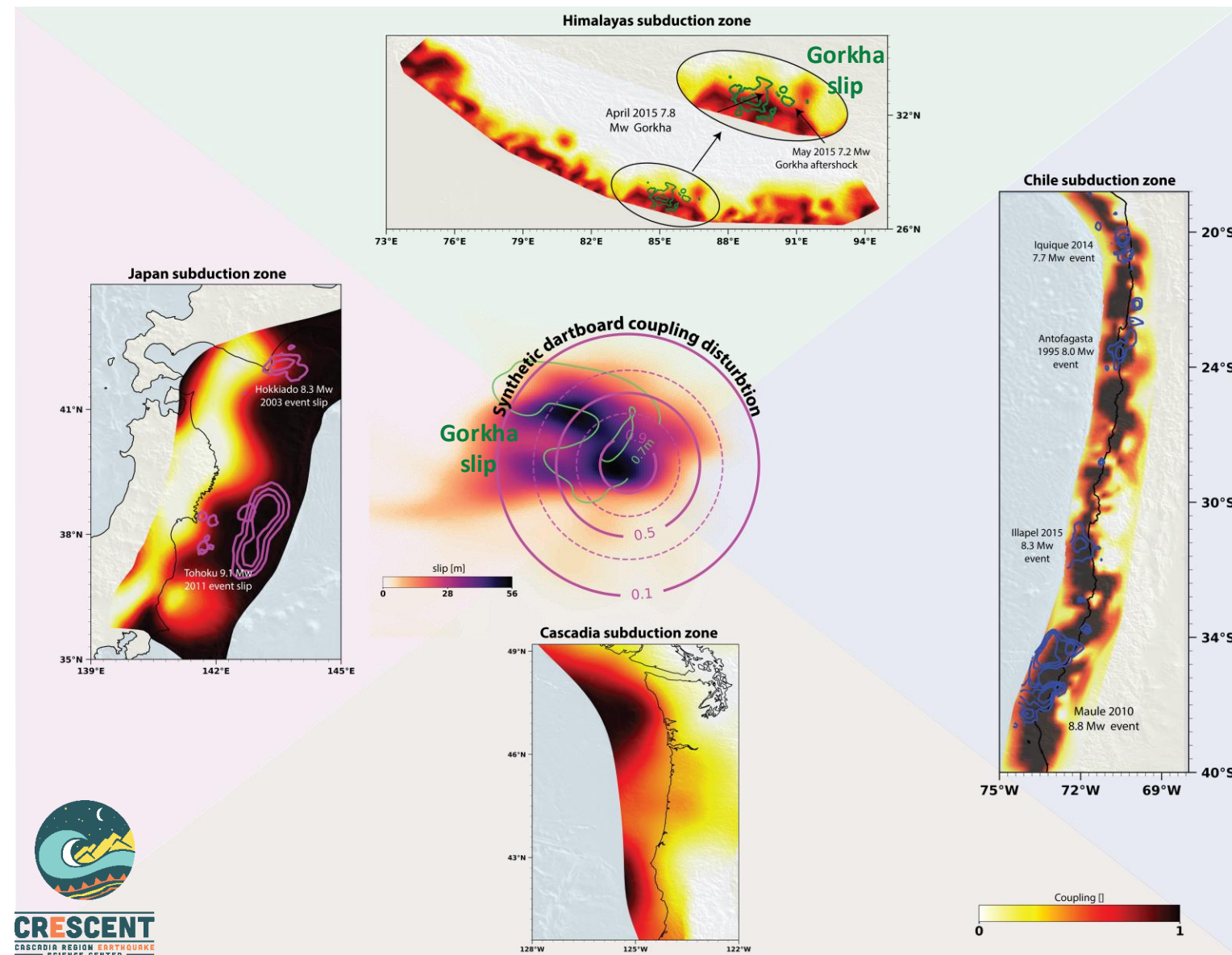


UNIFYING MEGATHRUSTS FAULTS USING OPTIMAL TRANSPORT AND MACHINE LEARNING TOOLS



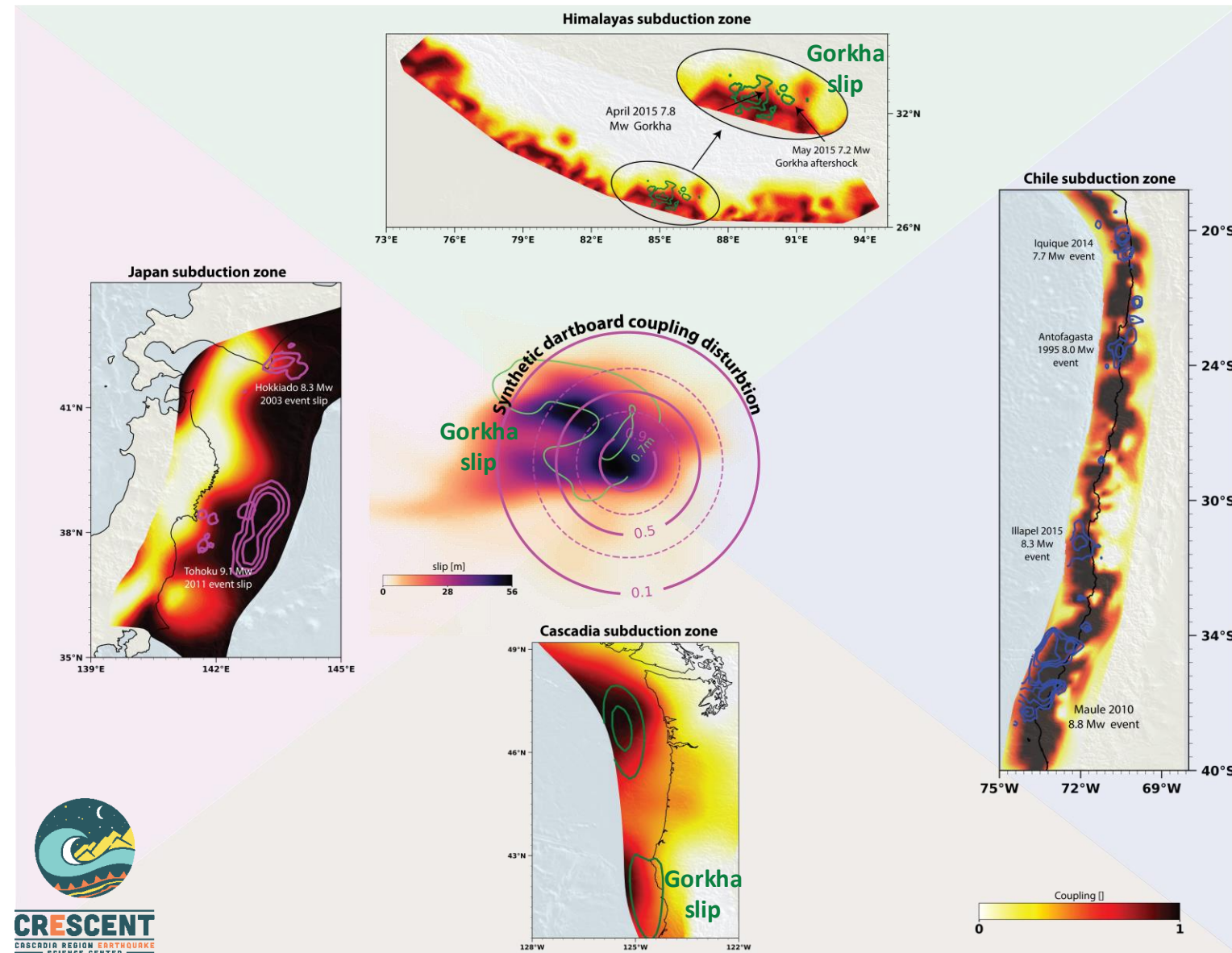
UNIFYING MEGATHRUSTS FAULTS USING OPTIMAL TRANSPORT AND MACHINE LEARNING TOOLS

- Seismo-geodetic observations span **decades at each subduction zone**.
- My group will use machine learning and optimal transport tools to compute geodetically and physically consistent **geometric mappings between megathrusts**.



UNIFYING MEGATHRUSTS FAULTS USING OPTIMAL TRANSPORT AND MACHINE LEARNING TOOLS

- Seismo-geodetic observations span **decades at each subduction zone**.
- My group will use machine learning and optimal transport tools to compute geodetically and physically consistent **geometric mappings between megathrusts**.
- This approach will **extend our seismo-geodetic observational record several-fold** and allow us to assess seismic hazard more robustly.



ACKNOWLEDGEMENTS



Alice Gabriel
Boris Gailleton
Dave May
Heather Savage
Jean-Arthur Olive
Jeena Yun
Lucile Bruhat
Luca Malatesta
Mike Steckler
Roger Buck
Romain Jolivet



